

The Effect of Process Variables on the Dispersion Process with Applications to Paint Processing

By

Callisto Kazembe

Thesis submitted in partial fulfilment of the requirements for the degree of Master of Science in
Engineering (Chemical Engineering) in the Department of Process Engineering at the
University of Stellenbosch



Supervisor: Professor J.H. Knoetze

Stellenbosch
April 2003

Declaration

I, the undersigned, hereby declare that the work contained in this thesis is my own original work and that I have not previously in its entirety or in part submitted it at any university for a degree.

Callisto Kazembe

11th March 2005



Summary

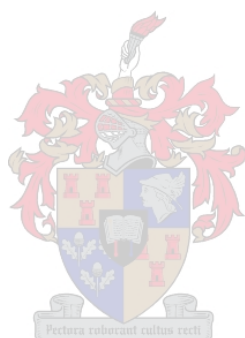
Paint manufacturing through the dispersion process is an important part of the chemical industry that relies on limited and expensive supplies of titanium dioxide pigment. The aims of the project were to: (i) identify and evaluate the factors that affect the opacity and flocculation gradient, (ii) establish and evaluate the mechanism of the process, and (iii) evaluate and apply the rheology of the dispersion process.

The mechanism of the dispersion process can be broken down into the following steps: (i) wetting, (ii) particle break down, and (iii) stabilisation against agglomeration. Wetting can be further broken down into adhesional, immersional and spreading wetting, which can be evaluated in terms of the contact angle. Titanium dioxide pigment particles are held together in the agglomerate state through attractive Van der Waals forces. These forces must be broken down through shear stresses applied through the Cowles mill or the homogeniser. The sensitivity analysis that was carried out confirms that Van der Waals forces are effective only for sub-micron-sized particles. Acoustic cavitation also increases the rate of particle break down in a homogeniser and it depends on turbulence intensity. The mechanism of dispersion can be evaluated in terms of the Reynolds number.

The opacity and flocculation gradient of paint were found to depend on: (i) the mean pigment particle size of titanium dioxide and extender, (ii) the particle size distribution of titanium dioxide, (iii) the pigment volume concentration of titanium dioxide and extender, and (iv) the wavelength of the incident radiation. Correlations of opacity (contrast ratio) or flocculation gradient could be set up on the basis of the above explanatory variables in terms of a multiple linear regression. However, it was found out that the methods used for measuring the contrast ratio and flocculation gradient were unreliable. In the case of the contrast ratio, there was no standard procedure for preparing pigment dispersion samples, thus resulting in values that were very high and insensitive to process changes. Samples whose contrast ratio has to be determined must be diluted with resin. Measurements of the flocculation gradient were found to be erratic with very low linear association.

Samples of pigment dispersions processed through the dispersion process were found to be shear thinning. Flow curves obtained showed that the high shear rate and low shear rate behaviour of dispersions were significantly different. Of the processing variables investigated, dispersant had the greatest impact on the dispersion process. It significantly affects wetting and the particle break down rate. Samples of dispersions from the dispersion process are thixotropic and recover their structure in a reasonable time after the application of shear stress.

Overall, the agitator speed and diameter did not impart a significant effect on the dispersion process.



Opsomming

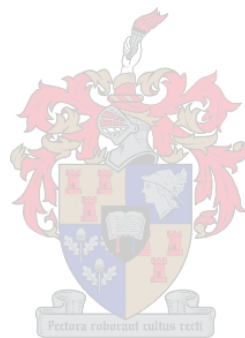
Die vervaardiging van verf met die dispersie proses vorm 'n belangrike deel van die chemiese industrie wat staatmaak op die verskaffing van 'n beperkte voorraad, duur titaniumdioksied pigment. Die doel van hierdie projek was om (i) die faktore te identifiseer en te evalueer wat die ondeurskynendheid en flokkulasie gradiënt beïnvloed, (ii) die meganisme van die proses vas te stel en te evalueer, en (iii) die reologie van die dispersie proses te evalueer.

Die meganisme van die dispersie proses kan verdeel word in die volgende stappe: (i) benatting, (ii) afbreking van partikels, (iii) stabilisering teen agglomerasie. Benatting kan verder verdeel word in adhesiebenatting, onderdompelingsbenatting en spreibenatting, wat dan in terme van die hoek van kontak ge-evalueer kan word. Titaniumdioksied pigment partikels word deur Van der Waals kragte bymekaar gehou in die agglomeraattoestand en hierdie kragte moet gebreek word met behulp van skuifspanning wat deur die Cowles Meul en Homogeniseerder aangewend kan word. 'n Sensitiwiteits analise het bevestig dat die Van der Waals kragte slegs effektief is vir sub-mikron grootte partikels. Akoestiese kavitasie verhoog die tempo waarteen partikels breek in die (homogeniser) en dit hang af van die intensiteit van die turbulensie. Die meganisme van dispersie kan in terme van die Reynolds getal ge-evalueer word.

Daar is gevind dat die ondeurskynendheid en flokkulasie gradiënt van die volgende afhanklik is: (i) die gemiddelde pigment partikel grootte van die titanium dioksied en aanvuller, (ii) die partikelgrootteverspreiding, (iii) die pigment volume konsentrasie van die titanium dioksied en die aanvuller, en (iv) die golflengte van die invallende bestraling. Korrelasies van die ondeurskynendheid of flokkulasie gradiënt kan opgestel word op grond van die bogenoemde verduidelikende veranderlikes in terme van 'n veelvuldige linêre regressie. Daar is egter gevind dat die metodes vir die meet van die ondeurskynendheid en flokkulasie gradiënt nie betroubaar is nie. In die geval van die ondeurskynendheid was daar geen standaard prosedure vir die voorbereiding van die pigment dispersie monsters nie en die gevolg was waardes wat baie hoog was en onsensitief was vir proses veranderinge. Monsters waarvan die ondeurskynendheid bepaal moet word behoort met 'n hars verdun te word of by relatiewe lae vastestof inhoude te wees. Flokkulasie gradiënt metings was baie wisselvallig.

Pigment monsters wat deur die dispersie proses geprosesseer is, is pseudoplasties. Die vloeikurwes dui daarop dat die hoë skuif tempo en die lae skuif tempo gedrag van die dispersies grootliks verskil. Van die proses veranderlikes wat ondersoek is het die dispersant die grootste invloed op

die dispersie proses gehad het. Dit het die benatting en partikel afbreking grootliks beïnvloed. Dispersie monsters van die dispersie proses is thixotropies en herwin hul struktuur redelik gou na die aanwending van skuifspanning. Die roerspoed het geen betekenisvolle invloed op die dispersie proses gehad nie binne die beperkte grense in roerspoed wat ondersoek is.



Acknowledgements

To Plascon, Scanning Electron Microscope Unit, Process Engineers Workshop, Professor Knoetze and *the living memory of my parents.*

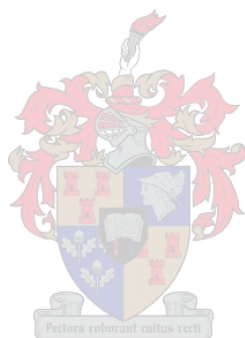


Table of Contents

| | |
|--|-----------|
| DECLARATION | I |
| SUMMARY | II |
| OPSOMMING | IV |
| ACKNOWLEDGEMENTS | VI |
| CHAPTER 1. INTRODUCTION | 1 |
| 1.1 Background | 1 |
| 1.1.1 The conventional paint-making process | 1 |
| 1.1.2 Potential use of the homogeniser in paint making | 3 |
| 1.1.3 Pigment blending | 4 |
| 1.1.4 Stabilisation against agglomeration | 4 |
| 1.2 The critical issues | 5 |
| 1.3 Objectives | 6 |
| CHAPTER 2. FUNDAMENTALS OF DISPERSION | 7 |
| 2.1 The paint-making process | 7 |
| 2.2 The dispersion process | 9 |
| 2.2.1 The formation of flocculates, agglomerates and aggregates | 10 |
| 2.2.2 The sub-process of the dispersion process | 11 |
| 2.2.2.1 The wetting sub-process | 11 |
| 2.2.2.2 Adhesional wetting | 13 |
| 2.2.2.3 Immersional wetting | 13 |
| 2.2.2.4 Spreading wetting | 13 |
| 2.2.3 The complete wetting process | 14 |
| 2.2.4 The mechanical breakdown of agglomerates | 14 |
| 2.2.5 Stability of against agglomeration | 15 |
| 2.3 The effect of the solid-liquid interface on dispersion | 17 |
| 2.3.1 Forces between particles | 17 |
| 2.3.1.1 The attractive Van der Waals forces and its sensitivity analysis | 17 |
| 2.3.2 The interface | 21 |
| 2.3.3 Wetting and contact angle | 23 |
| 2.4 Surface active agents in pigment dispersion | 25 |
| 2.4.1 Surface activity | 25 |
| 2.4.2 Properties of surface active agents | 26 |
| 2.4.3 The selection of surface active agents (HLB – balance) | 27 |

| | | |
|-------------------|---|-----------|
| 2.5 | The breakdown of agglomerates | 29 |
| 2.5.1 | The mechanical breakdown of agglomerates | 29 |
| 2.5.1.1 | The mechanical breakdown of agglomerates through shear stress | 29 |
| 2.6 | The mechanism of homogenisation | 32 |
| 2.7 | Pigment properties that influence the dispersion process | 36 |
| 2.7.1 | Pigment properties that influence wetting | 36 |
| 2.7.2 | Pigment properties that influence breakdown of agglomerates | 36 |
| 2.8 | The opacity of a dispersion | 38 |
| 2.8.1 | The interaction of light with a paint film | 38 |
| 2.8.2 | Light-scattering theories | 39 |
| 2.8.3 | Factors that affect the opacity of titanium dioxide pigments | 40 |
| 2.8.3.1 | The effect of pigment loading on opacity | 40 |
| 2.8.3.2 | The influence of extender on pigment crowding | 41 |
| 2.9 | The rheological behaviour of pigment dispersions | 42 |
| 2.9.1 | The behaviour of a dispersion subjected to shear stress | 42 |
| 2.9.1.1 | Newtonian and non-Newtonian fluid flow (Sherman, P. 1970) | 42 |
| CHAPTER 3. | TECHNICAL ASPECTS OF THE DISPERSION PROCESS | 45 |
| 3.1 | An introduction to the technical aspects of the dispersion process | 45 |
| 3.2 | Milling equipment for the dispersion process | 45 |
| 3.2.1 | Dispersion with a Cowles mill | 47 |
| 3.2.1.1 | The effect of tank: impeller diameter ratio on dispersion | 48 |
| 3.2.1.2 | Charge depth | 49 |
| 3.2.1.3 | Agitator location | 49 |
| 3.2.1.4 | Rotor speed | 49 |
| 3.2.1.5 | Milling time | 50 |
| 3.2.2 | Dispersion using a homogeniser | 50 |
| 3.2.2.1 | The effect of pressure drop on dispersion | 52 |
| 3.2.2.2 | The effect of groove diameter on dispersion | 52 |
| 3.2.2.3 | The effect of flow velocity on dispersion | 52 |
| 3.2.2.4 | The effect of groove length | 52 |
| 3.2.2.5 | The effect of number of (i) grooves per stage and (ii) stages | 53 |
| 3.2.2.6 | The effect of viscosity on dispersion | 53 |
| 3.3 | Methods for the evaluation of the efficiency of the dispersion process | 53 |
| 3.3.1 | The scanning electron microscope | 54 |
| 3.3.1.1 | Particle size analysis | 55 |
| 3.3.3 | Opacity | 55 |
| 3.3.3.1 | Contrast ratio | 56 |
| 3.3.3.2 | The contrast ratio colorimeter | 56 |
| 3.3.3.3 | The determination of contrast ratio | 56 |
| 3.3.4 | Flocculation gradient | 57 |
| 3.3.4.1 | The flocculation gradient monitor | 57 |
| 3.3.4.2 | The experimental determination of flocculation gradient | 60 |
| 3.3.4.3 | Sample testing and evaluation of flocculation gradient | 60 |
| 3.3.5 | Evaluation of the rheology of the dispersion process | 61 |
| 3.3.5.1 | Analytical determination of viscosity in the paint industry | 61 |

| | | |
|------------------|--|-----------|
| 3.3.5.2 | Rheology of the dispersion process | 62 |
| 3.3.5.2.1 | The physica MCR 300 rheometer | 62 |
| 3.4.1.1 | Rotational rheometric methods | 63 |
| 3.4.1.1.1 | Controlled shear rate tests (CSR) and controlled shear stress tests (CSS) | 64 |
| 3.4.1.2 | The evaluation of flow curves | 64 |
| 3.4.1.2.1 | Yield stress | 64 |
| 3.4.1.2.2 | Rate of change of viscosity | 64 |
| 3.4.1.3 | Classification of flow | 65 |
| 3.5 | Repeatability of analytical methods | 66 |
| 3.5.1 | Analysis of particle size and particle size distribution | 66 |
| 3.6 | Scale-up of dispersion vessels | 72 |
| 3.6.1 | Scale-up of agitated vessels through similitude | 72 |
| 3.6.1.1 | Geometrical similarity | 72 |
| 3.6.1.2 | Kinematic similarity | 73 |
| 3.6.1.3 | Dynamic similarity | 73 |
| 3.6.2 | Model based approach for scale up | 74 |
| 3.6.3 | Scale-up of the homogeniser | 76 |
| CHAPTER 4 | MATERIALS AND METHODS | 77 |
| 4.1 | Materials | 77 |
| 4.2 | Methods | 78 |
| 4.2.1 | Experimental design and philosophy | 78 |
| 4.3.1 | Experimental design for the cowles mill | 79 |
| 4.3.2 | Experimental design for the homogeniser | 80 |
| 4.3.3 | Rheology of the dispersion process | 81 |
| 4.4 | Experiments that were carried out with Cowles and Homogeniser mills | 82 |
| 4.5 | Analysis of Cowles/homogeniser experimental runs | 82 |
| CHAPTER 5 | RESULTS AND DISCUSSION – DISPERSION OF TITANIUM DIOXIDE | 83 |
| 5.1 | Results and discussion – dispersion in a Cowles mill | 83 |
| 5.1.1 | Evaluation of design 1 | 87 |
| 5.1.1.2 | Ten minutes of processing | 87 |
| 5.1.1.3 | Fifteen minutes of processing | 89 |
| 5.1.1.4 | Twenty minutes of processing | 91 |
| 5.1.1.5 | Thirty minutes of processing | 93 |
| 5.2 | The overall change in particle size during the dispersion process | 95 |
| 5.3 | The effect of agitator speed on the dispersion process | 96 |
| 5.3.1 | The effect of speed after ten minutes | 96 |
| 5.3.2 | The effect of speed after fifteen minutes | 97 |
| 5.3.3 | The effect of speed after twenty minutes | 98 |
| 5.3.4 | The effect of speed after thirty minutes | 99 |
| 5.3.5 | The mean particle size profiles for batches 2 and 4 | 101 |
| 5.3.6 | Summary of the effect of speed on the dispersion process | 101 |
| 5.3.7 | The contrast ratio for batches 2 and 4 | 102 |

| | | |
|--|---|------------|
| 5.3.7.1 | Empirical correlation of the contrast ratio of the dispersion process | 103 |
| 5.3.8 | The flocculation gradient for batches 4 | 104 |
| 5.3.8.1 | The flocculation gradient after processing batch 4 for ten minutes | 104 |
| 5.3.8.2 | The flocculation gradient after fifteen minutes of processing | 106 |
| 5.3.8.3 | The flocculation gradient after twenty minutes of processing | 107 |
| 5.3.8.4 | The flocculation gradient after thirty minutes of processing | 108 |
| 5.4 | Overall changes in flocculation gradient for the agitated dispersion process | 109 |
| CHAPTER 6 RESULTS AND DISCUSSION – DISPERSION OF STEOPAC TALC | | 112 |
| 6.1 | The dispersion of talc | 112 |
| 6.2 | Evaluation of the effect of speed on the dispersion of steopac talc extender | 114 |
| 6.2.1 | The effect of speed after ten minutes of processing | 114 |
| 6.2.2 | The effect of speed after fifteen minutes of processing | 115 |
| 6.2.3 | The effect of speed after twenty minutes of processing | 116 |
| 6.2.4 | The effect of speed after thirty minutes of processing | 117 |
| 6.3 | The particle size profile for the dispersion of steopac talc | 118 |
| 6.4 | The evaluation of the contrast ratio of batches F, G and H | 118 |
| 6.4.1 | The correlation for contrast ratio | 119 |
| CHAPTER 7 RESULTS AND DISCUSSION – HOMOGENISATION OF TITANIUM DIOXIDE | | 121 |
| 7.1 | Results and discussion – evaluation of dispersion in the homogeniser | 121 |
| 7.2 | The effect of flow rate on the dispersion process | 122 |
| 7.2.1 | Effect of flow rate after two passes | 122 |
| 7.2.2 | Effect of flow rate after four passes | 123 |
| 7.2.3 | The effect of flow rate after six passes | 124 |
| 7.2.4 | The effect of flow rate after eight passes | 126 |
| 7.2.5 | The effect of flow rate after ten passes | 126 |
| 7.2.6 | The effect of flow rate on the particle size profile for the dispersion of titanium dioxide | 127 |
| 7.3 | The contrast ratio for designs A and B | 128 |
| 7.4 | The correlation of contrast ratio | 131 |
| CHAPTER 8 RESULTS AND DISCUSSION – BLENDING OF DISPERSIONS | | 132 |
| 8.1 | Effect of extender on optical properties of titanium dioxide dispersions | 132 |
| 8.1.2 | preparation of blends of titanium dioxide and steopac talc of different compositions | 132 |
| 8.1.3 | The effect of steopac talc on the optical properties of titanium dioxide | 134 |
| 8.1.4 | The effect of kulu 2 on the optical properties of titanium dioxide | 135 |
| 8.1.5 | Correlating flocculation gradient of titanium dioxide dispersions blended with extender | 136 |

| | | |
|--------------------------|---|------------|
| CHAPTER 9 | RESULTS AND DISCUSSION – RHEOLOGY OF THE DISPERSION PROCESS | 138 |
| 9.1 | The effect of speed on the rheology of the dispersion process | 138 |
| 9.1.1 | The effect of speed on the titanium dioxide dispersion process. | 138 |
| 9.1.1.1 | The effect of speed after ten minutes of processing | 138 |
| 9.1.1.2 | The effect of speed after twenty minutes of processing | 140 |
| 9.1.2 | Evaluation of the effect of dispersant | 142 |
| 9.1.3 | Rheology of the dispersion process and particle size and distribution | 144 |
| 9.2 | The time dependent behaviour of Titanium dioxide dispersions | 144 |
| CHAPTER 10 | CONCLUSIONS | 146 |
| 10.1 | Conclusions of the literature review | 146 |
| 10.1.1 | The mechanism of the dispersion process | 146 |
| 10.1.2 | The theory of optical properties of the dispersion process | 147 |
| 10.1.3 | The theory of the rheology of dispersion | 147 |
| 10.1.4 | Application of the analytical techniques to the dispersion process | 148 |
| 10.1.4.1 | Contrast ratio | 148 |
| 10.1.4.2 | Flocculation gradient | 148 |
| 10.1.4.3 | Particle size analysis | 148 |
| 10.1.4.4 | Flow curves | 148 |
| 10.2 | Conclusions for the experimental results | 149 |
| 10.2.1 | Dispersion of titanium dioxide through the Cowles mill | 149 |
| 10.2.2 | Dispersion of steopac talc through the Cowles mill | 149 |
| 10.2.3 | Homogenisation of titanium dioxide | 150 |
| 10.2.4 | Pigment blending | 150 |
| 10.2.4 | The rheology of the dispersion process | 151 |
| CHAPTER 11 | RECOMMENDATIONS | 153 |
| 11.1 | Mechanism of dispersion and simulation | 153 |
| 11.2 | Analytical techniques | 153 |
| 11.2.1 | Contrast ratio | 153 |
| 11.2.2 | Flocculation gradient | 153 |
| 11.2.3 | Rheology of the dispersion process | 153 |
| 11.3 | Experimental technique | 154 |
| 11.4 | Blending of pigment dispersions | 154 |
| 11.5 | Rheology and modelling | 154 |
| 11.6 | Scale up of dispersion equipment | 154 |
| REFERENCES | | 156 |
| GLOSSARY OF TERMS | | 159 |

| | |
|---|------------|
| APPENDICES | 166 |
| A RAW MATERIAL PROPERTIES AND PIGMENT DISPERSION FORMULATIONS | 167 |
| A1 Raw Materials | 167 |
| A2 Formulation of Titanium Dioxide TR93 Dispersion | 168 |
| A3 Formulation of Steopac Talc Extender Dispersion | 169 |
| A4 Formulation of Kulu2 Extender Dispersion | 170 |
| B MILL GEOMETRY | 171 |
| B.1 Cowles mill Geometry | 171 |
| B.1.1 Geometry of Cowles Mill for Batches Investigated | 171 |
| B.1.1.1 Design of the Cowles Used To Disperse Titanium Dioxide Batches | 171 |
| B.1.1.2 Design of Cowles Mill Used To Disperse Steopac Talc Batches | 171 |
| B.2 Plunger Geometry of The Homogeniser | 172 |
| B2.1 Plunger Geometry For The Batches That were Homogenised | 172 |
| C SCANNING ELECTRON MICROGRAPHS AND PARTICLE SIZE DISTRIBUTION(ON CD) SAVED AS WORD DOCUMENT, APPENDIX C.DOC | 173 |
| D CONTRAST RATIO OF PIGMENT DISPERSIONS | 221 |
| D.1 Contrast ratio of Titanium Dioxide Dispersed in Cowles Mill | 221 |
| D.2 Contrast Ratio of Steopac Talc Batches Dispersed in Cowles Mill | 222 |
| D.3 Contrast Ratio of Homogenised Titanium Dioxide Batches | 223 |
| E OTHER VARIABLES WITH AN EFFECT ON THE DISPERSION PROCESS | 225 |
| E.1 The effect of Agitator diameter on the dispersion of Titanium Dioxide | 225 |
| E.2 The effect of agitator diameter on the dispersion of steopac talc | 229 |
| E3 the effect of plunger diameter on the homogenisation of titanium dioxide | 233 |
| F TEMPERATURE CHANGES IN THE COWLES DISPERSION OF TITANIUM DIOXIDE | 238 |
| 15 | 238 |
| G RHEOLOGY OF THE DISPERSION PROCESS | 239 |
| G1 Flow Curves For Batches A1, A2, and A3 | 239 |
| G.1 Viscosity of Titanium Dioxide Batches Dispersed in Cowles Mill | 252 |

| | | |
|----------------|--|------------|
| G3 | Viscosity of Titanium Dioxide Dispersed through Homogeniser | 254 |
| G4 | Viscosity Data for the Rheology of Titanium Dioxide Dispersed through The Cowles Mill | 256 |
| G.4.1 | The effect of speed on rheology of titanium dioxide dispersions | 256 |
| G.4.1.1 | Low Shear Conditions(Read off from the relevant flow curve) | 256 |
| A1 | | 256 |
| A1 | | 257 |
| G.4.1.1 | High Shear Conditions(Read off from the relevant flow curve) | 257 |
| A1 | | 257 |
| A1 | | 257 |
| G.4.2 | The effect of Dispersant on rheology of titanium dioxide dispersions | 259 |
| G.4.1.2 | Low Shear Conditions (Read off from the relevant flow curves) | 259 |
| | Effect of dispersant (10min) \ Batch | 259 |
| A1 | | 259 |
| G.4.1.2 | High Shear Conditions(Read off from the relevant flow curves) | 260 |

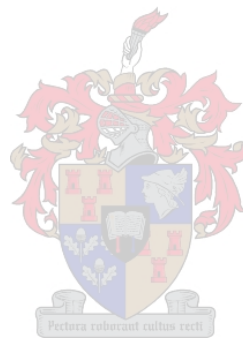
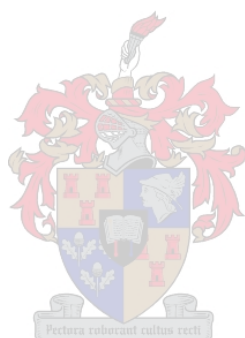


Table of Figures and Tables

| | |
|--|-----|
| Figure 2.4 Sensitivity of van der waals potential energy to the Hamaker constant and inter-particulate distance. | 20 |
| Figure 3.10 Particle size distribution for first hundred particles | 69 |
| Figure 3.11 Particle size distribution for first two hundred particles | 69 |
| Table 4.1 Properties and classification of raw materials | 77 |
| Table 5.1 Processing conditions for production of titanium dioxide dispersions | 84 |
| Table 5.2 Shear stress, viscosity and Reynolds numbers for titanium dioxide dispersions of batch 2 | 86 |
| Figure 5.1 The micrograph for design 1 after ten minutes of processing with mean 413.6nm | 88 |
| Figure 5.7 The micrograph for design 1 after thirty minutes of processing, mean particle size of 364.4nm | 94 |
| Figure 5.8 The particle size distribution for the dispersion based on design 1 after thirty minutes of processing. | 94 |
| Figure 5.9 The particle size profile for the dispersion based on design 1 | 95 |
| Figure 5.10 The effect of speed on the particle size distributions for batches 2 and 4 after ten minutes of processing. | 96 |
| Figure 5.11 The effect of speed on the dispersion process after fifteen minutes of processing in a Cowles mill. | 97 |
| Figure 5.13 The effect of speed on the dispersion process after thirty minutes of processing | 100 |
| Figure 5.14 The changes in the mean particle size of batches 2 and 4 with process time. | 101 |
| Table 5.3 Changes in contrast ratio and mean particle size with processing time | 102 |
| Table 5.4 Measurements required for the development of correlation for contrast ratio and flocculation gradient | 103 |
| Table 5.5 Film thickness and percentage back scatter for samples of titanium dioxide | 105 |
| Figure 5.16 The flocculation gradient for the dispersion process of batch 4 after fifteen minutes of processing. | 107 |
| Figure 5.17 The flocculation gradient after processing batch 4 for twenty minutes. | 108 |
| Figure 5.18 The flocculation gradient for the dispersion of batch 4 after thirty minutes of processing. | 109 |
| Figure 5.19 The changes in flocculation gradient with process time for batch 4 | 110 |
| Table 5.6 Changes in mean particle size and flocculation gradient during dispersion | 111 |
| Table 6.1 Agitator speed used in the preparation of steopac talc | 113 |
| Figure 6.2 The effect of agitator speed (after fifteen minutes of processing) on the particle size distributions for the dispersion of steopac talc (mean particle size in legend) | 115 |
| Figure 6.5 The change in particle size for steopac talc batches F, G and H with time. | 118 |
| Table 6.2 Changes in contrast ratio with processing time for steopac talc | 119 |
| Table 6.3 The mean particle sizes corresponding to the contrast ratios in table 6.1 | 119 |
| Table 7.1 The major dimensions for designs A - E of titanium dioxide dispersions | 121 |
| Figure 7.3 The effect of flow rate through the homogeniser after six passes. | 125 |
| Figure 7.4 The effect of flow rate through the homogeniser after eight passes. | 126 |
| Figure 7.6 The effect of flow rate on particle size of batches A and B passed through the homogeniser. | 128 |
| Table 7.3 Contrast ratio and particle size changes during homogenisation of batch A | 129 |
| Table 7.4 The mean particle size for batches A and B | 129 |
| Table 8.1 Preparation and optical properties of blend between dispersions of titanium dioxide and steopac talc | 133 |

| | |
|--|-----|
| Table 8.2 Preparation and optical properties of blend between dispersions of titanium dioxide and kulu 2 calcite | 135 |
| Table 9.1 The effect of speed on titanium dioxide dispersions (10min) | 139 |
| Figure 9.1 The effect of speed after ten minutes of processing | 140 |
| Table 9.2 The low and high shear rate behaviour of dispersion (20minutes of processing) | 141 |
| Figure 9.2 The effect on the rheology of the dispersion process after twenty minutes | 142 |
| Figure 9.3 The effect of dispersant after twenty minutes of processing. | 143 |
| Table 9.3 The effect of dispersant on the dispersion process | 143 |
| Figure 9.4 The time dependent behavior of titanium dioxide dispersions | 145 |

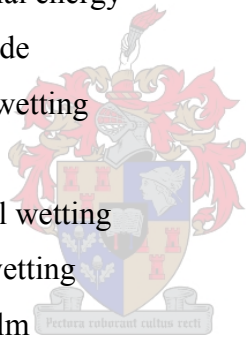


Nomenclature

| | | |
|-------------|--|--|
| a | Diameter of pigment particles | [μm] |
| A | The Hamaker constant | [J] |
| A_{ij} | Mixed Hamaker constant for phases i and j | [J]] |
| \hat{A} | Helmholtz free energy per unit surface area | [kJ.mol ⁻¹ .m ⁻²] |
| \bar{A}_m | The number average particle size for a sample consisting of m particles | [μm] |
| B_x | The percentage back scattered radiation | [%] |
| C.R. | Contrast ratio of a paint film | [...] |
| D^* | Adjusted shear stress in an environment that is influenced by both shear and Brownian motion | [N.m ⁻²] |
| D_i | Impeller diameter | [cm] |
| D_T | Diameter of tank | [cm] |
| F | Force | [N] |
| F_j | Force acting at point j in a dispersion vessel | [N] |
| Fr | Froude number | [...] |
| FR | Fresnel's Reflectivity | [...] |
| G | Gibbs free energy | [kJ/kmol] |
| \hat{G} | Gibbs free energy per unit area | [kJ.mol ⁻¹ .m ⁻²] |
| H | Depth of tank | [cm] |
| H.L.B. | Hydrophilic – Lipophilic Balance | [...] |
| I | Probability of collision of two particles due to Brownian motion | [...] |
| J_c | Probability of collision of two particles due to shear | [...] |
| M | The total number of particles measured | [...] |
| Mw | Molecular weight | [kg.kmol ⁻¹] |
| N | The refractive index at a characteristic frequency | [...] |
| n | Total number of particles in a dispersion | [...] |
| N_p | Power number | [...] |
| N_R | Impeller speed / number of revolutions per minutes | [min ⁻¹] |
| P | Pressure | [Pa] |
| P | Power supplied to the dispersion vessel | [W] |



| | | |
|----------------|--|--|
| PVC | Pigment volume concentration | [%] |
| R | Distance between particle centres | [μm] |
| R _s | Radius of a sphere | [μm] |
| R _b | Reflectance of a paint film applied over a black substrate | [...] |
| R _w | Reflectance of a paint film applied over a white substrate | [...] |
| S | Ratio of the distance between particle surfaces R, to their radii, a | [...] |
| \hat{S} | Entropy per unit surface area | [kJ.mol ⁻¹ .m ⁻²] |
| SEM | Scanning electron microscope | [...] |
| t | Time | [hr] |
| T | Temperature of a system | [K] |
| T _c | The critical temperature of the pigment particles | [K] |
| V | Volume | [m ³] |
| V _A | The attractive Van der Waals potential energy | [J] |
| V _R | The repulsive potential energy | [J] |
| W | Width of agitator blade | [cm] |
| W _a | Work of adhesional wetting | [J.m ⁻²] |
| W _d | Work of dispersion | [J.m ⁻²] |
| W _i | Work of immersional wetting | [J.m ⁻²] |
| W _s | Work of spreading wetting | [J.m ⁻²] |
| X | Thickness of paint film | [μm] |



| | | |
|----------------------|---|-------------------------|
| $\dot{\gamma}$ | Shear rate | [s ⁻¹] |
| $\dot{\gamma}_{ang}$ | Angular shear rate | [rad.s ⁻¹] |
| γ_0 | Surface tension | [N.m ⁻¹] |
| $\gamma_{l/v}$ | Interfacial tension between liquid and vapour phases | [N.m ⁻¹] |
| $\gamma_{s/l}$ | Interfacial tension between solid and liquid phases | [N.m ⁻¹] |
| $\gamma_{s/v}$ | Interfacial tension between solid and vapour phases | [N.m ⁻¹] |
| γ_E | Extrapolated yield stress | [N.m ⁻²] |
| γ_{max} | Upper yield stress | [N.m ⁻²] |
| γ_{min} | Lower yield stress | [N.m ⁻²] |
| δ | Thickness of absorbed layer on a particle | [μm] |
| Δ | Surface to surface separation between particles with a solvate layer | [μm] |
| η | Fluid viscosity | [Pa.s] |
| θ | Contact angle between liquid and solid phases | [degree] |
| ρ | Density of a material | [kg.m ⁻³] |
| τ_{ij} | The sheer stress acting in the j th direction along a plane that is perpendicular to the i th axis. | [N.m ⁻²] |
| μ_i | Chemical potential of species i | |
| λ | Wavelength of light | [μm] |
| Δn | Difference in refractive indices between pigment and medium | [...] |

Chapter 1. Introduction

1.1 Background

The paint industry is a global business that produces about 24 million tons per annum (Gous, K., 2003). Twenty-five percent of this production consists of latex paint, which is a water-based decorative paint (Gous, K., 2003). The major raw materials of all paints are: resin, solvent, pigment (which accounts for about ninety-five percent of the paint) and additives. The pigment imparts opacity on a substrate on which it is applied, while the resin binds the pigment onto the surface of application. On the other hand, the water enhances the spreading of the pigment and binder during application. The additives make up about five percent of the paint and these are: thickeners, surface active agents and defoamers. Thickeners are used in paint to enhance processing, for application rheology and to prevent sedimentation. Surface active agents enhance wetting of pigments during processing and help to stabilise the pigments against flocculation / agglomeration.

The major cost component in paints is the pigment titanium dioxide, which costs about R30.00 / kg (Gous K., 2003). It is the natural choice for opacification of paint, since it has the highest refractive index of all pigments. The opacity of paint is dictated by the difference in the refractive indices of the pigment and the binder and the higher this difference, the greater is the opacity. The refractive index of a pigment is more or less like an intrinsic constant that cannot be manipulated. Apart from its high cost, demand is beginning to outstrip supply. Therefore alternatives must be considered in order to attain the desired opacity in latex paints. One approach that is being used involves partial replacement of titanium dioxide pigment with vesiculated beads (Gous K., 2003). A different approach could be the improvement of the rate of particle break down and stabilisation of pigment particles during the dispersion process. Another alternative is the optimisation of blending of titanium dioxide and extender dispersions.

1.1.1 The conventional paint-making process

This section briefly describes how paint is made using the conventional process and the challenges that the traditional methodology presents. In general, dispersing pigment in a mixture of water, additives and resins in a Cowles mill makes paint.

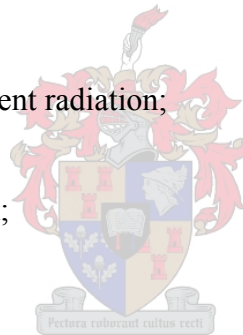
Dispersion is achieved through the supply of mechanical energy to the mill which:

- (i) Wets the pigment particles;
- (ii) Breaks down agglomerates;
- (iii) Stabilises broken-down pigments against re-agglomeration.

Contact between pigment particles and water is achieved through wetting. The energy supplied to the mill breaks down the agglomerates through laminar shear stress. The efficiency of dispersion of the paint produced is largely based on opacity and rheology. The effect of the difference in refractive index between pigments and the binder was explained above.

The opacity of paint is normally expressed through the contrast ratio, which represents the most important quality performance criterion. It is known that the opacity of paint depends upon (Tioxide®):

- i. Wavelength of the incident radiation;
- ii. Particle size;
- iii. Particle size distribution;
- iv. Pigment loading.



Although opacity is a very important quality property, its utility is reduced through the manner it is being implemented by the paint industry. Paint is sampled from the mill and its contrast ratio obtained through an off-line measurement. If the contrast ratio obtained is not the desired value, the mill and formulation variables are adjusted through a trial and error approach. The success of this approach depends on the experience of the operators and could possibly be time consuming.

Such an experience-based approach used to adjust the formulation and process fails to take advantage of the relationship between contrast ratio, mean pigment particle size and particle size distribution. A major reason for this dilemma is the lack of availability of easy to use, reliable and cost-effective particle size analysers. The common particle size analysers for dispersions of sub-micron-sized pigments such as titanium dioxide are the scanning electron microscope and laser diffraction.

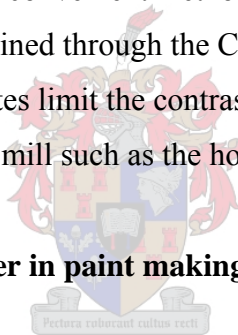
Controlling contrast ratio at the process stage is equivalent to manipulation of laminar shear stresses, which in turn manipulates the particle size and particle size distribution of the dispersion. Shear stress can be manipulated in the Cowles mill through:

- i. The speed of the stirrer;
- ii. Tank: agitator diameter ratio;
- iii. Charge depth of the mill base;
- iv. Pigment loading.

The viscosity, opacity or flocculation gradients share similar explanatory variables. It could be possible to investigate the relationships between these variables. This is important in establishing an economic online method for monitoring and manipulation of contrast ratio of flocculation gradient during processing.

Apart from the need to establish convenient methods for the estimation of mean pigment particle size, the dispersion obtained through the Cowles mill has a significant fraction of agglomerates. These agglomerates limit the contrast ratio of the paint. This necessitates further processing in a different mill such as the homogeniser.

1.1.2 Potential use of the homogeniser in paint making



The conventional Cowles disperser cannot break down all the agglomerates, since it does not develop sufficiently strong shear stress. It is felt that a homogeniser could improve the degree of dispersion of paint. The homogeniser is a set of valve-regulated orifices. The power, which operates the valve and forces the dispersion through the orifices is supplied by high-pressure pumps. The shear stress that is applied to the mill base passing through the orifices depends upon:

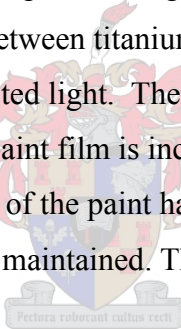
- i. Pressure drop across the orifice;
- ii. Radius of the orifice;
- iii. Residence time.

The residence time depends upon the length of the orifices and the number of passes.

The homogeniser has been applied to emulsion polymerisation of vermiculated beads, with the result that the size of the beads was reduced to about 1 micrometer (Gous K, 2003). Therefore it appears as if it is possible to use the homogeniser in the breakdown of pigment agglomerates. Should the homogeniser prove to be a suitable mill, it would be connected to the Cowles disperser in a semi-batch process that would complement the actions of each mill. In so doing the cost of paint would be reduced through the use of less titanium dioxide. A second approach for reducing the amount of titanium dioxide used in paint is pigment blending. Pigment blending is a possible formulation alternative that could be used to reduce the cost of titanium dioxide.

1.1.3 Pigment blending

Apart from titanium dioxide, which is the main opacifier in paint, there are other pigments called extenders that can be added to paint. Extender pigments have a similar refractive index to that of the binder. They impart rheological and optical properties to the paint. The extender acts as spacer particles between titanium dioxide particles. This reduces multiple scattering and absorption of refracted light. Therefore the amount of back-scattered radiation that emerges out of the paint film is increased, with a consequent increase in opacity. Once the desired opacity of the paint has been achieved in the process, there is a need for ensuring that it would be maintained. This involves stabilisation against flocculation or agglomeration.



1.1.4 Stabilisation against agglomeration

A pigment dispersion must be stabilised to prevent re-flocculation once the dispersing force is inactivated. Stabilisation is achieved through the addition of a surface active compound (surfactant) during the dispersion process. Ionic surface active compounds are suited for the stabilisation of aqueous pigment dispersions. Stability can only be effected to the pigment dispersion once the surface active compound has been adsorbed to the pigment particles. Once the ionic surfactant has been adsorbed onto the dispersed pigment particles, it repels neighbouring particles. Surfactants are known to have effects that are detrimental to the dispersion process, which means that they must be used cautiously or in conjunction with defoamers.

1.2 The critical issues

The mechanism of pigment dispersion is not understood in full (Floury *et al.*, 2004). This makes it difficult to scale up or predict the performance of different processing conditions. An understanding of the mechanism makes it convenient to monitor and control the pigment dispersion process.

The mechanism of the dispersion process relates process conditions to the mean particle size and distribution. Although mean particle size and distribution are important properties in the paint industry, they are not quality properties. Contrast ratio and flocculation gradient are the most important quality properties of pigment dispersions. Therefore, it is necessary to find a way of relating contrast ratio or flocculation gradient to mean particle size and distribution. This link enables the interfacing of quality properties with the mechanism of pigment dispersion. Furthermore, contrast ratio or flocculation gradient then become online variables making it convenient to monitor and manipulate them.

The mechanism is an overall tool for understanding the pigment dispersion process. However, pigment dispersion must be implemented in a mill. It is known that pigment dispersions produced using the Cowles mill contain a fraction of agglomerates, which is controlled by the equipment variables and the formulation. In addition the homogeniser has been applied in emulsion polymerisation to produce fine vesiculated beads. This mill could be important in reducing the mean particle size and the flocculation gradient of pigment dispersions.

Apart from reduction of flocculation, titanium dioxide pigment dispersion can be blended with extender minerals such as talc and calcite. Although the flocculation gradient deteriorates slightly, the cost of the paint can be drastically reduced. This approach requires determination of the optimum fraction of extender minerals that could blend into the titanium dioxide pigment dispersion. The objectives of this research are presented below.

Once the Cowles mill and Homogeniser have been investigated on a laboratory scale, it is necessary to explore the methods that can be used to scale these mills.

1.3 Objectives

The objectives of the project are to:

- i. Review the pigment dispersion process and to identify mechanisms, processes, analytical procedures and correlations;
- ii. Experimentally investigate the Cowles process for pigment dispersion;
- iii. Experimentally investigate the homogeniser for pigment dispersion;
- iv. Compare the Cowles process and homogeniser and identify the critical parameters.

Chapter 2 reviews the fundamentals of the dispersion process.



Chapter 2. Fundamentals of dispersion

The fundamentals of the dispersion process that are covered in this section help in the:

- i. Selection and evaluation of raw materials;
- ii. Design and operation of the dispersion process;
- iii. Evaluation of the efficiency of the dispersion process.

These issues are reviewed in detail in this thesis. However, the initial focus is placed on the paint production process. This is done using a process flow sheet. The rest of this section is structured as follows:

1. The paint-making process;
2. The dispersion process;
3. The effect of the solid-liquid interface on dispersion;
4. Surface active agents in pigment dispersion;
5. The break down of agglomerates;
6. The mechanism of homogenisation;
7. Pigment properties that influence the dispersion process;
8. The opacity of a dispersion;
9. The rheological behaviour of pigment dispersions.

2.1 The paint-making process

Paint is a dispersion of pigment particles suspended in a medium that contains resin. The major raw materials needed to make paint were identified in the introduction as: pigments, medium and additives. The roles of these raw materials were spelt out sufficiently in Chapter 1 and will not be repeated in this section. The set of raw materials and the order of addition during processing are called a formulation. This is as important as the raw materials.

Once the formulation is in place, a process is required to convert the raw materials into the product paint. This conversion is facilitated through the dispersion process, which is consists of the following steps:

- i. Wetting of pigments;
- ii. Mechanical break down of agglomerates;
- iii. Stabilisation of pigment particles against re-flocculation.

Wetting of pigments will be reviewed in section 2.2.2, while the breakdown of agglomerates is reviewed in section 2.2.3. Finally the stability of pigment dispersions is reviewed in section 2.2.4. This section briefly describes the paint-making process, while highlighting theoretical and technical aspects that still need an in-depth review.

To produce paint the dispersion process is technically implemented in a set of equipment units. A general flow sheet for the implementation of the dispersion process is shown in Figure 2.1.

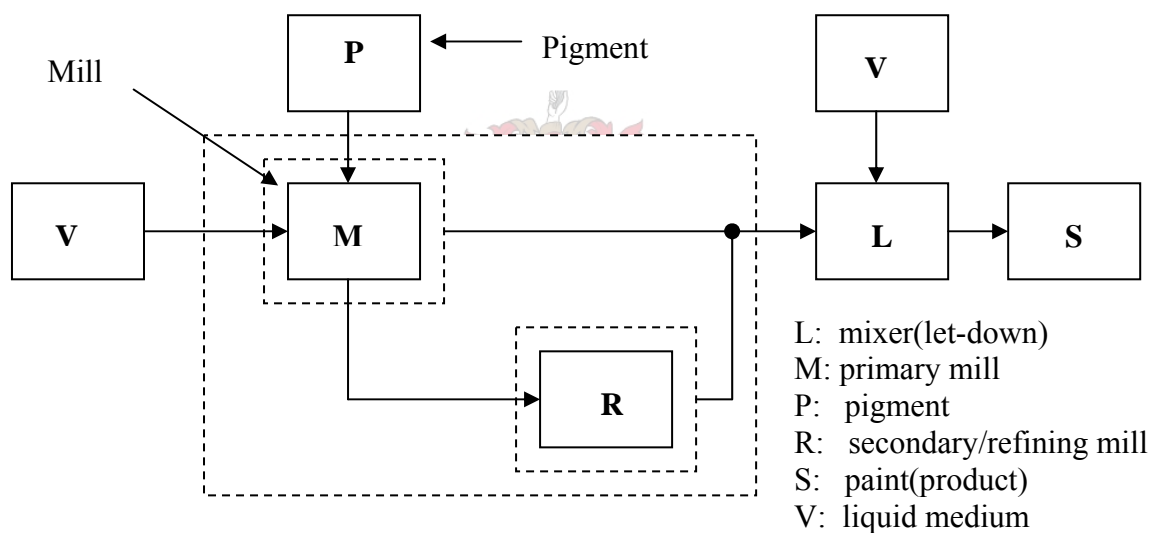


Figure 2.1 A multi-purpose (batch/continuous) dispersion process flow sheet.

Water and additives are loaded into mill M and thoroughly mixed before the addition of pigment can commence. Pigment is added gradually to the mill M, whilst ensuring that it wets out before any further additions. Once all the pigment has been added, the mill is run at a higher speed. During this period agglomerates are broken down, further wetting occurs and the smaller particles are stabilized. A number of mills are available for the dispersion process and these are reviewed in section 3.2. Milling is stopped once the desired degree of dispersion has been achieved. It is possible that mill M fails through limitations of design to achieve the desired degree of dispersion. Another mill must then be used.

Further improvements in the degree of dispersion can be achieved through the use of a semi-batch process as shown in Figure 2.1. Mill base from mill M flows to another mill R, where a further breakdown of agglomerates, wetting and stabilisation occurs. This project's focus is on:

- i. Determining if a single mill M produces mill base of the desired degree of dispersion; and/if
- ii. A second mill can improve the degree of dispersion further.

Mill base from R flows back to mill M in a recycle, while part of it is tapped off as product.

The paint-making process is complete when the product mill base has been evaluated; this is achieved using:

- i. Particle size and distribution;
- ii. Contrast ratio;
- iii. Flocculation gradient;
- iv. Rheology.



The efficiency of the dispersion process is reviewed in section 3.3, while the dispersion process is reviewed next in sub-section 2.2.

2.2 The dispersion process

Pigments exist as particles that are held together through Van der Waals attractive forces in agglomerates. Agglomerates are clusters of primary particles held together through attractive Van der Waals forces. The role of the dispersion process is to separate the particles in the agglomerates. In so doing, the optimum opacity is imparted to the dispersion. Although separation of particles was mentioned as part of the dispersion process, the other sub-processes in the dispersion process are: wetting and stabilisation of pigment particles. This section reviews:

- i. The formation of flocculates, agglomerates and aggregates;
- ii. The wetting sub-process;
- iii. Stabilisation against flocculation.

The major focus of the above method of reviewing this section is to identify the significant theory that is required to fully understand the dispersion process. It may not be possible to discuss all the theory for each of the dispersion processes in this section, but the appropriate section that further develops the required theory will be identified.

2.2.1 The formation of flocculates, agglomerates and aggregates

During the drying process, the pigment particles come together to form large clusters. Such clusters tend to reduce the opacity of the pigment particles since their size is larger than the optimum size required. The formation of the cluster of particles is driven by the instability of the individual pigment particles.

Individual pigment particles of colloidal dimensions have a high surface free energy and thus are unstable. Surface free energy \hat{A} is a measure of thermodynamic stability. A system of particles achieves greater stability whenever the surface free energy is made more negative. The only way for the particles to reduce their surface free energy would be to attract each other, thus forming clusters. The ways in which the attracting particles contact each other is used to classify the cluster of particles.



When pigment particles touch at points, they form a flocculate. Pigment agglomerates are formed when pigment particles contact each other through their edges. The surface free energy of agglomerates is lower than that of flocculates. Therefore agglomerates are more stable than flocculates. Put differently, the forces of attraction that hold agglomerates together are much stronger than those that hold flocculates together. The forces that hold flocculates or agglomerates together are called Van der Waals attractive forces, and these will be reviewed in section 2.3.1. An understanding of Van der Waals forces is critical in the determination of the force required to separate particles held up in flocculates or agglomerates. This aspect of the breakdown of agglomerates will be reviewed in section 2.6.

Flocculates and agglomerates are not the only oversized particles that are encountered in a batch of dry pigment powder. Aggregates are more compact particles that are formed through sintering of pigment particles. The conditions that provide sintering are high

pressures exerted on the pigment particles. Sintering is the result of fusion of two or more particles, which contact each other through sharp points when these sharp points are exerted by high pressure. When we discuss the breakdown of clusters in section 2.6, we do not refer to aggregates since the equipment used cannot break them down. As will be highlighted in section 2.6, aggregates can only be broken down through impact, which is not a mechanism that features significantly in the equipment we will discuss. The next sub-section reviews the sub-processes of the dispersion process.

2.2.2 The sub-process of the dispersion process

Dispersion is the complete process of incorporating a powder homogeneously in a liquid medium (Parfitt, G.D., 1981). The processes involved in dispersion are:

- i. Wetting of pigment particles;
- ii. Break down of agglomerates;
- iii. Stabilisation against agglomeration.

The above sub-processes are reviewed in this section.



2.2.2.1 The wetting sub-process

One reason mentioned for the instability of pigment particles is their high surface free energy. A possible way of lowering this surface free energy of the solid surface is through adsorption of another phase. Wetting is the process through which a solid surface adsorbs a liquid phase. The driving force behind wetting is surface free energy, which will be discussed in detail in section 2.3.2. Wetting can be analysed according to Osterhof *et al.* (1930) in terms of:

- i. Adhisional wetting;
- ii. Immersional wetting;
- iii. Spreading wetting.

Wetting is the work done in replacing a solid/air interface with a solid/liquid interface. Only equilibrium wetting is assumed in this section and it is described by the Dupré

equation (Dupré, A., 1865). Figure 2.2 shows the geometrical relationship between the variables that define the Dupré equation.

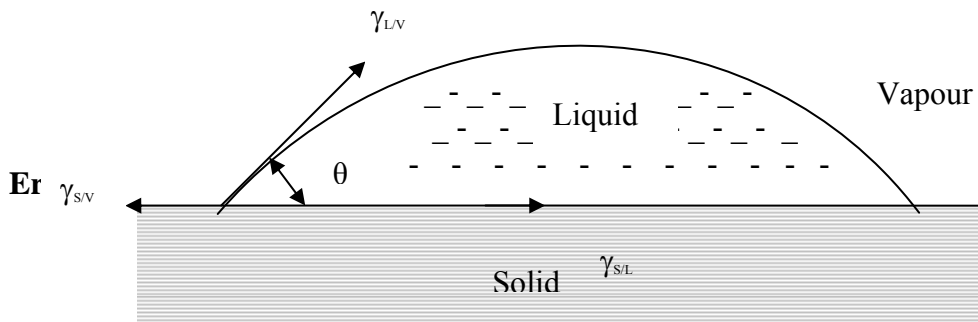


Figure 2.2 The interfacial tensions acting between the boundaries of any two phases

The Dupré equation is:

$$\cos \theta = \frac{(\gamma_{s/v} - \gamma_{s/l})}{\gamma_{l/v}} \quad 2.1$$

where: θ is the contact angle

$\gamma_{s/v}$ is the interfacial tension between the solid and vapour boundary

$\gamma_{s/l}$ is the interfacial tension between the solid and liquid boundary

$\gamma_{l/v}$ is the interfacial tension between the liquid and vapour boundary

The interfacial tension between any two phases is a measure of the stability or instability of the boundary between the phases. Interfacial tensions will be the subject of the discussion in section 2.3.2, where they are defined in terms of the surface free energy \hat{A} , which is a measure of thermodynamic stability. The difference of the interfacial tensions ($\gamma_{s/v} - \gamma_{s/l}$) expresses the total force from boundary effects that act along the solid surface. Therefore the cosine of the contact angle is a measure of the relative stability of the different forces ($\gamma_{s/v} - \gamma_{s/l}$) with respect to the interfacial tension of the liquid/vapour tension.

The Dupré equation assumes that:

- i. The solid phase is perfectly smooth;
- ii. Contacting phases are homogeneous.

The above refinements of the Dupré equation are described by Jaycock (1981). A review of the individual wetting sub-processes is presented below.

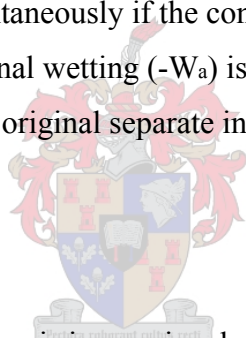
2.2.2.2 Adhesional wetting

The first step in wetting is adhesional wetting. It is the replacement of the unit surface area of each of the solid and liquid surfaces with a single unit area of a new solid/liquid interface (Parfitt, G.D., 1981). According to Dupré (1865) the work of adhesional wetting W_a is:

$$W_a = -\gamma_{lv}(\cos \theta + 1) \quad 2.2$$

where: W_a is the work of adhesional wetting per unit interfacial area

Adhesional wetting occurs spontaneously if the contact angle is less than 180° . The negative of the work of adhesional wetting ($-W_a$) is called the work of adhesion, which is the work required to restore the original separate interfacial phases.



2.2.2.3 Immersional wetting

The second step in the mechanism is immersional wetting and is the total immersion of unit square of solid surface by exchange of solid/vapour with solid/liquid interface, without any change in the extent of the liquid surface (Parfitt, G.D., 1981). The immersional work W_i is:

$$W_i = -4\gamma_{lv} \cos \theta \quad 2.3$$

where: W_i is the work of immersional wetting per unit surface area of particles

Immersional wetting is spontaneous for contact angles that are less than 90° .

2.2.2.4 Spreading wetting

Spreading wetting is the last step in the wetting mechanism and is the work required to create an equivalent solid/liquid interface from separate solid and liquid interfaces (Parfitt, G.D., 1981). It is given by:

$$W_s = -\gamma_{l/v}(\cos\theta - 1) \quad 2.4$$

where: W_i is the work of spreading wetting per unit interfacial area

2.2.3 The complete wetting process

The complete wetting process is obtained by combining adhesional, immersional and spreading wetting. The complete wetting process is shown diagrammatically through transitions a → d in Figure 2.3. Transition a → b represents adhesional wetting, transition b → c represents immersional wetting, while transition c → d represents spreading wetting. The addition of these transitions is equivalent to transition a → d, which is the total wetting process. The total work of wetting W_d , in terms of the contact angle θ is:

$$W_d = -6\gamma_{l/v} \cos\theta \quad 2.5$$

where: W_d is the total work of wetting per unit interfacial area

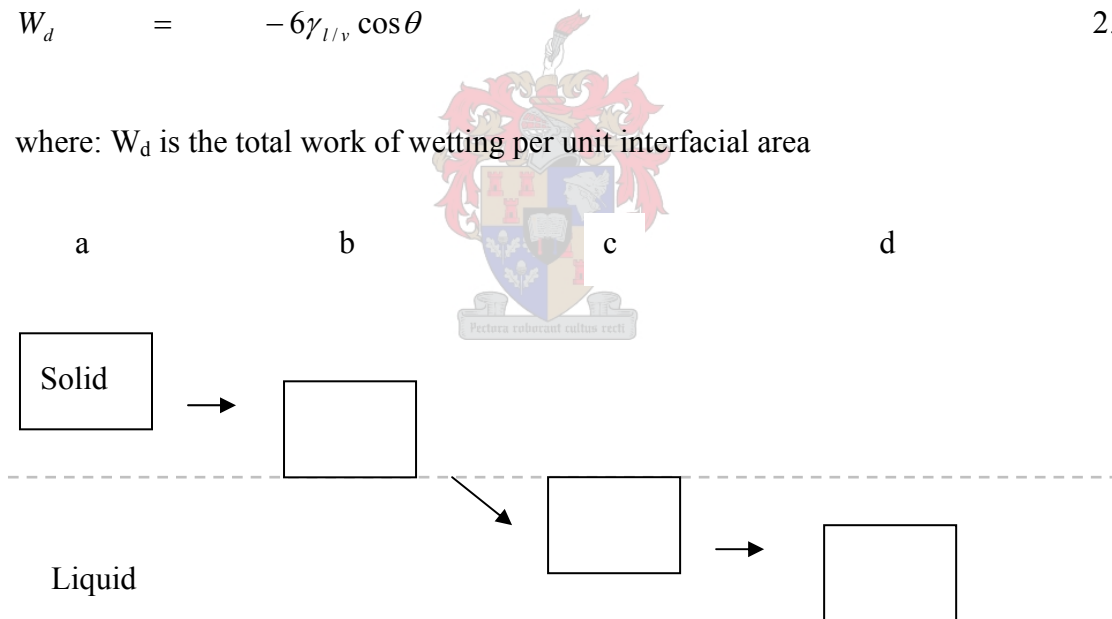


Figure 2.3 The sub-processes of the wetting mechanism

Shear stresses can act on the agglomerates causing particle breakdown once pigment particles have been wetted. The mechanical breakdown of agglomerates is reviewed in section 2.2.4.

2.2.4 The mechanical breakdown of agglomerates

The purpose of the mechanical breakdown of agglomerates is to overcome attractive Van der Waals forces between particles in agglomerates through laminar shear stress. Van der Waals attractive forces will be dealt with in greater detail in section 2.3.1.

Agglomerates are broken down by laminar shear stresses applied through the mill. It is essential to select the appropriate mill in which control of laminar shear stress is convenient. Laminar shear stresses are reviewed in greater detail in section 2.6.3. Section 2.6.3 will show that, when using laminar shear stress to breakdown agglomerates, it is necessary to combine the process with a macro-mixing facility. This creates extra challenges, since macro-mixing is promoted by turbulent flow. Therefore it is necessary to select equipment and processing conditions appropriately. The selection of equipment and processing conditions to manipulate shear stress appropriately is reviewed in detail in section 3.2.

Breakdown of agglomerates on its own is inadequate to produce a dispersion of the desired degree, since it results in a finer product whose surface energy is very high, resulting in instability. Such instability can be avoided provided that the particulate system is stabilised against re-agglomeration.

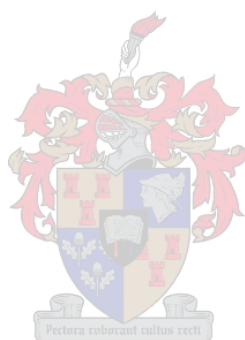


2.2.5 Stability of against agglomeration

The inherent thermodynamic instability of colloidal particles was noted in the concluding paragraph of sub-section 2.2.3. Therefore it is necessary to stabilize a dispersion to prevent re-agglomeration. Stability against agglomeration is achieved by preventing close approach of particles in a dispersion. The exact method used depends on the nature of the dispersion. However, close approach is prevented in any case through the use of surface active agents. Surface active agents are described in section 2.5. The first step in stabilizing pigment particles against agglomeration is adhesion, which is discussed in section 2.3.4. Adhesion attaches the surface active agent onto the surface of the pigment particles. It is an interfacial process and it is also responsible for wetting. A surface active agent functions through steric hindrance or electric repulsion. For aqueous dispersions the surface active agents employed function through repulsion.

A simple approach that is used to address the stability of a dispersion is the HLB (hydrophile-lipophile balance). It is a systematic procedure for the selection of surface

active agents and it is described in section 2.5. Section 2.3 reviews the solid/liquid interface and provides a thermodynamic approach to the stabilities of interfaces.



2.3 The effect of the solid-liquid interface on dispersion

This section reviews the forces between particles, interfacial processes, wetting and contact angle.

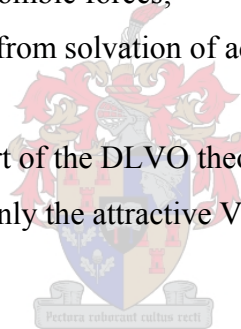
2.3.1 Forces between particles

An understanding of the forces of interaction between particles in a dispersion is important in: (i) production and stabilisation of the dispersion and (ii) an understanding of the fundamental causes of agglomeration.

The major forces of interaction between particles in a dispersion are (Parfitt, G.D., 1981):

- i. Attractive Van der Waals forces;
- ii. Repulsive/attractive coulombic forces;
- iii. Repulsive forces arising from solvation of adsorbed layers.

Effects (i) and (ii) above are part of the DLVO theory (Deryaguin, B.V. *et al.*, 1941 and Verwey, E.J.W. *et al.*, 1948). Only the attractive Van der Waals forces are reviewed in detail.



2.3.1.1 The attractive Van der Waals forces and its sensitivity analysis

Van der Waals forces are the major causes of the formation of agglomerates. Knowledge of the strength of the Van der Waals attractive forces is important in determining the magnitude of:

- i. Shear stress required to disrupt agglomerates;
- ii. Repulsive force required stabilise a dispersion against re-agglomeration.

This section explores all significant variables that have an effect on the size of the van der Waals attractive forces. The size of the repulsive force that is required to stabilize aqueous dispersions is not reviewed in depth, since it is equivalent to the attractive Van der Waals force.

Van der Waals forces of attraction originate from electromagnetic interactions between induced or permanent dipoles in particles (Hamaker, 1937). The Van der Waals forces are obtained by integrating attractive interactions over all pairs of molecules.

The Van der Waals attractive potential energy, V_A , between any two spheres is given by (Parfitt, G.D., 1981):

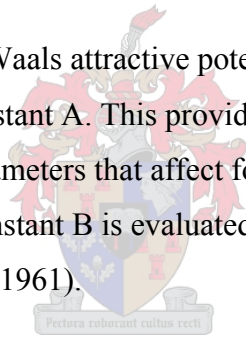
$$V_A = -\frac{A}{6} \left(\frac{2}{S^2 - 4} + \frac{2}{S^2} + \ln \left(\frac{S^2 - 4}{S^2} \right) \right) \quad 2.6$$

where: V_A is the van der Waals attractive potential energy

A is the Hamaker constant

S is the ratio of the distance between the surfaces of interacting particles and their centres

The evaluation of the Van der Waals attractive potential energy is critically dependent on knowledge of the Hamaker constant A . This provides the focus of this section, since the Hamaker constant contains parameters that affect formulation and stabilization against agglomeration. The London constant B is evaluated through the modified Slater–Kirkwood expression (Moelwyn–Hughes, 1961).



The Hamaker constant analysed above was for particles in the absence of a medium. When the medium surrounds pigment particles, then its role is that of transmitting the attractive force between the particles. The medium reduces the attractive force, thereby providing some stabilization (Parfitt, G.D., 1981). For a two-phase system the effect of the medium can be incorporated as shown below (Hamaker, H.C., 1937):

$$A = \left(A_{pp}^{1/2} - A_{mm}^{1/2} \right)^2 \quad 2.7$$

where: A_{pp} is the combined Hamaker constant for two particle-particle interactions

A_{mm} is the combined Hamaker constant for two medium-medium interactions

Where the subscripts p and m refer to particle and medium as the interacting species respectively. Equation 2.7 is like a mixing rule used for estimating the Hamaker constant in a mixture.

The Hamaker treatment can also be extended to dispersions with dissimilar particles (Parfitt, G.D., 1981), which is of practical importance in the treatment of Van der Waals forces that involve pigment blending.

The effect of the medium on the transmission of force is through the permeability of the medium. Therefore the attractive potential V_A must be reduced by a factor equal to the dielectric constant of the medium at electronic frequency. In turn the dielectric constant is related to the refractive index of the medium.

Further refinements address the effect of an adsorbed layer having a Hamaker constant that is different to that of the suspended particles. According to Vold (1961), an adsorbed layer leads to a decrease in the attractive energy. This will become apparent when surface energy is discussed in section 2.3.2. The adsorbed layer causes changes in the Hamaker constant as a result of two effects. The attractive energy is inversely proportional to the minimum surface separation between the two particles. Therefore the addition of an adsorbed layer leads to an increase in separation between the core particles. Thus adsorption of a fluid surface layer imparts steric stabilization by increasing the separation between attracting particles, which effectively reduces the attractive potential energy, according to equation 2.6.

An improved expression for the attractive potential must incorporate the effect of the adsorbed layer as highlighted in the previous paragraph. The treatment of the effect of an adsorbed layer on the attractive potential was analysed by Vold (1961).

According to Parfitt (1981), incorporation of the effects of adsorbed layers into the Hamaker constant leads to the following conclusions:

- i. The solvate layer can stabilise only very small particles less than 10nm in radius;
- ii. Homogeneous adsorbed layers are more effective than solvent layers;
- iii. Oriented amphipathic molecules in a homogeneous layer increase the stabilisation due to homogeneous layers;

- iv. The thickness of the adsorbed layer required for adequate stabilisation depends on the radius of the particle. As an example, an adsorbed layer of about 10nm is required for particles of about 1 μ m in radius.

Sensitivity of van der Waals potential energy to the Hamaker constant

A sensitivity analysis of van der Waals attractive potential energy to the Hamaker constant was carried out. According to Parfitt(1982), the Hamaker constants for metals and ionic solids lie between 10 e-20 J to 30e-10 J. titanium dioxide pigments were assumed to be ionic solids and thus their Hamaker constants lie in the range above. The mean pigment particle size was assumed to be 400nm. The distance between particles was varied between 0.01nm and 0.1nm. It must be noted that the distance between particles must be smaller than the diameter of the particles. The resulting graph is shown below.

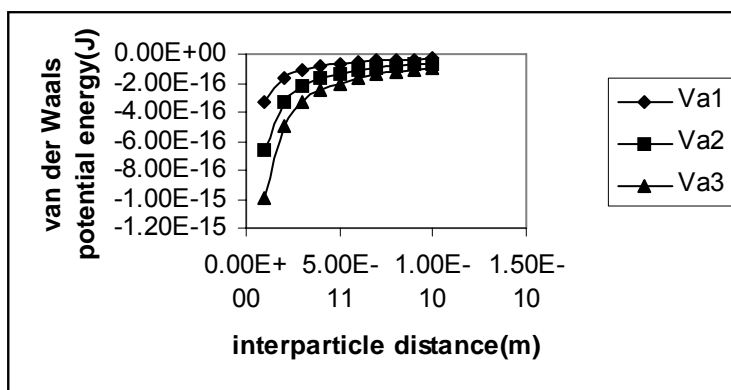


Figure 2.4 Sensitivity of van der waals potential energy to the Hamaker constant and inter-particulate distance.

In the sensitivity analysis above, the legend is explained below:

- i. Va1, is the curve for a Hamaker constant of 10×10^{-20} J;
- ii. Va2, is the curve for a Hamaker constant of 20×10^{-20} J;
- iii. Va3, is the curve for a Hamaker constant of 30×10^{-20} J.

For a distance of 0.01nm, the van der Waals potential energy is:

- i. -3.33×10^{-16} J for a Hamaker constant of 10×10^{-20} J;
- ii. -6.67×10^{-16} J for a Hamaker constant of 20×10^{-20} J;

iii. -1.00×10^{-15} J for a Hamaker constant of 30×10^{-20} J.

It can be noted that the van der Waals potential energy increases with the magnitude of the Hamaker constant.

For a distance of 0.1nm the van der Waals potential energy is:

- i. -3.33×10^{-17} J, for a Hamaker constant of 10×10^{-20} J
- ii. -6.67×10^{-17} J, for a Hamaker constant of 20×10^{-20} J;
- iii. -1.00×10^{-16} J, for a Hamaker constant of 30×10^{-20} J.

As in the previous case, the van der Waals potential energy increases when the hamaker constant is increased.

When we compare the effect of the distance between interacting particles and keep the Hamaker constant fixed, it is observed that the van der Waals potential energy increases with decreasing interparticulate distance.

The van der Waals potential energy is thus a function of both inter-particulate distance and the Hamaker constant. At very small inter-particulate distances the van der Waals potential energy becomes significantly strong. When stating the size of the van der Waals potential energy, it is necessary to state the inter-particulate distance and the Hamaker constant used.

2.3.2 The interface

This section will complement the review of section 2.2.2 by analysing wetting in thermodynamic terms. Therefore at the end of this section the reasons why wetting and adsorption occur will be clear. This section seeks to determine the:

- i. Driving force behind interfacial processes;
- ii. Description of the interface;
- iii. Manipulation of interfacial processes.

An interface is defined as the intervening phase between two distinct phases (Gibbs, J.W., 1928; Guggenheim, E.A., 1928). The interface assumes properties of the two distinct

phases. It can be viewed as a form of a boundary layer. Volds (1961) who analysed the contribution of adsorbed layers to the attractive potential energy, as described in section 2.3.1.1, was actually analysing the effect of interfaces on the stability of particles. However, that treatment provided by Vold was not thermodynamic. This section develops the analysis of interfaces in thermodynamic terms.

The instability of the surface of a phase is due to the fact that bulk molecules are strongly attracted to each other through adhesive forces compared to surface molecules (Young, T., 1805). Therefore the free energy of surface molecules is higher than that for bulk molecules. As a consequence the surface molecules seek to stabilize themselves if an opportunity for doing so exists. If this is possible, the free energy of the phase as a whole is reduced. The Gibbs free energy A is one way of characterizing the stability of a phase. The change in the Gibbs free energy is given by:

$$dG = -s dT + V dP + \gamma_0 dG + \mu dn \quad 2.8$$

where: G is the Gibbs free energy

s is the entropy

V is the volume

P is the pressure

γ_0 is the tension

μ is the chemical potential

n is the number of moles



The above equation leads to a definition of surface tension at constant temperature, volume and concentration as:

$$\gamma_0 = \hat{G} + G \left(\frac{\delta \hat{G}}{\delta G} \right)_{T,P,n} \quad 2.9$$

Where: \hat{G} is the Helmholtz free energy per unit surface area.

T is the temperature of the system

For liquid/gas interfaces, the partial derivative in the above equation is equal to zero, while it is non-zero for solid/liquid interfaces. Therefore surface tension is a measure of the stability of unit area of the surface of a phase. Alternatively surface tension can be said to be a measure of the thermodynamic spontaneity of the surface to achieve thermodynamic equilibrium or stability. It thus becomes apparent that, since the Dupré equation (equation 2.1) is described in terms of interfacial tensions, it is an expression of the relative thermodynamic interfacial stability.

2.3.3 Wetting and contact angle

When the Dupré equation is used in conjunction with the work of adhesion, Young's equation for the work of adhesion is obtained.

$$W_a = \left(\hat{G} + G \left(\frac{\delta \hat{G}}{\delta G} \right)_{T,P,N} \right) (1 + \cos \theta) \quad 2.10$$

The utility of expressing adhesional wetting in terms of the Gibbs free energy is its ability to be linked to thermodynamic changes in temperature. This allows for the manipulation of the work of adhesion as a function of temperature.

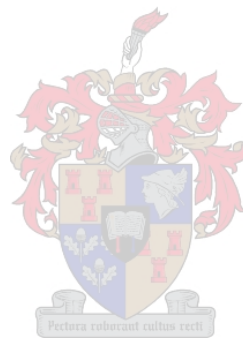
The difference between adhesion and wetting is that adhesion quantifies the force of attraction between the interfacial phase and the surface, while wetting describes the thermodynamic changes that occur at the interface between two phases when wetting occurs.

The force of adhesion, AF between a surface and an interfacial phase is given by Jaycock, M.J. (1981):

$$AF = 4\pi R\gamma \quad 2.11$$

where: AF is the force of adhesion
R is the radius of curvature

Adhesion refers to the force acting between two particles separated by a thin film of medium. It is responsible for the stickiness of particles (Lin, L., 2000). The above expression for the adhesive force between particles gives an indication of the strength of the shear stresses required to overcome particles sticking to each other.



2.4 Surface active agents in pigment dispersion

Surface active compounds are required to enhance:

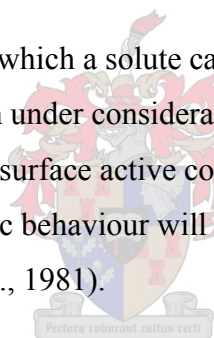
- i. Wetting; and
- ii. The stability of pigment dispersions.

This section will focus on surface active compounds under the categories:

- i. Surface activity – physical requirements and general properties;
- ii. Selection of surface active compounds;
- iii. Application of surface active compounds in aqueous media.

2.4.1 Surface activity

Surface activity is the extent to which a solute can be adsorbed from the liquid phase at one or more interfaces of the system under consideration (Black, W., 1981). There are a number of ways through which surface active compounds can be adsorbed. However, absorption based on amphipathic behaviour will be described in this section, since it is the most general method (Black, W., 1981).



A compound is said to be amphipathic if it possesses a hydrophilic and a hydrophobic radical. The hydrophobic radical is not wetted by an aqueous phase, since it is not readily ionisable, while the hydrophilic radical is readily wetted, since it is ionisable in an aqueous medium. There are several amphipathic surface active agents. When an amphipathic compound is mixed with water, the hydrophobic radical will be oriented away from water. On the other hand, the hydrophilic radical will be oriented towards the water.

Surface active compounds can be classified according to the solubilising group.

Classification is thus in terms of cationic, anionic or non-ionic surface active compounds. The action of the surface active agent is based on its interaction with the surface of the particle. Two special interactive effects associated with surface active agent are:

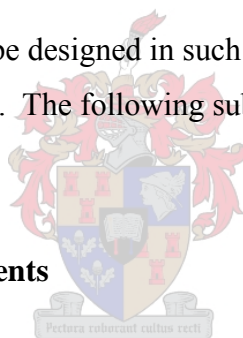
- i. Specific adsorption due to strong attractions being set up between polar groups of a surface active compound and specific groups on the surface of pigment particles;

- ii. Reversed orientation adsorption, in which the hydrophobic groups are forced to orientate towards the aqueous phase.

There is a difference between amphipathic and specific adsorption. Amphipathic adsorption is based on the expulsion of a hydrophobic radical from an aqueous phase, while the polar radical is solvated. Specific adsorption occurs through the interaction between the surface and the surface active molecule.

Polymeric surface active compounds differ in their mode of action to the two methods mentioned in the previous paragraph. According to Jenckel *et al.* (1951), the interaction between polymeric surface active compounds and pigment particles is weak since attachment occurs through a few points, and the remainder of the molecule extends into the medium. In this case, stabilization occurs through steric hindrance, which is an entropic phenomenon.

Surface active compounds can be designed in such a way that they assume characteristics from the different groups above. The following sub-section, 2.5.2, reviews the properties of surface active agents.



2.4.2 Properties of surface active agents

The important parameters for studying surface active agents are based on:

- i. Surface tension;
- ii. Thermodynamics of the adsorption processes and wetting;
- iii. The problems associated with the forces between colloidal particles.

This section deals with the properties of surface active agents with respect to their ability to modify the above parameters.

Surface active agents are organic compounds. Therefore their stability can be treated from an organic perspective. Stability of the surface active agent is an important attribute that must be considered when selecting an agent for an application (Black, W., 1981). The applied surface active agent must be stable to the environment with respect to pH, heat and chemicals (Black, W., 1981).

A universal property amongst virtually all surface active agents is their ability to form molecular aggregates of micelles at certain concentrations. Micelle formation is the result of re-orientation of the surface active agent's molecule. In an aqueous medium the re-orientation results in polar groups facing the water. The interior of the micelle in aqueous medium exhibits organic properties. The formation of micelles is thermodynamically driven, since it results in the reduction of the total free energy of the dispersion. An important property of micelles at or above the critical micelle concentration (c.m.c.) is their ability to increase the solubility of chemicals that have limited solubility in a solvent (Black, W., 1981).

The efficiency of a surface active agent is determined by the polarity and size of the constituent radicals. Therefore the balance of polar and non-polar groups in the surface active compound plays an important role in the selection of the agent (Black, W., 1981). The quantity that measures the above balance is the hydrophile-lipophile balance, which is considered under the section on selection of the surface active agents.

A complete review on surface active compounds must include adsorption and wetting. These concepts were reviewed in section 2.2 and 2.3, and must be considered when selecting surface active agents. Section 2.5.3 reviews the HLB balance, which is a systematic procedure for the selection of surface active agents.

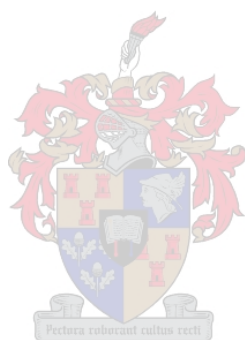
2.4.3 The selection of surface active agents (HLB – balance)

There are several surface active agents available and the hydrophile-lipophile balance (HLB) makes the selection process manageable (Griffin, 1954). The HLB balance was conveniently modified by Davies (1957) and is defined as:

$$HLB = \sum (\text{hydrophilic group numbers}) - n * (\text{group numbers per } CH_2 - \text{group}) \quad 2.12$$

The HLB is a method for quantifying the surface activity of a compound on the basis of the size and polarity of the hydrophilic and lipophilic radicals in the molecule (Black, W., 1981).

The HLB concept has limitations of its own. Griffins (1945) has showed that different surface active compounds could have the same HLB number. Another limitation is that HLB numbers are temperature sensitive (Shinoda *et al.*, 1977). Finally, the multitude of possible interactions between the constituents of a dispersion can swamp the concept of the HLB number (Black, W., 1981).



2.5 The breakdown of agglomerates

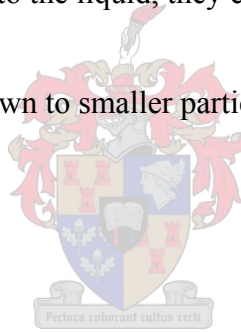
This section seeks to review the various forces/stresses that are responsible for particle breakdown during the dispersion process. The forces that cause particle break-down are laminar shearing, impact and extension. The major method leading to particle break down is laminar shearing and it will be reviewed in depth in this section.

2.5.1 The mechanical breakdown of agglomerates

This section reviews the process of mechanical breakdown of agglomerates in terms of the relevant shear forces. Mechanical break down of agglomerates can only occur once the pigment particles have been wetted sufficiently. This converts the pigment's particle-air interface to a particle-liquid interface. In so doing, pigment particles become homogeneously incorporated into the suspending liquid. Once pigment agglomerates are homogeneously incorporated into the liquid, they can interact with the forces of fluid flow.

Agglomerates can be broken down to smaller particles in the dispersion through (Wheeler, D.A., 1981):

- i. Impact;
- ii. Extension;
- iii. Shear.



Breakdown through impact involves collisions of agglomerates with a static surface (Wheeler, D.A., 1981). It is promoted by increasing the kinetic energy of the dispersion, whilst lowering its viscosity (Wheeler, D.A., 1981), which leads to disintegration of the primary particles, which is not the goal of pigment dispersion. Therefore, impact must be depressed in any pigment dispersion application. Breakdown of agglomerates through extension is not normally encountered in the paint industry. Only mechanical breakdown of agglomerates through shear stress is reviewed in greater detail.

2.5.1.1 The mechanical breakdown of agglomerates through shear stress

The action of shear stress on agglomerates is best illustrated through Figure 2.6a. It shows an ideal laminar flow velocity profile and the difference in velocity between stream lines

causes shear stress to be exerted according to Newton's second law of motion. Figure 2.6b shows shear forces τ_{ij} acting on the wetted agglomerate interface, which overcome the attractive Van der Waals forces, provided that they are sufficiently strong. Finally, Figure 2.6c shows the broken down agglomerate particles that were produced through the action of the laminar shear stresses. It is clear that the shear forces are the link between the mechanical energy supplied to the process and particle breakdown. For particle breakdown to occur, it is essential for laminar flow to be active.

Laminar flow is emphasised rather than turbulent shear stress, since it is responsible for the breakdown of agglomerates (Wheeler, 1981). On the other hand, turbulent shear stress promotes back mixing, which is responsible for wetting (Wheeler, 1981). The demarcation between laminar and turbulent flow is defined in terms of the Reynolds number (N_R), which is a function of the system geometry and flow viscosity.

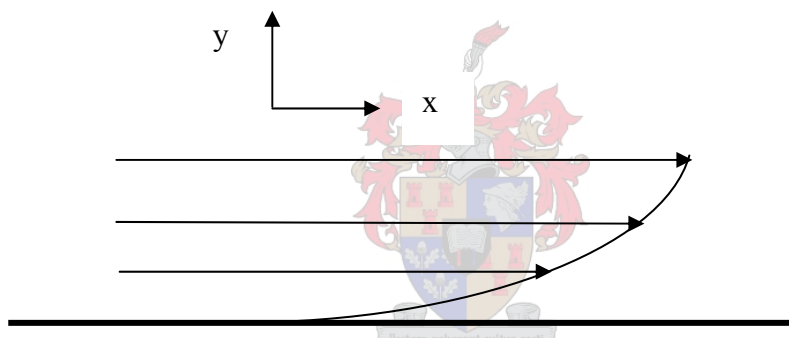


Figure 2.5 The mechanism of dispersion: ideal laminar velocity flow profile in a viscous system

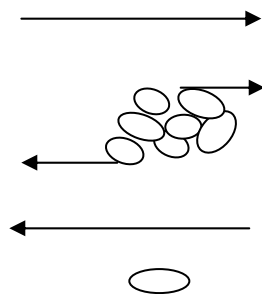


Figure 2.6 The mechanism of dispersion: movement of wetted agglomerate in viscous system.

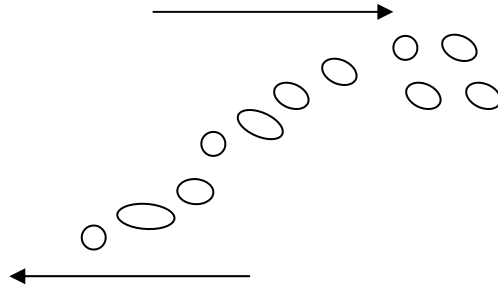


Figure 2.7 The mechanism of dispersion: Partial break down of agglomerate before complete distribution of discrete particles

It must be noted that system geometry depends upon the unit in question and that this differs between a tank and a tube. However, efficient dispersion requires both laminar and shear stresses, since dispersion involves both wetting and particle break-down (Wheeler, 1981). Shear stress is defined according to equation 2.27 (Welty, J.R. *et al.*, 1984):

$$\tau = \eta * \dot{\gamma} \quad 2.13$$

where: τ is the shear stress

η is the viscosity of the fluid

$\dot{\gamma}$ is the shear rate



Equation 2.13 shows that shear stress is the product of fluid viscosity and the rate of strain. The viscosity of a dispersion is an expression of the resistance of a fluid element to distortion. The shear stress required to break down agglomerates is theoretically equivalent to the attractive Van der Waals forces between the agglomerates.

The selection of a mill for effecting dispersion of titanium dioxide depends on the degree of dispersion that is required. This is equivalent to selecting a mill in which the desired magnitude of shear stress is achieved.

2.6 The mechanism of homogenisation

The mechanism of homogenisation can best be understood through numerical simulation based on computational fluid dynamics (Floury *et al.*, 2004). This requires solving the material and momentum balances associated with the flow through the homogeniser valve. A renormalized group RNG k- ϵ turbulence model is used to describe any possible eddy effects within the homogeniser. A number of mechanical processes occur within the homogeniser depending upon the actual flow. According to Floury *et al.* (2004), the general flow occurring within the homogeniser can be depicted as shown in Figure 2.7.

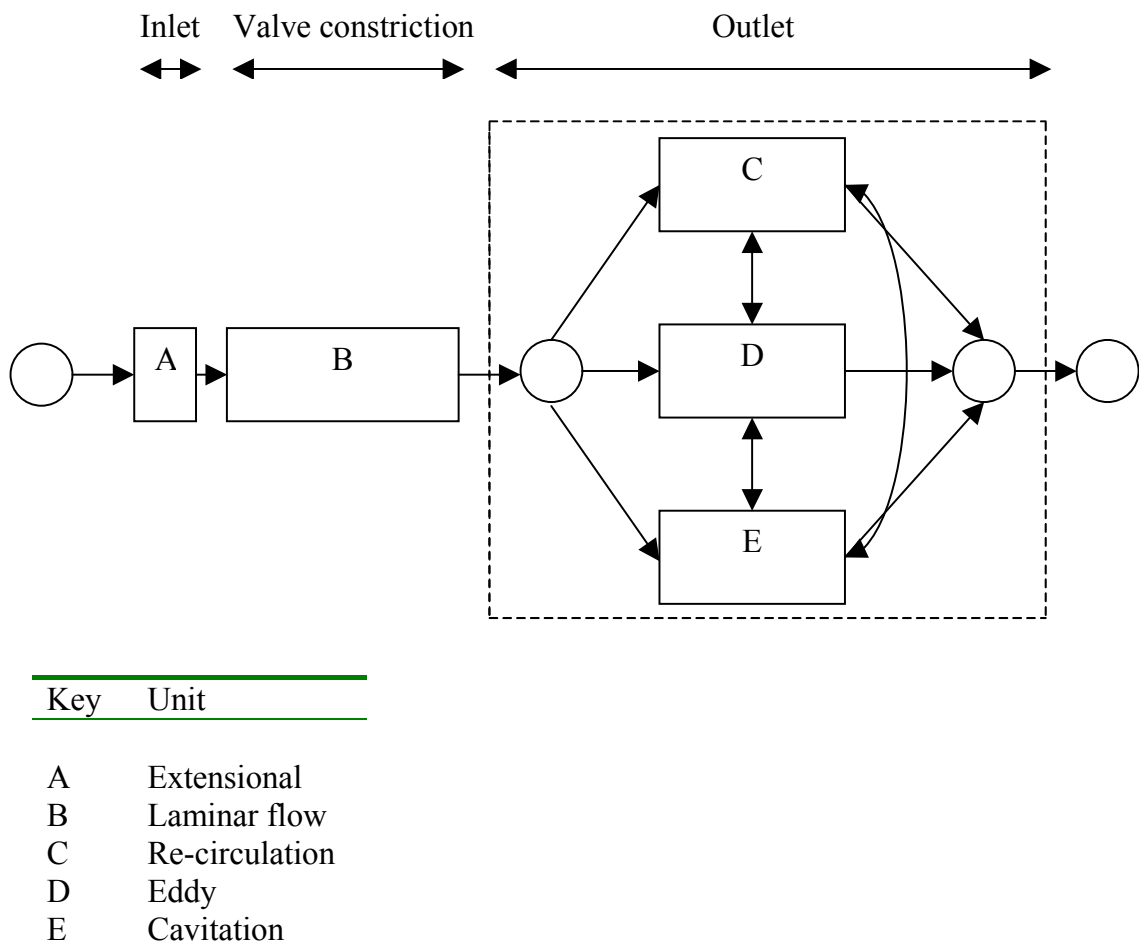


Figure 2.8 Demarcation and interaction of different flow regimes within the homogeniser.

Figure 2.8 shows that the flow within the homogeniser can be partitioned into three different compartments: the inlet, valve constriction and the exit units. Each of these units is characterised by its Reynolds number. The exit unit is by far the most complex as it can further be divided into the eddy, re-circulation and cavitation units. The processes occurring in all these units are described below.

The dispersion that enters the homogeniser is confronted with a sudden constriction, which results in an abrupt conversion of pressure energy to kinetic energy. This abrupt mechanical energy conversion means that a slow-moving agglomerate suddenly accelerates. That is, an agglomerate approaching the inlet of the constriction is subjected to two different head and tail velocities, with the head velocity far larger than its tail velocity (Floury *et al.*, 2004). This is equivalent to a stretching force being subjected to the agglomerate. Such a stretching effect is commonly called elongational/extensional shear stress. According to the simulations of Floury *et al.* (2004), the strength of the extensional shear stress is inadequate, so that no disruption of agglomerates occurs.

The stretched agglomerates at the inlet eventually enter the constriction in which they are subjected to laminar shear stress. The small diameter constriction and the low velocity due to the low pressure drop used in this current project mean that the flow is always laminar. Some disruption of agglomerates occurs within the constriction. Agglomerates leaving the constriction enter the exit part of the homogeniser.

The transition from the constriction to the outlet of the homogeniser is characterised by a sudden expansion, which leads to flow separation that results in transitional or turbulent flow characterised by eddies. The eddies are equivalent to inertial waves that transfer energy to the agglomerates, which could cause disruption of agglomerates. The eddy unit is denoted D in the above diagram. Agglomerate break up is increased by turbulence intensity.

Floury *et al.* (2004) also show that a large area downstream of the constriction is subjected to local pressure that is lower than the thermodynamic vapour pressure of the continuous phase. This causes evaporation and the formation of cavities, which collapse further downstream when the pressure recovers. Such a collapse is associated with the generation of acoustic cavitation waves, which could cause resonant disruption of agglomerates. Cavitation occurs in unit E, as shown in the above diagram. Cavitation depends upon turbulent intensity, as shown by the simulations of Floury *et al.* (2004). The areas of the eddy and cavitation units overlap, since they both depend upon turbulence intensity, and hence exchange of material between the two should be possible as shown in the diagram above.

The effect of eddies and cavitation is similar in that both lead to the disruption of agglomerates. Recirculation is another effect that occurs in the outlet and it depends on turbulent intensity or an increase in pressure drop or a reduction in the diameter of the constriction. The flow separation that occurs at the exit from the constriction leads to re-circulation. Re-circulation is essentially back mixing or turbulent flow. It leads to collisions between particles with the possibility of re-agglomeration. The probability of collision between particles in the re-circulation unit is governed by the turbulence intensity of the flow. The recirculation unit is a sub-unit of the outlet and is denoted by C in the above diagram. Although the recirculation unit is a part of the outlet, it is a unit that is separate from the eddy and cavitation units in terms of area, as shown by the profiles obtained by Flourey *et al.* (2000). However, it is connected to both the eddy and cavitation units.

According to Flourey *et al.* (2004), turbulence intensity seems to become significant above twenty bars. The pressure drop in the current project was 4bars. Therefore it is reasonable to assume that exit effects such as eddy inertial forces, cavitation and back mixing are negligible. Instead only laminar shear stresses are active in the outlet zone.

Flourey *et al.* (2004) identify two important dimensionless groups for characterising the dispersion process occurring in the homogeniser. These are the Reynolds number, Re and the cavitation number, C_v . Flourey *et al.* (2004) define three different Reynolds numbers, one for each of the inlet, constriction and exit sections of the homogeniser. The geometry of the homogeniser used in this project is different to that of the homogeniser. A Reynolds number is used in this project and it is defined as:

$$Re = 4\rho Q \left(\frac{1}{\pi \eta d} \right) \quad 2.14$$

where: Re is the Reynolds number

ρ is the density of the fluid

d is the diameter of a cylindrical constriction

Q is the flow rate of a fluid

The Reynolds number is used to characterise flow into either laminar or transitional or turbulent. This characterisation based on the magnitude of the Reynolds number is useful in

assigning a mechanism to the observed results, as presented in the results and discussion section below.

The second dimensionless group, defined by Shirgaonkar *et al.* (1998), is the cavitation number.

$$C_v = \left(\frac{P_2 - P_1}{\frac{1}{2} \rho v_{gap}^2} \right) \quad 2.15$$

where: C_v is the cavitation number

v_{gap} is the fluid velocity in the constriction

P_1 and P_2 are the pressures at points 1 and 2 in a flow system

According to Flourey *et al.* (2004), the cavitation number is also a function of geometry and this is not reflected above. This number will not be used in this project since the relationship with geometry is unknown. The cavitation number is used in the results and discussion to determine if additional particle breakdown occurs through acoustic cavitation. The extent of particle breakdown through acoustic cavitation depends on the turbulence intensity. Although turbulence intensity is important in particle breakdown through acoustic cavitation, it promotes recirculation of dispersion in the exit unit, resulting in collisions that could lead to re-agglomeration.

The simulations of Flourey *et al.* (2004) are based on simple Newtonian liquids like water and simple oil. Pigment dispersions are known to exhibit non-Newtonian flow behaviour. In addition, their simulations are limited to a single pass, while the present research emphasises multiple passes through the homogeniser.

2.7 Pigment properties that influence the dispersion process

Pigment properties can influence the dispersion process if they have an effect on one or more of the following: wetting, breakdown of agglomerates and stabilisation against re-agglomeration. The influence of pigment properties on the dispersion process is reviewed here according to the sub-processes above.

2.7.1 Pigment properties that influence wetting

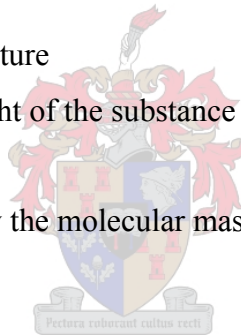
Interfacial tension can be predicted from thermodynamic properties and this is shown in equation 2.16 (Johansen, R.T. *et al.*, 1953).

$$\gamma = \frac{K(T_c - T)}{(M / \rho)^{2/3}} \quad 2.16$$

where: T_c is the critical temperature

M is the molecular weight of the substance

Therefore wetting is affected by the molecular mass, density and critical temperature of the pigment.



Interfacial tensions between phases in a dispersion are related to the Dupré equation through the contact angle θ . The Dupré equation assumes that the contact angle is relative to a smooth surface and roughness can be accounted for through the rough surface contact angle θ' (Wenzel, 1936). Unfortunately, surface roughness cannot be modified in the dispersion process under normal conditions and the pigment manufacturer can only manipulate it.

2.7.2 Pigment properties that influence breakdown of agglomerates

The breakdown of agglomerates affects the dispersion process, since it is one of the essential sub-processes. This breakdown of particles held in the agglomerate state is effectively the disruption of Van der Waals attractive forces between particles. Although attractive Van der Waals forces were reviewed previously, an expanded form is presented here.

The attractive potential V_A is defined in a previous section. However, this section examines the attractive Van der Waals force in an expanded form and this is shown through equation 2.17.

$$V_A = -\left(\frac{A}{6}\right)\left[\frac{2\alpha^2}{(r+2\alpha)(r-2\alpha)} + \frac{\alpha^2}{r^2} + \ln(r+2\alpha) + \ln(r-2\alpha) - \ln(r^2)\right] \quad 2.17$$

where: r is the distance between the centres of interacting particles

α is the surface to surface distance between two interacting particles

Physically the distance between the centres of the interacting particles r must be greater than twice the radius of the particles. The term outside the square bracket is the Hamaker constant.

For terms in the square brackets:

The first term is sensitive to the size of the particles, provided the distance between interacting particles is of the same order as the radius of the particles;

The second term is also sensitive to particle size along the same argument as in (i);

The third and fourth terms are logarithmic, which means that large changes in the particle size are required for any significant impact;

The last term is independent of particle radius.

It appears as if large changes are required to change the attractive potential energy.

Therefore particle size will only have a significant effect if its dimensions are colloidal (less than $1\mu\text{m}$).

The effect of adsorbed layers can also be incorporated into the above discussion. The thickness of the adsorbed layer effectively increases the separation between particles and this effect can be regarded as increasing the effective size of the pigment particle. In this regard the attractive potential energy is reduced, since the particle size effectively increases on adsorption of a fluid layer

2.8 The opacity of a dispersion

Opacity is a quality property of a dispersion. It quantifies the extent to which a film of pigment applied as paint obliterates a substrate. A common measure of opacity is the contrast ratio. Opacity can be understood by reviewing: (i) interaction of light with a paint film (section 2.8.1), (ii) the modified Kubelka-Munk light scattering theory (Kubelka *et al.*, 1931), and (iii) the effects of particle size, pigment loading and extender on opacity.

2.8.1 The interaction of light with a paint film

When light is incident on a paint film, the following happens: (i) reflection at the paint/air surface (specular reflection), (ii) refraction of light, (iii) absorption by pigment particles and (iv) reflection of light (back scatter) by pigment particles. Figure 2.9 shows the interaction of light with a surface of a pigment film and pigment particles.

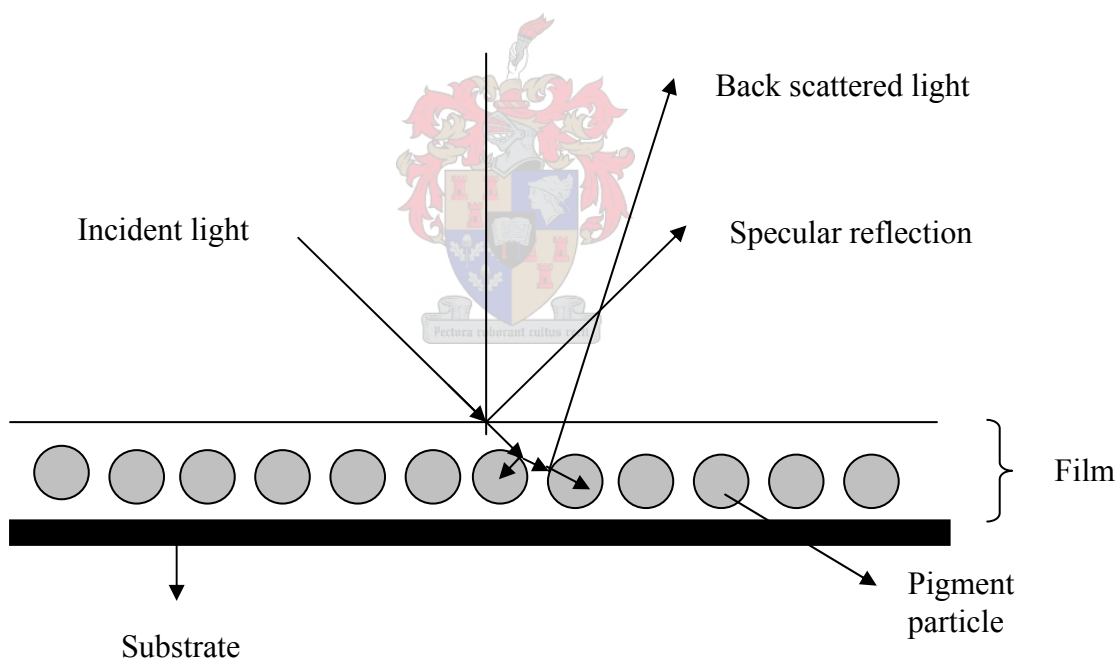


Figure 2.9 The interaction of light with pigment particles

Back scattered radiation is the main way from which the opacity of a paint film arises. Back scattered radiation is described through the light scattering theories explained in 2.8.2. The other involves the difference between the refractive index of the pigment particles and the binder in the paint film. The relevant relationship was defined by Fresnel and is indicated below (Tioxide):

$$FR = \left(\frac{\Delta n}{n_1 + n_2} \right)^2 \quad 2.18$$

where: FR is the Fresnel's reflectivity

n_1 and n_2 are the refractive indices of materials 1 and 2

Δn is the difference in refractive indices of materials 1 and 2

Fresnel's reflectivity depends on the refractive indices of the binder and the pigment, as shown through equation 2.18. This equation shows that Fresnel's reflectivity is increased when the difference in refractive indices between pigment and binder is large. This can be achieved by choosing a pigment that has the highest refractive index, which is titanium dioxide. Unfortunately there is very little scope in manipulating opacity on the basis of refractive indices, since these are constants. Opacity is also imparted to a pigment film through light scattering.

2.8.2 Light-scattering theories

Light-scattering theories describe the opacity of a paint film based on back-scattered radiation. In so doing they relate important parameters like film thickness x , particle size, pigment loading and wavelength of incident radiation to the opacity. A prediction of opacity on the basis of particle size would be important in the assessment of the efficiency of dispersion. In a similar manner, wavelength of incident light affects the maximum back-scatter for a given particle size. In this regard the discussion in this section is relevant to flocculation gradient.

The main theories of opacity (light scattering) are:

- i. Rayleigh's theory (Rayleigh, 1871);
- ii. Mie's theory (Mie, G., 1908);
- iii. Kubelka-Munk's theory (Kubelka *et al.*, 1931);
- iv. The modified Kubelka-Munk theory (Turnstal *et al.*, 1971).

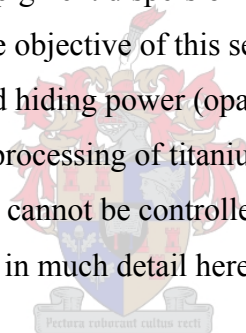
Rayleigh's and Mie's theory cannot describe most practical applications and will not be reviewed any further. The Kubelka-Munk theory is important, but it was later modified since it could not account for the effect of crowding.

The Kubelka-Munk theory gives a relationship between reflectance, scattering, absorption and film thickness (Kubelka *et al.*, 1931). The scattering and absorption are reported as the scattering coefficient and absorption coefficient. Scattering and absorption coefficients are the only unknown variables in the Kubelka-Munk theory (Kubelka *et al.*, 1931). These coefficients can be evaluated at two different film thicknesses.

An improvement of the Kubelka-Munk light-scattering theory is the modified Kubelka-Munk light-scattering theory, which accounts for the surface reflectance (Turnsta *et al.*, 1971).

2.8.3 Factors that affect the opacity of titanium dioxide pigments

The opacity of a white paint depends on: (i) pigment loading, (ii) mean crystal size, (iii) mean particle size, (iv) state of pigment dispersion and (iv) the titanium dioxide content of the pigment (Parfitt, 1981). The objective of this section is to establish relationships between the variables above and hiding power (opacity), which is of importance in guidelines for formulation and processing of titanium dioxide-containing paints. The only variable from the above list that cannot be controlled by the formulator is the mean crystal size and it will not be discussed in much detail here (Hird, M.J., 1973).



2.8.3.1 The effect of pigment loading on opacity

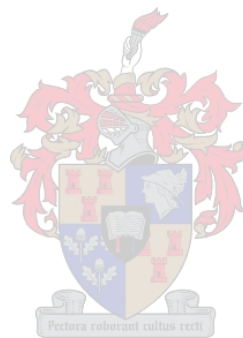
Pigment loading is quantified through the pigment volume concentration (PVC) and it controls the distance between pigment particles in a dispersion. When pigment loading is increased beyond 10 percent PVC, the distance between pigment particles is appreciably reduced. This results in the interaction of the scattering behaviour of the pigment particles and leads to a gradual reduction in the scattering power of the paint film. The consequent reduction in opacity that occurs due to the close proximity of the pigment particles is termed particle crowding.

Turnstall *et al.* (1974) were able to show that the scattering efficiency depended on the mean surface-to-surface distance, a , between pigment particles and also on the wavelength of light, λ .

2.8.3.2 The influence of extender on pigment crowding

When extenders are used to control crowding in paints, they must be chosen in such a way that their refractive indices are comparable to those of the medium. The range of refractive indices must be in the range 1.45 to 1.70. Extenders can reduce the flocculation between titanium dioxide particles by acting as spacers.

Extenders cannot increase the scattering efficiency of a dispersion that contains titanium dioxide. This can be confirmed from the equation of Fresnel's reflectivity. It was noted that the reflectivity of a coating depends upon the difference in refractive index between the medium and the pigment. The difference in refractive index between medium and extender is very small. Therefore the reflectivity of the dispersion is small and insignificant.



2.9 The rheological behaviour of pigment dispersions

The rheological behaviour of a pigment dispersion is very important during its processing and application on a substrate and, according to Weltmann (1960), it is dependent on:

- i. Particle size and particle size distribution;
- ii. Stability of the dispersion;
- iii. Particle shape;
- iv. Temperature.

Conversely, knowledge of the rheological behaviour of a dispersion gives an indication of its particle size and distribution. Although this relationship is not clearly understood, it finds application in the evaluation of the state of a pigment dispersion. The present section focuses on the classification of the rheological behaviour of a pigment dispersion. A brief theoretical analysis of rheological behaviour concludes the section.

2.9.1 The behaviour of a dispersion subjected to shear stress

The classification of the rheological behaviour of a dispersion is based on how it reacts to shear stress acting on it. The manner in which the dispersion reacts depends upon its viscosity, which is its resistance to flow under the action of a shearing stress. The viscosity of a dispersion depends upon (Frisch *et al.*, 1956): (i) shape, size, distribution and mass of dispersed particles, (ii) PVC, (iii) flexibility and ease of deformation of particles and (iv) thermodynamic conditions of the disperse system.

2.9.1.1 Newtonian and non-Newtonian fluid flow (Sherman, P. 1970)

Figure 2.10 shows a dispersion between two discs. The upper disc can rotate if a force F is applied to it, while the bottom disc remains stationary. The rotating force F applied to the top disc is associated with a rate of strain. The force F is gradually increased, while noting the corresponding rate of strain. The force F is converted to shear stress τ_{θ} by dividing it with the area A of the disc.

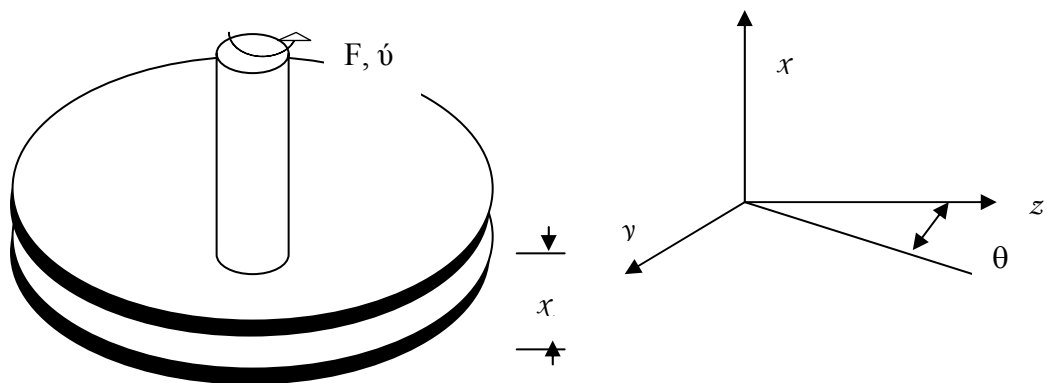
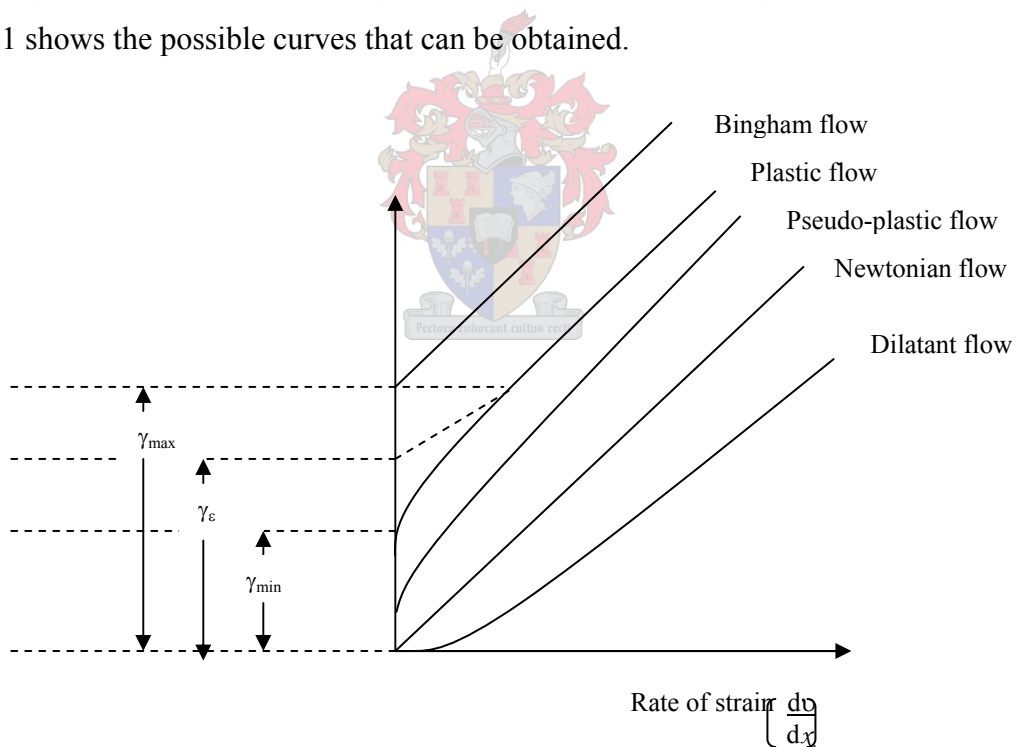


Figure 2.10 Action of shear stress on a dispersion between two plates

Where: F is the force applied to the fluid system

A graph of shear stress τ is then plotted against the core corresponding rate of strain. Figure 2.11 shows the possible curves that can be obtained.



Key

- γ_{max} upper yield value (Houwink)
- γ_{ϵ} Extrapolated yield value (Bingham)
- γ_{min} Lower yield value (Houwink)

Figure 2.11 Categorisation of the flow behaviour of a dispersion

Figure 2.11 is used below to define the different types of flow behaviour. Flow is said to be Newtonian, if it is instantaneous on the application of any shear stress τ_{x_0} .

In other words, there is no barrier that must be overcome for flow to occur. It differs from pseudo-plastic flow in that its viscosity does not depend on the rate of strain and is constant for all possible values. Newtonian flow characterises the flow of all simple liquids.

Pseudo-plastic flow is characterised by the non-existence of a barrier to flow. It differs from Newtonian flow in that the viscosity initially increases when the rate of strain is increased and remains constant beyond a rate of strain value that is particular to the given liquid.

In plastic flow a minimum shear stress is required before the fluid can flow. This minimum shear stress is termed the lower yield value. Once the fluid starts flowing, there is a gradual reduction in viscosity when the rate of strain is increased. Beyond a characteristic rate of strain, the viscosity becomes constant.

Dilatant flow can be classified in terms of yield stress. Dilatant flow without a yield stress is shown in Figure 2.11. In the case of all dilatant flow, the viscosity increases as the rate of strain is increased and this is the opposite of flow, which is shear thinning. The term shear thickening is sometimes used as an alternative to dilatant flow. In dilatant flow, the rate of increase in the viscosity gradually slows down as the rate of strain is increased. This type of flow is associated with high p.v.c., which causes the dispersion to assume a closely packed structure. When shear stress is applied to the dispersion the closely packed structure is disturbed, leading to irregularities in the packing. Bridging occurs between the particles reducing the amount of medium needed to lubricate the particles with a consequent increase in viscosity. Dilatancy is an example of a flocculation, deflocculating process. The technical aspects of the dispersion process are reviewed in Chapter 3.

Chapter 3. Technical Aspects of the Dispersion Process

Technical aspects of the dispersion process refer to the practical issues of carrying out the dispersion process and the methods for evaluation of the dispersion. In this regard the technical aspects seek to implement the fundamentals of the dispersion process in the production and testing of dispersions.

This chapter is organised into the following sections:

The major purpose for presenting and evaluating the link between fundamentals and technical aspects of the dispersion process is to:

- i. Provide an introduction to the technical aspects of the dispersion process;
- ii. Describe the equipment necessary for the dispersion process;
- iii. Outline the methods for the evaluation of the efficiency of the dispersion process.

3.1 An introduction to the technical aspects of the dispersion process

The technical aspects refer to the fundamentals of the dispersion process that are used in a practical manner in the processing of a dispersion in order to attain the desired state and performance properties. They encompass:

- i. The design and evaluation of dispersion equipment(mills);
- ii. Identification of significant mill variables;
- iii. Establishment of correlations that could simplify the operation of the process.

3.2 Milling equipment for the dispersion process

There are a number of mills in use in the paint-making industry(Tioxide). Only the Cowles mill is reviewed in this section. Before the review can commence, a brief diagrammatic summary of the dispersion process is provided in Figure 3.1.

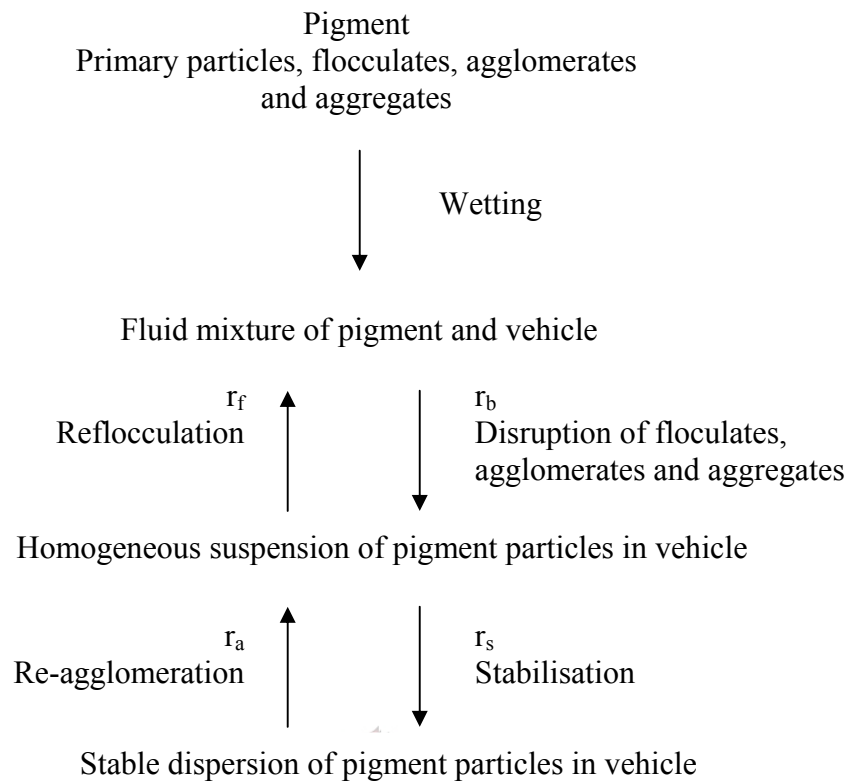


Figure 3.1 The mechanism of pigment dispersion

Where: r_b is the rate of particle break down

r_s is the rate of particle stabilisation

r_a is the rate of particle re-agglomeration

r_f is the rate of re-flocculation

Figure 3.1 shows the relationships between the sub-processes of dispersion and their associated rates. The first step in dispersion is wetting, followed by breakdown of agglomerates. Breakdown of agglomerates occurs at a rate r_b and that for reflocculation occurs at a rate r_f . Breaking of agglomerates to form smaller particles results in an unstable state, since this increases the surface energy of the dispersion. Furthermore, Brownian dispersion, as was stated in section 2.9, is responsible for perikinetic reflocculation.

From a formulation and milling point of view, conditions must be such as to maximize breakdown whilst minimizing reflocculation. In terms of the mill, the speed of milling must be increased. On the other hand, the viscosity of the mill base must allow for faster

breakdown, but must be unfavourable for reflocculation. The focus of this section for each mill is to establish:

- i. The manipulated variables that would increase the rate of break down;
- ii. The formulation that could enhance the rate of break down.

Unfortunately, there is limited scope for manipulation of the rate of breakdown of agglomerates, since this process occurs concurrently with wetting. Effective dispersion calls for the coupling of a macro- and a micro-mixing units in the mill. The macro-mixing unit is responsible for pigment wetting, while the micro-mixing unit breaks down agglomerates. Breakdown of agglomerates occurs in the laminar shear unit, while wetting occurs in the macro-mixing unit, with the macro-mixing unit operated under turbulent flow, which tends to promote re-flocculation due to its mixing capabilities. The major challenge that must be tackled is to specify design and processing conditions that use the laminar shearing and macro-mixing facilities in a manner that produces the required degree of dispersion. The complexity of this challenge is increased through the fact that dispersion also depends upon formulation.

The rest of Figure 3.1 shows the steps that occur after breakdown of agglomerates, such as stabilization and destabilization. The major aim is to allow breakdown of agglomerates to occur to a satisfactory degree before stabilization can be effected. If stabilization were hastily effected, agglomerates would then be stabilized rather than primary particles.

3.2.1 Dispersion with a Cowles mill

The Cowles mill is commonly used in the paint industry either for the production of the desired paint or for pre-mixing pigment with medium before further processing. The Cowles mill is shown in Figure 3.2(Tioxide).

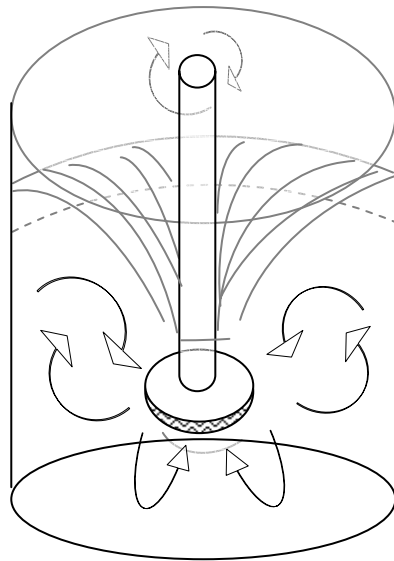


Figure 3.2 The structure and flow pattern in a Cowles mill

Figure 3.2, shows the structure and flow pattern that occurs in a Cowles mill. It consists of an impeller that is concentrically mounted within a tank. The impeller is an assembly of a shaft that supports a Cowles blade, which is a serrated disc with alternating teeth on either face. The Cowles mill is operated after it has been loaded with mill base. The physical variables of the Cowles mill are:

- i. Agitator speed, v ;
- ii. Charge depth, H ;
- iii. Tank: impeller diameter ratio, D ;
- iv. Agitator location, h .

These variables can be used to manipulate the shear stress that is applied to a dispersion.

3.2.1.1 The effect of tank: impeller diameter ratio on dispersion

The tank diameter and mill base compositional effects appear to be interdependent. Therefore different proportions are required for different media. In general, the tank to impeller diameter ratio lies between 2.0 and 2.5. However, for dilatant or thixotropic mill bases, the tank to impeller diameter ratio can be as small as 1:3.

3.2.1.2 Charge depth

Charge depth refers to the height of the mill base above the base of the tank. Charge depth appears to control the possible fractions of the mill base that fall into either the laminar or turbulent flow regimes. The charge depth must not be smaller than the diameter of the agitator.

3.2.1.3 Agitator location

The agitator location refers to the height of the agitator above the base of the tank. Dowling(1961) recommends the impeller to be located a third of the charge depth above the container's bottom. However, Patton(1970) recommends that the impeller must be above the tank's bottom by a distance that must be less than the mill base viscosity in poises. This ensures that flow within the agitated tank is laminar.

3.2.1.4 Rotor speed

The optimum rotor speed depends on the impeller diameter and the composition of the mill base. In general, high peripheral velocities will cause a transition from laminar to turbulent flow, resulting in a poorer degree of dispersion. Thus it is necessary to think of manipulating speed relative to the given formulation.

In general, a formulation must have a high pigment volume concentration if a good degree of dispersion is to be realised. However, milling such a formulation at high speeds could result in setting due to excessive dilatancy. The recommended impeller peripheral speed should lie between 1050 to 1350 metres per minute. The actual speed depends upon the formulation and charge volume. A general formula for rotor speed is:

$$N_r = \frac{\text{peripheral speed(metres / min)} * 31.8}{2kT} \quad 3.1$$

where: N_r is the peripheral speed of the agitator

k is a constant

3.2.1.5 Milling time

The optimum milling time is about fifteen minutes. Ten minutes of milling should suffice. Excessive milling times cause a temperature rise that lowers the mill base viscosity to an extent of shifting laminar flow to turbulent flow. Therefore breakdown of agglomerates may cease with prolonged milling times. In general, a cut-off of thirty minutes must be used to decide if the particular formulation will ever mill satisfactorily. It appears as if re-formulation of the mill base would be necessary when the degree of dispersion is poor after thirty minutes of milling(Tioxide). An alternative is to consider the use of a different mill.

3.2.2 Dispersion using a homogeniser

The homogeniser is similar in principle to a Cowles mill. The major difference is the way in which the dispersive force is generated. In a Cowles mill, the dispersive force is generated through rotational motion while this is achieved flow generated by pumping dispersion into the homogeniser. In both cases dispersion is through laminar shear forces. It appears as if it is difficult to have both laminar flow and macro-mixing occurring together in a homogeniser and in that regard a homogeniser requires pre-mixed mill base.

The homogeniser can be viewed as a constricted valve through which mill base flows resulting in breakdown of agglomerates. Homogenisers find application in the dairy and pharmaceutical industries and recently in the processing of vesiculated beads(Gous, K., 2003). A typical pressure operated laboratory scale homogeniser is presented in figure 3.4.

Figure 3.4 shows the homogeniser inlet cone supported on an arc stand. A cylinder is attached at the base of the cone. It houses the plunger, which rests on a spring. The cylinder is in turn attached to a pneumatically operated handle. The plunger and spring combination function as a non-return valve. Gous(2003) presents a detailed mechanical drawing of the homogeniser and its internals.

The most important part of the homogeniser is the spindle that supports a number of orifice grooves arranged in parallel and in stages. A drawing of a two-stage spindle and its dimensions is shown in appendix B.2. The important design variables of the homogeniser valve are the length and diameter of the grooves, the density of the grooves per stage and

the number of stages. The important variables of the homogeniser are the operating pressure drop, mill base flow rate and the supporting spring back pressure.

It appears as if the homogeniser has more variables that can be used to manipulate shear stress compared to the cowles mill. However it is apparent that most of the variables are in fact used in the manipulation of the residence time of the mill base within the homogeniser, which is equivalent to the batch processing time for the cowles mill. One of the objectives of this research would be to establish the most significant residence time manipulating variable.

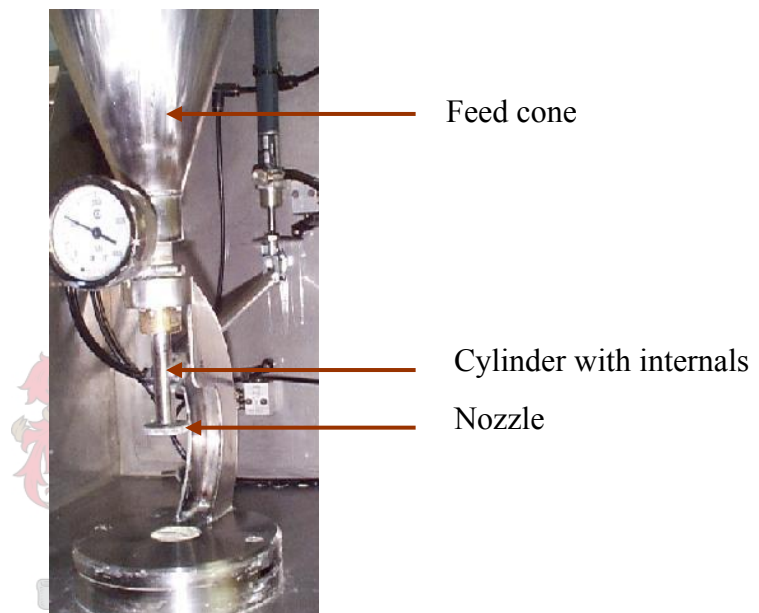


Figure 3.4 A pressure operated laboratory scale homogeniser (Gous, K., 2003)

The effects of the individual manipulated variables of the homogeniser are discussed in detail below. These can be categorised as (i) Shear control and (ii) Residence time control.

The shear control variables are those that have an impact upon shear stress and these are:

- i. Pressure drop
- ii. Spring back pressure
- iii. Plunger velocity
- iv. Groove diameter

Residence time control variables do not have an effect on the shear stress and they essentially control how much time a mill base element spends in the homogeniser valve.

The residence time control variables are: (i) groove length, (ii) Number of grooves per stage and (iii) Number of stages and the flow rate.

An alternative and extension to the number of stages appears to be the number of homogeniser passes, which can also be interpreted as the recycle ratio but it is clearly a means of controlling the residence time. The effects of these variables on the dispersion process carried out in the homogeniser are discussed below.

3.2.2.1 The effect of pressure drop on dispersion

Pressure drop is one of the variables that is used to manipulate shear stress in the homogeniser and affects the flow rate of mill base. According to Farrall, an increase in pressure drop results in finer break up of agglomerates with excessive pressure drops causing re-agglomeration (Gous, K., 2003)

3.2.2.2 The effect of groove diameter on dispersion

Groove diameter affects the pressure drop and residence time of the mill base. A large reduction in groove diameter causes a large pressure drop that in turn would result in the development of high shear forces. Therefore finer break up of agglomerates should occur.

3.2.2.3 The effect of flow velocity on dispersion

The flow velocity affects the flow rate through the homogeniser and it defines the Reynolds number. An increase in flow velocity should result in an increase on the shear stress leading to finer break up of agglomerates. The flow velocity determines the flow rate and is in turn affected by the pressure drop.

3.2.2.4 The effect of groove length

The length of the groove should not affect the shear forces acting on the mill base.

Instead it appears as groove length affects the residence time of the mill base within the groove. Therefore it must also affect the pressure drop. However pressure drop will not be significantly affected by length since the distances encountered are too small.

3.2.2.5 The effect of number of (i) grooves per stage and (ii) stages

The number of stages and grooves per stage affect the residence time of the mill base. These variables also reduce the fraction of slip or by-pass. Therefore a narrower size distribution would be expected.

3.2.2.6 The effect of viscosity on dispersion

The shear stresses developed in a fluid flow application depend on the velocity of the flow. Shear stress in laminar flow is directly proportional to the flow velocity. A thickener can be added to the dispersion to control its viscosity and this can control the shear stresses that act on the dispersion.

3.3 Methods for the evaluation of the efficiency of the dispersion process

The efficiency of dispersion is normally referred to as the degree of dispersion or the level of dispersion (Lawrence, S.G., 1981) and it ultimately describes the mean particle and size distribution of the opacifying pigment.

The major analytical techniques for evaluating the degree of dispersion are:

- i. Scanning electron microscope(SEM)
- ii. Hiding power or contrast ratio
- iii. Flocculation gradient
- iv. Rheology

Another method of evaluating the degree of dispersion is fineness of grid(FOG), (Lawrence, S.G., 1981). It is limited to particle sizes greater than 10 micrometers (Lawrence, S.G., 1981) and it is not discussed further.

The above methods for evaluating the degree of dispersion are discussed below. The efficiency of dispersion depends on: (i) Energy input into the mill, (ii) Forces of adhesion between the particles in the pigment and (iii) Interaction between pigment and the medium.

3.3.1 The scanning electron microscope

The scanning electron microscope is used to obtain micrographs of a paint film that can be used to determine the mean particle and size distribution. A block diagram of the scanning microscope is shown in figure 3.5

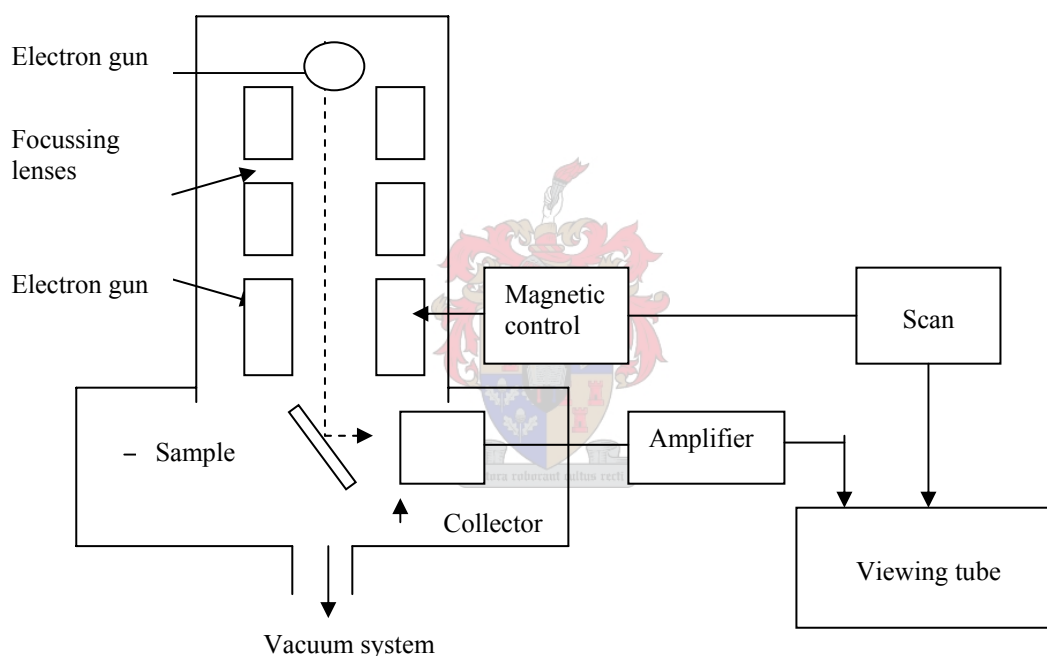


Figure 3.5 Block diagram of scanning electron microscope (Hearle, J.W.S., 1973)

The scanning electron microscope is shown in figure 3.5 and it functions as follows:

- i. Electron beam generated by electron gun
- ii. Electron beam focussed onto sample by electromagnetic lenses
- iii. Electron beam scanned across sample
- iv. Collection of image and its manipulation
- v. Display of image through viewing tube

The image is formed when electrons in the beam collide with orbital electrons in the pigment particles resulting in the ionisation of the particles(Gous, K., 2003). A secondary electron detector, detects the electrons that are ionised from the pigment particles, resulting in the formation of the image. The ionisation of electrons from the pigment particles can be amplified by coating the sample with gold under low vacuum.

3.3.1.1 Particle size analysis

The scanning electron micrograph is analysed using an image analysis software package, Analysis TM. It assigns particle size, using a click and drag technique and it requires preliminary calibration. The result of the analysis is a particle size distribution. The Analysis TM software creates a spreadsheet of the particle size distribution, which can be exported to Microsoft Excel for statistical analysis. The number averaged mean particle size \bar{a}_m , is defined in equation 3.2.

$$\bar{a}_m = \sum_{i=1}^m \frac{a_i}{m} \quad 3.2$$

Where:

a_i is the size of the i th particle measured

m is the number of particles measured

\bar{a} is the mean particle size

Each statistical analysis requires at least hundred particles. The opacity of a film of the dispersion is reviewed in the next section.

3.3.3 Opacity

The following happens when light is incident on a paint film(section 2.8):

- i. Reflection at the paint/air interface(specular reflection)
- ii. Refraction at the paint/air interface

Refraction at the paint/air interface leads to absorption and reflection (diffuse reflection) of the incident light by the pigment particles. Diffuse reflection is also referred to as back scattering and is responsible for obliterating the substrate to which a paint film is applied, thus imparting opacity to a paint film. The factors that maximise back scattering lead to the optimisation of opacity. Opacity is commonly measured through the contrast ratio.

3.3.3.1 Contrast ratio

Contrast ratio (CR) of a paint film is defined as:

$$CR = \frac{R_B}{R_W} \quad 3.3$$

where: CR is the contrast ratio

R_B is the reflectance of a pigment film applied over a black substrate

R_W is the reflectance of a pigment film applied over a white substrate

According to equation 3.3, contrast ratio is the ratio of reflectance measured over a black substrate R_B with respect to the reflectance measured over a white substrate R_W . Contrast ratio depends on film thickness x . When evaluating contrast ratio, it is necessary to state the nominal wet film thickness. This also applies to flocculation gradient as will be seen in section 3.3.3. In this research a nominal wet film thickness of 200 micrometers is used. The reflectance over the black and white substrates is measured using a colorimeter.

3.3.3.2 The contrast ratio colorimeter

A colorimeter based on a photo-electric instrument is used to measure reflectance. It basically provides contrast ratio relative to the observation that a normally sighted human observer would experience. Therefore it is calibrated with C I E illuminant C or D65, which matches a normally sighted human being. The main unit in the contrast ratio colorimeter is the integrating sphere, which is also common to the flocculation gradient monitor.

3.3.3.3 The determination of contrast ratio

The procedure for the determination of contrast ratio is laid out in point form below.

- i. Dispersion coated onto contrast ratio card using a 200 μm applicator gauge
- ii. Dry the coated contrast ratio card
- iii. Calibrate calorimeter using CIE illuminant C or D65
- iv. Place black and white portions of card into sample port and record reflectance
- v. Evaluate the contrast ratio using the measured reflectances

3.3.4 Flocculation gradient

Flocculation gradient is a measure of the degree of flocculation or agglomeration of titanium dioxide pigment in a paint film (TiO₂). Flocculation gradient and contrast ratio are complementary. Contrast ratio defines how efficient titanium dioxide pigment is, in obliterating a substrate on the basis of scattering of visible light. In contrast flocculation gradient is not based on the scattering of infra-red radiation. Since contrast ratio and flocculation gradient are based on back scattered radiation, their instrumental analysis is similar, figure 3.6.

Flocculation occurs through the collision of particles with the result that a larger particle is formed. The wavelength at, which maximum scattering occurs for agglomerates is around 2.5 μm . For contrast ratio, maximum scattering occurs at a wavelength of about 0.5 μm .

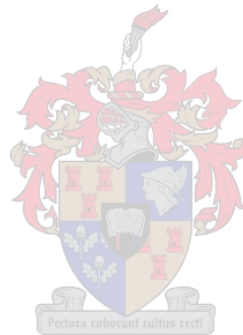
3.3.4.1 The flocculation gradient monitor

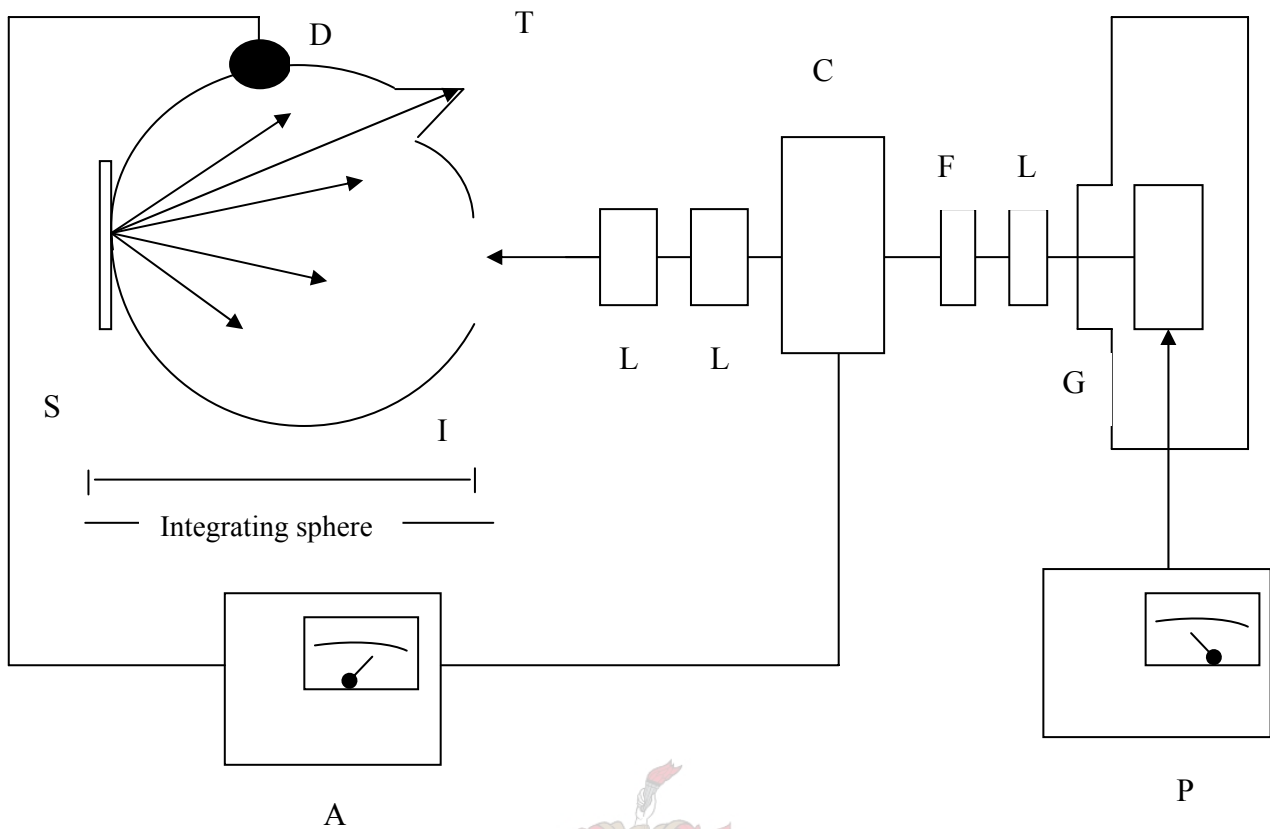
Figure 3.6 shows the components of the flocculation gradient monitor, which is used in the evaluation of flocculation gradient. The radiation source G is a tungsten filament lamp and a beam from the lamp passes through a filter, which removes all other wavelengths except that at 2.5 micrometers. The monochromatic beam from the filter is then chopped at a frequency of 400Hz. Part of the beam proceeds to the lock-in-amplifier while the rest is incident on a polyester sheet located in the integrating sphere, to which a paint film of nominal wet film thickness 24, 36, 50 or 60 micrometers has been applied. The integrating sphere shown as part of figure 3.6 performs the following:

- i. Filters specular from diffuse radiation through trap T

- ii. Detects diffuse reflection through the photo-electric transducer, D and
- iii. Transmits the detected signal to an analyser, A for calculation of reflectance

While white light is used for the measurement of contrast ratio, infra-red is used for the determination of flocculation gradient. The back scattered infra-red radiation is sensed by an infra-red detector that transduces it into a current with a corresponding potential difference. The current is transmitted to the lock-in amplifier where its frequency is compared to another current from the chopper at 400 Hz, before amplification. This procedure enables the flocculation gradient monitor to reject erroneous radiation that was detected in the integrating sphere. It is necessary to calibrate the colorimeter with a barium sulphate standard.





- | | | |
|------|------------------------|------------------------|
| Key: | A - Lock in amplifier | I - integrating sphere |
| | C - Light chopper | L - collimating lens |
| | D - infra-red detector | P - power supply |
| | F - filter | S - sample |
| | G - infra-red source | T - specular trap |

Figure 3.6 The flocculation gradient monitor

The percentage back scatter B_x is related to the potential differences according to:

$$B_x = \frac{V_F(x)}{V_B} * 100 \quad 3.4$$

Where:

$V_F(x)$ is the voltage obtained for the sample of thickness x

V_B is the voltage obtained for the barium sulphate standard

B_x is the percentage back scatter for a dry film thickness x

X is the film thickness in micrometers

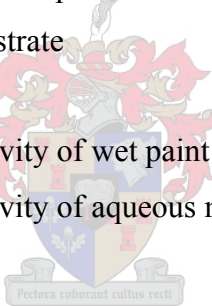
The flocculation gradient M_F is obtained as the slope of a graph of percentage back scatter B_x against the dry film thickness X.

The dry film thickness, X is calculated using the equation below(Tioxide®).

$$X = \frac{w_f * 10^4}{\frac{A_x * S_a}{\frac{100}{C_w} - \frac{(100 - S_a)}{R_s}}} \quad 3.5$$

Where :

| | | |
|-------|------------------------------------|--------------------|
| X | Dry film thickness | μm |
| w_f | Weight of dried paint film | g |
| A_x | Area of substrate | cm^2 |
| S_a | Ash content | % by weight |
| C_w | Specific gravity of wet paint | g.cm^{-3} |
| R_s | Specific gravity of aqueous medium | g.cm^{-3} |



3.3.4.2 The experimental determination of flocculation gradient

The samples required in the determination of flocculation gradient are prepared in a similar way to those for contrast ratio, however the substrate is a polyester sheet (125 μm thick). Four samples, per formulation must be coated onto the polyester sheets using applicator bars, of gauge thickness, 24, 36, 50 and 60 μm . The samples are dried before a 6 x 6 cm^2 is cut from each polyester sheet. The samples are then mounted onto a special sample holder that can fit into a sample slot located within the flocculation gradient monitor.

3.3.4.3 Sample testing and evaluation of flocculation gradient

The flocculation gradient monitor is standardized with a barium sulphate standard. Samples are then placed into the sample port where they are illuminated with infrared

radiation. The diffuse radiation from each sample is converted into percentage back scatter, which is plotted against its corresponding film thickness. The slope of this graph is equivalent to the flocculation gradient.

3.3.5 Evaluation of the rheology of the dispersion process

The evaluation of the rheology of the dispersion process is important in establishing the shear stresses required to break down agglomerates and the viscosity of the dispersion. The viscosity of the dispersion is important in the development of a correlation for particle size. Such a correlation could be important in the online prediction of contrast ratio and flocculation gradient.

3.3.5.1 Analytical determination of viscosity in the paint industry

Viscosity is determined in the paint industry using the Krebbs-Stormer viscometer.

The Krebbs-Stormer viscometer is presented in figure 3.7.

The heart of the Krebbs-Stormer viscometer is the pulley system that is operated through a load, which can be adjusted by the addition of weights into an attached pan. The pulley transmits rotational kinetic energy to a paddle that is immersed in the dispersion, which then shears the dispersion. To operate the Krebbs-Stormer viscometer, it is necessary to wind-up the pulley through a winding handle and then the pulley is locked. A standard weight is placed in the pan and the pulley unlocked. The paddle rotates provided a sufficient load that can overcome the shear stress required to cause flow was used. A rotational speed is displayed on a dial not shown in figure 3.8. If the speed is 200rpm, the load in the pan is recorded. Otherwise a trial and error procedure is used until a velocity of 200rpm is observed. The Krebbs-Stormer viscosity, corresponding to the load is then read off the associated chart.

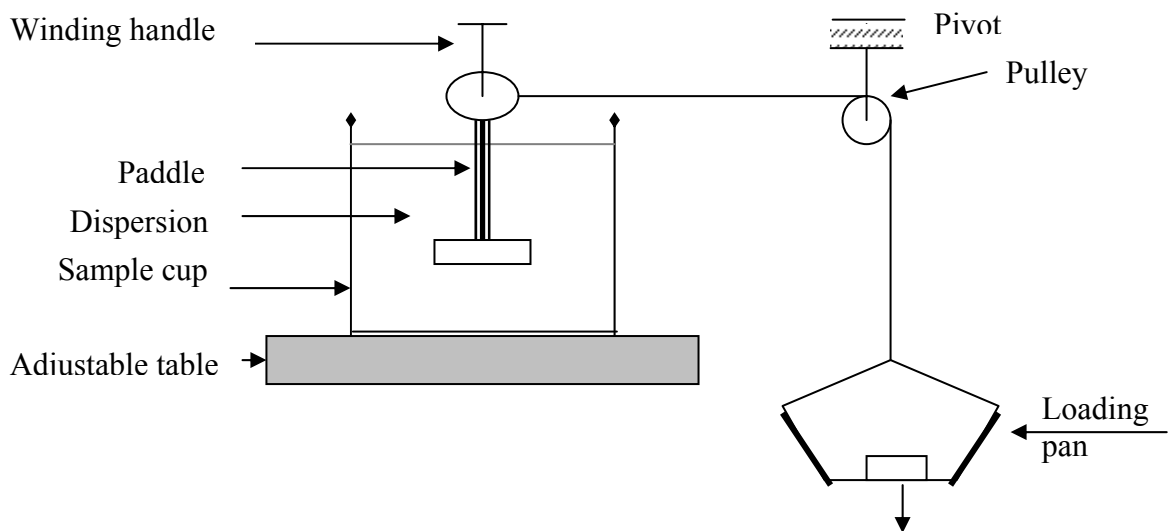
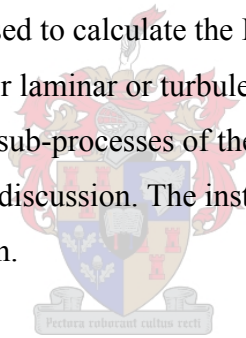


Figure 3.7 The Krebs-Stormer viscometer

The Krebs-Stormer viscosity obtained must be converted to units of pascal-seconds (Pa.s). Once this has been done, it is used to calculate the Reynolds number Re , which can be used in charactering the flow as either laminar or turbulent. The Reynolds number is important in assessing the progress of the sub-processes of the dispersion process and this will be demonstrated in the results and discussion. The instrumental analysis of flow curves is presented in the next sub-section.



3.3.5.2 Rheology of the dispersion process

Although viscosity is important in the manipulation of wetting and particle break down sub-processes, it by no means adequate in answering all the processing and formulation requirements of the dispersion process. The broad term rheology includes flow diagrams that are the subject of this section. Flow curves are required in the processing and re-formulation of dispersions.

3.3.5.2.1 The physica MCR 300 rheometer

The physica MCR 300 rheometer is used to establish the flow curves of a dispersion and it is presented in figure 3.8



Figure 3.8 The physica MCR 300 rheometer(Moolman, P.L., 2003)

The most important unit in the rheometer is the measuring system, which consists of a stationary disc and another disc or cone above it, through which a shear stress is applied. The sample is placed between the bottom disc and either the other disc(plate) or cone. The measuring systems come in different sizes, which determine the nature of measurements that can be made. In this project only the rotational measuring systems are described.

3.4.1.1 Rotational rheometric methods

The determination of flow curves depends on the rotation of the upper plate in the measuring system, which imparts shear stress onto the sample. The rotational rheometric methods used for flow analysis are:

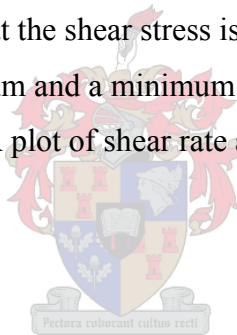
- i. Controlled shear-rate (rate of strain) tests (CSR);
- ii. Controlled shear stress tests (CSS).

3.4.1.1.1 Controlled shear rate tests (CSR) and controlled shear stress tests (CSS)

The independent variable in the shear rate test (CSR) is shear rate (rate of strain). It is programmed between two limits, while recording the corresponding shear stress. The shear rate program is either as a ramp / linear / constant change and the corresponding shear stress must be recorded in the same mode as the shear rate. The other critical aspects of the procedure are: total test and time duration for the collection of data. The data gathered are plotted to obtain a shear stress against shear rate flow curve.

The procedure for the controlled shear stress test (CSS) is similar to that for the controlled shear rate test (CSR), except that the shear stress is controlled. Therefore, shear stress is programmed between a maximum and a minimum value. Increases in the shear stress are either ramp / linear / constant. A plot of shear rate against shear stress is then made.

3.4.1.2 The evaluation of flow curves



A number of properties can be evaluated from a flow curve. They include yield stress, rate of change of viscosity and classification of flow.

3.4.1.2.1 Yield stress

Practically all particulate dispersions exhibit a yield stress. The yield stress represents the shear stress required to overcome attractive or adhesive forces between particles in agglomerates. The magnitude of the yield stress gives an indication of the minimum force required to break agglomerates during processing.

3.4.1.2.2 Rate of change of viscosity

If the purpose is to determine the change in viscosity either when shear rate or shear stress is controlled, then the slope gives the viscosity at a controlled value. If the rate of change

of viscosity needs to be controlled, then it appears as if this gives information on the choice in surfactant that must be made (Moolman, P.L., 2003).

3.4.1.3 Classification of flow

Flow curves were classified in terms of the shape of the curve obtained as described in section 2.9.1.1 The flow curve obtained must be classified as any of the following: Bingham flow, plastic flow, pseudo-plastic flow, Newtonian flow, dilatant flow or yield limited dilatant flow. All forms of plastic flow will not regain the original state once the action of shear rate or shear stress is stopped. This information should be important in the processing of a dispersion, since it gives an indication of the nature of the surfactant that must be used. For dilatant flow, it is well known that the pigment loading would be too high, thus causing an increase in viscosity with either controlled shear rate or controlled shear strain. In that case, it is necessary to reduce the pigment loading or otherwise processing at a lower shear rate would be required.



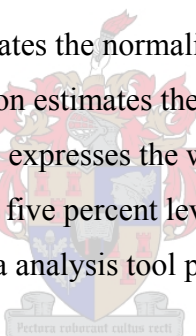
3.5 Repeatability of analytical methods

This section evaluates the performance of the analytical methods that were used to analyse the experimental data. The repeatability of mean particle size measurements for sub-micrometer-sized particles (titanium dioxide) is presented, since size is seen as the most critical property that defines quality properties such as contrast ratio and flocculation gradient.

3.5.1 Analysis of particle size and particle size distribution

Particle size analysis is carried out in order to obtain the mean particle size and distribution. It is necessary to evaluate the reliability of the mean particle size. Estimating the standard error, standard deviation and the confidence level does this.

The standard error basically estimates the normalised error associated with the mean particle size. The standard deviation estimates the absolute error of finding the mean particle size. The confidence level expresses the width of locating the mean with a certain probability. In this case the ninety five percent level is used. The statistical analyses in this section were carried out using data analysis tool pack in Microsoft Excel.



The evaluation of particle size and particle size distribution was achieved by preparing two titanium dioxide pigment dispersions of TR 93 using a homogeniser. These dispersions are denoted A and B. The scanning electron micrograph of sample A is presented in Figure 3.9 below and its particle size and distribution are evaluated first.

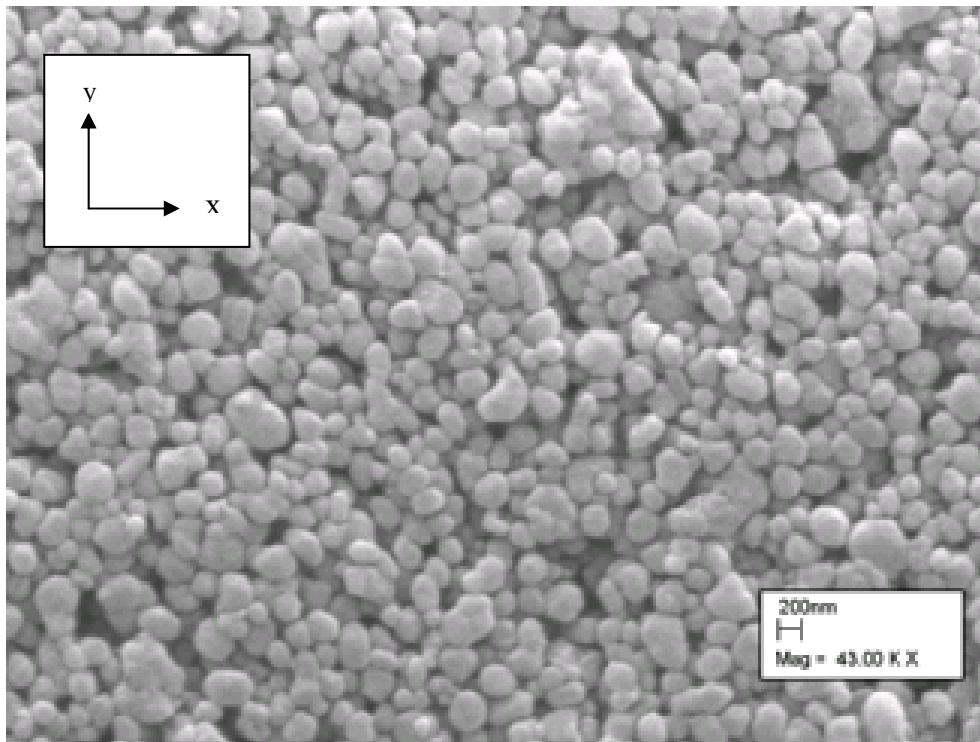


Figure 3.9 The scanning electron micrograph of sample A

The Analysis™ software can analyse particle size in either the vertical (y) or the horizontal (x) directions. The horizontal direction was chosen for the analysis of this micrograph. Such a choice depends upon the sample and, in this case, observing that the particles appear to be circular led to this decision. Therefore the particles are approximately symmetrical and either x or y directions can be used.

As part of the project scope, at least one hundred particles must be analysed. One hundred particles were seen as the minimum number of representative particles and this section serves to explore this assumption.

Almost all the particles of sample A were analysed using Analysis™ software. The particle sizes were then partitioned into consecutive sets of a hundred. The mean particle size (nm) of each of these sets is shown in the table below.

Table 3.1 The reproducibility of mean particle size based on the same sample size

| Particle set | Mean size(nm) | Standard error | Standard deviation(nm) | Confidence interval(95%),[nm] |
|--------------|---------------|----------------|------------------------|-------------------------------|
| 1st | 383.0 | 11.68 | 116.80 | 23.18 |
| 2nd | 361.9 | 10.39 | 103.92 | 20.62 |
| 3rd | 382.0 | 12.01 | 120.08 | 23.83 |
| 4th | 392.7 | 12.52 | 125.17 | 24.84 |

The results of the statistical analysis show that the second set is statistically different to the other sets. Otherwise there is good agreement between the remainder of the sets. If we consider sets 1, 3 and 4 as being representative, then the ranges of the statistical descriptors are:

- i. Standard error(11.68 to 12.52)
- ii. Standard deviation(116.8nm to 125.17nm)
- iii. Confidence level(95%),(23.18nm to 24.84nm)

The standard error can be considered to be significant, meaning that the reliability is not that good. The confidence interval at the ninety five percent level is reasonably good meaning that the mean can be located fairly accurately.

The variability in the statistical analysis based on counting an equal number of particles in different portions of the scanning electron micrograph can be accounted for. The difference in the mean particle sizes observed in different regions is due to:

- i. Non-spherical particles;
- ii. Random analytical errors.

Analyst training would minimise random analytical errors. Counting all the particles, which is impractical in terms of time, can eliminate the first reason.

The particle size distributions for sample A based on counting hundred particles from different portions of the micrograph are shown below.

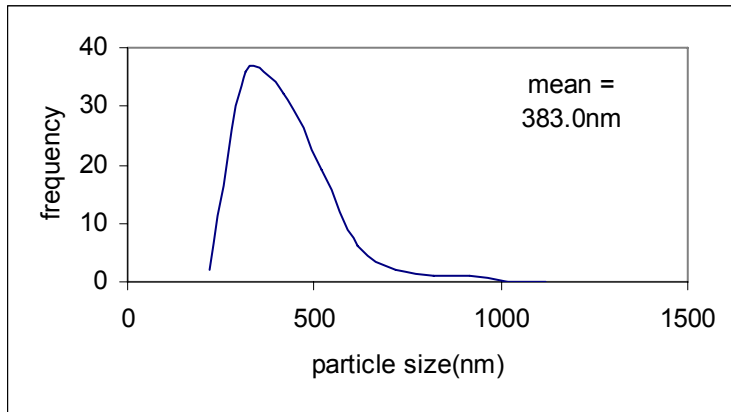


Figure 3.10 Particle size distribution for first hundred particles

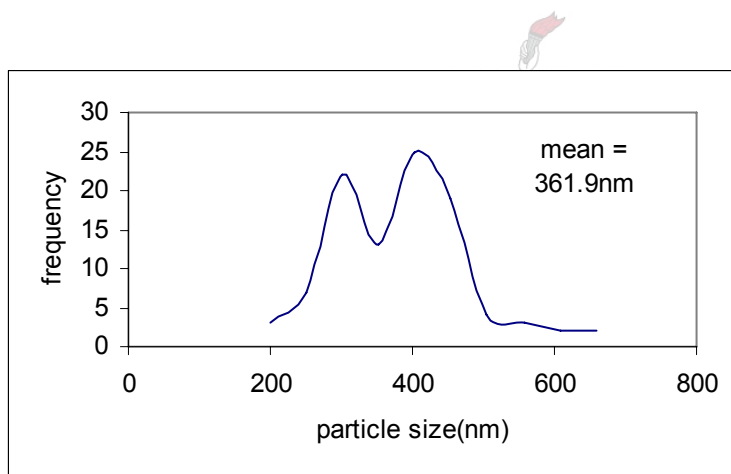


Figure 3.11 Particle size distribution for first two hundred particles

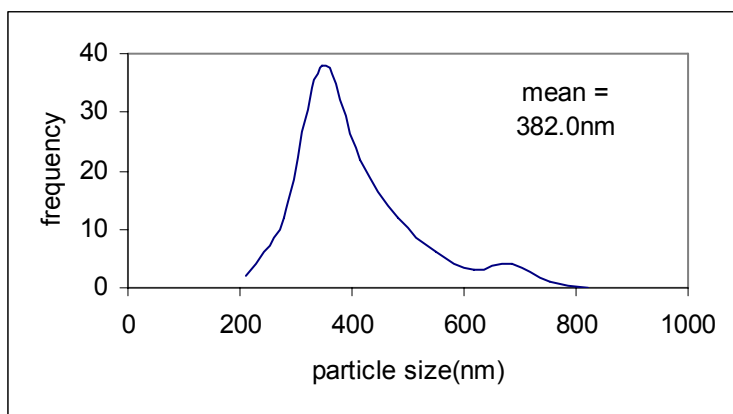


Figure 3.12 Particle size distribution for the first four hundred particles.

A cumulative approach based on successively increasing the sample size by hundred particles starting with an initial hundred was also investigated.

The mean particle size obtained through this cumulative approach in which the sample size becomes progressively bigger is shown in the table below.

Table 3.2 The reproducibility of mean particle size based on different sample sizes

| Cumulative set | Mean size(nm) | Standard error | Standard deviation(nm) | Confidence level(95%),(nm) |
|----------------|---------------|----------------|------------------------|----------------------------|
| 100 | 383.0 | 11.49 | 114.87 | 22.79 |
| 200 | 372.4 | 10.54 | 105.43 | 20.92 |
| 300 | 375.6 | 10.76 | 107.17 | 21.35 |
| 400 | 379.9 | 11.26 | 110.76 | 22.34 |

The statistical analysis of particle size based on increasing the number of particles counted is shown in table 3.2. The ranges of the statistical descriptors is shown below:

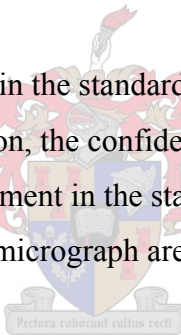
- i. Mean particle size(372.4nm to 383.0nm)
- ii. Standard error(10.54 to 11.26)
- iii. Standard deviation(105.43 to 114.87nm)
- iv. 95percent confidence level(20.92nm to 22.79nm)

The standard deviation is a measure of the width of the particle size distribution. When used in particle size analysis, the standard deviation does not give an indication of the error in the mean particle size. The standard error, described below gives a measure of the error in the mean particle size.

The standard error for the different sample size is in the range 10.54 to 11.26. Since the difference between these values of standard errors is small, it can be concluded that the error in the mean particle size is not significantly affected by sample size.

The confidence level tells us the range in which we can locate the central moment of a distribution for a stated probability. From table 3.2 and item (iv) just below the table, the confidence level is in the range 20.92nm to 22.79nm. This range is small and it means that there is no statistical difference between a sample size of hundred or four hundred particles. Therefore we can use a sample size of hundred particles for our particle size analysis.

There is no definite improvement in the standard error or standard deviation when the sample size is increased. In addition, the confidence level does not change that significantly. The lack of improvement in the statistical descriptors indicates that the particles in the scanning electron micrograph are not uniformly distributed.



When the method of counting only hundred particles and the cumulative approach are compared, it can be seen that:

- i. the two methods give similar results;
- ii. increasing the size of particles counted results in marginal improvements.

From the discussion in this section, the experimental determination of mean particle size used a sample of hundred particles from the scanning electron micrographs obtained.

3.6 Scale-up of dispersion vessels

Scale up of dispersion mills is broken down according to the type of mill used (cowles mill or homogeniser).

3.6.1 Scale-up of agitated vessels through similitude

Agitated vessels can be scaled using dimensionless numbers based on similar behaviour in the two units (Coulson and Richardson, 1996). Similitude is classified into:

- i. Geometric similarity
- ii. Kinematic similarity
- iii. Dynamic similarity

Figure 3.13, shows the relationships between the dimensions of an agitated vessel required in the definition of similitude.

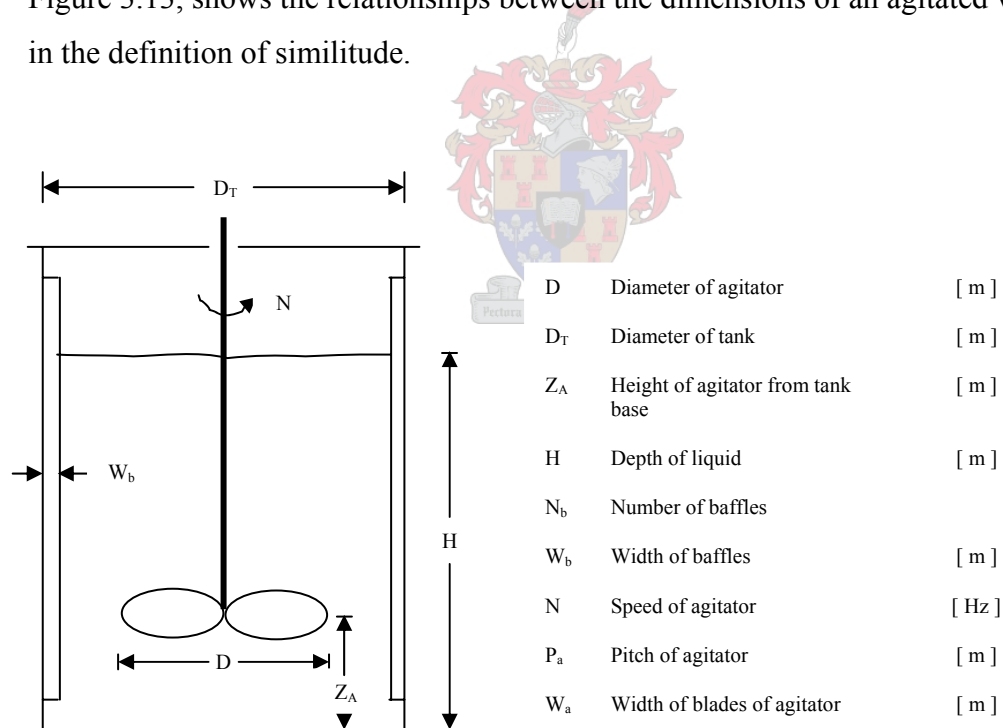


Figure 3.13 The dimensions of an agitated vessel

3.6.1.1 Geometrical similarity

Two dispersive systems are said to be geometrically similar if all their counterpart length dimensions exhibit a constant ratio. The geometrical ratios are shown below.

$$\frac{D_T}{D_i} \quad ; \quad \frac{Z_A}{D_i} \quad ; \quad \frac{W_b}{D_i} \quad ; \quad \frac{W_a}{D_i} \quad ; \quad \frac{H}{D_i}$$

This implies that the corresponding ratios must be equal in the two vessels on scale-up.

3.6.1.2 Kinematic similarity

Kinematic similarity exists between two vessels when the velocities at counterpart positions within the two vessels have a constant ratio, provided the dispersive systems are geometrically similar. It is important to note that the condition of geometrical similarity is necessary in order to define kinematic similarity.

3.6.1.3 Dynamic similarity

Dynamic similarity occurs in two dispersive systems if forces at counterpart locations have a constant ratio on condition that the two systems are geometrically similar. The condition of geometrical similarity is important just like in the case of kinematic similarity.

If the two systems being compared are denoted 1 and 2, then dynamic similarity mathematically be defined in two ways as:

$$\frac{F_{a1}}{F_{a2}} = \frac{F_{b1}}{F_{b2}} = \frac{F_{c1}}{F_{c2}} = \dots = \quad \quad \quad 3.6$$

Dynamic similarity can also be defined in terms of dimensionless group. The dimensionless groups that arise from geometric similarity are Reynolds, Froude and Weber numbers (Coulson and Richardson I). For two dynamically similar vessels the corresponding dimensionless groups must be the same.

The method of similitude is difficult to use in principle because of its strict requirement for corresponding ratios to be equal. Modelling is a convenient method that can be used for scale-up.

3.6.2 Model based approach for scale up

The scale-up of a cowles mill can be achieved once the model that describes the change in the mean particle size has been established. Terblanche(2003) established that the significant variables during emulsification of vesiculated beads are:

- i. Agitator speed.
- ii. Impeller diameter.
- iii. Impeller/tank diameter ratio.

The work of Terblanche established that impeller diameter had a more significant impact upon the emulsification process(2003). According to Klein et al(1996), the stability of a dispersion during processing can be determined by operating the mill above a minimum speed. The minimum speed required to prevent coagulation in a cowles mill given by Grossman(1980):

$$N_{\min} = 0.2 \left(\frac{D_T}{D_i} \right) D_i^{-0.765} \left(\frac{\Delta \rho g}{\eta_c} \right)^{0.294} \left(\frac{\gamma}{\rho_c} \right)^{0.353} (1 - \phi_d)^{1.37} (1 + 3.5)^{0.59} \left(\frac{h}{D_T} \right)^{0.4} \quad 3.7$$

Where:

| | |
|---------------|--|
| N_{\min} | Minimum agitator speed(revolutions/s) |
| D_T | Vessel diameter(m) |
| D_i | Impeller diameter(m) |
| $\Delta \rho$ | Density difference between monomer and continuous phase (kg/m ³) |
| G | Acceleration due to gravity(m/s ³) |
| η_c | Viscosity of the continuous phase |
| γ | Interfacial tension (mN/m) |
| ρ_c | Density of continuous phase |
| Φ_d | Volume fraction of dispersed phase(m ³ /m ³) |
| h | Distance of impeller from the bottom of the tank(m) |

The above model was applied to emulsification and there are some terms that would probably not exist when considering the pigment dispersion process. For instance the second bracketed term in equation 3.7 should assume a value of one since. This is due to the fact that it refers to two different fluids for emulsion but it is assumed that there is only

one fluid during the dispersion process. The volume fraction becomes the pigment volume fraction if we consider the application of equation 3.7 in pigment dispersion.

Equation 3.7 can be simplified if it is assumed that geometric similarity applies on scale-up and that the properties of the fluids remain constant. This leads to the simplified equation(Terblanche, J.C., 2003):

$$D_i^{0.765} N_{\min} = \text{constant} \quad 3.8$$

The above model can be made to apply to practical situations, which are non-geometrically similar. In that case it simplifies to (Terblanche, J.C., 2003):

$$\bar{a}_n = kN^w D_i^x \left(\frac{D_i}{D_T}\right)^y \quad 3.9$$

Where:

- \bar{a} Mean particle size based on the standard emulsification time(μm)
- K Constant
- w,x,y Model exponents



The standard emulsification time could be equivalent to the minimum time required to obtain appreciable particle break down. When values of the mean particle size and the explanatory variables in equation 3.9 are available the exponents can then be estimated. A model similar to equation 3.9 can be constructed where time is a variable.

The model of equation 3.9 was applied to a 5 and a 20 litre agitated vessel where agitator speed and diameter were varied individually. It was found that it could predict particle size reasonably well(Terblanche, J.C., 2003). The same model was applied to a pilot plant of a large size and was found to perform satisfactorily when agitator speed or diameter was varied(Terblanche, J.C., 2003). However, it was observed that agitator speed had a greater impact on particle size reduction(Terblanche, J.C., 2003).

3.6.3 Scale-up of the homogeniser

The homogeniser is scaled-up on the basis of geometrical similarity. The basic length dimensions of the homogeniser are shown in figure 3.14.

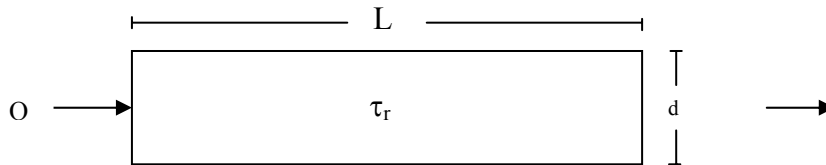


Figure 3.14 The length dimensions, residence time and flow-rate of a homogeniser

Where: τ_r is the residence time

L is the length of the plunger

The model in figure 3.14 is that for the plunger, which is shown in greater detail in appendix B.2. The length of the plunger is L while its diameter is d . Dispersion flows through the homogeniser at a volumetric flow-rate Q and is processed for a residence time τ_r .

The requirement for scale-up of the homogeniser is geometric similarity, which requires the aspect ratio (L/d) in the laboratory scale to be equal to that in the pilot scale (Gous, K., 2003). The volumetric flow-rate on scale-up is obtained by assuming that the residence times in the two units are the same. The alternative scale-up method for the homogeniser is to use a number of smaller plungers in parallel.

Chapter 4. Materials and Methods

This chapter describes the materials and methods that were used to carry out the aims of this project. A description of the materials is given first followed by the methods.

4.1 Materials

The important materials, their characterisation and physical properties that were used are presented in Table 4.1 below.

Table 4.1 Properties and classification of raw materials

| Raw material | Classification | SG |
|-------------------|----------------------|-------|
| Foamaster VL | Defoamer | 0.890 |
| Acticide HF | Bactericide | 1.025 |
| Attagel 50 | Clay thickener | 2.360 |
| AMP 95 | Ph modifier / alkali | 0.940 |
| Alcosperse 700 | Surfactant | 1.100 |
| Kulu 2 | Extender | 2.700 |
| Kulu 5 | Extender | 2.700 |
| Steabrite Talc | Extender | 1.100 |
| Steopac Talc | Extender | 1.000 |
| RCR 40 | Opacifier | 4.052 |
| TR 93 | Opacifier | 4.000 |
| Titanium TR 93 | Opacifier | 4.000 |
| Cellosize QP 4400 | Cellulose thickener | 1.390 |
| Propylene Glycol | Antifreeze | 1.038 |
| Water | Diluent / vehicle | 1.000 |

Where: SG is the specific gravity

The above materials were used in a formulation that was used to prepare the dispersions that were processed. These formulations are described in detail in the relevant results and discussion sections.

4.2 Methods

The initial focus of this section (4.2) is devoted to planning in order to address the following issues:

- i. How many experimental runs to implement;
- ii. Strategy used to run an experiment;
- iii. Evaluation of the effect of manipulated variables.

4.2.1 Experimental design and philosophy

In section 4.2.2 it was observed that the number of experiments that are required to investigate the effect of manipulated variables on the efficiency of dispersion depended on whether the pigment was an opacifier or an extender. For opacifiers, the attractive Van der Waals forces have a significant effect on both dispersion and stability, while their role is insignificant for extenders. Section 4.2.2 thus recommended a factorial design for opacifiers and relaxed this for extenders.

Section 4.2.1 clearly identified the machine variables that are used to manipulate shear stress in the Cowles disperser and in the homogeniser. These variables are different in the two mills. Therefore the experimental designs for the two mills are different. The objective in this section is to determine the essential number of experiments that must be carried out for the Cowles mill and the homogeniser.

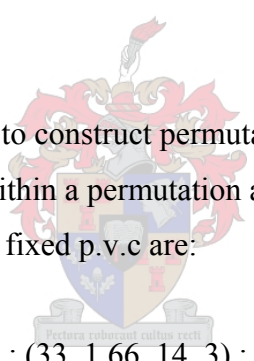
Three levels were chosen according to the available experimental equipment and their range of application and formulation. The next step in the procedure was to find all the possible permutations of the levels from different variables. The experimental designs for the Cowles mill and the homogeniser are now discussed.

4.31 Experimental design for the cowles mill

The significant shear stress manipulating variables of the cowles mill were reviewed in section 3.2.1 and these are: impeller speed, charge depth, impeller location and tank: impeller diameter ratio.

The base / medium levels that were chosen for each variable shown in figure 4.2 are: impeller speed (36Hz), impeller location (3cm), charge depth (14cm) and tank: impeller ratio (2.00). The levels of each variable are now discussed. The motor speed is very flexible and can be varied between 0 and 50 Hertz. Therefore it is possible to define low, medium and high levels for the impeller speed. Thus the levels for the impeller speed is the set {32.4, 36.0, 39.6 Hz}. Two Cowles blades were available and these resulted in tank: impeller ratio set, {1.66 and 2.00}. For charge depth, the design levels are {12, 14.0cm}. The only practical impeller location was 3cm. The tree in table Table 4.2 shows all possible design permutations of levels.

As an example table 4.2, is used to construct permutations that include the low frequency value. The sequence of levels within a permutation are (frequency, ratio, charge depth, location). The permutations at a fixed p.v.c are:

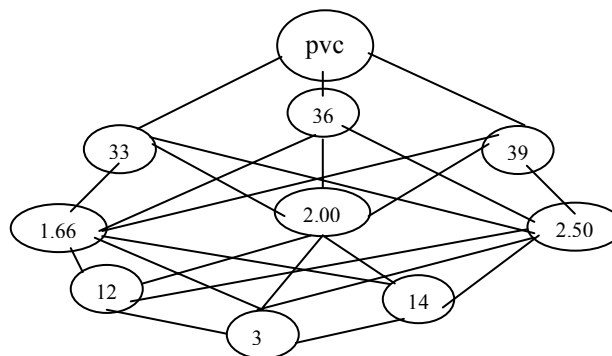


(33, 1.66, 12, 3) ; (33, 1.66, 14, 3) ; (33, 1.66, 16, 3)
(33, 2.00, 12,3) ; (33, 2.00, 14, 3) ; (33, 2.00, 16, 3)
(33, 2.50, 12, 3) ; (33, 2.50, 14, 3) ; (33, 2.50, 16, 3)

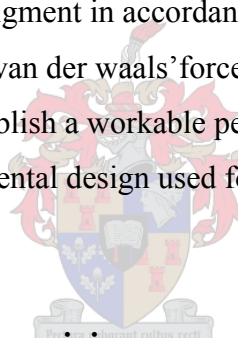
The tree in table 4.2 shows that for each frequency level, there are nine possible permutations that involve it. There are three levels of frequency, thus leading to a total of twenty-seven permutations at a fixed formulation. There are two titanium dioxide pigments, which are regarded as two different formulations and it leads to a total of fifty four experimental runs. If the number of levels of charge dept is reduced from three to two, the number of experimental runs becomes thirty-six, which was adopted since it is manageable.

Table 4.2 Level permutation tree for shear manipulating variables in the dispersion of titanium dioxide pigments using a Cowles disperser

| Stress manipulating variable | Low value | Medium value | High value | Units |
|------------------------------|-----------|--------------|------------|----------|
| | - 1 | 0 | + 1 | |
| Formulation | | | | %(ml/ml) |
| Frequency (speed) | | | | Hz |
| Tank: Impeller ratio | | | | |
| Charge depth | | | | cm |
| Impeller location | | | | cm |



The number of experiments that need to be performed for four different extender pigments is strictly four runs, one for each pigment in accordance with our assumption of the insignificant effect of attractive van der waals' forces on the dispersion process. A trial and error procedure was used to establish a workable permutation for each extender. The next paragraph describes the experimental design used for the dispersion of a titanium dioxide dispersion using a homogeniser.



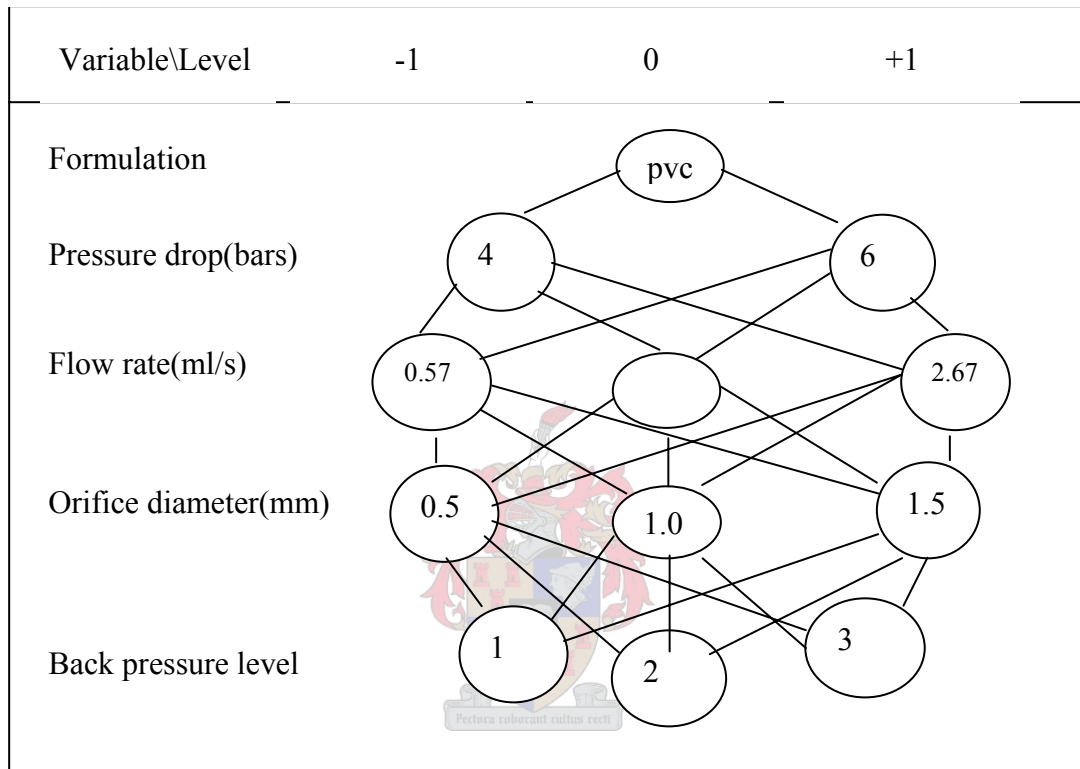
4.3.2 Experimental design for the homogeniser

The use of the homogeniser was justified for titanium dioxide only on the basis of the significance of flocculation / agglomeration. Section 2.8 reviewed the effect of particle size on the opacity and flocculation gradient of titanium dioxide dispersions and it was established that its opacity could be increased through the reduction of flocculation. Thus it is justifiable to investigate the potential of the homogeniser in reducing flocculation. In that case a detailed experimental design for the dispersion of titanium dioxide in a homogeniser must be attempted. Only one design is required, since the best pigment (formulation) would have been selected, after the analysis and evaluation of the dispersion process carried out using the cowles mill. The next paragraph describes how the homogeniser was investigated.

The shear stress manipulating variables for the homogeniser are: pressure drop, flow rate, orifice diameter, back pressure and number of stages (kept constant at a value of two). The

effective number of manipulated variables was thus four. The total possible permutations shown in Table 4.3 is 27 for each pressure. Since there are two pressures the total number of experimental runs is 27 x 2 or fifty four. Table 4.3 shows the possible combinations of designs that can be implemented with the homogeniser.

Table 4.3 Level permutation tree for shear manipulating variables in the dispersion process of the optimum titanium dioxide dispersion using a homogeniser



The establishment of permutations that need to be considered have been described for both the Cowles disperser and the homogeniser, using a detailed experimental design. Only the dispersion of titanium dioxide warrants a detailed design of experiments since particles of titanium dioxide are colloidal. As a result the attractive van der Waals potential energy for titanium dioxide is significant.

4.3.3 Rheology of the dispersion process

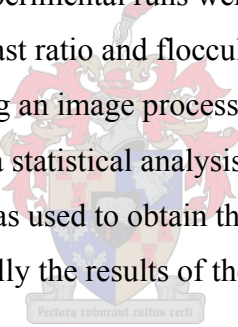
The effect of agitator speed and level of dispersant on the rheology of the dispersion process was investigated. Two agitator speed levels of 30Hz and 35Hz were used while the dispersant level was reduced by fifty percent. The agitator speed used was 30Hz when the level of dispersant was reduced.

4.4 Experiments that were carried out with Cowles and Homogeniser mills

The detailed designs provided above were trimmed to a few variables when it was realised that there was no significant difference in the levels. Several experiments with the levels suggested in the experimental design were carried out. When they were analysed, it became apparent that they did not show significant response. As a result these analyses are not reported in this project. A few of the variables are analysed to show the typical response that would be obtained. One of the recommendations is re-design the experiment used such that the variables used show significant differences in size.

4.5 Analysis of Cowles/homogeniser experimental runs

Samples obtained during the experimental runs were analysed for their scanning electron micrographs, flow curves, contrast ratio and flocculation gradients. The scanning electron micrographs were analysed using an image processor in order to obtain particle sizes. The particle sizes were subjected to a statistical analysis using a software package in Microsoft Excel. The statistical analysis was used to obtain the mean particle size and particle size distribution of the samples. Finally the results of the analysis were interpreted in light of the theory of the dispersion process.

A faint watermark of a university crest is visible in the background of the text. The crest features a shield with various symbols, topped with a crown and a crest. Below the shield is a motto scroll with the Latin text "Pectora roburant cultus recti".

Chapter 5 Results and Discussion – Dispersion of Titanium Dioxide

This section evaluates the effects of:

- i. Agitator speed on the dispersion process;
- ii. Agitator diameter on the dispersion process.

The initial focus is on the effect of the process on the mean particle size and size distribution in terms of the mechanism that was proposed. The changes in the mean particle size distribution are then used to qualitatively predict the contrast ratio and flocculation gradient expected of the dispersion. Finally, the two effects above are compared in terms of significance to development of opacity.

5.1 Results and discussion – dispersion in a Cowles mill

Dispersion of titanium dioxide in a Cowles mill was carried out using the formulation specified in appendix A2. This formulation was used to make five-kilogram batches and the mill configurations supplied in appendix B. The designs that were used for the dispersion of titanium dioxide in particular are described in appendix B.1.1.1.

The pigment volume concentration (PVC) is 37.2 percent and it is calculated from knowledge of the total volume of the dispersion and the mass of the pigment in the formulation as shown below.

| | |
|------------------------------|--------------------------------------|
| Mass of titanium dioxide: | 5.211kg |
| Density of titanium dioxide: | 4.000kg/litre |
| Volume of titanium dioxide: | $(5.211/4.000)$ litres or 1.30litres |
| Total volume of dispersion: | 3.500litres |

$$P.V.C = \frac{\text{Total volume occupied by pigment particles}}{\text{Total volume of the dispersion}} * 100\%$$

$$\text{Total volume occupied by pigment particles} = \frac{\text{mass of pigment particles}}{\text{density of pigment}}$$

$$P.V.C = \left(\frac{\left(\frac{5.211}{4.0} \right)}{3.5} \right) * 100\% = 37.2\%$$

The following designs presented in Table 5.1 were used for producing the titanium dioxide TR 93 dispersion.

Table 5.1 Processing conditions for production of titanium dioxide dispersions

| Design | D(m) | N(Hz) | % Alcosperse |
|--------|------|-------|--------------|
| 1 | 0.10 | 30 | 1.37 |
| 2 | 0.10 | 35 | 1.37 |
| 3 | 0.12 | 30 | 1.37 |
| 4 | 0.12 | 35 | 1.37 |

Samples were obtained from the mill after ten, fifteen, twenty and thirty minutes for each design that was investigated. The temperature, viscosity, contrast ratio and flocculation gradient of each sample were measured.

Viscosity was measured using the Krebbs-Stormer viscometer. Unfortunately, the Krebbs-Stormer viscosity does is carried out at a shear rate of $3.33s^{-1}$, which does not correspond to the shear rate in the Cowles mill. The viscosity of the dispersion at the shear rate that corresponds with the process conditions is important in the calculation of the Reynolds number. In order to obtain an idea of the shearing occurring in the Cowles mill, it was decided to use the speed and dimensions of the Krebbs-Stormer viscometer. An illustrative calculation is provided below for batch 2 after ten minutes of dispersion in the Cowles mill.

The spindle used in the Krebbs-Stormer viscometer had a width and a diameter of 0.5cm and 6.0cm respectively. This is equivalent to an area of $3cm^2$. The mass used to achieve a

spindle speed of 200rpm was 330g and it is equivalent to a gravitational force of 3.23N. This force is exerted onto the dispersion through the spindle area calculated above. The area and the force can be used to calculate the shear stress as shown below.

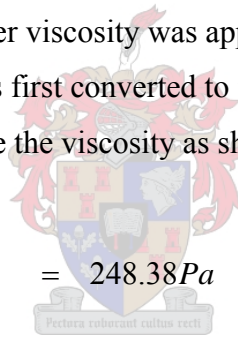
$$\tau = \frac{3.23N}{3 * 10^{-4} m^2} = 10762.4Pa$$

The spindle speed of 200rpm corresponds to the shear rate calculated below.

$$\dot{\gamma} = 13 * (200/60)s^{-1} = 43.33s^{-1}$$

The factor 13 used in the calculation above is an approximation used to convert impeller speeds to shear rates(Coulson and Richardson, 1996). The value 13 is an empirical constant used to convert measurements of impeller speeds to shear rates. The spindle used in the determination of Krebbs-Stormer viscosity was approximated to be equivalent to an impeller. The spindle speed was first converted to its SI equivalent. The shear rate and shear stress are used to calculate the viscosity as shown below.

$$\eta = \frac{10762.40Pa}{43.33s^{-1}} = 248.38Pa$$



The viscosity of the dispersion for batch 2 after fifteen minutes of processing is 249.28Pa.s. The Reynolds number Re for the first design is estimated from:

$$Re = \frac{\rho D^2 N}{\eta} \tag{5.2}$$

The Reynolds number for the flow in the Krebbs-Stormer viscometer is calculated as shown below. The density of the titanium dioxide dispersion is 2000kg.m⁻³. The diameter of the spindle was 6cm.

$$Re = \frac{2000kg.m^{-3} * (0.06m)^2 * (200rev/60s)}{248.38Pa} = 0.0966$$

The calculations shown above were compiled for batch 2 in table 5.2 below

Table 5.2 Shear stress, viscosity and Reynolds numbers for titanium dioxide dispersions of batch 2

| | | | | |
|----------------------------------|----------|---------|---------|---------|
| Time(min) | 10 | 15 | 20 | 30 |
| Mass(kg) | 0.330 | 0.305 | 0.280 | 0.250 |
| F(N) | 3.23 | 2.99 | 2.74 | 2.45 |
| Shear stress(N.m ⁻²) | 10762.40 | 9966.66 | 9133.33 | 8166.66 |
| Viscosity(Pa.s) | 248.38 | 230.02 | 210.79 | 188.46 |
| Re | 0.097 | 0.104 | 0.114 | 0.127 |
| Viscosity(KU) | 98 | 95 | 93 | 89 |

The dimensions of the Krebbs-Stormer viscometer are shown below:

| | |
|------------------------------|-------------------------|
| Breadth | 0.5 10cm |
| Diameter | 6 cm |
| Area | 3.00E-04 m ² |
| N _r | 200 rpm |
| Shear rate(s ⁻¹) | 43.33 |
| Density | 2000 kg.m ⁻³ |



Similar calculations for evaluating the flow conditions in the mill are done for the other dispersion times and for other batches. Appendix G.1 shows the flow conditions for all the sampling times and flow conditions for the dispersion process of titanium dioxide in a Cowles mill. The flow conditions in the Krebbs-Stormer viscometer will be assumed to correspond to the process conditions in the Cowles mill.

In conclusion, the Krebbs-Stormer viscosity, shear rate used for determining the Krebbs-Stormer viscosity and the Reynolds number do not represent the dispersion process. They are misleading and also apply at a single point rather than for the whole system. As a result

they do not give the best representation of the changes in particle size that occur during the dispersion process. In chapter 9, it will be shown how flow curves relate to the particle size changes occurring during the dispersion process.

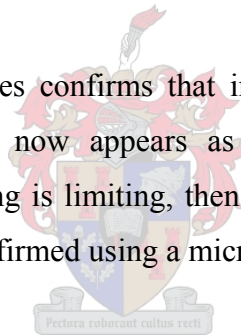
5.1.1 Evaluation of design 1

The micrograph of the process for ten minutes is shown below.

5.1.1.2 Ten minutes of processing

The micrograph for ten minutes of processing is shown Figure 5.1. It shows a variety of particle shapes ranging from oval to spherical. It shows that the dispersion still contains a sizeable fraction of agglomerates, which will be confirmed, using its particle size distribution. The mean particle size of the dispersion is 413.6nm.

The appearance of agglomerates confirms that inadequate wetting and minimal particle breakdown have occurred. It now appears as if the wetting agent does not cause instantaneous wetting. If wetting is limiting, then increased processing time could lead to overcoming it. This can be confirmed using a micrograph for longer processing time.



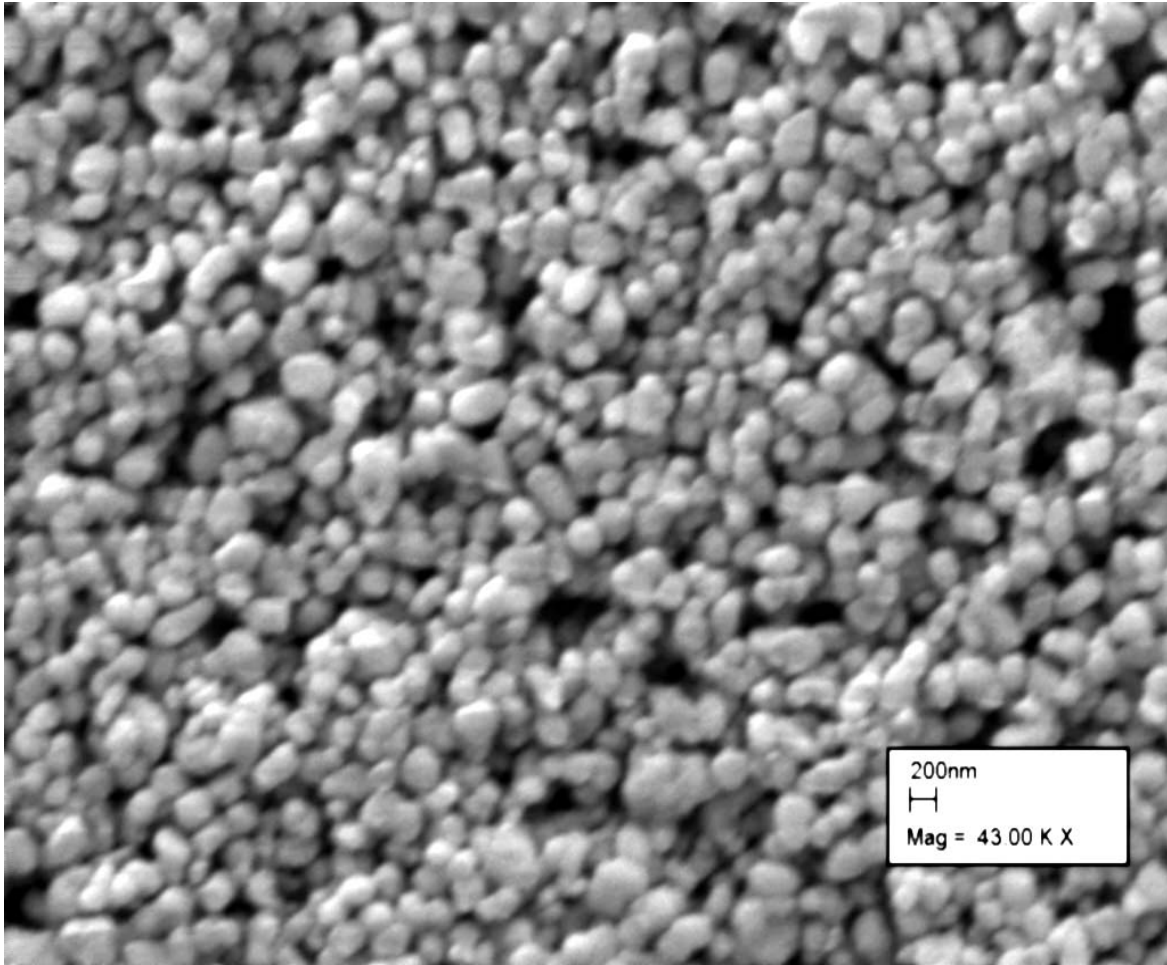


Figure 5.1 The micrograph for design 1 after ten minutes of processing with mean 413.6nm

Since the process was not operated for a long enough time, it appears as if the particles did not wet adequately. The particle size distribution for the above micrograph shown in Figure 5.1 is presented in Figure 5.2.

The particle size distribution above is bimodal or it can be assumed to have a broad upper tail. The broad tail in the distribution shows that there are some particles at large sizes that are stable for the processing conditions used. This could confirm that the particles in the dispersion have not wetted adequately.

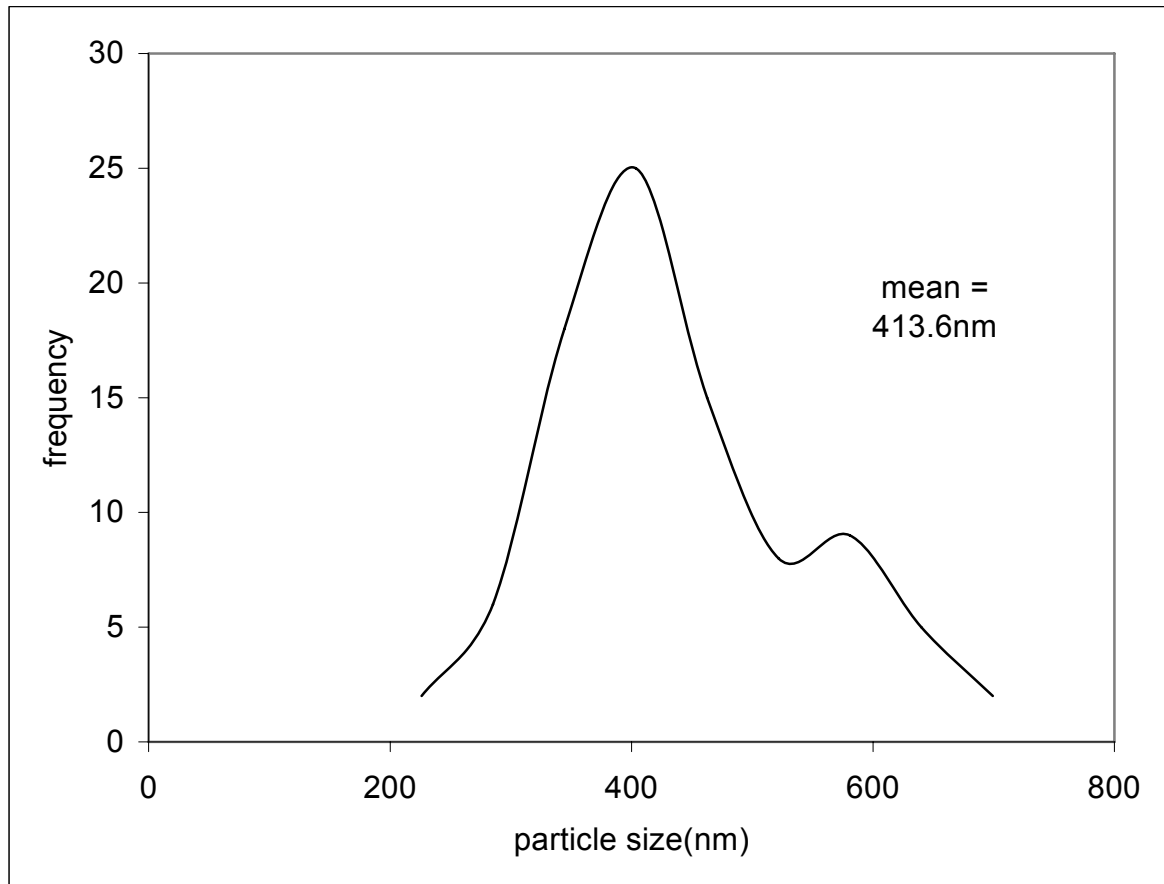


Figure 5.2 The particle size distribution after ten minutes of processing

5.1.1.3 Fifteen minutes of processing

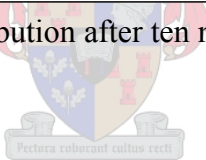


Figure 5.3 is the micrograph for the process after fifteen minutes of operation. The micrograph shows a variety of particle shapes from oval to spherical. The dispersion still contains some agglomerates and the mean particle size is now 388.1nm. This confirms that significant particle size reduction occurred between ten and fifteen minutes of operation. In order for that to happen, there must have been a significant improvement in wetting of particles.

Figure 5.4 shows the particle size distribution for the process after fifteen minutes. The broad tail has diminished in size and this indicates that particle break-down occurred between ten and fifteen minutes. Therefore wetting limitations must have been overcome between ten and fifteen minutes. The appearance of a small peak in the tail suggests that some stable particles seem to resist the shearing action.

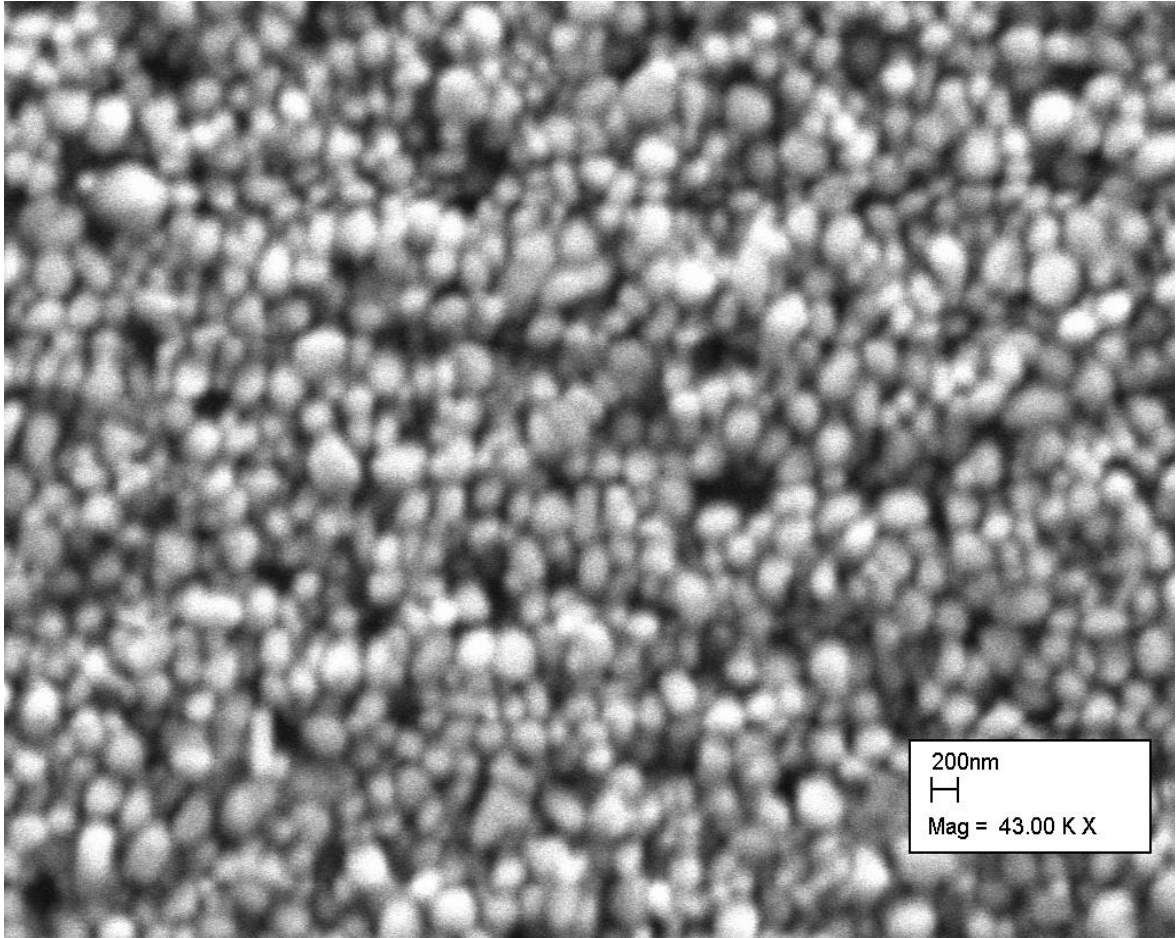


Figure 5.3 Dispersion after fifteen minutes of processing with mean particle size 388.1nm.



The presence of agglomerates in the dispersions after ten minutes of processing could indicate inadequate wetting of pigment particles. Therefore wetting of pigment particles seems not to be instantaneous.

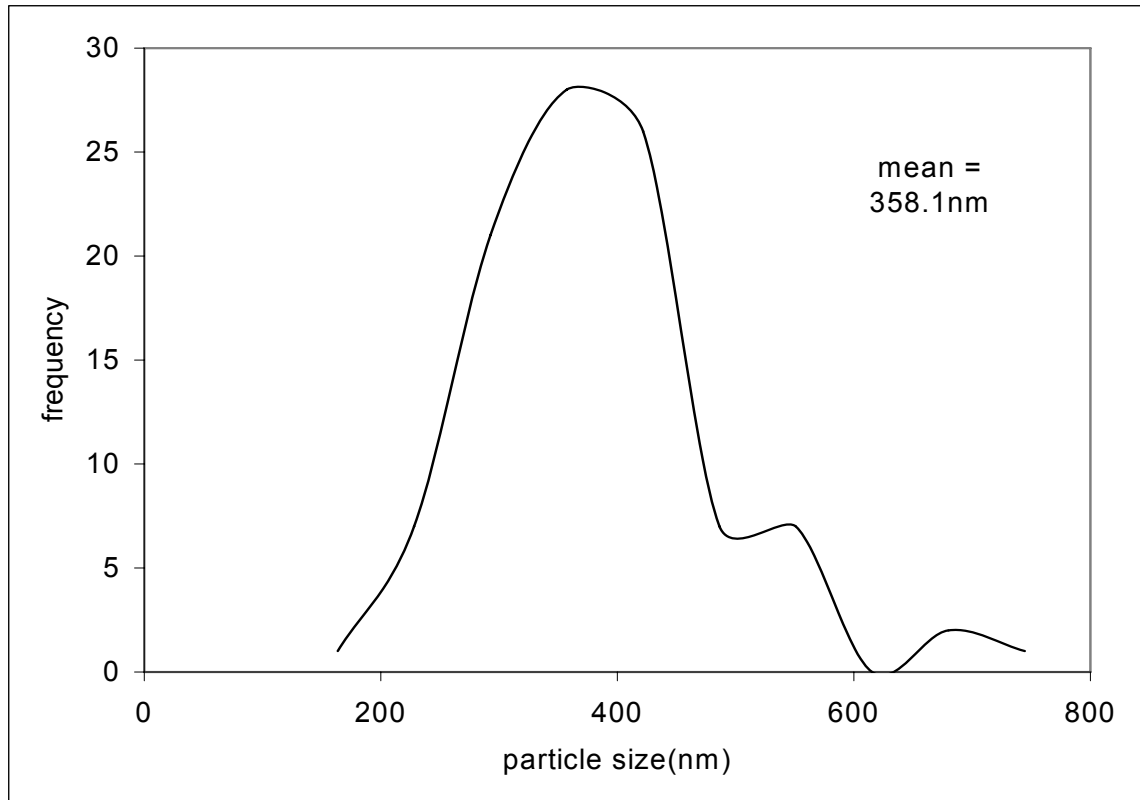


Figure 5.4 The particle size distribution after fifteen minutes

5.1.1.4 Twenty minutes of processing



The scanning electron micrograph after twenty minutes of processing is shown in Figure 5.5. The particles are more rounded in shape compared to the shape after fifteen minutes. Therefore agglomerate breakdown occurred between fifteen and twenty minutes. Since more particle breakdown occurred, the particles must have wetted adequately.

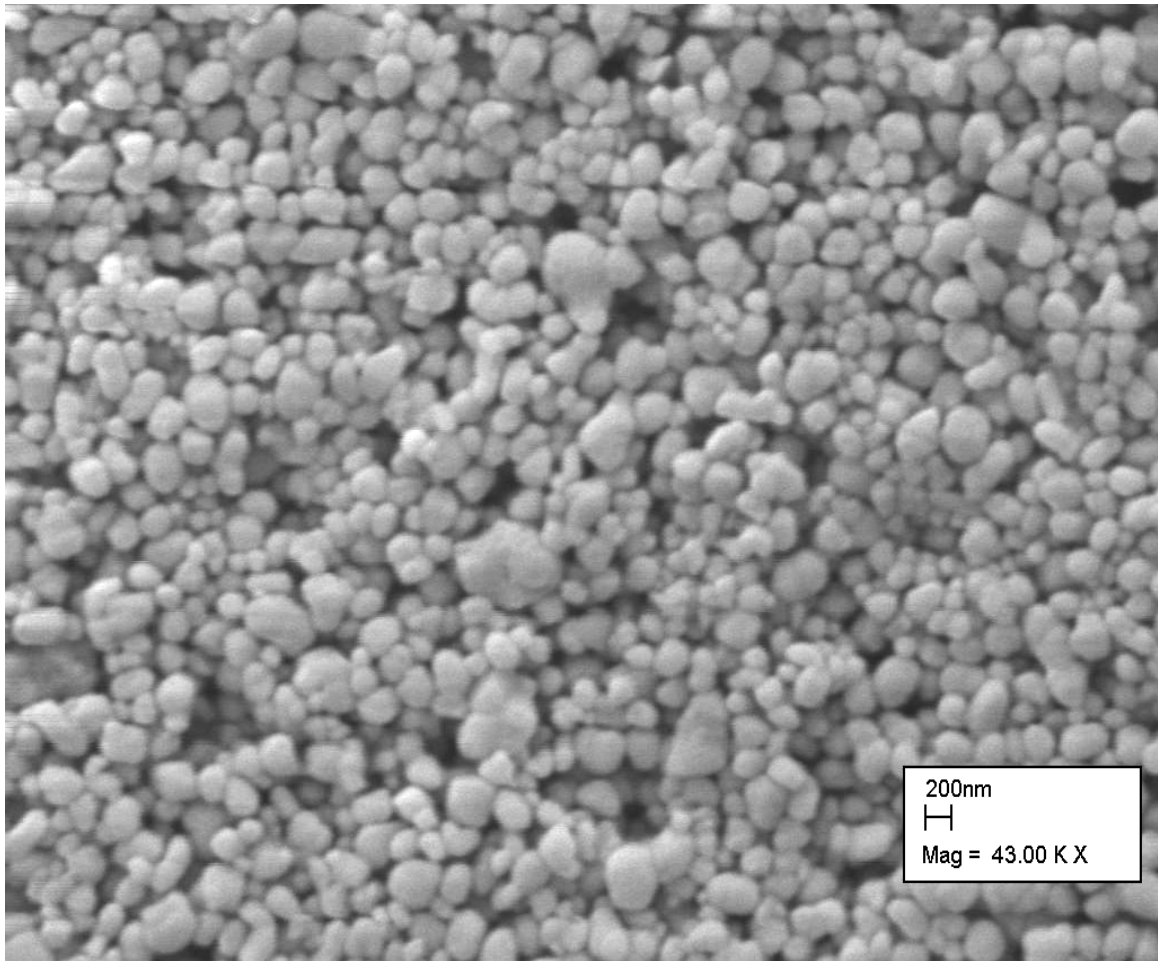


Figure 5.5 Micrograph for design 1 after 20 minutes of processing, mean size 370.0nm

The particle size distribution is shown in Figure 5.6 has a mean size of 370.0nm. Its particle size ranges is between 200 – 800nm and has a near symmetrical central region. This is an indication of a smaller fraction of agglomerates compared to smaller processing times. The tail of the distribution has a single peak which is small compared to those observed for shorter processing times, suggesting that most of the agglomerates were progressively broken down.

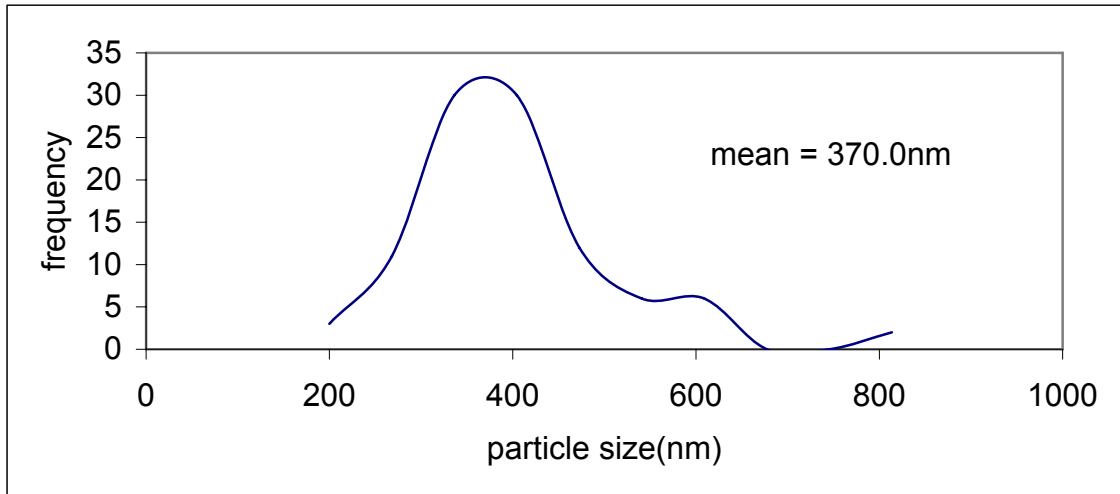


Figure 5.6 The particle size distribution of design 1 after twenty minutes of processing

The secondary peak in the distribution suggests that a fraction of the particles still exist as agglomerates. Therefore they offer resistance to particle break down and are thus stable under the present processing conditions. The process is next evaluated after thirty minutes of operation.



5.1.1.5 Thirty minutes of processing

The micrograph for the dispersion process based on design 1 after thirty minutes of processing is given in Figure 5.7. The mean particle size for thirty minutes of processing is 364.4nm. Most of the particles in the micrograph of Figure 5.7 are almost spherical, with fewer agglomerates than preceding times. Therefore particle break down through shearing assumes significance progressively with time and the rate of particle break down appears to be superior to the rate of flocculation. Furthermore, it appears as if the dispersant provides adequate stabilisation against flocculation. The particle size distribution for this micrograph is shown in Figure 5.8.

The particle size distribution for thirty minutes of processing is shown in Figure 5.8 and has a mean of 364.4nm with a particle size range from 172.0 to 800nm. It does not have a secondary peak in its tail and it is almost symmetrical.

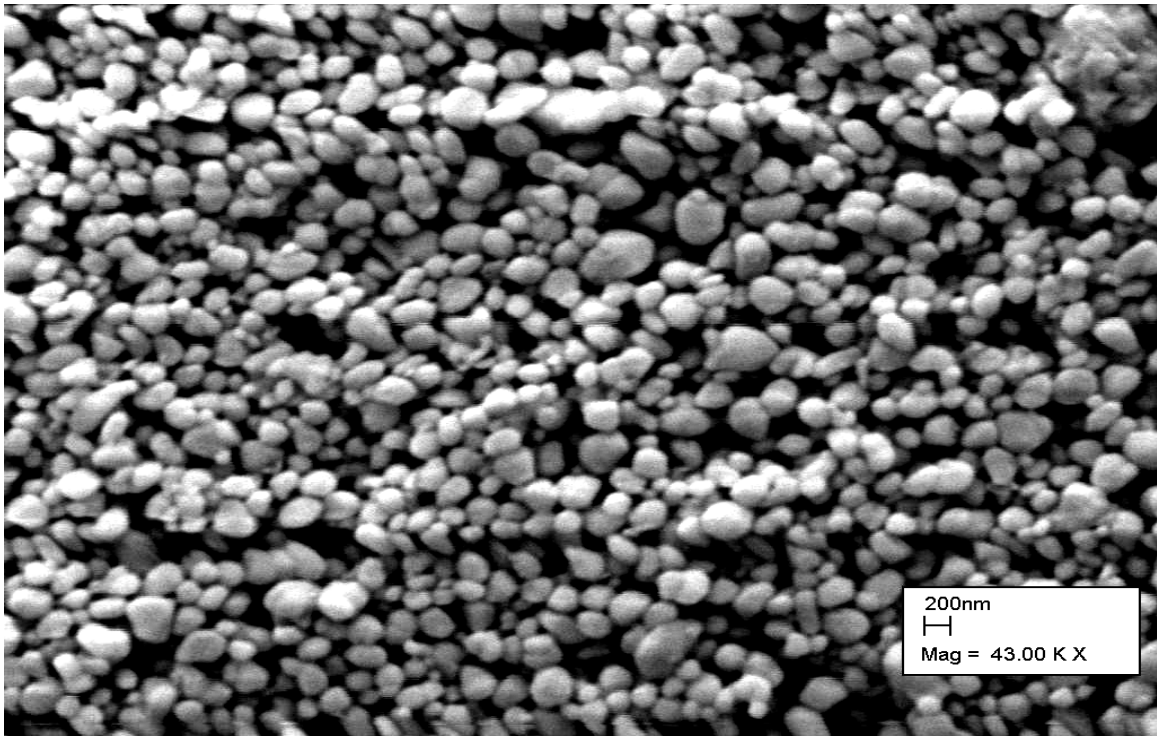


Figure 5.7 The micrograph for design 1 after thirty minutes of processing, mean particle size of 364.4nm

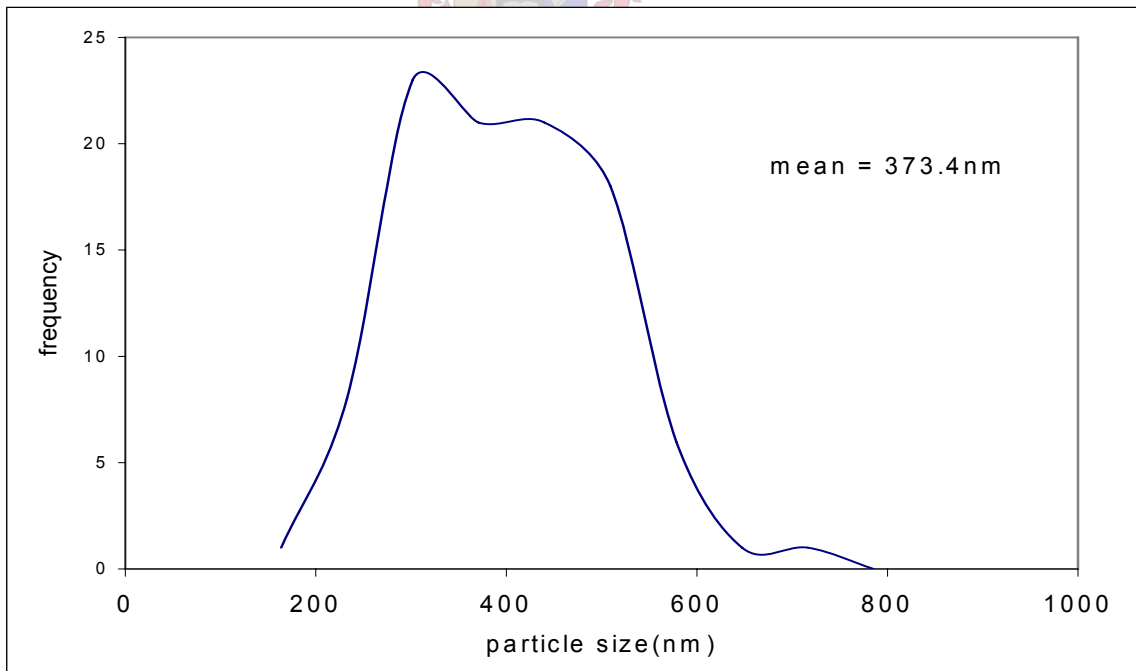


Figure 5.8 The particle size distribution for the dispersion based on design 1 after thirty minutes of processing.

The absence of a secondary peak means that all the particles are sampled from the same distribution. The rate of particle break down slows down between twenty and thirty minutes of processing. Therefore the milling process must be terminated after thirty minutes of processing.

5.2 The overall change in particle size during the dispersion process

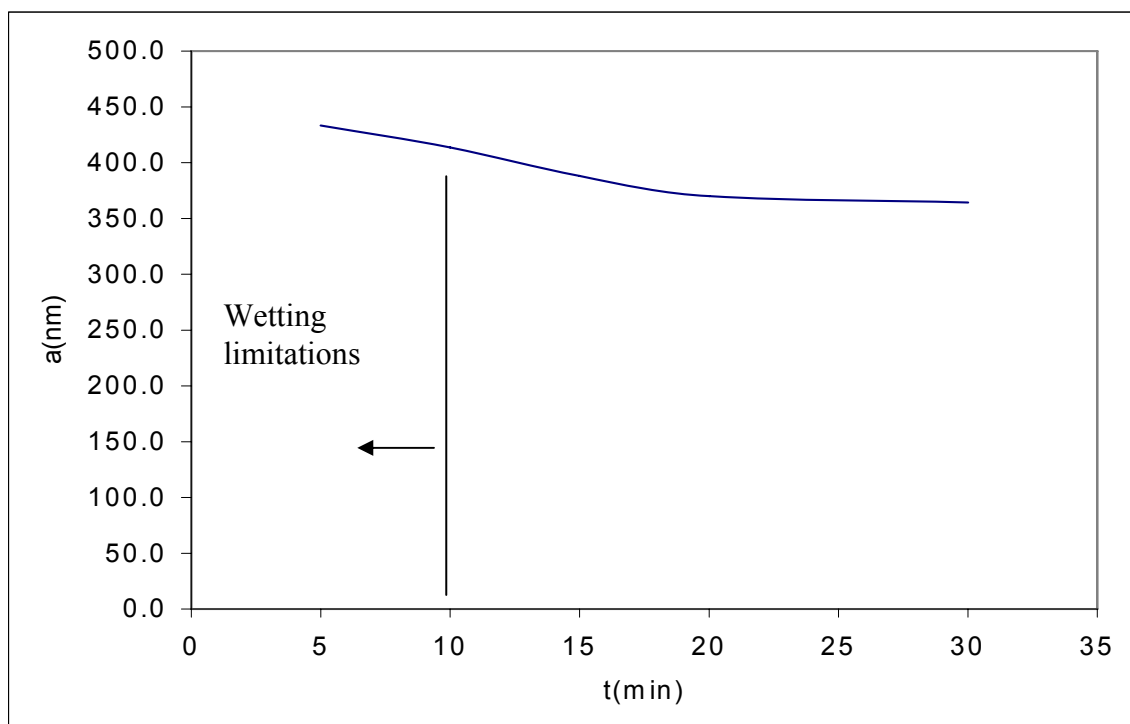


Figure 5.9 The particle size profile for the dispersion based on design 1

Figure 5.9 shows that the dispersion process starts off with a mean particle size of 433.4 nm and after thirty minutes of processing this size is reduced to 364.4nm. The process appears to have a limitation in one of the wetting sub-processes up to fifteen minutes of processing. The distribution up to fifteen minutes contains a secondary peak, which progressively becomes smaller with time. The secondary peak is an indicator of the fraction of agglomerated particles. Other designs were evaluated in a similar manner as done for design 1. The effect of speed on the dispersion process is evaluated in section 5.3.

5.3 The effect of agitator speed on the dispersion process

The speed of agitation in a Cowles mill affects the shear rate and the Reynolds number during the dispersion process, which in turn influences the mechanism of dispersion. Batch runs 2 and 4 were used to evaluate the effect of speed. Batch 2 was operated a speed of 30Hz while Batch 4 was operated at a speed of 35Hz. The particle size distributions from batches 2 and 4 are analysed simultaneously at each sampling time. The mechanism operating in each batch is proposed. Furthermore, a qualitative judgement on the possible changes in opacity and flocculation gradient are provided at each time.

5.3.1 The effect of speed after ten minutes

The particle size distributions after ten minutes are shown in Figure 5.10. The particle size distributions are similar in shape except for the secondary peak in batch 2. Both distributions are broad and have a particle size range between 200 and 800nm. The mean particle size for batch 2 is 433.4nm, while it is 413.6nm for batch 4.

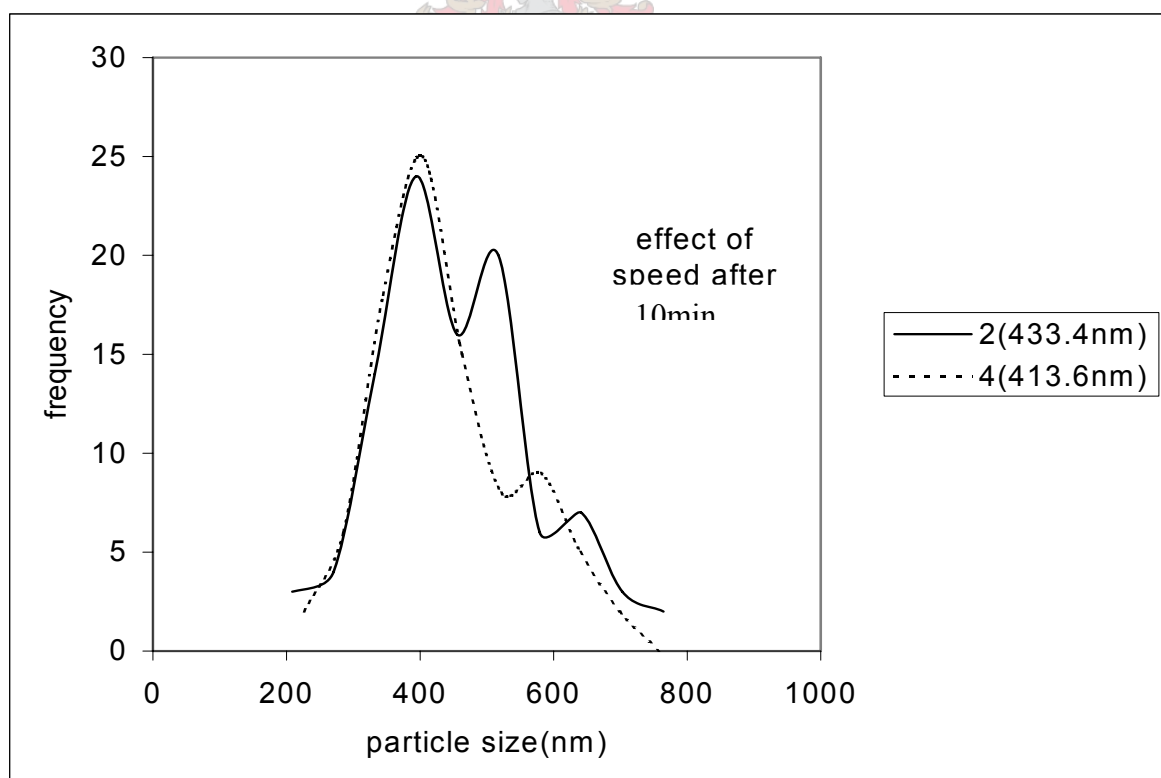


Figure 5.10 The effect of speed on the particle size distributions for batches 2 and 4 after ten minutes of processing.

The wide range of particle sizes suggests that both batches contain a significant fraction of agglomerates. The secondary peak in the distribution of batch 2 indicates that it has a higher fraction of agglomerates than batch 4, since its secondary peak is located at a higher particle size. This large fraction of agglomerates suggests limitations in the wetting of pigment particles and it agrees with the interpretation of the micrographs.

Batch 4 is operated at a larger shear rate than batch 2. Therefore the Reynolds number in batch 4 must be larger than in batch 2 leading to better particle breakdown. This is confirmed by the distributions in Figure 5.10. The opacity for batch 4 must be higher than for batch 2, while the flocculation gradient for batch 4 must be lower than for batch 2. Operation for fifteen minutes is evaluated below.

5.3.2 The effect of speed after fifteen minutes

The particle size distributions for batches 2 and 4 for fifteen minutes of processing are shown in Figure 5.11.

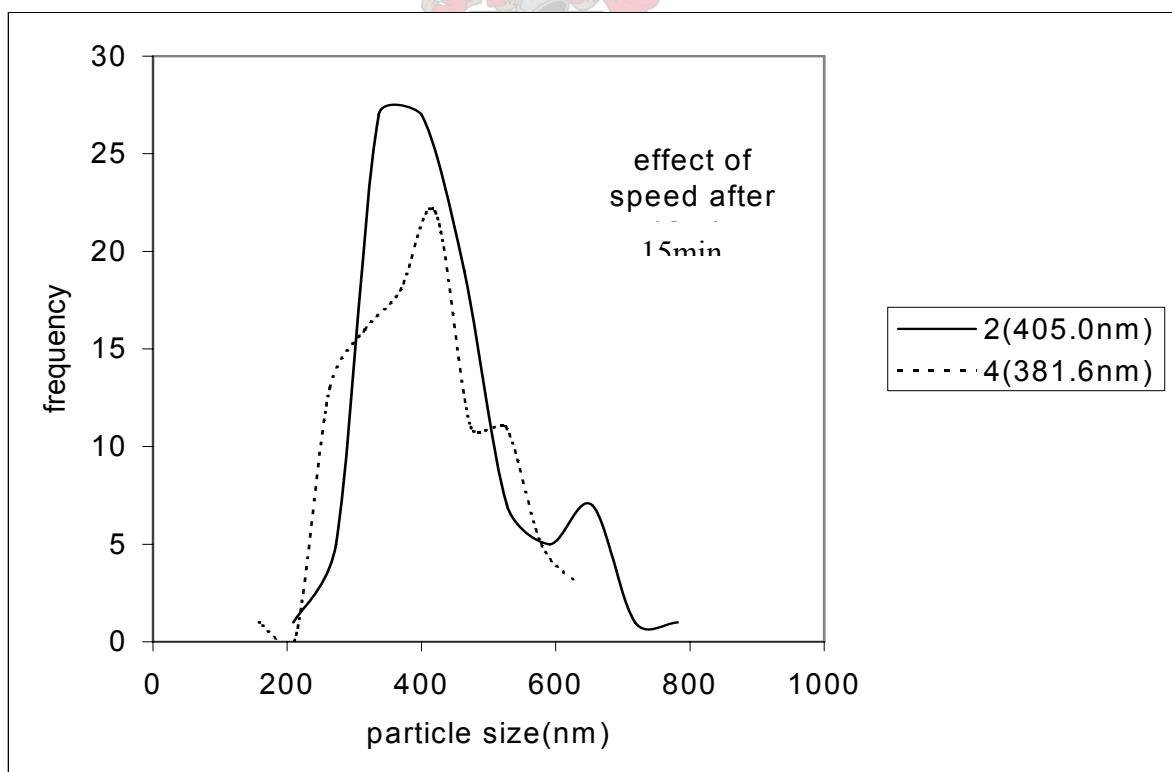


Figure 5.11 The effect of speed on the dispersion process after fifteen minutes of processing in a Cowles mill.

The distributions for batches 2 and 4 after fifteen minutes of processing practically overlap each other. The slight difference is that the particle size range for dispersion from batch 4 is slightly narrower. Furthermore, the particle size distribution for batch 2 has a secondary peak around 650nm.

The overlap between distributions for batches 2 and 4 suggests that the processes are behaving in a similar manner. That is the rates of wetting and particle breakdown are almost similar in magnitude. However, the above particle size distributions suggest that the rates of wetting and particle breakdown for batch 4 are slightly superior.

Batch 2 exhibits a secondary peak in its tail around 650nm. It appears as if it is a meta-stable collection of particles, which increases the fraction of agglomerates in batch 2. Therefore it may indicate limitations to wetting and particle breakdown. It suggests that the low speed at which the mill was operated when processing batch 2 is inadequate for overcoming possible wetting and particle break-down process.

The mean particle sizes for batches 2 and 4 after fifteen minutes of processing are 405.0 and 381.6nm, respectively. That the mean particle size for batch 2 is larger than that for batch 4 was an expected result, since batch 2 has a lower shear rate and Reynolds number. Therefore the rate at which shear stress is applied in batch 2 is lower than in batch 4. Furthermore, the strength of the laminar shear stresses in batch 2 are expected to be lower than in batch 4 since the Reynolds number for batch 2 is smaller than in batch 4.

The mean particle sizes in both batches 2 and 4 after fifteen minutes are smaller than after ten minutes of processing. This result was expected, since the dispersions in both mills had more contact time with the shear stresses, which led to further particle breakdown.

5.3.3 The effect of speed after twenty minutes

The particle size distributions for batches 2 and 4 for twenty minutes of processing are shown in Figure 5.12.

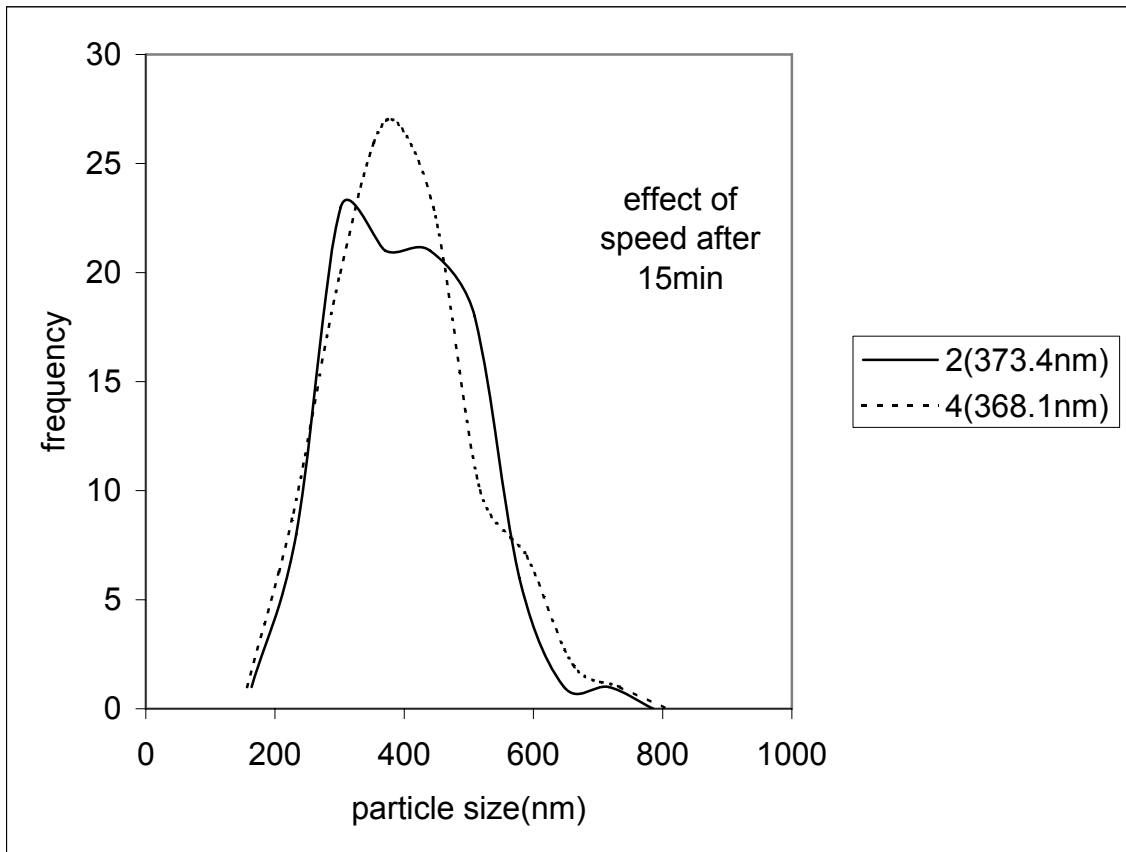


Figure 5.12 The effect of speed on the dispersion process after twenty minutes of processing in a Cowles mill.

The particle size distributions for batches 2 and 4 almost overlap as shown in the Figure 5.12. The particle size range is between 180 and 750nm, while the mean particle sizes for batches 2 and 4 are 373.4 and 368.1nm, respectively.

The similarity of the particle size distributions and mean particle sizes for batches 2 and 4 indicates that the processes occurring are similar. Therefore the rates of wetting and particle breakdown are expected to be similar in magnitude. This seems to confirm that, as processing time is increased, the influence of agitator speed is diminished. This reduced influence of speed with processing time seems to indicate that wetting is complete and that the shear stresses being applied are limited in their ability to separate particles.

5.3.4 The effect of speed after thirty minutes

The distributions for batches 2 and 4 for thirty minutes of processing are shown in Figure 5.13. The differences between the particle size distributions after thirty minutes of processing in batches 2 and 4 are minor. This is similar to the trends that were observed for fifteen and twenty minutes of processing. The particle size range for batches 2 and 4 is 180 to 700nm. Furthermore, the mean particle size for batch 2 and 3 are 368.6 and 356.7nm respectively.

The similarity of the particle size distributions for batches 2 and 4 suggest that similar processes are occurring in both batches during the dispersion process. Therefore the rates of wetting and particle breakdown are similar in the two batches. Since the two batches are approximately similar (overlapping shapes and similar mean particle sizes), it appears as if speed does not have a differentiating effect between the two batches.

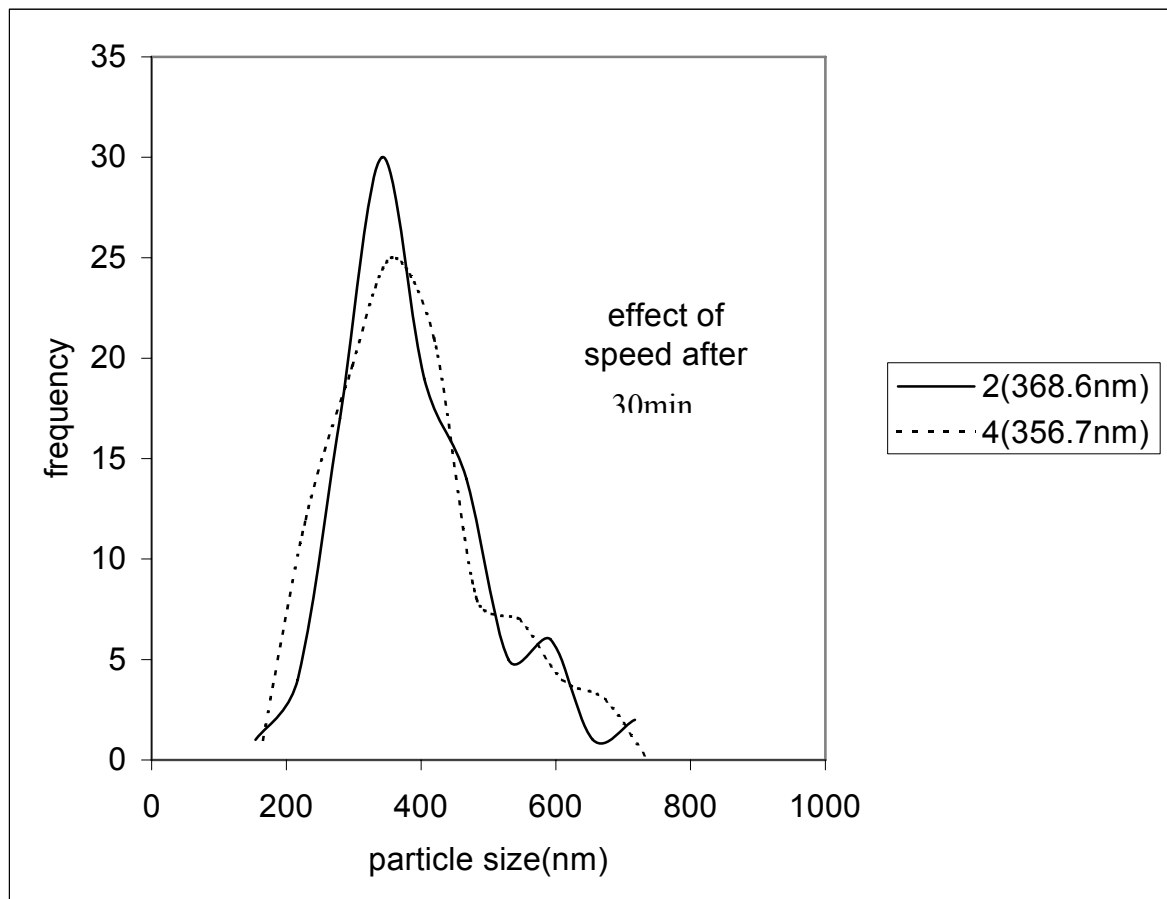


Figure 5.13 The effect of speed on the dispersion process after thirty minutes of processing

The similar particle size and distributions for batches 2 and 4 are caused by the depletion of agglomerates leading to the formation of fine particles with process time. This leads to increased resistance to further breakdown increases since the attractive Van der Waals forces become more significant.

5.3.5 The mean particle size profiles for batches 2 and 4

A representative graph that shows the changes in the mean particle size for batches 2 and 4 with time is shown in Figure 5.14.

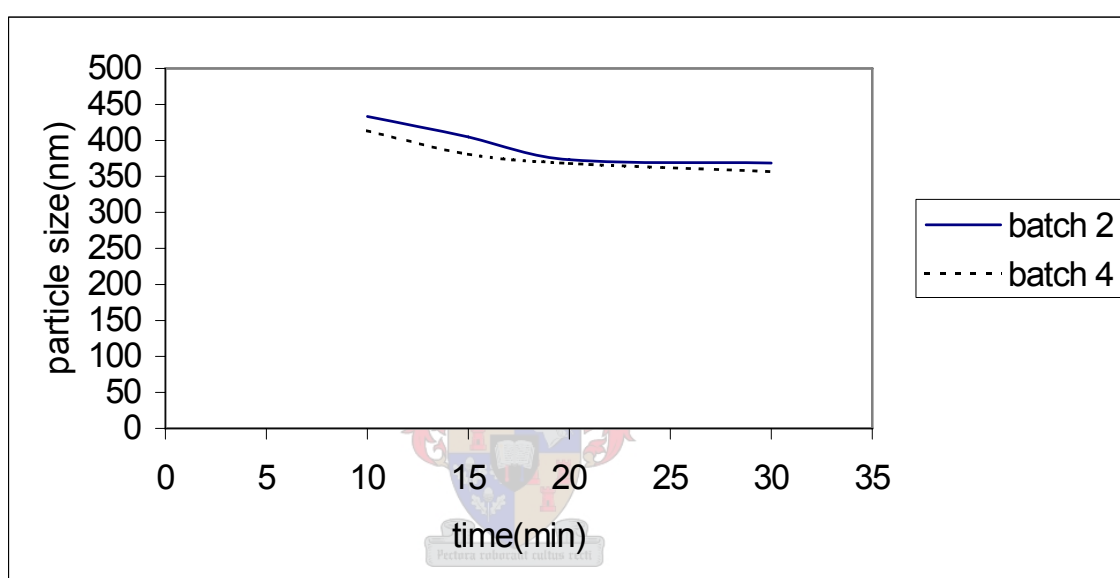


Figure 5.14 The changes in the mean particle size of batches 2 and 4 with process time.

Figure 5.14 shows that the mean particle size drops with dispersion time when batches 2 and 4 are processed using a Cowles mill. Furthermore, the mean particle size for batch 4 is always smaller than the mean particle size of batch 2 for the same processing times.

5.3.6 Summary of the effect of speed on the dispersion process

For short times of processing (ten to fifteen minutes), speed has a significant effect on the dispersion process. An increase in the speed of agitation results in enhancing the wetting of pigment particles and breakdown of agglomerates. This is supported by the fact that speed increases the Reynolds number affecting the wetting processes and particle breakdown due to shear stress.

Increasing the processing time beyond fifteen minutes causes the behaviour of batches 2 and 4 to become similar. This is due to the depletion of agglomerates, which are acted upon by the shear stresses. Furthermore, the agglomerates are converted to even smaller particles for which the attractive Van der Waals forces become significant, retarding further breakdown. Therefore, for large process times the Reynolds number does not control the dispersion process. Evaluation of contrast ratio and flocculation gradients for batches 2 and 4 is provided in section 5.3.7.

5.3.7 The contrast ratio for batches 2 and 4

Evaluation of contrast ratio and flocculation gradient was carried out for batches 2 and 4 during the dispersion process. The contrast ratio was obtained by dividing the reflectance over the black substrate by the reflectance over the white substrate. Table 5.3 shows the contrast ratios that were obtained for batches 2 and 4. The reflectance over the black substrate and the reflectance over the white substrate used to calculate the contrast ratio are shown in appendix D1 for the dispersion of titanium dioxide in a Cowles mill.

Table 5.3 Changes in contrast ratio and mean particle size with processing time

| Time(min) | C.R(batch2) | C.R(batch4) | Size(nm) | Size(nm) |
|-----------|-------------|-------------|----------|----------|
| 10 | 0.974 | 0.973 | 433.4 | 413.6 |
| 15 | 0.976 | 0.976 | 405.0 | 381.6 |
| 20 | 0.977 | 0.981 | 373.4 | 368.1 |
| 30 | 0.978 | 0.983 | 368.6 | 356.7 |

When the contrast ratios for batch 2 and the corresponding mean particle sizes are compared, there is an increase in the contrast ratio as the particle size decreases with processing time. This was expected from light scattering theory, which states that the contrast ratio increases when the particle size becomes smaller. A similar trend is observed between the contrast ratio and mean particle size for batch 4. when the contrast ratio for batches 2 and 4 are compared at corresponding times, batch 4 is expected to exhibit a higher value of contrast ratio, since its mean particle size is smaller than that for batch 2. this is true for twenty and thirty minutes of processing. Experimental errors affect the

contrast ratios at ten and fifteen minutes of processing for batch 4 such that its contrast ratios are similar to those of batch 2.

5.3.7.1 Empirical correlation of the contrast ratio of the dispersion process

Models for contrast ratio can be set up for the effect of agitator speed and diameter using multiple linear regression. The model of contrast ratio based on the effect of agitator speed for an operation time of thirty minutes is described in this section.

The reviews of Chapters 2 and 3 clearly state that the opacity (contrast ratio) of titanium dioxide dispersions depends on: (i) pigment volume concentration, (ii) mean titanium dioxide pigment crystal size, (iii) pigment volume concentration of extender, (iv) the grade of titanium dioxide extender, and (iv) the particle size distribution(PSD). Table 5.4 shows the measurements that would have been made.

Table 5.4 Measurements required for the development of correlation for contrast ratio and flocculation gradient

| PSD | Particle size(nm) | Contrast Ratio | Flocculation Gradient |
|--------------------|---------------------------------|----------------------------------|----------------------------------|
| PSD ₁ | A (30 min, PSD ₁) | CR (30 min, PSD ₁) | FG (30 min, PSD ₁) |
| PSD ₂ | A (30 min, PSD ₂) | CR (30 min, PSD ₂) | FG (30 min, PSD ₂) |
| ... | ... | ... | ... |
| Psd _{n-1} | A (30 min, psd _{n-1}) | CR (30 min, psd _{n-1}) | FG (30 min, psd _{n-1}) |
| Psd _n | A (30 min, psd _n) | CR (30 min, psd _n) | FG (30 min, psd _n) |

The multi-linear correlation assumed that particle size distribution and the mean particle size are the only variables, since the other variables are held constant during dispersion. The proposed model is shown below.

$$Y = k_0 + k_1 * X_1 + k_2 * X_2 \quad 5.3$$

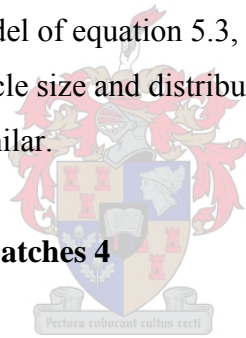
Where:

| | | |
|----------------|----------------|----|
| Y | Contrast ratio | % |
| X ₁ | Particle size | Nm |
| X ₂ | PSD | Hz |
| K ₀ | Coefficient | |
| K ₁ | Coefficient | |
| K ₂ | Coefficient | |

It would have been important to test for auto-correlation between particle size and the particle size distribution. On the other hand, if the multi-linear correlation had failed, it would have been necessary to include higher powers of X₁ and X₂ in the correlation. A model for the contrast ratio needs to be evaluated for each agitator speed.

The contrast ratio and corresponding values of mean particle size and distribution cannot be used to test the multi-linear model of equation 5.3, since the speeds used do not have a significant effect on mean particle size and distribution. Furthermore, the values of contrast ratio for batches 1 and 2 are similar.

5.3.8 The flocculation gradient for batches 4



The flocculation gradient of a dispersion is important in that it provides a quantitative idea of the impact of flocculation gradient on the opacity of the dispersion. This subsection provides calculations and an interpretation of the flocculation gradient for batch 4.

5.3.8.1 The flocculation gradient after processing batch 4 for ten minutes

The flocculation gradient is calculated according to the equations presented in Chapter 3. The data required for this calculation are provided below. It is assumed that the density of the dispersion remains constant. The calculation for film thickness, X.

| | |
|----------------|-------------------|
| w _f | 0.43g |
| A _x | 36cm ² |
| S _a | 65% by weight |

$$C_w = 2.0 \text{g.cm}^{-3}$$

$$R_s = 1.0 \text{g.cm}^{-3}$$

$$X = \frac{\frac{0.43 * 10^4}{36 * 65} \mu m}{\frac{100}{2} - \frac{(100 - 65)}{1}} \quad 5.4$$

The film thickness obtained is equivalent to 27.6µm and it corresponds with a back scatter of 19.8 percent. Four points in all are required for plotting the graph used to determine the flocculation gradient. The results of all the four points are shown in the table below.

Table 5.5 Film thickness and percentage back scatter for samples of titanium dioxide

| Mass of film(g) | X(µm) | % Back scatter |
|-----------------|-------|----------------|
| | | 0.0 |
| 0.43 | 27.6 | 19.8 |
| 0.60 | 38.5 | 20.0 |
| 0.62 | 39.7 | 22.0 |
| 0.84 | 53.8 | 60.0 |

The data in Table 5.5 were used to plot a graph (Figure 5.15), for which a linear correlation was fitted. The gradient of the graph, including its R² value, is shown below.

The flocculation gradient is equivalent to the gradient in the graph of Figure 5.15 and it has a value of 1.61 with a linear association, Pearson coefficient of correlation R² value of 0.77. This shows that the dispersion is highly flocculated, since the flocculation gradient is large. The points in the graph could be fitted by a polynomial.

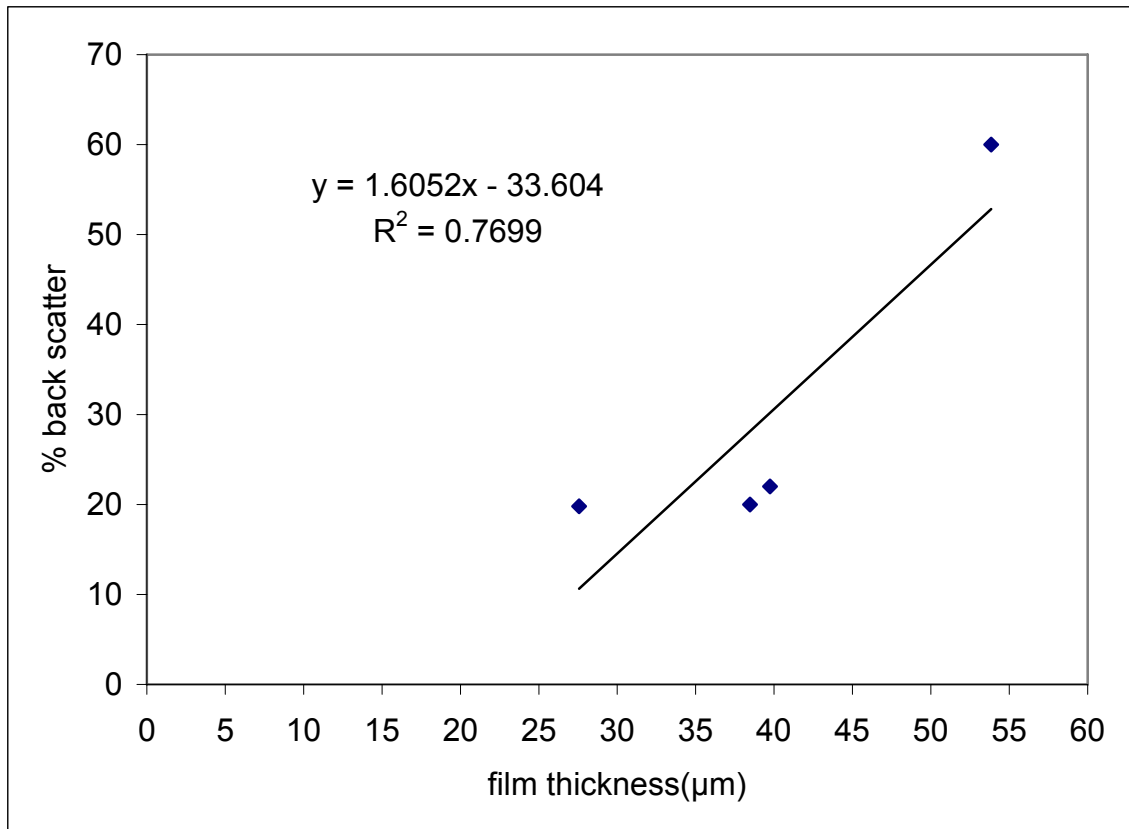
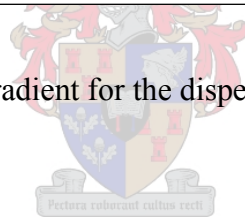


Figure 5.15 The flocculation gradient for the dispersion of batch 4 after ten minutes of processing.



Evaluation of the flocculation gradient after fifteen minutes is provided in section 5.3.8.2.

5.3.8.2 The flocculation gradient after fifteen minutes of processing

The flocculation gradient of batch 4 is 1.88 (Figure 5.16). This is higher than for ten minutes of processing. Therefore it indicates that flocculation increased between five and ten minutes of processing. This contradicts the particle breakdown that occurred corresponding to a drop in size from 413.6nm to 381.6nm. Therefore the flocculation gradient that was observed is not leading to the true interpretation of the changes that occurred. Although the R^2 value is 0.87, the points in the graph could have been better fitted through a curve rather than a straight line.

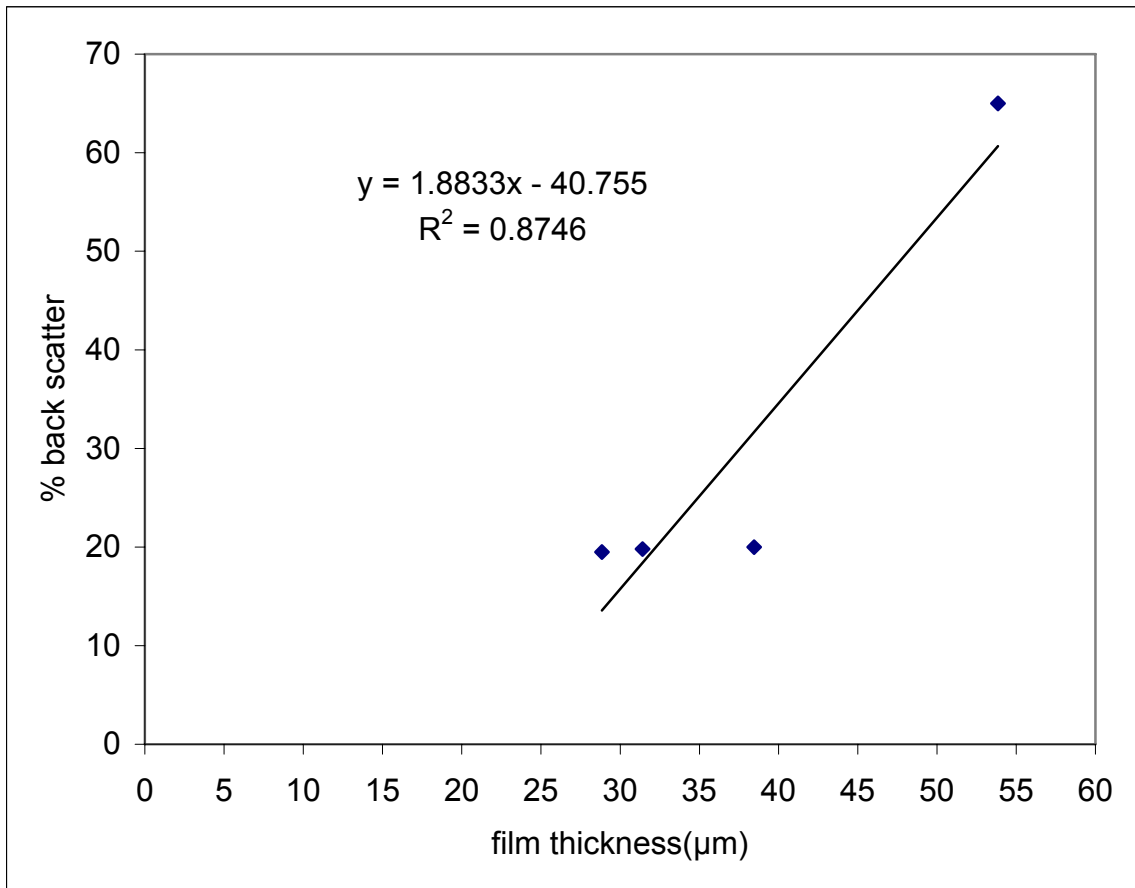
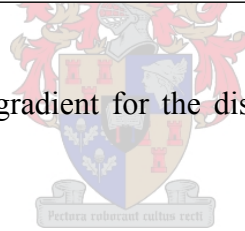


Figure 5.16 The flocculation gradient for the dispersion process of batch 4 after fifteen minutes of processing.



5.3.8.3 The flocculation gradient after twenty minutes of processing

The flocculation gradient after twenty minutes is equivalent to 1.48 (Figure 5.17). This value is smaller than that corresponding with ten minutes of processing. Therefore, it indicates that particle break-down occurred between fifteen and twenty minutes of processing. During the same time interval the mean particle size dropped from 381.1nm to 368.1nm, thus corresponding to particle breakdown. Therefore the decline in the magnitude of the flocculation gradient is in agreement with the reduction in the mean particle size that occurred between fifteen and twenty minutes.

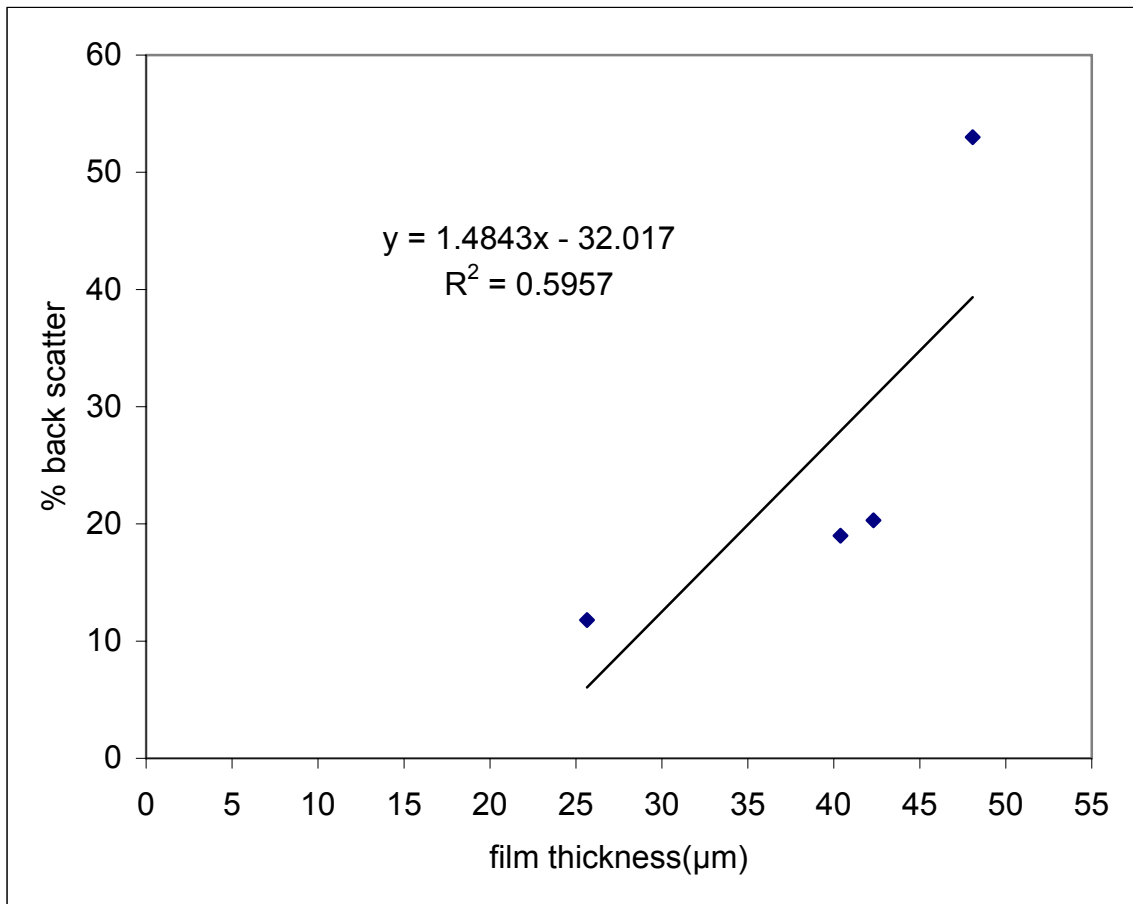


Figure 5.17 The flocculation gradient after processing batch 4 for twenty minutes.

5.3.8.4 The flocculation gradient after thirty minutes of processing

Figure 5.18 shows that the flocculation gradient for the dispersion process after thirty minutes is 1.48 and it is similar to that after twenty minutes of processing. This is an indication that negligible particle break down occurs between twenty and thirty minutes of processing. It can be noted that the mean particle size decreases from 368.1nm to 356.7nm in the same time interval and this represents negligible changes in the mean particle size. This explains why the flocculation gradients for twenty and thirty minutes are similar in magnitude.

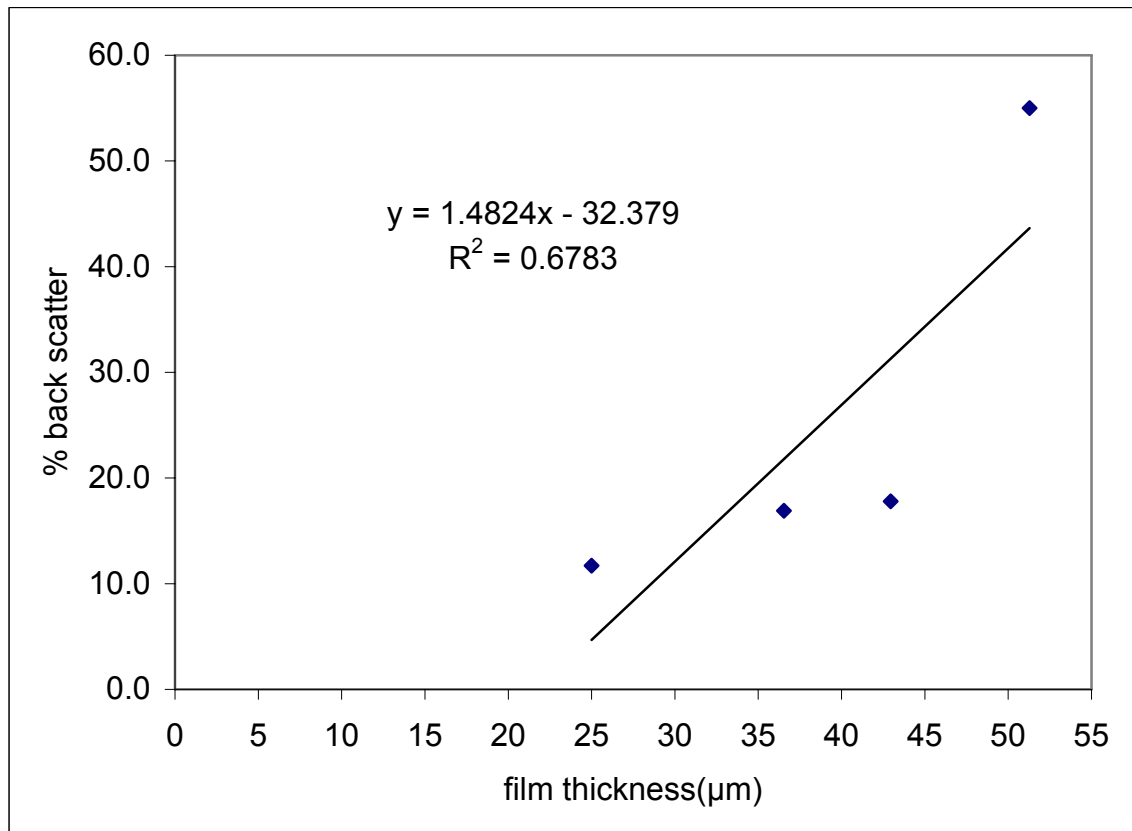
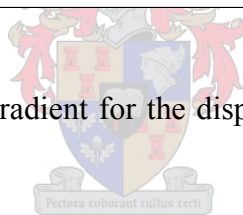


Figure 5.18 The flocculation gradient for the dispersion of batch 4 after thirty minutes of processing.



The overall changes that occurred in flocculation gradient are evaluated below.

5.4 Overall changes in flocculation gradient for the agitated dispersion process

The graph in Figure 5.19 shows changes in flocculation gradient for batch 4 (solid line) with processing time. An initial increase in the flocculation gradient between ten and fifteen minutes occurs and this was unexpected, given that during the same time interval there was a reduction in the mean particle size. This should have led to a reduction in the flocculation gradient. A sudden reduction in the flocculation gradient occurs between fifteen and twenty minutes, which agrees with the change in particle size (381.6nm to 368.1nm) in the same time interval. This is followed by another reduction in the flocculation gradient between

twenty and thirty minutes, which correspond to a reduction in mean particle size (368.1nm to 356.7nm).

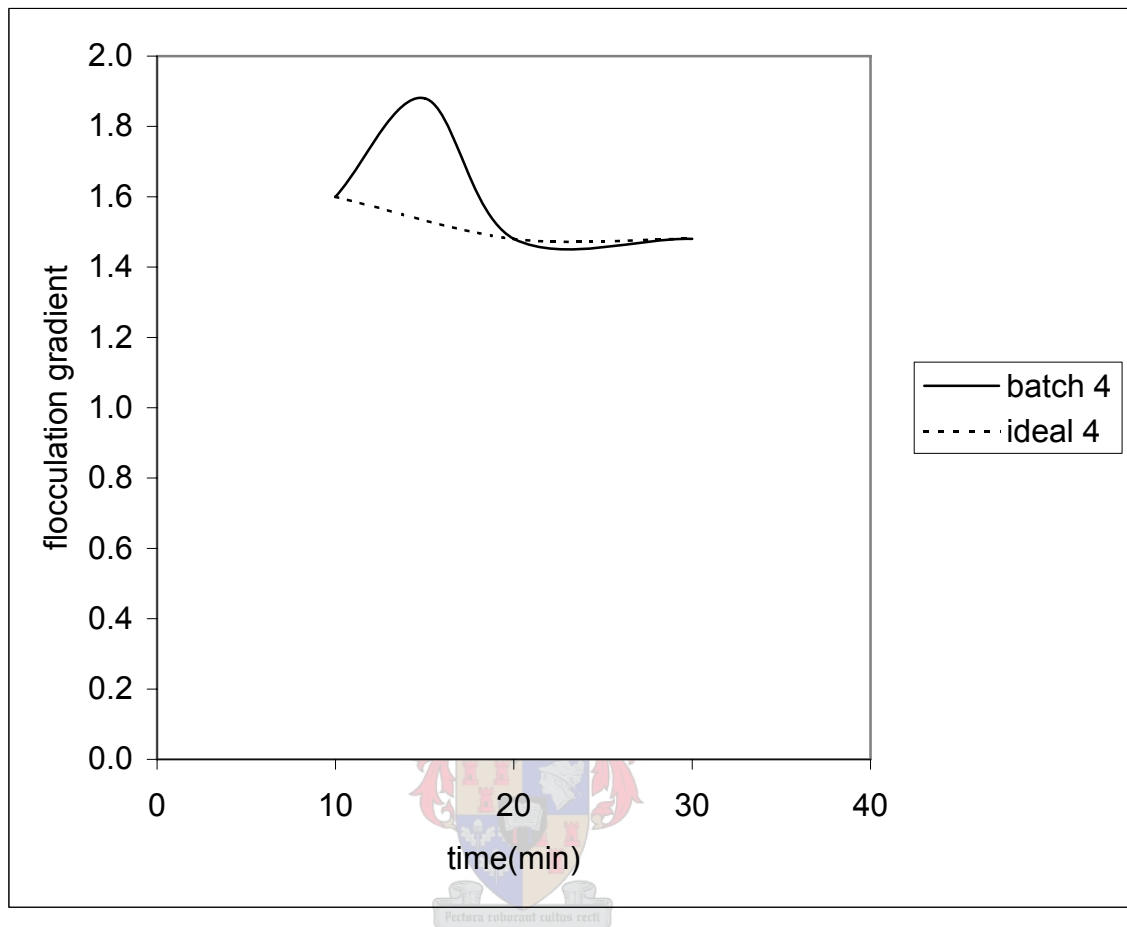


Figure 5.19 The changes in flocculation gradient with process time for batch 4

A dashed trend line (ideal 4) superimposed in Figure 5.19 indicates the expected gradual reduction in the flocculation gradient of batch 4 on the basis of the changes in mean particle size. Table 5.6 shows all the corresponding values of the flocculation gradient and their strengths of linear association R^2 values and mean particle size.

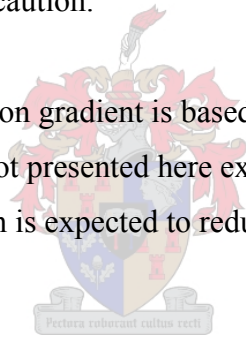
The Pearson correlation coefficient for processing times between ten and thirty minutes is 0.77, 0.87, 0.60 and 0.67. The linearity for processing times ten, fifteen, twenty and thirty minutes is in doubt, since their Pearson correlation coefficients are less than 0.77. In addition the individual plots from which the flocculation gradients were calculated appears to be best fitted by a polynomial rather than a straight line.

Table 5.6 Changes in mean particle size and flocculation gradient during dispersion

| Time(min) | Flocculation gradient | R ² value | Particle size(nm) |
|-----------|-----------------------|----------------------|-------------------|
| 10 | 1.61 | 0.77 | 413.6 |
| 15 | 1.88 | 0.87 | 381.6 |
| 20 | 1.48 | 0.60 | 368.1 |
| 30 | 1.48 | 0.67 | 356.7 |

It appears as if the values of the flocculation gradient for batch 4 are statistically inconsistent. The major reasons are the poor values of the Pearson correlation coefficients and the possibility of fitting other polynomials to the data. It is acknowledged that the use of the flocculation gradient is important in the study of pigment dispersion. However, it appears as if the calibration of the micron-sized gauge that is used to apply the film could be faulty. Therefore the flocculation gradient for the estimation of the extent of flocculation must be used with caution.

The correlation of the flocculation gradient is based on the same explanatory variables as that for contrast ratio and it is not presented here except to point out the differences. Increasing the speed of agitation is expected to reduce the flocculation gradient, while it increases the contrast ratio.



The flocculation gradients are shown in appendix E. It must be pointed out that a limited number of flocculation gradients were obtained. This is due to the experimental difficulties that were encountered whilst measuring quantities required in the evaluation of contrast ratio.

In conclusion, the reduction in the particle with processing time supports the observed reduction in flocculation gradient. According to the theory reviewed in chapter 3, a reduction in flocculation gradient indicates that the fraction of agglomerates becomes small. Since the flocculation gradient decreases with processing time

Chapter 6 Results and Discussion – Dispersion of Steopac Talc

The following evaluations are provided in this chapter:

- i. The effect of agitator speed on the dispersion process;
- ii. The effect of agitator diameter on the dispersion process.

The structure used to evaluate these results is similar to that laid out in Chapter 5 for the evaluation of the dispersion of titanium dioxide in a Cowles mill. The initial focus is on the effect of the process on the mean particle size distribution in terms of the mechanism. Changes in the mean particle size and distribution are then used to qualitatively predict the contrast ratio and flocculation gradient expected of the dispersion. Finally, the two effects above are compared in terms of significance in the development of opacity.

6.1 The dispersion of talc

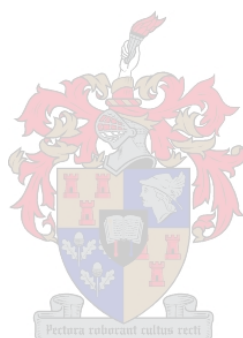
Dispersion of talc was carried out in a Cowles mill; using different batches F, G, H and J. The mill configurations that correspond to these batches are shown in appendix B.1.1.2. Changes in viscosity occurring in the Cowles mill had not been determined during the project. Therefore, it is not possible to predict the flow occurring in the dispersion process of steopac talc. An approach similar to the one presented when evaluating the dispersion process of titanium dioxide in a Cowles mill could be used. This section assumes that the weights used in the determination of the Krebs-Stormer viscometer for steopac talc and titanium dioxide dispersions are similar. Therefore the flow conditions evaluated for titanium dioxide dispersed through a Cowles mill are similar to those for steopac talc.

In total, four batches were run. Batches F, G and H are similar and differ only in the speed of the agitator. In batches F, G and H the objective is to determine the effect of operating speed on the degree of dispersion. Batch J is similar to H and they differ in the diameter of the agitator. Batches H and J therefore investigate the effect of agitator diameter on the dispersion. batches F, G and H were prepared using the levels shown in the table below.

Table 6.1 Agitator speed used in the preparation of steopac talc

| Batch | Agitator speed(Hz) |
|-------|--------------------|
| F | 30 |
| G | 35 |
| H | 40 |

Table 6.1 shows that the speed of agitation is increased in the order, $F < G < H$. The steopac talc, which was prepared using the above agitator speeds, was based on the formulation provided in the appendix A3. The agitator diameter used was 0.1m. The effect of agitator speed on the dispersion of batches F, G and H is discussed in detail below.



6.2 Evaluation of the effect of speed on the dispersion of steopac talc extender

Three different agitator speeds of 30, 35 and 40Hz, corresponding to batches F, G and H respectively, were selected for significance testing. The agitator diameter selected was 0.1m and was used in a tank of diameter 0.20m.

6.2.1 The effect of speed after ten minutes of processing

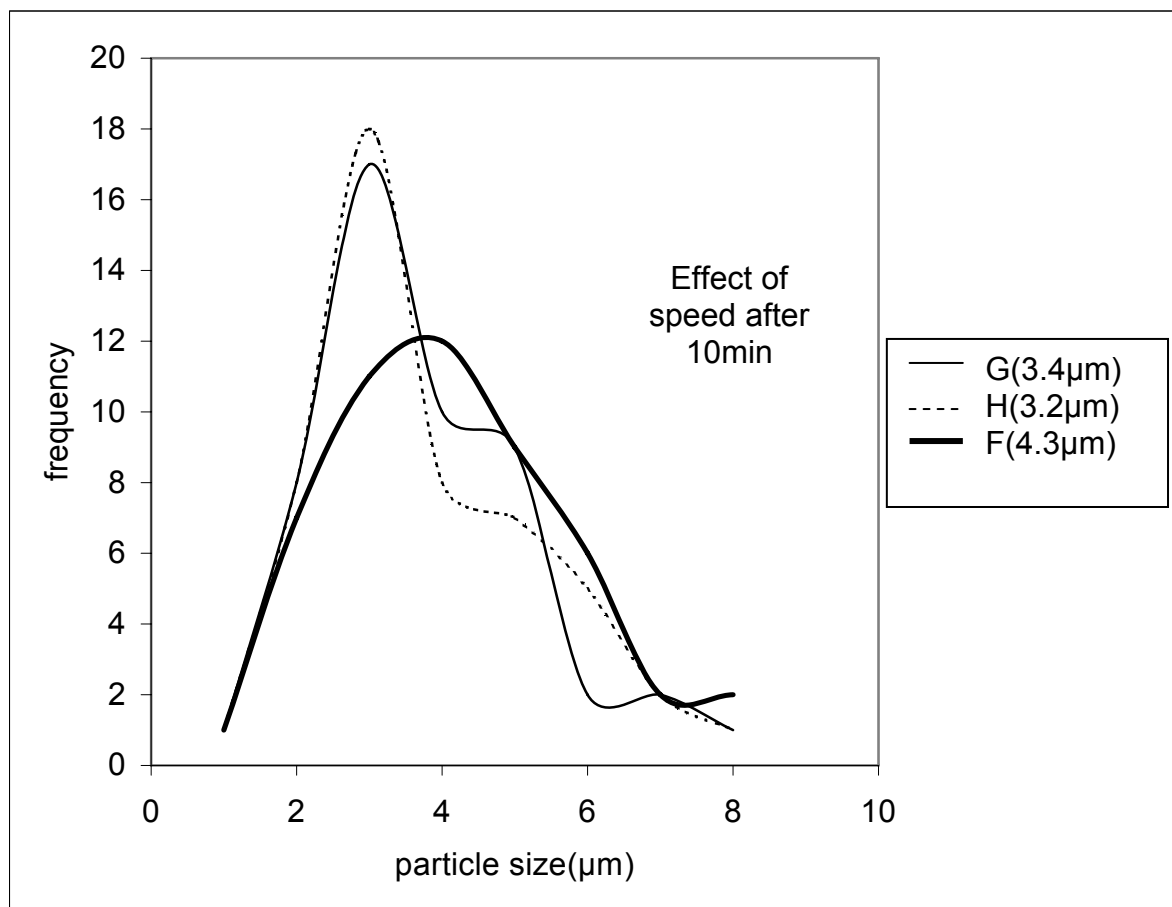


Figure 6.1 The effect of agitator speed after ten minutes of processing on the particle size distributions for the dispersion of talc (mean particle size shown in brackets in legend).

Figure 6.1 shows that the distributions for batches F and H are broad compared to G. Therefore distributions F and H appear to have a greater proportion of coarse particles or agglomerates compared to G. However, their corresponding micrographs do not exhibit any agglomerates.

The mean particle sizes are: F (4.3 μm), G (3.4 μm) and H (3.2 μm). These mean particle sizes are almost equal. This could be expected since the dispersions may not have wetted adequately after this short period of operation. The mean particle sizes decrease in the order according to batch: $F > G > H$ and this was expected since the shear rates for the dispersion according to batch are: $F < G < H$. Therefore it is to be expected that the order of mixing is $F < G < H$, since this is the order for the shear rates.

6.2.2 The effect of speed after fifteen minutes of processing

The particle size distributions and their mean particle sizes for the dispersion after fifteen minutes are shown Figure 6.2.

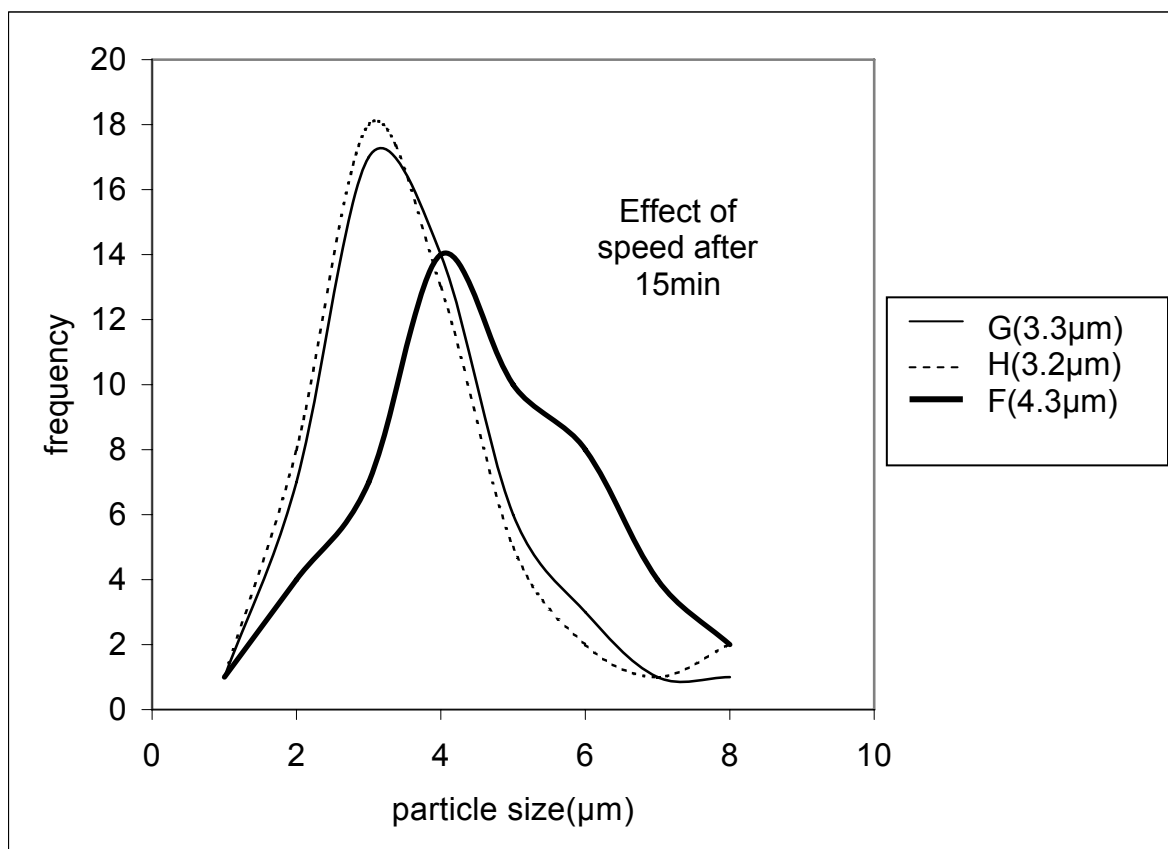


Figure 6.2 The effect of agitator speed (after fifteen minutes of processing) on the particle size distributions for the dispersion of steopac talc (mean particle size in legend)

The mean particle sizes for batches F, G, H after fifteen minutes of agitation are 4.3 μm , 3.3 μm and 3.2 μm . There is a significant difference in the effect of agitator speed between 30 and 35Hz. Speeds of 35Hz and 40Hz have a similar effect on the mean particle size. The

three distributions are all broad. When the distributions for ten and fifteen minutes of processing are compared, they show no significant difference in the mean particle size. The similarity in the mean particle size for ten and fifteen minutes of processing was expected since steopac talc is relatively free of agglomerates. The relative ease of dispersion after fifteen minutes of processing can be confirmed from the scanning electron micrographs of batches F, G and H after fifteen minutes of processing.

6.2.3 The effect of speed after twenty minutes of processing

The particle size distributions for twenty minutes of processing are shown in figure 6.3 below.

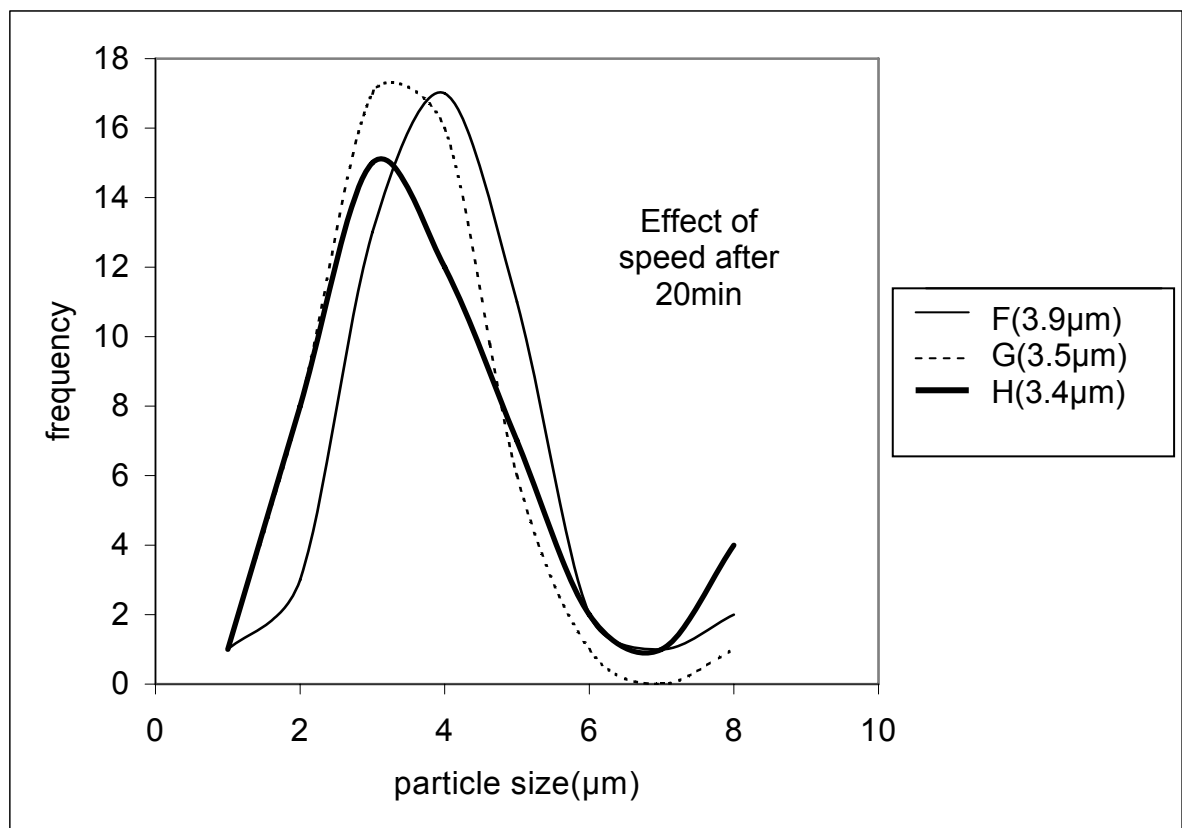


Figure 6.3 The effect of speed on the dispersion process of steopac talc after 20 minutes of operation.

Figure 6.3 shows the particle size and distribution for twenty minutes of processing. The mean particle sizes for batches F, G and H are 3.9µm, 3.5µm and 3.4µm respectively. The trends in the mean particle size are the same as those for ten and fifteen minutes of processing. The only significant change is that the mean particle size for batch F dropped

from 4.3 μm to 3.9 μm . Furthermore, the mean particle sizes for batches G and H increased slightly. This could be due to the error in the particle size analysis. The scanning electron micrographs for batches F, G and H after twenty minutes of processing do not show any significant fraction of agglomerates.

6.2.4 The effect of speed after thirty minutes of processing

Figure 6.4 shows the particle size and distributions for thirty minutes of processing. After thirty minutes of processing the particle size distributions for batches F, G and H begin to converge. This indicates that the rate of particle breakdown process slows down, since the resistance due to attractive Van der Waals forces increases when size decreases.

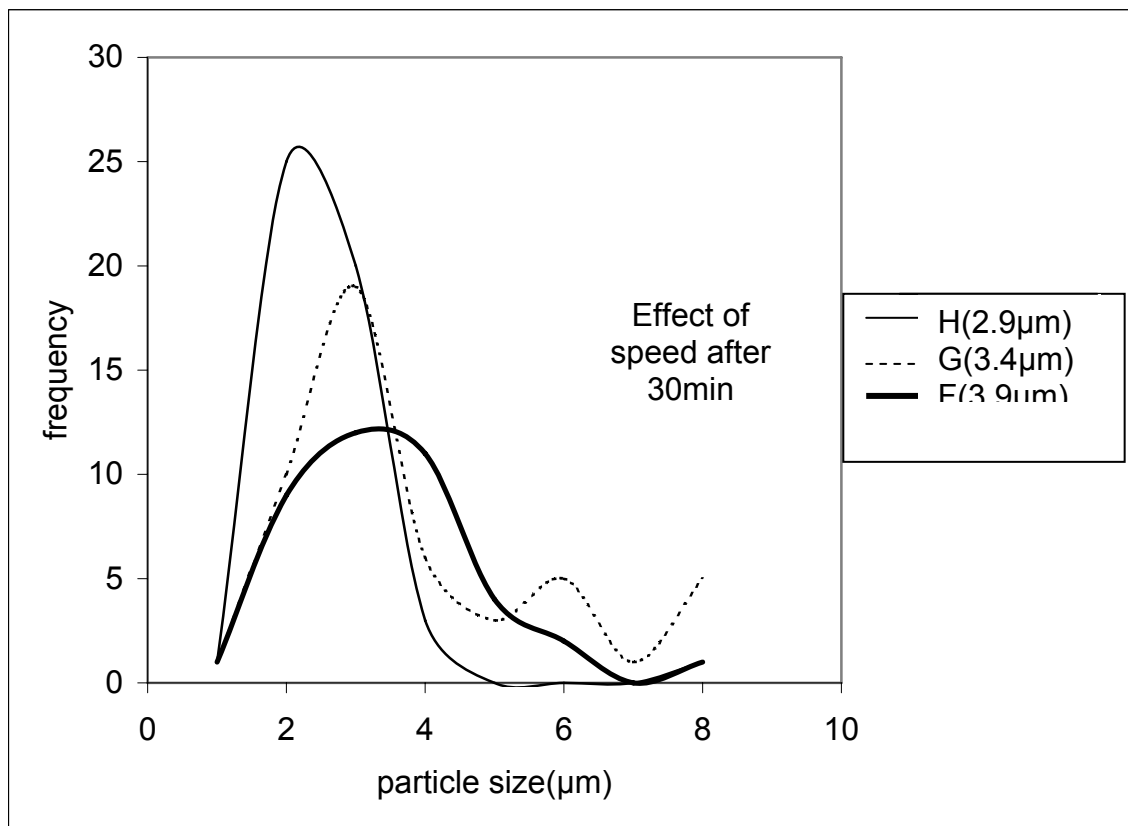


Figure 6.4 The effect of agitator speed (after thirty minutes of processing)

The mean particle sizes of the dispersions for batches F, G and H are all 3.7 μm . Therefore speed does not have an effect upon the particle size and particle size distribution for long processing times.

6.3 The particle size profile for the dispersion of steopac talc

The trend lines of mean particle size for batches F, G, and H are shown in the graph of Figure 6.5.

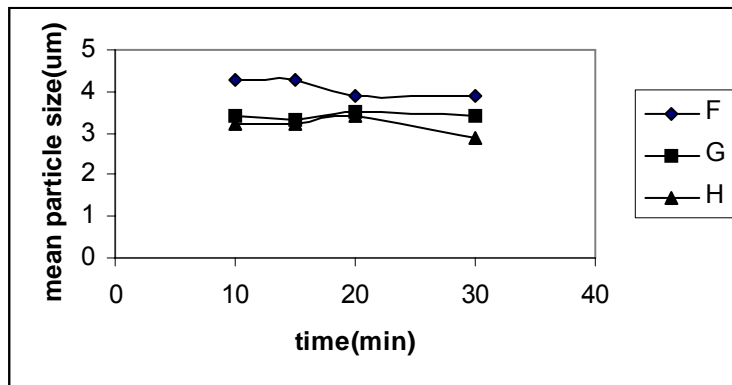


Figure 6.5 The change in particle size for steopac talc batches F, G and H with time.

Figure 6.5 shows that the particle size decreases as the processing time is increased for all three batches. Batches G and H have a small increase in the mean particle size after twenty minutes of processing. This is due to experimental error. It would have been expected that the particle sizes after twenty minutes would have been lower than those after fifteen minutes of processing. For similar processing times, the order of decreasing mean particle size is Batch F > G > H. The shear stress acting on the steopac talc particles increases with the speed of agitation. Since batch F is subjected to the lowest speed of agitation it is expected that its mean particle size would be the smallest. On the other hand batch H is subjected to the largest agitator speed and it is expected that its mean particle size is the smallest among the three batches processed. Finally, batch G is subjected to an intermediate agitator speed and its mean particle size lies between that of batch F and H.

6.4 The evaluation of the contrast ratio of batches F, G and H

The contrast ratio for batch F, G and H are shown in Table 6.2. The corresponding mean particle sizes are shown in table 6.3.

Table 6.2 Changes in contrast ratio with processing time for steopac talc

| Time (min) | CR(batch F) | CR(batch G) | CR(batch H) |
|------------|-------------|-------------|-------------|
| 10 | 0.946 | 0.947 | 0.946 |
| 15 | 0.950 | 0.948 | 0.947 |
| 20 | 0.951 | 0.951 | 0.951 |
| 30 | 0.951 | 0.951 | 0.951 |

Table 6.3 The mean particle sizes corresponding to the contrast ratios in table 6.1

| Time(min) | Particle size(batch F) | Particle size(batch G) | Particle size(batch H) |
|-----------|------------------------|------------------------|------------------------|
| 10 | 4.3 μ m | 4.3 μ m | 3.2 μ m |
| 15 | 4.3 μ m | 3.3 μ m | 3.2 μ m |
| 20 | 3.9 μ m | 3.5 μ m | 3.4 μ m |
| 30 | 3.9 μ m | 3.4 μ m | 2.9 μ m |

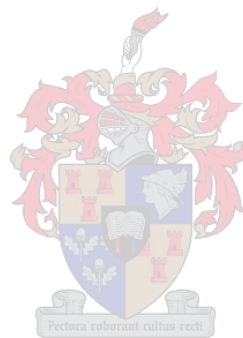
Table 6.2 shows that the contrast ratio is essentially not affected by the speed of the agitator or processing time. The values of reflectance of black substrate and white substrate used for calculating the above contrast ratios are shown in appendix D2. The mean particle sizes that correspond to the contrast ratios in table 6.2 are shown in table 6.3. The contrast ratios do not show much variation since the changes in the mean particle size, which affects contrast ratio are small. Table 6.3 includes values of mean particle sizes that correspond to the contrast ratios shown in table 6.1. Table 6.2 shows that there is an increase in the contrast ratio with processing time at all the speeds investigated. This was expected. However, it is not in agreement with the mean particle sizes for batches G and H after twenty minutes of processing. It was expected that the contrast ratio would decrease in batches G and H after 20 minutes of processing. Since this did not happen, it confirms that there was an error in the particle size determination for batches G and H after twenty minutes of processing.

6.4.1 The correlation for contrast ratio

The correlations of contrast ratio and flocculation gradients are expected to be similar to their counterparts for the dispersion of titanium dioxide in a Cowles mill. Therefore correlations based on multiple linear regression are proposed. The difference between correlations for titanium dioxide and steopac talc for dispersion in a Cowles mill would lie

in the magnitude of the coefficients. The coefficients for particle size in correlations for contrast ratio and flocculation gradient for steopac talc are expected to be close to zero.

The effect of agitator diameter was not evaluated separately in this section since it is similar to that for speed. The scanning electron micrographs, particle size distributions for batch J, are shown in appendix C.2. The change in contrast ratio for batch J is shown in appendix D.2.4. Chapter 7 evaluates the effect of homogenisation on a dispersion of titanium dioxide.



Chapter 7 Results and Discussion – Homogenisation of Titanium Dioxide

The results for the dispersion in a homogeniser are evaluated in this section. They include the evaluation of the effect of:

- i. Flow rate on homogenisation;
- ii. Spindle diameter on homogenisation.

In the experimental design carried out in chapter 4, it had been anticipated that more variables would be investigated. The number of variables to be analysed was reduced when it became apparent that the levels involved did not differ significantly. The initial focus is on the effect of the above variables on the evolution of mean particle size and size distribution during processing in terms of the mechanism proposed by Flourey *et al.* (2004).

7.1 Results and discussion – evaluation of dispersion in the homogeniser

The formulation of the titanium dioxide dispersion used for dispersion in the homogeniser is the same as that presented in the results and discussion section for dispersion in a Cowles mill. However, the homogeniser uses dispersion processed using the Cowles mill as its feed. A diagram of the plunger geometry is shown in appendix B.2. Table 7.1 shows the important dimensions for the designs that were investigated.

Table 7.1 The major dimensions for designs A - E of titanium dioxide dispersions

| Design | Level of spring back pressure | Valve diameter D (mm) | Flow rate Q (ml/s) |
|--------|-------------------------------|-----------------------|--------------------|
| A | Low | 0.7 | 0.54 |
| B | Low | 0.7 | 2.67 |
| C | Medium | 1.4 | 0.92 |
| D | Medium | 1.4 | 1.67 |
| E | High | 1.1 | 1.38 |

Designs A and B have a similar geometry. However, the plunger was set at a high speed level in design B while it was set at a low level in design A.

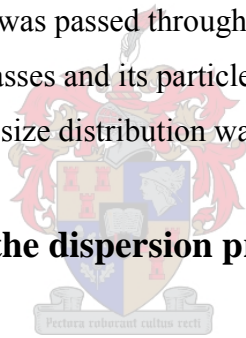
The flow within the homogeniser can be characterised using flow curves. However, these flow curves were unavailable for the study of the homogeniser. An estimate of the flow conditions can be obtained from measurements obtained using the Krebbs-Stormer viscometer. The shear rate in the homogeniser required for this calculation is given below.

$$\dot{\gamma} = \frac{4Q}{\pi d^3} \quad 7.1$$

The Reynolds numbers obtained for designs A and B are 1.59×10^{-3} and 1.83×10^{-3} respectively. These are very small and do not make much sense and will not be used for explanation of the homogenisation process.

For each design the dispersion was passed through the homogeniser ten times. A sample was collected after every two passes and its particle size was analysed using the scanning electron microscope. A particle size distribution was then obtained for each sample.

7.2 The effect of flow rate on the dispersion process



The effect of flow rate is investigated in this section. Designs A and B were used to evaluate the effect of the flow rate on homogenisation. The designs A and B are similar, except for their flow rates (Table 7.1). The flow rate for design B is 2.67ml/s, while that for design A is 0.57ml/s.

7.2.1 Effect of flow rate after two passes

The particle size distributions that correspond with the process after two passes are shown in Figure 7.1.

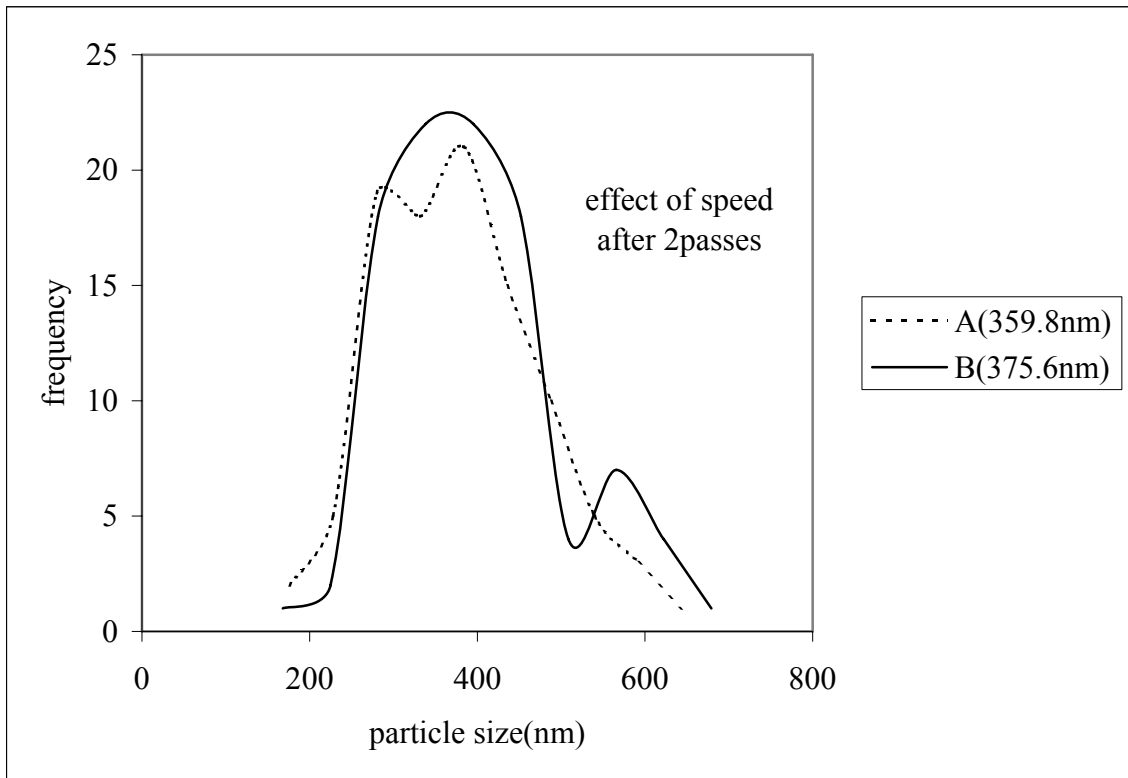


Figure 7.1 The effect of flow rate through the homogeniser after two passes.

The particle size distributions after two passes are similar for designs A and B and the mean particle sizes are 359.8nm and 375.6nm for designs A and B, respectively. The corresponding micrographs show that some particle stretching occurs in design B. Both designs exhibit some agglomerates.

Stretching in design B indicates that when the dispersion is in the homogeniser spindle for two passes, its particles re-agglomerate. On the other hand, the agglomerates that are processed through design A break up.

7.2.2 Effect of flow rate after four passes

The particle size distributions after four passes are shown in Figure 7.2.

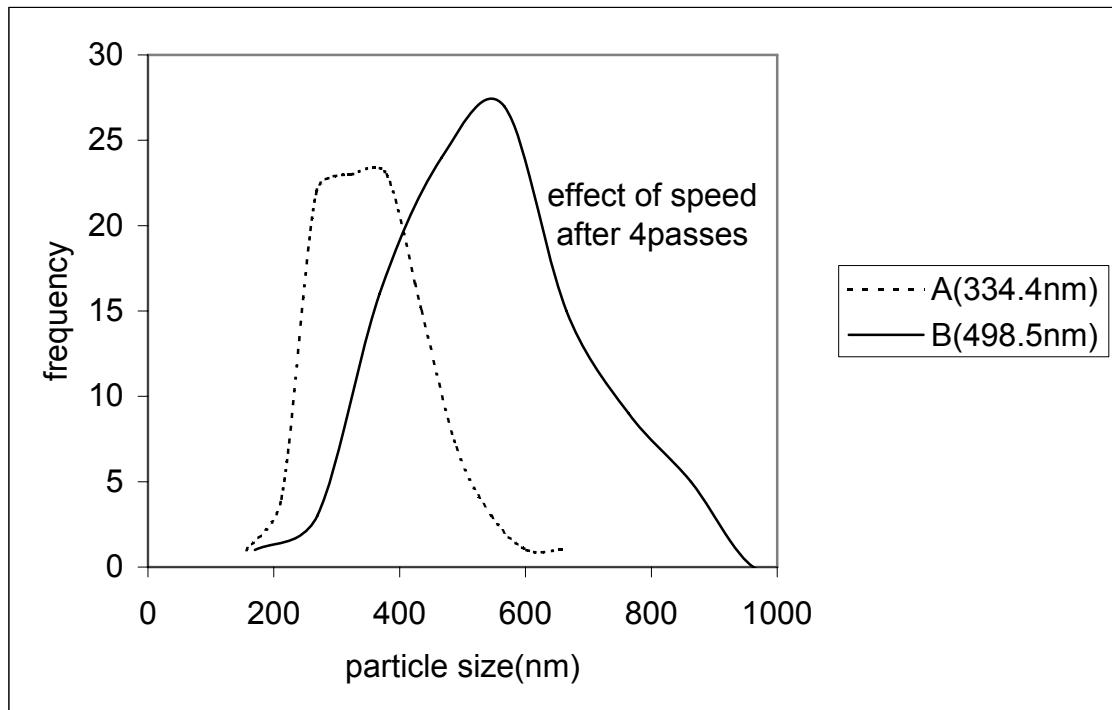


Figure 7.2 The effect of flow rate through homogeniser after 4 passes

The distribution for design B is broader than that for design A. This shows that design B has a wider range of particle sizes than design A and this can be confirmed from the micrographs in which design B exhibits a larger fraction of agglomerates than design A. The mean particle size for design A is 334.4nm, while that for design B is 498.5nm. Therefore design A exhibits more particle breakdown than design B. Furthermore, the mean particle size for design A decreased when the number of passes was increased to four, while this was the opposite for design B.

The changes in particle size for designs A and B show that the mechanisms of dispersion are different. The behaviour of agglomerates processed through design B after passing through the homogeniser for four passes is the same as that for two passes. the agglomerate size increases. on the other hand the size of agglomerates processed through design A decrease in size, which is the same trend as for two passes.

7.2.3 The effect of flow rate after six passes

The particle size distribution after six passes is shown in Figure 7.3.

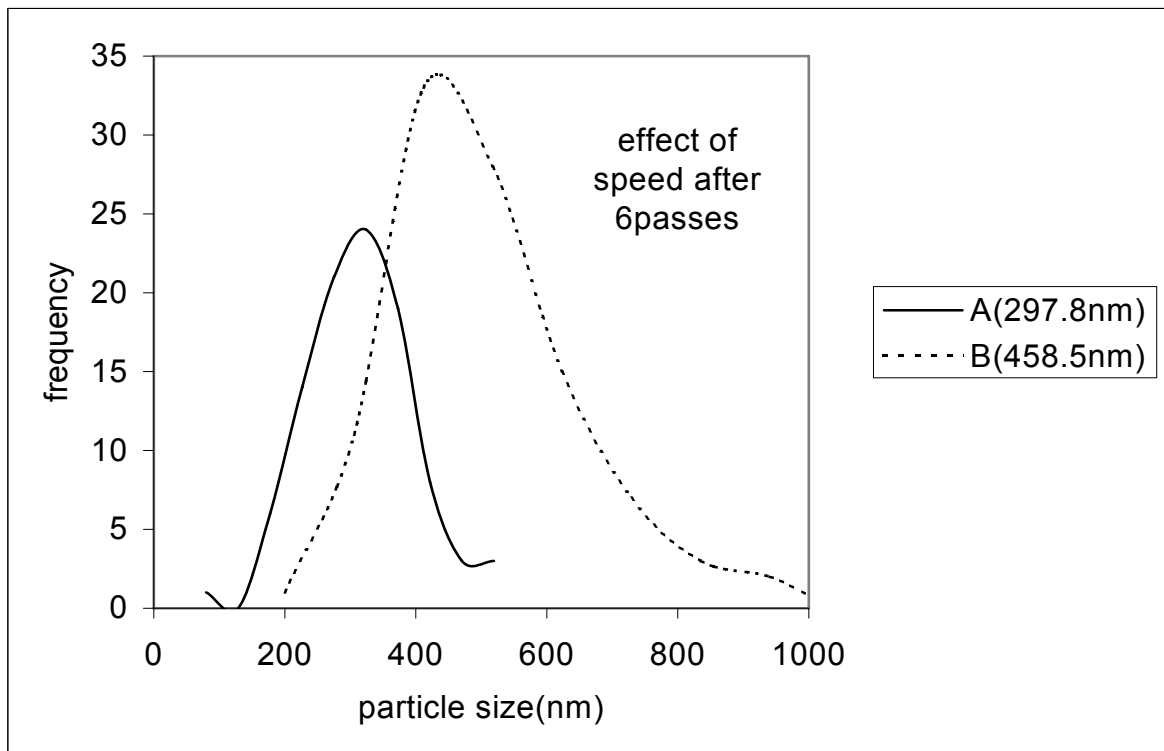


Figure 7.3 The effect of flow rate through the homogeniser after six passes.



The mean particle sizes for batches A and B are 297.8nm and 458.5nm respectively. When the above particle size distributions for six passes are compared to those for four passes, it can be noted that the trends are similar. For batch B, further re-agglomeration occurred in the re-circulation zone through collisions caused by back-mixing. In the case of batch A, further particle break down occurred through eddy and cavitation mixing.

7.2.4 The effect of flow rate after eight passes

The particle size distribution after eight passes is shown in the graph of Figure 7.4.

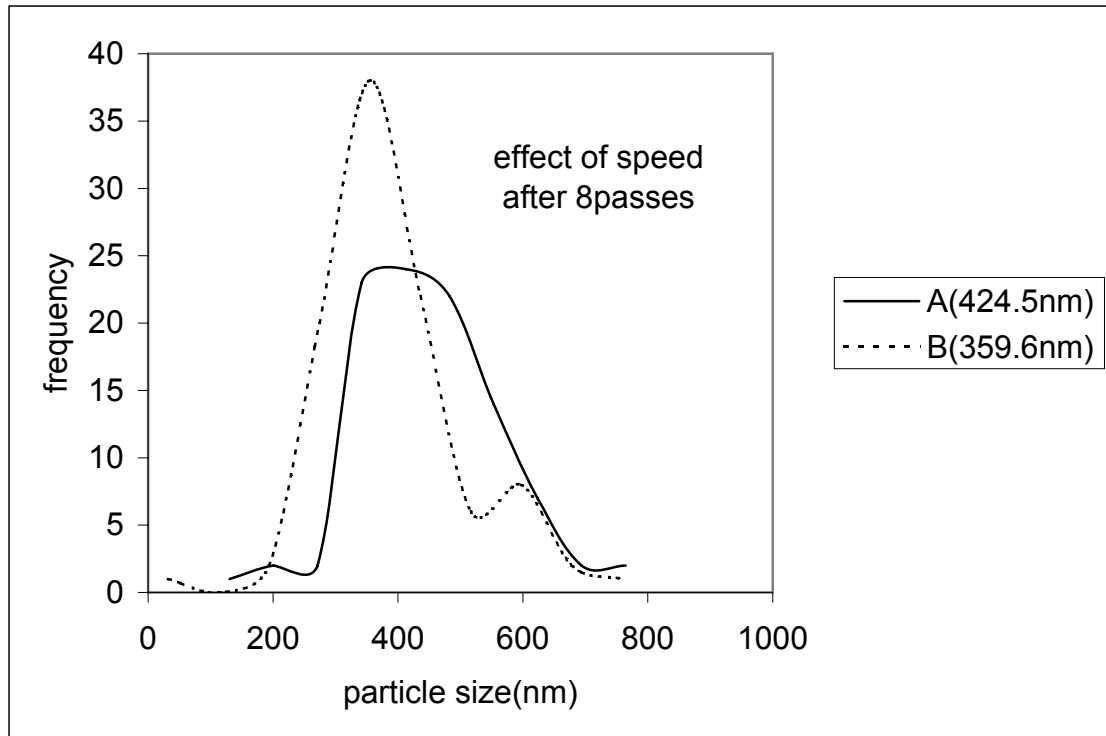


Figure 7.4 The effect of flow rate through the homogeniser after eight passes.

The mean particle size for design A (424.5nm) is now larger than for design B (359.6nm). The corresponding micrographs show that stretching occurs for design A and this explains the sudden increase in the fraction of agglomerates. However, the micrograph for design B shows a reduction in the fraction of agglomerates. The trends observed after eight passes are the opposite of those observed after four and six passes. This sudden change in the trends cannot be explained through the mechanism of Flourey *et al.*(2004).

7.2.5 The effect of flow rate after ten passes

The mean particle sizes for batches A and B are 357.4nm and 489.4nm respectively as shown in figure 7.5. The micrographs show that after ten passes the particles for design B

are stretched and this is due to extensional flow that occurs when flow approaches the inlet of the constriction in to the homogeniser spindle. The flow then passes through the remaining portion of the homogeniser spindle without further break down.

On the other hand, the mean particle size for design A after ten passes is 357.4nm, which is lower than the mean particle size for the same design after eight passes. Therefore particle break down occurred between eight and ten passes. This indicates that further particle break down occurs through eddy and cavitation mixing at the exit of the spindle.

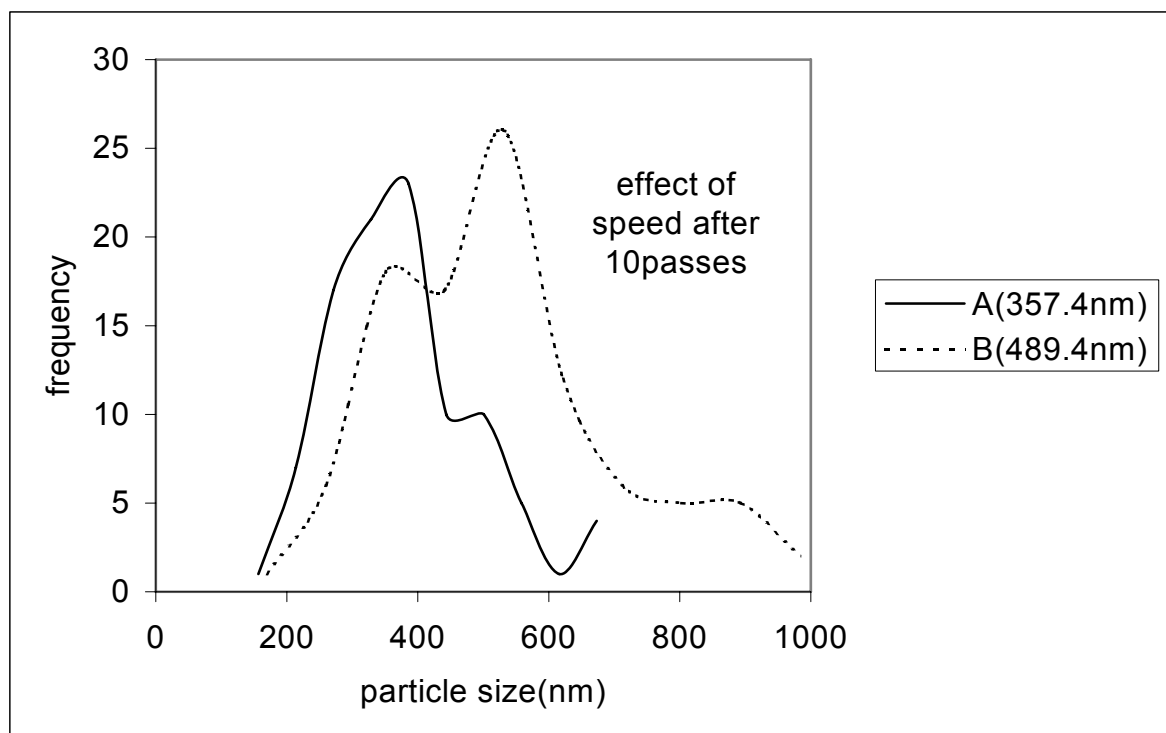


Figure 7.5 The effect of flow rate after ten passes through the homogeniser.

7.2.6 The effect of flow rate on the particle size profile for the dispersion of titanium dioxide

There are two different trends observed for the different flow rates. At the high flow rate, batch B, There is an initial increase in the mean particle size between two and six passes. This is followed by a reduction in the mean particle size between six and eight passes. Finally there is an increase in particle size between eight and ten passes. The first increase in particle size corresponds to re-agglomeration of particles. These agglomerates reach a

large particle size where they become unstable and break up between six and eight passes. For batch A, the agglomerates break up between two and four passes produces finer particles, which progressively become unstable. Between six and eight passes, the finer particles start to re-agglomerate.

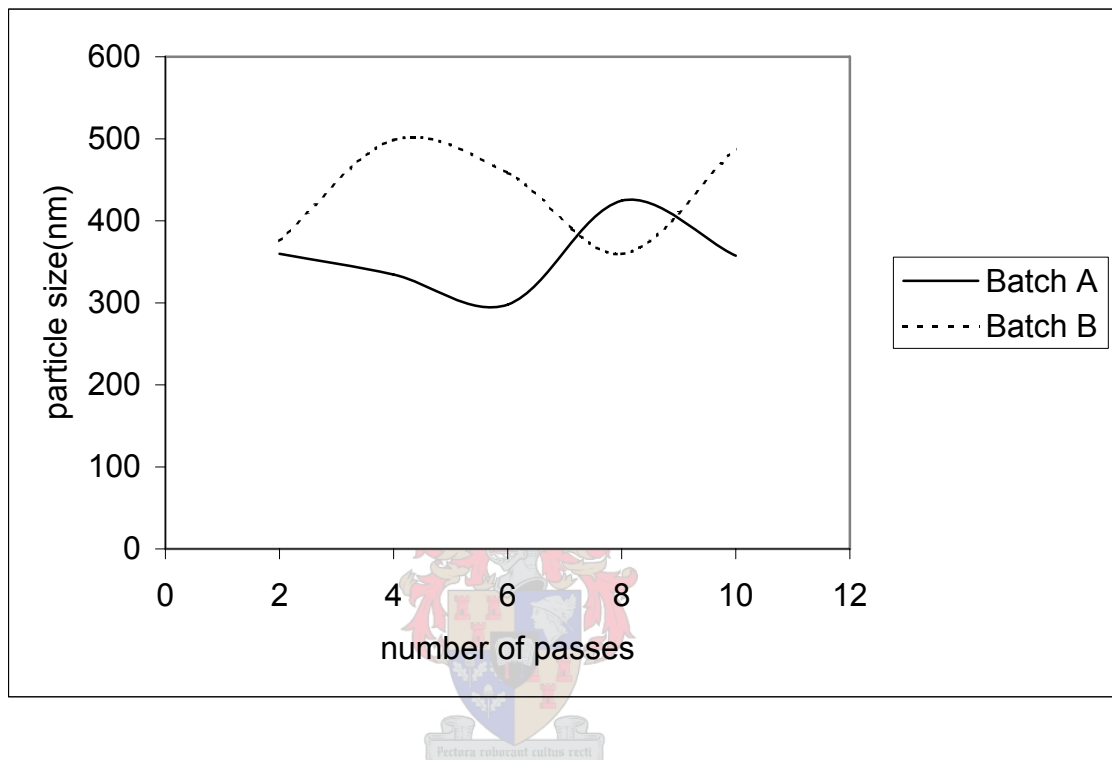


Figure 7.6 The effect of flow rate on particle size of batches A and B passed through the homogeniser.

The mechanism proposed by Flourey *et al.*(2004) does not fully explain the changes in mean particle size as the flow rate is increased. This mechanism does not explain why maximum and minimum particle sizes occur between two and ten passes.

7.3 The contrast ratio for designs A and B

The expected changes in the contrast ratio for the processing of dispersion from designs A and B were provided in the section on the evaluation of the mechanism. This section

evaluates the experimental contrast ratio and the possible correlations that could have been used. The contrast ratio for designs A and B appear in Tables 7.3 and 7.4.

Table 7.3 Contrast ratio and particle size changes during homogenisation of batch A

| Passes | CR(batch A) | CR(batch B) |
|--------|-------------|-------------|
| 2 | 0.978 | 0.973 |
| 4 | 0.979 | 0.967 |
| 6 | 0.983 | 0.968 |
| 8 | 0.975 | 0.970. |
| 10 | 0.978 | 0.970 |

Table 7.4 The mean particle size for batches A and B

| Passes | Mean particle size(nm) for batch A | Mean particle size(nm) for batch B |
|--------|---------------------------------------|---------------------------------------|
| 2 | 359.8 | 375.6 |
| 4 | 334.4 | 498.5 |
| 6 | 297.8 | 458.5 |
| 8 | 424.5 | 359.6 |
| 10 | 357.4 | 489.4 |

Table 7.3 shows the changes in the contrast ratio with the number of passes. Table 7.4 shows the corresponding mean particle sizes that occur with the number of passes. Table 7.4 can be used with table 7.3 to explain the changes in the contrast ratio in terms of particle size. In general, the contrast ratios in table 7.3 are in agreement with the changes in the mean particle size for batch A. However, the agreement in the change in contrast ratio and mean particle size is not as good as that for batch A. this indicates that there was some fair amount of error in either the instrument for contrast ratio or particle size analysis.

The mean particle size increases between two and six passes for batch B and this is accompanied by a reduction in the contrast ratio. According to the light scattering theory, the contrast ratio must decrease when the mean particle size increases. There is a reduction in the particle size between six and eight passes, however the contrast ratio for batch B

remains constant. This was not expected and indicates an experimental error. The increase in mean particle size between eight and ten passes resulted in a reduction in the contrast ratio. Such a reduction in contrast ratio when the mean particle size increased was expected on the basis of the light scattering theory.

In the case of batch A, the changes in the contrast ratio are in agreement with the changes in the mean particle size. When the mean particle size drops between two and six passes, the contrast ratio increases. Between six and eight homogeniser passes for batch A, during which the mean particle size increases, a reduction in the contrast ratio occurs. This reduction in contrast ratio was expected on the basis of the light scattering theory, which predicts that the contrast ratio becomes smaller when the mean pigment particle size increases. An increase in the contrast ratio occurred between eight and ten passes and was expected since a reduction in the mean particle size occurred in this range.

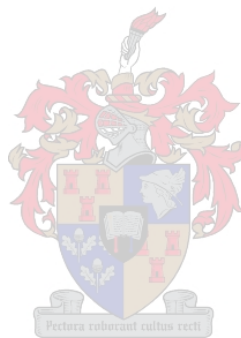
In general, the contrast ratios for batch A are higher than those for batch B after the same processing times. This was expected since the mean particle sizes for batch A are in general lower than those for batch B. the contrast ratios for batch A are generally larger than those for the dispersion of titanium dioxide through a Cowles mill. This was expected since the mean particle sizes for batch A are in general lower than those for the Cowles mill. In a similar manner, the contrast ratios for batch B are in general lower than those for the dispersion of titanium dioxide through a Cowles mill and this was expected on the basis of the large mean particle sizes for batch B.

The contrast ratios for the other batches that were homogenised are in appendix D.3. It can be seen that the changes that were used to manipulate particle size exerted a marginal influence on the contrast ratio. However, it can be noted that contrast ratio is logarithmic hence the marginal changes observed. In order to observe greater influence of process variables on the contrast ratio, it is necessary to formulate pigment dispersions with a lower pigment volume concentration.

7.4 The correlation of contrast ratio

The procedure for correlating contrast ratio described in chapter 5 applies in this section. Therefore it is not necessary to explain the correlation for contrast ratio using a homogeniser as it has the same form as that used for the Cowles mill.

The correlations for contrast ratio for dispersion processed with a Cowles mill and a homogeniser would differ in the coefficients. The coefficients for the correlation of contrast ratio based on the homogeniser are expected to be larger than that corresponding to the Cowles mill. This is due to the smaller particle size and distribution in the homogeniser.



Chapter 8 Results and Discussion – Blending of Dispersions

The results obtained during the blending of titanium dioxide and steopac talc or kulu 2 dispersions are discussed in this section.

8.1 Effect of extender on optical properties of titanium dioxide dispersions

The effect of the pigment volume concentration of extender on the contrast ratio and flocculation gradient of a dispersion of titanium dioxide extender is evaluated in this section. The extenders dispersions that were used are steopac talc and kulu 2.

The titanium dioxide dispersion was prepared using the formulation that was presented earlier. The formulation of the titanium dioxide dispersion has a pigment volume concentration of 37.2percent. A speed of 30Hz was used to prepare the dispersion.

Batches of steopac talc and kulu 2 were prepared in separate Cowles mills. The formulations used for the preparation of the batches of the steopac talc and kulu 2 are presented appendix A.3 and A.4 respectively. Agitator blades used for preparing the dispersions had a diameter of 0.1m and were operated at a speed of 35Hz.

8.1.2 preparation of blends of titanium dioxide and steopac talc of different compositions

The preparation and properties of the blend between titanium dioxide and steopac talc are provided in Table 8.1. The preparation of blend between titanium dioxide and extender dispersions always started with 6.829kg of titanium dioxide dispersion. The pigment volume concentration of titanium dioxide in the blend was reduced by successively increasing the mass of extender. The resulting blend had a lower pigment volume concentration of titanium dioxide but a higher pigment volume concentration of extender. The calculation of the pigment volume concentration of the blend between dispersions of titanium dioxide and steopac talc using the second row as an example is shown below.

Table 8.1 Preparation and optical properties of blend between dispersions of titanium dioxide and steopac talc

| | | P.V.C.(TR 93) | | P.V.C. (Talc) | | P.V.C R _B (%) | | |
|----------|----------|---------------|------|---------------|--------------------|--------------------------|-----------|--------|
| TR93(kg) | Talc(kg) | % | % | % | R _w (%) | C.R | F.G(%/μm) | |
| 6.829 | 0 | 37.2 | 0 | 37.2 | 96.79 | 98.97 | 0.978 | 0.9777 |
| 6.829 | 0.342 | 33.7 | 4.3 | 38 | 96.68 | 98.96 | 0.977 | 0.9854 |
| 6.829 | 0.683 | 30.7 | 7.8 | 38.5 | 96.48 | 98.95 | 0.975 | 1.0634 |
| 6.829 | 1.366 | 26.2 | 13.4 | 39.6 | 96.26 | 98.93 | 0.973 | 1.1299 |
| 6.829 | 2.049 | 22.8 | 17.4 | 40.2 | 95.97 | 98.94 | 0.970 | 1.2336 |

Where:

- TR 93 Titanium dioxide
R_B Percentage reflectance over a black substrate;
R_w Percentage reflectance over a white substrate;
C.R Contrast ratio;
F.G Flocculation gradient.

Titanium dioxide dispersion (6.829kg) was blended with steopac talc dispersion (0.3415kg). The density of a dispersion of steopac talc is 1.0082 kg/litre. Therefore the volume of the steopac talc dispersion is 0.339litres. The percentage of pigment in the steopac talc dispersion is 49.14 percent. Therefore the mass of steopac talc dispersion is 0.4914*0.342kg, which is equivalent to 0.1678kg. The density of steopac talc pigment is 1.1kg/litre. Therefore the volume equivalent to 0.3415kg of steopac talc dispersion is (0.3415/1.1)litres, that is 0.153litres. A similar calculation can be done for the 6.829kg of titanium dioxide dispersion used with a solid content of 70.1 percent, and a pigment density of 4.0kg/litre. The resultant volume occupied by titanium dioxide pigment is 1.196litres. The volume occupied by 6.829kg of the titanium dioxide dispersion is 3.214litres given that its density is 2.124kg/litre.

If it is assumed that there is no change in the enthalpy of mixing, the total volume of the blend between dispersions of titanium dioxide and steopac talc is the sum of their individual volumes, which is equivalent to 3.553litres.

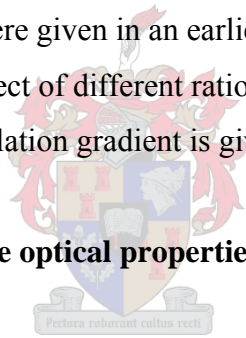
The volumes of pigment in the separate dispersions were given above as:

- i. 1.196litres for the dispersion of titanium dioxide;
- ii. 0.153litres for the dispersion of steopac talc.

The pigment volume concentration in a blend of titanium dioxide and steopac talc is obtained by dividing the individual pigment volumes by the total volumes. This is equivalent to pigment volume concentrations of 33.7 percent for titanium dioxide and 4.3 percent for steopac talc in the blend.

The sequence of calculations that was presented above can be repeated for the different ratios of titanium dioxide to steopac talc dispersions that were used in this project. The results of these calculations are shown in Table 8.1. The same table gives the corresponding contrast ratios and flocculation gradients. However, the calculations for the contrast ratio and the flocculation gradient were given in an earlier section and are not presented here again. The evaluation of the effect of different ratios of pigment volume concentration on the contrast ratio and the flocculation gradient is given below.

8.1.3 The effect of steopac talc on the optical properties of titanium dioxide



When the pigment volume concentration of titanium dioxide is reduced, by increasing the pigment volume concentration of steopac talc, the contrast ratio increases as shown in table 8.1. This is agreement with theory since the two minerals; titanium dioxide and steopac talc have different refractive indices. Titanium dioxide has a higher refractive index than steopac talc and it exhibits a larger contrast ratio than steopac talc. Therefore replacing titanium dioxide with a mineral of lower refractive index is expected to reduce the overall contrast ratio. The reduction in contrast ratio that is observed when the pigment volume concentration of titanium dioxide is reduced is accompanied by an increase in the flocculation gradient of the blend. This is expected from theory since a reduction in contrast ratio must be accompanied by an increase in flocculation.

8.1.4 The effect of kulu 2 on the optical properties of titanium dioxide

Table 8.2 presents the contrast ratio and flocculation gradients corresponding to the different pigment volume concentrations that were investigated. The preparation of the blend between dispersions of titanium dioxide and kulu 2 is similar to that presented for a blend between titanium dioxide and steopac talc.

Table 8.2 Preparation and optical properties of blend between dispersions of titanium dioxide and kulu 2 calcite

| TR93 (kg) | Kulu 2 (kg) | P.V.C. (TR 93) (%) | P.V.C. (kulu2) (%) | P.V.C (%) | R _B (%) | R _w (%) | C.R | F.G (%/μm) |
|--------------|----------------|-----------------------|-----------------------|--------------|-----------------------|-----------------------|-------|---------------|
| 6.829 | 0 | 37.2 | 0 | 37.2 | 96.63 | 98.80 | 0.978 | 0.9728 |
| 6.829 | 0.66 | 33.1 | 4.3 | 37.4 | 96.50 | 98.77 | 0.977 | 0.9797 |
| 6.829 | 1.35 | 29.7 | 7.8 | 37.5 | 96.18 | 98.75 | 0.974 | 1.0559 |
| 6.829 | 2.80 | 24.5 | 13.4 | 37.9 | 95.89 | 98.75 | 0.971 | 1.1180 |
| 6.829 | 4.30 | 20.7 | 17.4 | 38.1 | 95.60 | 98.76 | 0.968 | 1.1758 |

The trends that are observed for a blend between titanium dioxide and kulu 2 are similar to those for a blend between steopac talc and titanium dioxide dispersions. When the pigment volume concentration of titanium dioxide is reduced from 37.2 to 20.7, the contrast ratio decreases from 0.978 to 0.968. This trend is in agreement with theory since the reduction in the pigment volume concentration of titanium dioxide is achieved through replacement with a mineral of lower refractive index. The reduction in contrast ratio when the pigment volume concentration of titanium dioxide is reduced is accompanied by an increase in the flocculation gradient. This was expected since a reduction in contrast ratio is equivalent to an increase in the flocculation gradient.

When the contrast ratios of blend dispersions prepared with steopac talc and kulu 2 are compared, it is noted that they are similar. The contrast ratio is affected by:

- i. The pigment volume concentration of titanium dioxide and extender;
- ii. The mean particle size of the extender.

It can be noted that at the same pigment volume concentration of kulu 2 and steopac talc, kulu 2 causes a larger reduction in the pigment volume concentration of titanium dioxide. This large reduction in the pigment volume concentration that occurs with the addition of kulu 2 to titanium dioxide is due to the large density of kulu 2 compared to that of steopac talc. The effect of kulu 2 on the contrast ratio is based on pigment volume concentration and its smaller mean particle size compared to steopac talc. On the basis of pigment volume concentration, blends of kulu 2 are expected to exhibit a lower contrast ratio. However, the mean particle size of kulu 2 is smaller than that of steopac talc meaning that it should result in a larger contrast ratio than steopac talc. When these two effects are combined, the result is that blends of titanium dioxide with either kulu 2 or steopac talc have similar contrast ratios.

According to the theory presented in Chapters 2 and 3, the flocculation gradient in a dispersion of titanium dioxide that was blended with extender increases with the particle size of the extender. Since the mean particle size of steopac talc is larger than that of kulu 2, it is to be expected that the flocculation gradient for steopac talc should be larger than that for kulu 2. However, this expected trend was not entirely observed in the range of investigation. The discrepancy could be due to experimental error or the unreliability of the measurement of flocculation gradient as explained in chapter 5.



8.1.5 Correlating flocculation gradient of titanium dioxide dispersions blended with extender

The discussion above clearly shows that there is a need to correlate the flocculation gradient with:

- i. Pigment volume concentration of titanium dioxide in a blend, Y_0 ;
- ii. Pigment volume concentration of extender in a blend, Y_j ;
- iii. Mean particle size of titanium dioxide, a_0 ;
- iv. Mean particle size of extender, a_j .

Subscript j refers to the extender, which could be steopac talc, kulu 2 or any other extender. More than one or two extenders can be used to develop the correlation. In developing the correlation the assumptions that apply are:

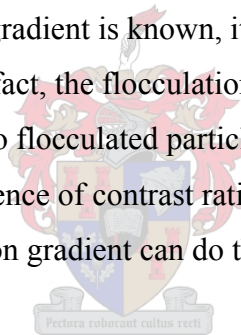
- i. Interactions between particles are assumed to be between the same mineral;
- ii. The refractive indices of blend and titanium dioxide dispersion are similar.

The multi-linear correlation of the form shown below would have been fitted on the flocculation gradient data:

$$F.G = c_0 + c_1 * y_0 + \sum_1^n a_j * y_j \quad 8.1$$

The above correlation would have been tested for auto-correlation. It is possible that the multilinear correlation could have failed to fit the data. In that case, some of the terms could have been raised to higher powers.

If a correlation of flocculation gradient is known, it becomes unnecessary to establish a correlation of contrast ratio. In fact, the flocculation gradient was defined to account for the reduction in contrast ratio due to flocculated particles in a pigment dispersion. Instead, it is necessary to establish a dependence of contrast ratio on flocculation gradient. Plotting contrast ratio against flocculation gradient can do this.



Chapter 9 Results and Discussion – Rheology of the dispersion Process

This section presents the results on the rheology of the dispersion process. It is limited to the rheology of the dispersion process of titanium dioxide using a Cowles mill. Three batches A1, A2 and A3 were used to investigate the rheological behaviour of titanium dioxide processed through a Cowles mill.

The formulation for preparing titanium dioxide dispersions specified in appendix A.2 was used. Batches of titanium dioxide dispersions were then prepared in a Cowles mill, whose dimensions are shown in appendix B.1. The agitator diameter was kept constant at 0.1m for all the batches. Agitator speeds of 30Hz and 35Hz were used for batches A1 and A2 respectively. Batch A3 was processed at an agitator speed of 30Hz but its dispersant level was reduced by fifty percent. Samples were withdrawn from the Cowles mill after ten, fifteen, twenty and thirty minutes of processing. The rheometer described in chapter 3 was used to prepare flow curves of the samples.

9.1 The effect of speed on the rheology of the dispersion process

Batches A1 and A2 were used to investigate the rheology of the dispersion process for titanium dioxide carried out in a Cowles mill. These flow curves were analysed for their appearance and structural behaviour.

9.1.1 The effect of speed on the titanium dioxide dispersion process.

9.1.1.1 The effect of speed after ten minutes of processing

Figure 9.1 shows the flow curves for batch A1 and A2 after ten minutes of processing. These flow curves show different behaviour under low and high shear rates. Table 9.1 shows the low shear rate flow values for batch A1 and A2.

Table 9.1 The effect of speed on titanium dioxide dispersions (10min)

| Effect of speed (10min) | A1(30Hz) | A2(35Hz) |
|---------------------------------|----------|----------|
| Shear rate(s^{-1}) | 385.7 | 529.8 |
| Shear stress(Pa) | 47.96 | 46.81 |
| Viscosity(Pa.s) | 0.1243 | 0.08834 |
| Mill speed(Hz) | 30 | 30 |
| Re | 48270.3 | 67919.4 |
| Mill temperature($^{\circ}C$) | 30 | 33 |
| Mean particle size(nm) | 416.2 | 403.9 |
| Particle size distribution(nm) | 663.6 | 457.1 |

The mean particle sizes for batch A1 and A2 are 416.2nm and 403.9nm respectively. The particle size distribution for the batches A1 and A2 are 663.6nm and 457.1nm. Batch A1 with the greater mean particle size and particle size distribution has a viscosity of 0.1243Pa.s while batch A2 has a viscosity of 0.08834Pa.s. The lower viscosity exhibited by batch A2 with respect to that for batch A1 is justified by theory since particles whose size do not differ significantly can readily overcome resistances to flow.



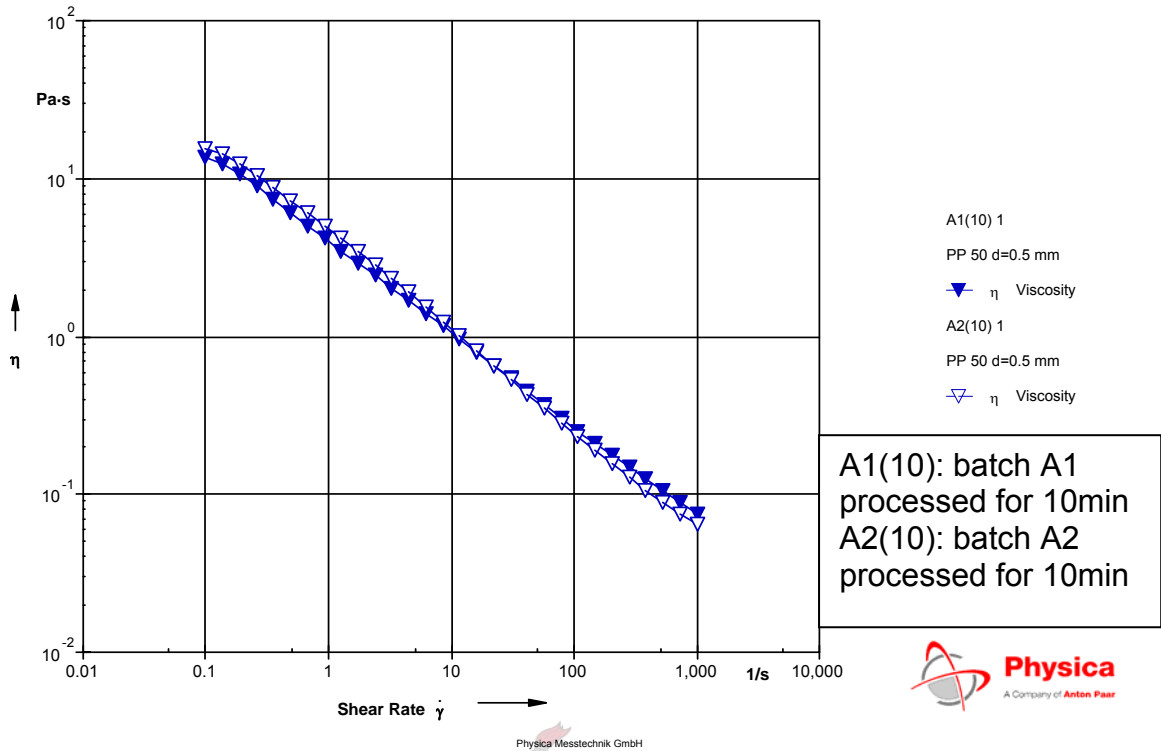


Figure 9.1 The effect of speed after ten minutes of processing

9.1.1.2 The effect of speed after twenty minutes of processing

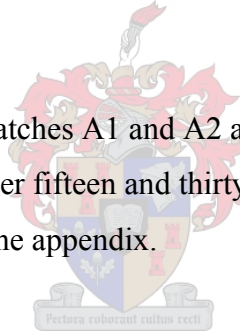
Figure 9.3 shows the flow curves for batch A1 and A2 after twenty minutes of processing. Table 9.2 shows the detailed rheological behaviour of batch A1 and A2 and complements the flow curves in figure 9.3.

The mean particle size after twenty minutes of processing for batches A1 and A2 are 393.1nm and 382.4nm respectively. The corresponding particle size distribution for batches A1 and A2 are 672.7nm and 636.4nm respectively. Therefore batch A2 processed at 35Hz has a lower mean particle size and distribution when compared to batch A1 processed at 30Hz. The viscosities of the batches A1 and A2 are 0.1286Pa.s and 0.08609Pa.s respectively. Batch A2 with the lower particle size and distribution corresponds to a lower value of viscosity compared to batch A1. This result was expected and it is in agreement with theory.

Table 9.2 The low and high shear rate behaviour of dispersion (20minutes of processing)

| Effect of speed (20min) | A1(30Hz) | A2(35Hz) |
|-----------------------------------|----------|----------|
| Shear rate(s^{-1}) | 385.7 | 529.8 |
| Shear stress(Pa) | 49.61 | 45.62 |
| Viscosity(Pa.s) | 0.1286 | 0.08609 |
| Mill speed(Hz) | 30 | 30 |
| Re | 46656.3 | 69694.5 |
| T($^{\circ}$ C) | 39 | 42 |
| Mean particle size(nm) | 393.1 | 382.4 |
| Particle size distribution(nm) | 672.7 | 636.4 |

The same trends observed for batches A1 and A2 after ten and twenty minutes of processing are also observed after fifteen and thirty minutes. The flow curves for these processing times are shown in the appendix.



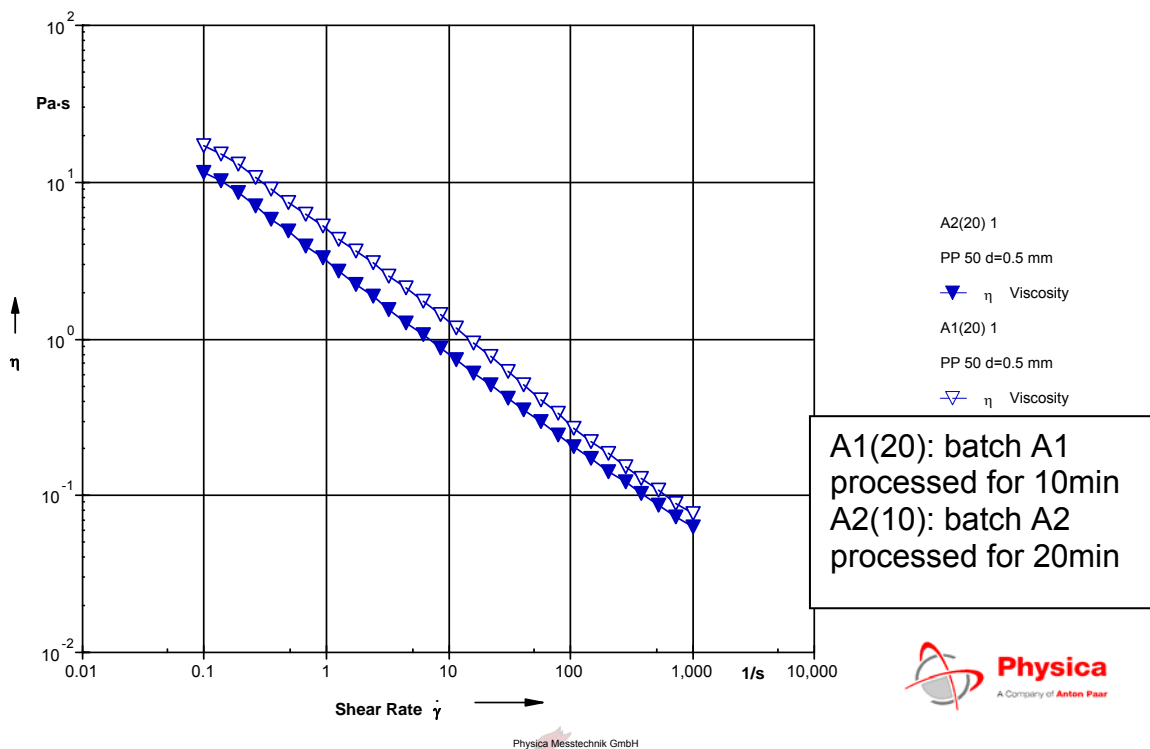


Figure 9.2 The effect on the rheology of the dispersion process after twenty minutes

9.1.2 Evaluation of the effect of dispersant

Batches A1 and A3 were processed at the same agitator speed. However, batch A3 contains fifty percent of the dispersant in batch A1. Batches A1 and A3 can be used to evaluate the effect of dispersant on the dispersion process. Flow curves were prepared for sample obtained from the mill after ten, twenty and thirty minutes of agitation. These flow curves exhibit a similar behaviour. The flow curve for twenty minutes of processing is discussed in detail and it is shown in figure 9.3 and its data is provided in table 9.3. The flow curves for ten and twenty minutes of processing are available in the appendix.

The viscosity of batch A1 is always lower than that for batch A3 at the same shear rates. However, the difference between the viscosities of the two flow curves decreases when the shear rate is increased. The high viscosities associated with batch A3 indicate that the pigment particles are poorly wetted compared to those for batch A1. This arises from the large fraction of agglomerates, which is mixed with a small fraction of fine particles. In

such a circumstance, large shear stresses must be applied in order to allow the small particles to slip past the large particles.

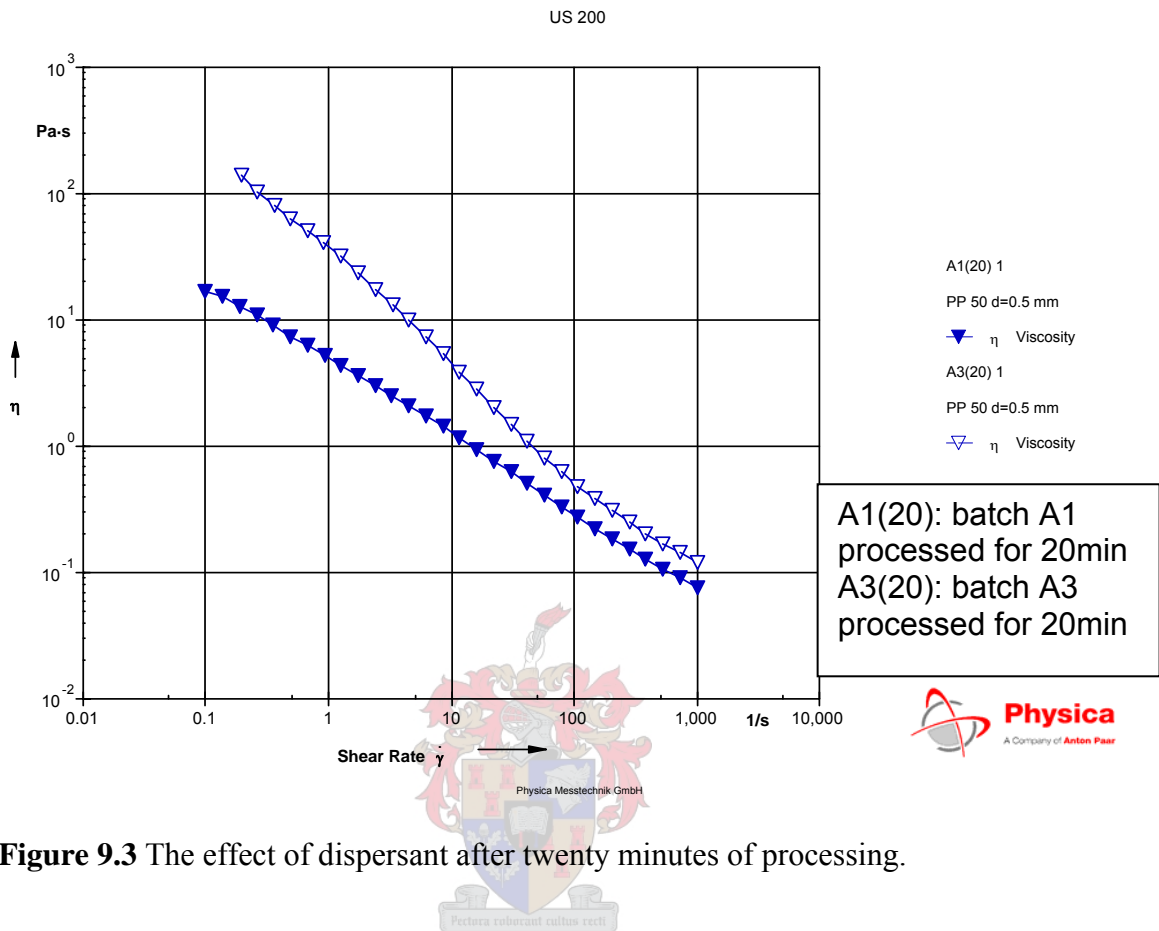


Figure 9.3 The effect of dispersant after twenty minutes of processing.

Table 9.3 The effect of dispersant on the dispersion process

| Effect of dispersant (10min) | Batch A1 | Batch A3 |
|---------------------------------|----------|----------|
| Shear rate(s^{-1}) | 385.7 | 385.7 |
| Shear stress(Pa) | 47.96 | 86.48 |
| Viscosity(Pa.s) | 0.1243 | 0.2242 |
| Mill speed(Hz) | 30 | 30 |
| Re | 48270.3 | 26761.8 |
| Mill Temperature($^{\circ}C$) | 30 | 34 |
| mean particle size(nm) | 416.2 | 458.5 |
| Particle size distribution(nm) | 663.6 | 681.8 |

Table 9.3 shows that at a shear rate of $385.7s^{-1}$, the viscosity of batch A1 is $0.1243Pa.s$ while that for batch A3 is $0.2242Pa.s$. Batch A3 contains fifty percent less dispersant than

batch A1. Since batch A3's viscosity is higher than that for batch A1, it confirms that batch A3 suffers from poor wetting compared to batch A1. therefore it contains a significant fraction of agglomerates than batch A1. As a result, fine particles are sandwiched between large particles making it difficult for the small particles to slip past the large particles. This slip resistance is manifested by a large value of viscosity in batch A3 than in batch A1.

9.1.3 Rheology of the dispersion process and particle size and distribution

The results and discussion of the effect of agitator speed and level of dispersant on the dispersion process show that the rheology changes when the mean particle size and particle size change. Flow curves for different flow and formulating conditions are different and are in agreement with theory. Therefore, rheology (flow curves should be used as an estimator of the level(degree) of dispersion.

9.2 The time dependent behaviour of Titanium dioxide dispersions

The time dependent behaviour of titanium dioxide dispersions was investigated using batch A1 sampled after thirty minutes of processing. The resultant flow curve is shown in figure 9.4. The dispersion is thixotropic. This figure shows that the storage modulus is always larger than the loss modulus. The storage modulus is a measure of the solid behaviour of the dispersion, while the loss modulus is a measure of the viscous behaviour of the dispersion. When the dispersion is sheared, its structure breaks after about hundred seconds. The structure starts to recover after break down. However, after three hundred seconds the dispersion has recovered up to about thirty percent of its original structure.

The time dependent behaviour of the dispersion after thirty minutes of processing exhibits a storage modulus, which is always larger than the loss modulus. This behaviour is undesirable in paint. Instead the loss modulus should be larger than the storage modulus.

US 200

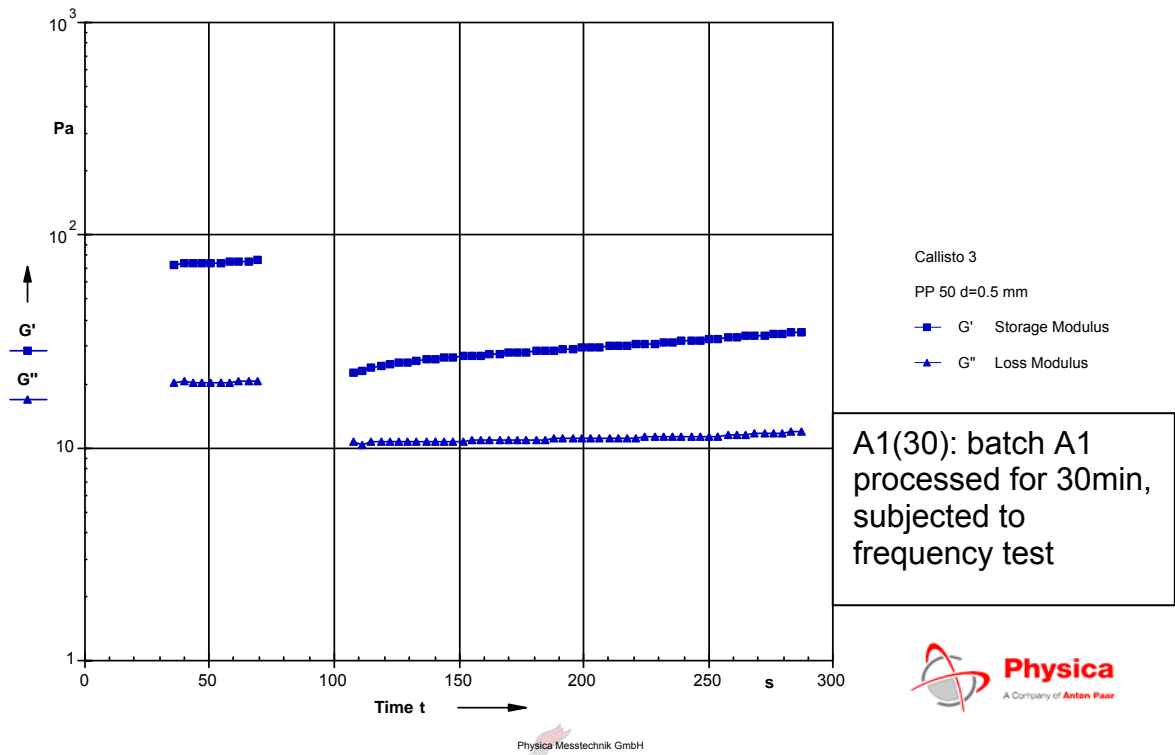


Figure 9.4 The time dependent behavior of titanium dioxide dispersions



Chapter 10 Conclusions

The conclusions of this research are presented in this section under the categories:

1. Literature review;
2. Experimental results of dispersion through the Cowles mill;
3. Experimental results of dispersion through the homogeniser;
4. Experimental results of the blending process;
5. Experimental results of the rheology of dispersion;
6. Recommendations.

10.1 Conclusions of the literature review

The conclusions pertaining to the theory of the dispersion process are presented below.

10.1.1 The mechanism of the dispersion process

The mechanism of the dispersion process involves four steps:

1. Pigment wetting;
2. Agglomerate breakdown;
3. Particle stabilisation against re-agglomeration;
4. Particle re-agglomeration.



Pigment wetting consists of the following three sub-processes:

1. Immersional wetting;
2. Adhesional wetting;
3. Spreading wetting.

Any or a combination of the above three wetting sub-processes could be limiting, depending on the formulation. The occurrence of wetting can be predicted from the contact angle.

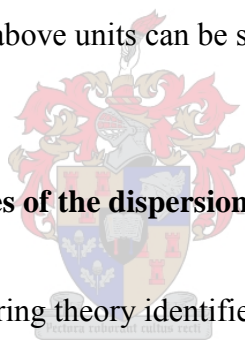
Particle break down is basically the overcoming of attractive van der Waals forces after which the freed particles must be stabilised against re-flocculation using a dispersant.

The homogeniser can be broken down into the following mixing units:

1. Entrance unit (extensional shearing);
2. Valve gap unit (laminar shearing);
3. Exit unit (eddy shearing, acoustic vibrations and recirculation).

The turbulence intensity plays an important role in defining the efficiency of particle breakdown due to cavitation. However, it promotes a side effect, namely recirculation of flow that causes re-agglomeration. An alternative parameter for evaluating the extent of cavitation is the cavitation number.

The processes occurring in the above units can be simulated using a computational fluid dynamics package.



10.1.2 The theory of optical properties of the dispersion process

The Kubelka-Munk light-scattering theory identifies the variables that affect the contrast ratio of a dispersion as:

1. Mean pigment particle size/state of the dispersion;
2. Particle size distribution;
3. Pigment volume concentration;
4. Wavelength of the incident radiation.

The flocculation gradient of a pigment dispersion is also affected by the above variables.

10.1.3 The theory of the rheology of dispersion

The viscosity of a dispersion depends upon:

1. Temperature of the dispersion;

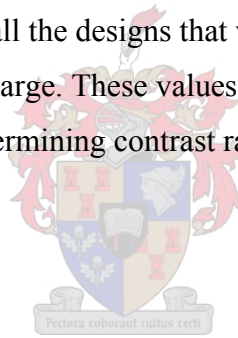
2. Mean pigment particle size;
3. Particle size distribution;
4. Particle shape;
5. Pigment volume concentration;
6. Shear rate.

The shear rate in an agitator is manipulated through the speed and diameter of the agitator, while it is manipulated through flow rate, spring back pressure or valve diameter in the homogeniser.

10.1.4 Application of the analytical techniques to the dispersion process

10.1.4.1 Contrast ratio

The contrast ratio obtained for all the designs that were investigated for all the sampling times or number of passes was large. These values did not reflect the changes in particle size and distribution. When determining contrast ratio, it is necessary to dilute samples with resin.



10.1.4.2 Flocculation gradient

The linear association for the graphs used to determine flocculation gradients were very low (R^2 values of about 0.75). The flocculation gradient method is thus unreliable and should not be used to quantify the level(degree) of dispersion.

10.1.4.3 Particle size analysis

More than a hundred particles should be counted in order for a reliable determination of particle size and distribution.

10.1.4.4 Flow curves

The flow curves for pigment dispersions show that:

- i. Flow is non-Newtonian;
- ii. The dispersions are shear thinning.

10.2 Conclusions for the experimental results

10.2.1 Dispersion of titanium dioxide through the Cowles mill

The mean particle size for titanium dioxide prepared at an agitator speed of 30Hz lies between 368.6nm and 433.4nm. The contrast ratio for at a speed of 30Hz lies in the range 0.974 to 0.978.

The mean particle size for titanium dioxide prepared at an agitator speed of 35Hz lies between 356.7nm and 413.6nm. The contrast ratio for at a speed of 30Hz lies in the range 0.973 to 0.985.

Increasing the speed of agitation causes an increase in the shear rate and thus the shear stress acting on the pigment particles. This results in an increase in particle break down and contrast ratio.

The flocculation gradients for an agitator speed of 35Hz lie in the range 1.6052 and 1.4824. However, there is a single value of flocculation gradient after fifteen minutes of processing that is larger than expected. The general trend is that an increase in the processing time leads to a reduction in the flocculation gradient.

The correlation of coefficient for the graph from which flocculation gradient is evaluated lies between 0.5957 and 0.8746. This suggests that flocculation gradient is an unreliable measure of the fraction of flocculated particles in a pigment dispersion.

10.2.2 Dispersion of steopac talc through the Cowles mill

Three agitator speeds were used in the dispersion of steopac talc, 30Hz, 35Hz and 40Hz. The agitator diameter was 0.10m. The mean particle size for speeds of 30Hz, 35Hz and

40Hz was between: 3.7 μ m and 5.0 μ m; 3.7 μ m and 4.9 μ m; and 3.6 μ m and 4.8 μ m respectively. The mean particle size decreased when the processing time was increased.

The contrast ratio for the speeds 30Hz, 35Hz and 40Hz was in the range: 0.946 to 0.951; 0.947 to 0.951 and 0.946 to 0.951 respectively. The contrast ratio increased with milling time for each speed of processing. When the agitator speed was increased, the contrast ratio was also increased. The results obtained are consistent with theory.

10.2.3 Homogenisation of titanium dioxide

The effect of flow rate on dispersion was investigated. Two flow rates 0.57ml/s and 2.67ml/s were used. The mean particle sizes for two, four, six, eight and ten passes were: 359.8nm, 334.4nm, 297.8nm, 424.5nm and 357.4nm respectively for a process flow rate of 0.57ml/s. The mean particle sizes for two, four, six, eight and ten passes were: 375.6nm, 498.5nm, 458.5nm, 359.6nm and 489.4nm respectively for a flow rate of 2.67ml/s. The changes in mean particle sizes for the two processing flow rates were erratic and could not be fully explained through the mechanism of Floury *et al.*(2004).

The contrast ratios for a flow rate of 0.57ml/s are in the range 0.978 and 0.983 while those for a flow rate of 2.67ml/s are in the range 0.967 and 0.973. These contrast ratios generally are in agreement with the particle size changes observed at the corresponding process flow rates.

10.2.4 Pigment blending

Dispersions of titanium dioxide were blended with either dispersions of steopac talc of kulu 2 to achieve different pigment volume concentrations of titanium dioxide.

The pigment volume concentration of titanium dioxide was varied between 37.2percent and 22.8percent when blended with steopac talc. The contrast ratio was observed to have dropped from 0.978 to 0.970, while the flocculation gradient increased from 0.977 to 1.234. The changes in contrast ratio and flocculation gradient are in agreement with the changes in the pigment volume concentration that were used. The increase in the flocculation gradient

is brought about when the large steopac talc particles replace the smaller sized particles of titanium dioxide.

The pigment volume concentration of titanium dioxide was varied between 37.2percent and 20.7percent when blended with kulu 2. The contrast ratio was observed to have dropped from 0.978 to 0.968, while the flocculation gradient increased from 0.973 to 1.176. The changes in contrast ratio and flocculation gradient are in agreement with the changes in the pigment volume concentration that were used. The increase in the flocculation gradient is brought about when the large kulu 2 particles replace the smaller sized particles of titanium dioxide.

Changes in pigment volume concentration of either steopac talc or kulu 2 of a similar magnitude produce similar effects in the contrast ratio and flocculation gradient. The difference between these two pigments is that the kulu 2 has a smaller mean particle size compared to steopac talc. Therefore kulu 2 is expected to result in less flocculation than steopac talc. Although kulu 2 generally has lower flocculation gradients than steopac talc, its contrast ratios are marginally smaller than those for steopac talc. This discrepancy is due to some experimental error.

10.2.4 The rheology of the dispersion process

The speeds used were 30Hz and 35Hz. These speeds corresponded to shear rates of $385.7s^{-1}$ and $529.8s^{-1}$. The viscosity for 30Hz was in the range of 0.1243Pa.s to 0.1132Pa.s and the corresponding mean particle size range was 416.2nm to 368.4nm. On the other hand the viscosity for an agitator speed of 35Hz was in the range 0.088Pa.s to 0.065Pa.s and the corresponding particle size range was 403.9nm to 359.8nm.

The changes in the viscosity at each processing speed are in agreement with the changes in the mean particle size. The viscosities corresponding to 35Hz are lower than those for 30Hz. In addition the mean particle sizes corresponding with 35Hz are lower than those for 30Hz. Changes in rheology can thus be used to monitor the changes in the level(degree) of dispersion.

Dispersions of titanium dioxide are thixotropic. When the action of shear stress on dispersions of titanium dioxide is suddenly terminated, it takes the dispersion about 200seconds to recover thirty percent of its structure.



Chapter 11 Recommendations

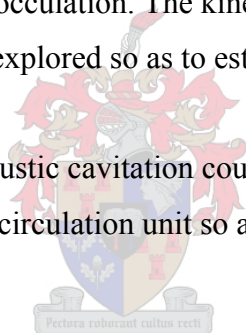
11.1 Mechanism of dispersion and simulation

The kinetics of the wetting sub-mechanism for non-instantaneous wetting should be evaluated and included in a comprehensive model for the dispersion process.

The numerical simulations of Flourey *et al.* (2004), using computational fluid dynamics, should be extended to: (i) non-Newtonian fluids, and (ii) multiple pass homogenisations. The flow model could be simulated at an even more microscopic level to determine the detailed kinetics by analysing the different mixing zones in the homogeniser.

A model for collisions leading to re-agglomeration in the recirculation zone could include ortho-kinetic and peri-kinetic flocculation. The kinetics of particle breakdown through acoustic cavitation needs to be explored so as to establish a detailed simulator.

Particle breakdown through acoustic cavitation could be intensified using a separate ultrasonic unit coupled to the recirculation unit so as to reduce re-agglomeration.



11.2 Analytical techniques

11.2.1 Contrast ratio

Samples for the determination of contrast ratio must be diluted with resin.

11.2.2 Flocculation gradient

Flocculation gradient is an unreliable measure of the fraction of flocculated particles in a pigment dispersion and its use would not be encouraged.

11.2.3 Rheology of the dispersion process

Flow curves are sensitive to the changes in pigment structure that occurs during dispersion. They should be used as a measure of the level(degree) of dispersion. They could be used to replace flocculation gradient as a measure of the fraction of flocculated particles in a pigment dispersion.

11.3 Experimental technique

The results obtained show that it is necessary to improve the precision and confidence of the experimental measurements. A design of experiment should also be used to determine the significant variables. Detailed experiments should then be carried out on the significant variables with an extensive number of levels.

11.4 Blending of pigment dispersions

Detailed blending experiments should be carried out to determine the optimum pigment volume concentration that does not significantly cause flocculation and thereby reducing the contrast ratio.

11.5 Rheology and modelling

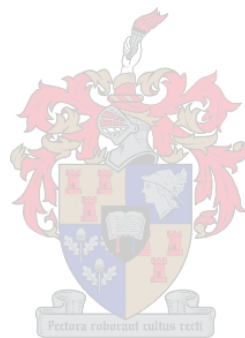
At present, there is no correlation for shear rate in a Cowles mill (Moolman, P.L., 2003). This correlation must be established.

The rheology of the dispersion process could be used in conjunction with measurements of contrast ratio of flocculation gradient to train a neural network that can predict contrast ratio. This could result in an economic method for online monitoring and manipulation of contrast ratio and flocculation gradient.

11.6 Scale up of dispersion equipment

The method proposed for the scale-up of emulsion reactors used for making vesiculated beads(Terblanche, J.C., 2003), should be used for the scale-up of the Cowles mill for pigment dispersion. The variables that are required for scale-up are:

- i. Agitator diameter;
- ii. Agitator/Tank diameter ratio;
- iii. Speed.



References

Black, W., 1981. Surface Active compounds, In: Parfitt, G.D. (Ed.), Dispersion of powders in liquids with special reference to pigments, Applied Science publishers, London, pp. 149 – 198

Coulson, J.M. and Richardson, J.F., 1996. Chemical Engineering: Fluid flow, heat transfer and mass transfer, vol. 1, 5th ed. Oxford: Butterworth-Heinemann

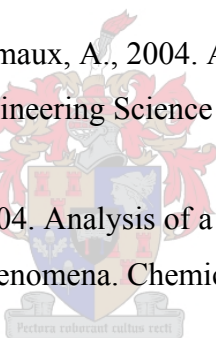
Davies, J.T., 1957. Proc. 2nd Int. Congress on Surface Activity, London, 1, 426

Deryaguin, B.V. and Landau, L.D., 1941. Acta Physicochim. URSS, 14, 633

Dupré, A., 1865. Ann. Chimie, (4) (6), 274

Floury, J., Bellettre, J., Legrand, J., Desrumaux, A., 2004. Analysis of a new type of homogeniser: A study of the flow pattern. Chemical Engineering Science 59, 843-853

Floury, J., Legrand, J., Desrumaux, A., 2004. Analysis of a new type of homogeniser: A study of the droplet break-up and recoalescence phenomena. Chemical Engineering Science 59, 1285-1294



Frisch, H.L. and Simha, R., 1956, Rheology, Volume 1, (Ed.) Eirich, F.R., Academic Press Inc., New York, p. 525

Gous, K., 2003. Continuous processing of vesiculated beads. MSc. Thesis. Stellenbosch: Stellenbosch University

Griffin, W., 1954. J. Soc. Cosmetic Chem., 5, 249

Grossman, H.; Phase inversion and minimum impeller speed for complete dispersion in agitated liquid-liquid systems; meeting of the working party, Vortrag, 1980

Guggenheim, E.A., 1929. J. Phys. Chem., 33, 842

Hamaker, H.C., 1937. *Physica*, 4, 1058

Hannam, A.R. and Patterson, D., 1963. *J. Soc. Dyers and Colourists*, 79, 192

Hearle, J.W.S., Sparrow, J.T. and Cross, P.M., 1973. *The use of the scanning electron microscope*, Pergamon Press, Oxford

Hird, M.J., 1973. Internal Publication, Tioxide Limited, BRD/723

Jaycock, M.J., 1981. *The Solid-Liquid Interface*, In: Parfitt, G.D. (Ed.), *Dispersion of Powders in Liquids with special reference to Pigments*, Applied Science Publishers, London, pp. 51 – 94

Johansen, R.J., Lorenz, P.B., Dodd, D.G., Pidgeon, F.D. and Davis, J.W., 1953. *J. Phys.Chem*, 57, 40

Klein, A.; Lowry, V.; some mixing scale-up considerations for emulsion polymerisation, *Advances in emulsion polymerisation and latex technology*, short course, Leigh University, Pennsylvania, 1996.

Kubelka, P., and Munk, F., 1931. *Z. Techn. Physik*, 12, 593

Lawrence, S.G., 1981. *Assessment of the state of dispersion*, in: Parfitt, G.D. (Ed.), *Dispersion of powders in liquids with special reference to pigments*, Applied Science Publishers, London, pp. 363 – 391

Lin, L., 2000. “Adhesion and Cohesion phenomena in pigment dispersion.”, *Surface Coatings International*, 6, pp. 289 – 296

Moelwyn-Hughes, E.A., 1961. “*Physical Chemistry*”, 2nd edition, Pergamon, London

Moolman, P.L., 2003. *Rheology of coating systems*, MSc thesis, Stellenbosch: Stellenbosch University

Osterhof, H.J. and Bartell, F.E., 1930. *J. Phys. Chem.*, 34 1399

Sherman, P., 1970. Industrial rheology with particular reference to foods, pharmaceuticals and cosmetics, Academic Press, London

Shinoda, K. and Kuneida, H., 1977. In: Micro-emulsions, Prince, L.M. (Ed.), Academic Press, London, pp. 58 – 59

Shirgaonkar, I.Z., Lothe, R.R., Pandit, A.B., 1998. Comments on the mechanism of microbial cell disruption in high-pressure and high speed devices. Biotechnology Progress 14, 657-660.

Terblanche, J.C., The development of vesiculated beads, MSc Ing Thesis, Department of Chemical Engineering, University of Stellenbosch, 2003.

Turnstall, D.F. and Dowling, D.G., 1971. J. Oil Col. Chem. Assoc., 54, 1007

Turnstall, D.F., 1972. J. Oil Col. Chem. Assoc., 55, 695

Turnstall, D.F., and Hird, M.J., 1974. J. Paint Tech., 46, 588, 33

Verwey, E.J.W., and Overbeek, J. Th.G., 1948. Theory of the stability of lyophobic colloids, Elsevier, Amsterdam

Vold, M.J., 1961. J Colloid Sci., 16, 1

Welty, J.R., Wicks, C.E. and Wilson, R.E.,(Eds), 1984. Fundamentals of Momentum, Heat and Mass Transfer, 3rd ed., New York, John Wiley and Sons

Weltmann, R.N. and Eirich, F.R. (Eds), 1960. Rheology, Academic Press, New York, 3, p. 189

Wenzel, R.N., 1936. Ind. Eng. Chem. (Anal.), 28, 988

Wheeler, D.A., 1981. Technical Aspects of Dispersion. In: Parfitt, G.D. (Ed.), Dispersion of Powders in Liquids with special reference to Pigments, Applied Science Publishers, London, pp. 327 – 361

Glossary of Terms

| | |
|--------------------|--|
| Additive | Materials added to paint in minute quantities that modify the interfacial properties of pigment or the dispersion. |
| Adhesional wetting | Replacement of unit surface area of each of the solid and liquid surface with a single unit area of a new solid/liquid interface. |
| Agglomeration | Process leading to particles establishing edge contact after collisions through attractive Van der Waals forces. |
| Aggregation | Process leading to particles establishing permanent contact after impact through sintering/fusion. |
| Apparent viscosity | The shear stress divided by the rate of strain when this quotient is dependent on the shear rate. |
| Back scatter | Irregular reflection occurring at surfaces of pigments within paint film. |
| Binder | A film-forming phase. |
| Bingham flow | Flow which exhibits elastic behaviour up till the yield point and whose shear rate is directly proportional to the shear stress less the yield stress above the yield point. |
| Brownian motion | Random motion of particles due to collisions with molecules of the continuous phase. |
| Cavitation | Formation of bubbles, when its? What? Vapour pressure under prevailing thermodynamic conditions exceeds liquid pressure. |

| | |
|-------------------|---|
| Cavitation noise | Acoustic vibrations dissipated with the collapse of cavities when the pressure exerted on dispersion during fluid flow exceeds liquid vapour pressure. |
| Cavitation number | The change in liquid potential energy relative to its kinetic energy. |
| c.m.c | Critical micelle concentration. |
| Contact angle | The angle between the interfacial tensions of the boundaries of the phases liquid/vapour and solid/liquid, which is important in defining the spontaneity of wetting. |
| Continuous phase | Phase, which suspends the discrete phase. |
| Contrast ratio | The ratio of the reflectance over a black substrate to the reflectance over a white substrate. |
| Correlation | Empirical mathematical model that does not rely on details of mechanism. |
| Cowles mill | Batch agitated vessel for wetting and imparting shear stress onto agglomerates in a mill base. |
| Dilatancy | The increase in the viscosity of a fluid when the shear stress is increased (shear thickening). |
| Discrete phase | The phase whose constituents are particles. |
| Dispersant | Additive that modifies interfacial properties of pigments resulting in better wetting, particle breakdown and stability. |
| Dispersion | A multiple phase system constituted by discrete and continuous phases. |

| | |
|-----------------------|--|
| Dispersion process | Process of homogeneously distributing particles in a continuous phase through wetting, particle breakdown, particle stabilisation or particle destabilisation. |
| Dynamic similarity | The similarity of forces at counterpart locations in two geometrically similar dispersive vessels. |
| Eddy | The combination of shear stress and fluctuations in inertial force during turbulent flow. |
| Extender | A particulate mineral that reduces point/edge contacts between pigment particles. |
| Extension/elongation | Stretching of agglomerates a sudden increase in the momentum of the agglomerates in the vicinity of an abrupt flow constriction. |
| FOG | Fineness of grind – a visual/experience-based scale for quantifying particle size. |
| Flocculation | Process leading to particles establishing point contact after collisions through attractive Van der Waals forces. |
| Flocculation gradient | The change in the percentage back scattered radiation relative to the change in the thickness of a paint film used as a measure of the fraction of flocculated particles in the paint. |
| Flow curve | A graphical representation of relationship between stress and shear rate. |
| Froude number | The ratio of inertial to gravitational forces in a flow system. |
| Geometric similarity | Two or more dispersive systems whose counterpart length |

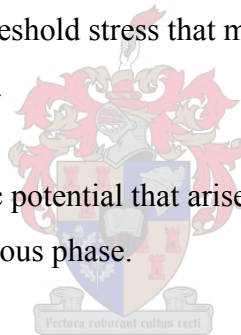
dimensions exhibit a constant ratio.

| | |
|----------------------|--|
| HLB | Hydrophile-lithophile balance – a method used for the selection of dispersants. |
| Homogeniser | A flow valve for imparting shear stress and cavitation noise onto agglomerates in a dispersion. |
| Immersional wetting | The total immersion of unit square of solid surface by exchange of solid/vapour with solid/liquid interface, without any change in the extent of the liquid surface. |
| Impact | Particle breakage from a sudden reduction in the momentum of particles after collision in a dispersion vessel. |
| Interfacial process | Processes that occur at interfaces altering the interfacial tension and stability of dispersions. |
| Interface | The surface/boundary between distinct phases. |
| Kinematic similarity | A constant ratio of velocities at counterpart positions within two vessels provided the dispersive systems are geometrically similar. |
| Laminar flow | Streamlined flow with Reynolds numbers less than 2000. |
| Manipulated variable | A quantity whose value can be altered. |
| Mean particle size | The average particle size of a discrete phase. |
| Mechanism | Sequence of steps through which overall process is expressed. |
| Mill | A piece of equipment in which the particulate phase is homogeneously distributed throughout the continuous phase. |

| | |
|----------------------------|---|
| Mill base | An inhomogeneous mixture of a discrete and continuous phase. |
| Model | A representation of a physical object or abstract concept. |
| Neural network | A computational tool with the ability to interpolate after learning from empirical data. |
| Non-Newtonian flow | Flow whose viscosity is sensitive to changes in shear stress. (This is the behaviour that is exhibited by dispersions.) |
| Newtonian flow | Flow whose viscosity is insensitive to changes in shear stress. |
| Opacity | Ability to obliterate a substrate. |
| Ortho-kinetic flocculation | Flocculation caused by the action of shear stress on particles. |
| Paint | Dispersion of pigment particles with binder and additives in the continuous phase. |
| Particle | Individual entity of a discrete phase. |
| Particle break down | Separation of flocculated/agglomerated particles by overcoming attractive Van der Waals forces between the particles. |
| Particle size | The physical dimension of a particle (length/area/volume). |
| Particle size distribution | The weighted particle size of particles spread in size bins of the size range. |
| Peri-kinetic flocculation | Flocculation caused by collisions due to Brownian motion of particles. |

| | |
|----------------------|---|
| Pigment | A particulate mineral/compound that imparts opacity to a substrate. |
| PVC | Pigment volume concentration, which is the fraction of volume occupied by pigment or extender in a dispersion. |
| Reynolds number | The ratio of inertial to viscous forces exerted onto fluid during flow. |
| Rheology | The study of the deformation effects of shear stress applied to a fluid. |
| Rheometer | An instrument for the analysis of the rheological behaviour of materials. |
| SEM | Scanning electron microscope – electro-optic instrument used to obtain pictures of particles in the analysis of particle size and distribution. |
| Sensitivity analysis | Technique for determination of the significance of explanatory variables either implicitly or explicitly. |
| Shear | The relative movement of layers of a material. |
| Shear rate | The change of shear stress |
| Shear stress | The force that causes deformation of layers of fluid by acting parallel to the layers. |
| Shear thinning | The reduction in the viscosity of a fluid when the shear stress is increased. |
| Specular reflection | Regular reflection, which occurs at a film/air boundary. |

| | |
|-------------------|---|
| Spreading wetting | Work required to create an equivalent solid/liquid interface from separate solid and liquid interfaces. |
| Thickener | Additive that increases the viscosity of a dispersion. |
| Transitional flow | Flow with Reynolds numbers between 2000 and 10000. |
| Turbulent flow | Flow with Reynolds numbers greater than 10000. |
| Viscosity | Expression of the resistance of a fluid to flow when exerted to shear stress. |
| Wetting | The process of replacing a solid/gas with a solid/liquid interface. |
| Yield stress | The threshold stress that must be applied before a fluid commences to flow. |
| Zeta potential | Electric potential that arises at the interface between particles and continuous phase. |



Appendices



A Raw Material Properties and Pigment Dispersion Formulations

A1 Raw Materials

| Description | Classification | SG |
|-------------------|----------------------|-------|
| | | |
| Foamaster VL | Defoamer | 0.890 |
| Acticide HF | Bacteriocide | 1.025 |
| Attagel 50 | Clay thickener | 2.360 |
| AMP 95 | Ph modifier / alkali | 0.940 |
| Alcosperse 700 | Surfactant | 1.100 |
| Kulu 2 | Extender | 2.700 |
| Steopac Talc | Extender | 1.000 |
| Titanium TR 93 | Opacifier | 4.000 |
| Titanium TR 93 | Opacifier | 4.000 |
| Cellosize QP 4400 | Cellulose thickener | 1.390 |
| Propylene Glycol | Anti freeze | 1.038 |
| Water | Diluent / vehicle | 1.000 |

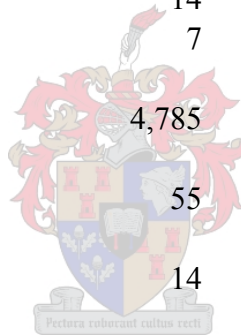
A2 Formulation of Titanium Dioxide TR93 Dispersion

TITANIUM DISPERSION

| | Mass(g) | % |
|------------------|---------|-------|
| Water | 743 | 10.89 |
| Water | 341 | 5.00 |
| Acticide HF | 20 | 0.30 |
| Water | 95 | 1.39 |
| Propylene Glycol | 616 | 9.01 |
| Water | 95 | 1.39 |

High speed

| | | |
|-------------------|-----------|--------|
| Alcosperse 700 | 44 | 0.64 |
| Foamaster VL | 14 | 0.20 |
| Cellosize QP 4400 | 7 | 0.10 |
| Titanium TR 93 | 4,785 | 70.07 |
| Water | 55 | 0.80 |
| AMP 95 | 14 | 0.20 |
| Sum | 6,829 | 100.00 |
| F: | 0.4350000 | |
| Volume | 3,214 | |
| % solids | 0.701 | |



P.V.C 37

High speed for 30 min

A3 Formulation of Steopac Talc Extender Dispersion

| Steopac Dispersion(Talc) | | |
|----------------------------|----------|---------|
| | Mass(g) | % |
| Water | 1,191 | 33.753 |
| Water | 94 | 2.662 |
| Acticide HF | 20 | 0.573 |
| Water | 30 | 0.860 |
| Propylene Glycol | 283 | 8.010 |
| Water | 30 | 0.860 |
| <u>Low speed</u> | | |
| Alcosperse 700 | 81 | 2.285 |
| Foamaster VL | 8 | 0.228 |
| Cellosize QP 4400 | 8 | 0.240 |
| Attagel 50 | 12 | 0.344 |
| Titanium TR 93 | 4 | 0.113 |
| Steopac Talc | 1,734 | 49.140 |
| Water | 29 | 0.819 |
| AMP 95 | 4 | 0.115 |
| Sum | 3,529 | 100.000 |
| F: | 0.361300 | |
| Volume | 3,500 | |
| P.V.C | | 45.046 |



High speed for 30 min

A4 Formulation of Kulu2 Extender Dispersion

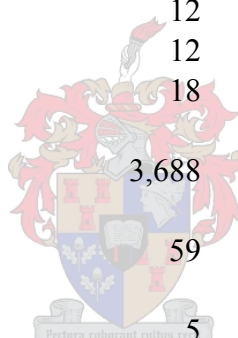
KULU 2 DISPERSION

| | Mass(g) | % |
|------------------|---------|-------|
| Water | 1,368 | 23.42 |
| Water | 322 | 5.51 |
| Acticide HF | 19 | 0.32 |
| Water | 117 | 2.00 |
| Propylene Glycol | 59 | 1.00 |
| Water | 117 | 2.00 |

High speed

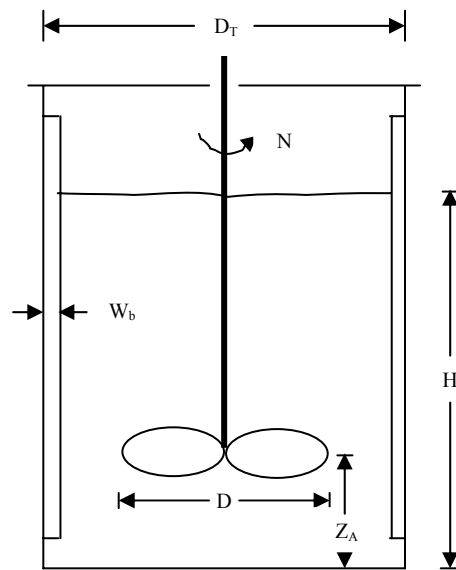
| | | |
|-------------------|-----------|---------|
| Alcosperse 700 | 47 | 0.80 |
| Foamaster VL | 12 | 0.20 |
| Cellosize QP 4400 | 12 | 0.20 |
| Attigel 50 | 18 | 0.30 |
| Kulu 2 | 3,688 | 63.15 |
| Water | 59 | 1.00 |
| AMP 95 | 5 | 0.08 |
| Sum | 5,840 | 2029.36 |
| F: | 1.1706700 | |
| Volume | 3,500 | |
| P.V.C | | 39.03 |

High speed for 30 min



B Mill Geometry

B.1 Cowles mill Geometry



B.1.1 Geometry of Cowles Mill for Batches Investigated

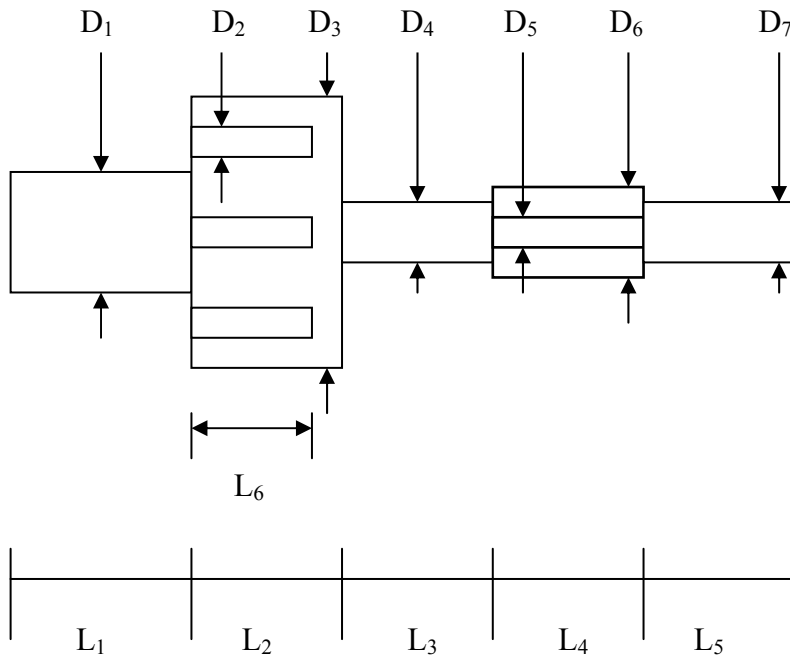
B.1.1.1 Design of the Cowles Used To Disperse Titanium Dioxide Batches

| Batch | D(cm) | Z _A (cm) | H(cm) | D _T (cm) | W _b (cm) | N(Hz) |
|-------|-------|---------------------|-------|---------------------|---------------------|-------|
| 1 | 0.10 | 5 | 15 | 20 | 0 | 30 |
| 2 | 0.10 | 5 | 15 | 20 | 0 | 30 |
| 3 | 0.12 | 5 | 15 | 20 | 0 | 30 |
| 4 | 0.10 | 5 | 15 | 20 | 0 | 35 |

B.1.1.2 Design of Cowles Mill Used To Disperse Steopac Talc Batches

| Batch | D(cm) | Z _A (cm) | H(cm) | D _T (cm) | W _b (cm) | N(Hz) |
|-------|-------|---------------------|-------|---------------------|---------------------|-------|
| F | 0.10 | 5 | 15 | 20 | 0 | 30 |
| G | 0.10 | 5 | 15 | 20 | 0 | 35 |
| H | 0.10 | 5 | 15 | 20 | 0 | 40 |
| J | 0.12 | 5 | 15 | 20 | 0 | 40 |

B.2 Plunger Geometry of The Homogeniser



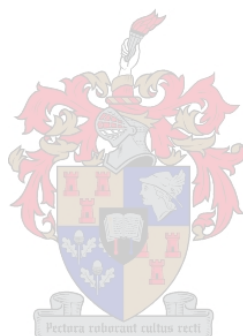
B2.1 Plunger Geometry For The Batches That were Homogenised

| Dimension\Plunger | 1 | 2 |
|-------------------|-----|------|
| D_1 (mm) | 3 | 4 |
| D_2 (mm) | 1.5 | 0.5 |
| D_3 (mm) | 8 | 8 |
| D_4 (mm) | 2.5 | 2.5 |
| D_5 (mm) | 1 | 0.24 |
| D_6 (mm) | 3.5 | 3.5 |
| D_7 (mm) | 2 | 2 |
| L_1 (mm) | 8 | 8 |
| L_2 (mm) | 8 | 7 |
| L_3 (mm) | 7 | 7 |
| L_4 (mm) | 8 | 8 |
| L_5 (mm) | 6 | 7.5 |
| L_6 (mm) | 6 | 5 |

C Scanning Electron Micrographs and Particle Size Distribution(on CD) saved as word document, Appendix C.doc

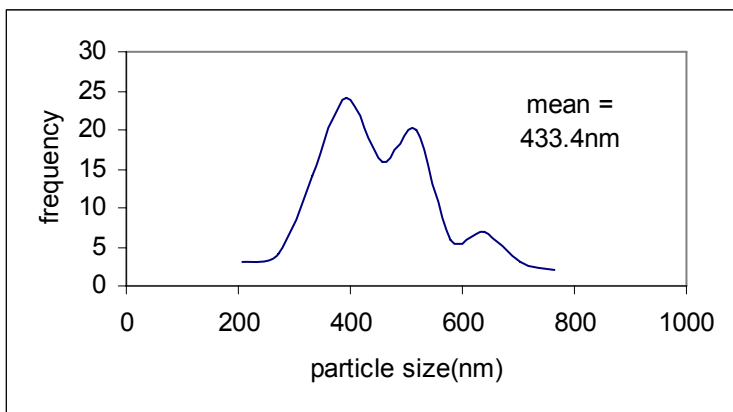
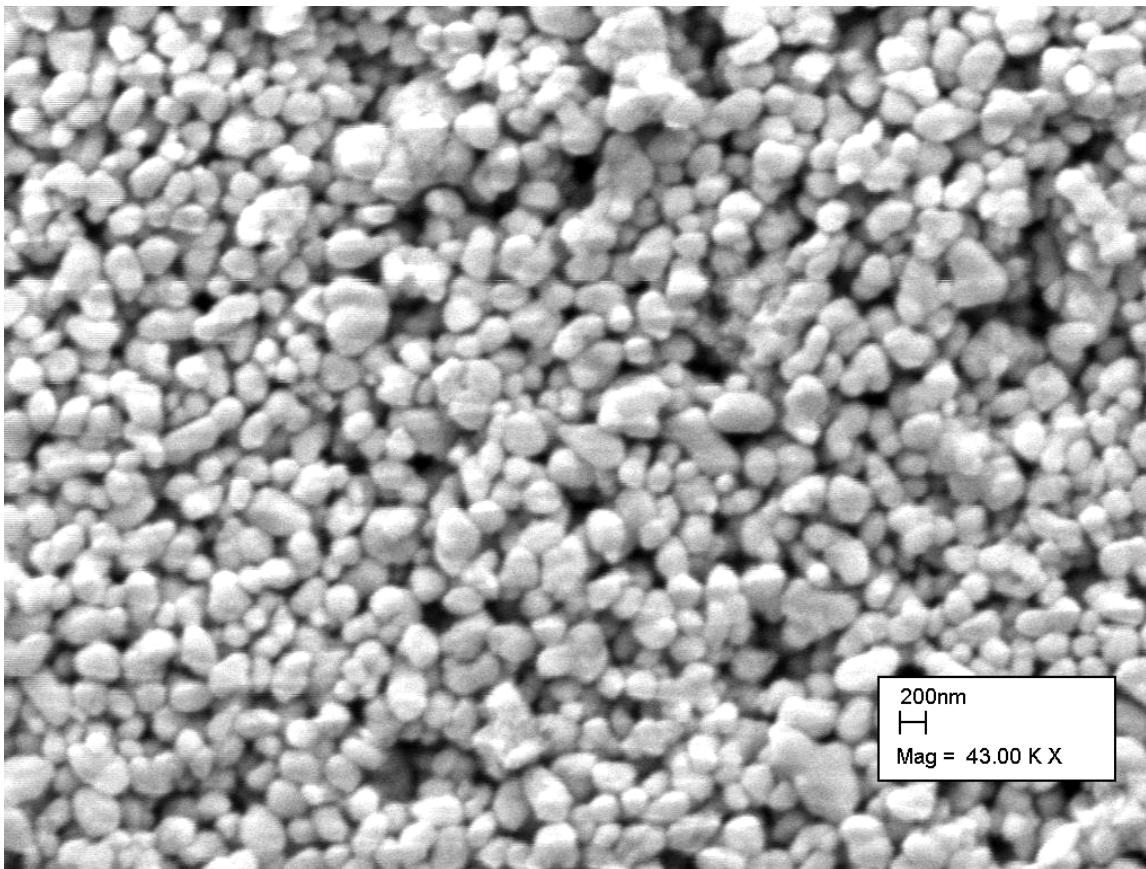
C.1.1 SEM and PSD for Batch 1

... included in chapter 5

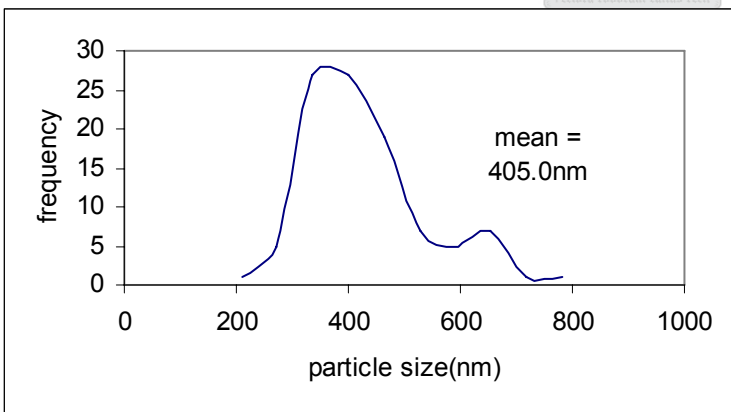
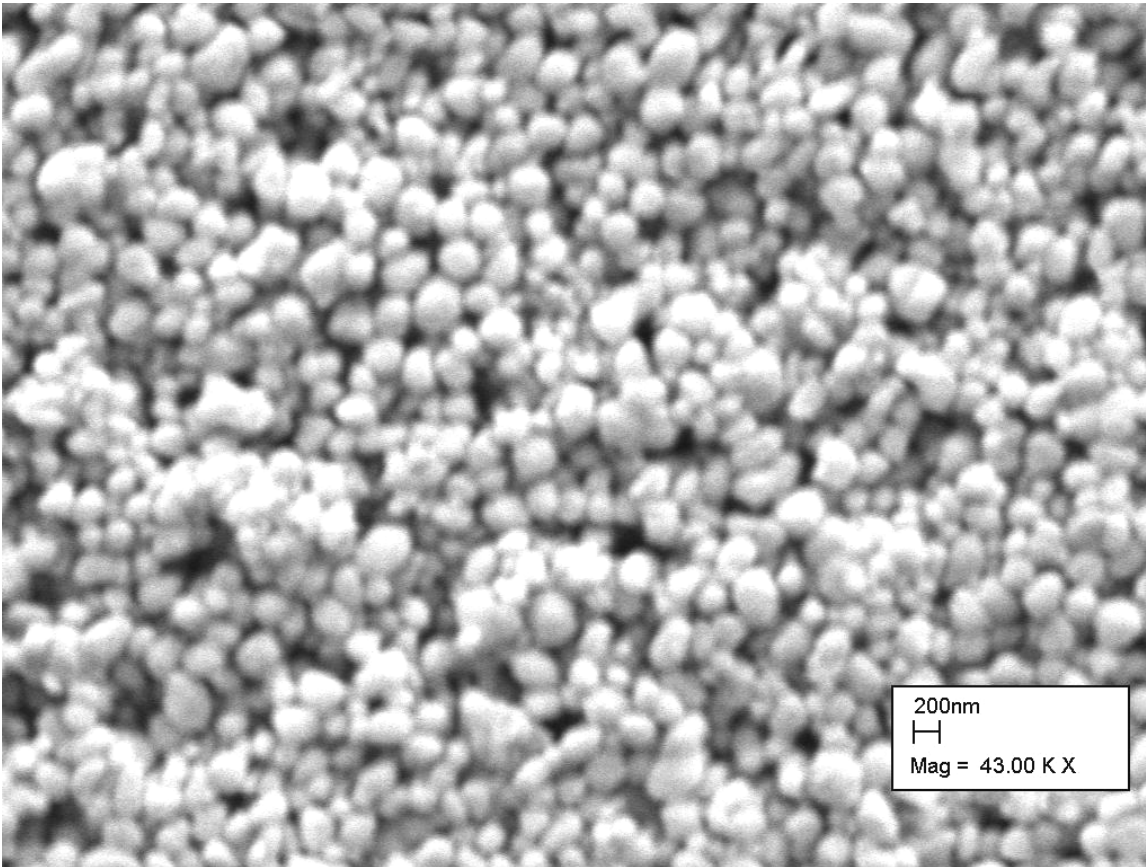


C.1.2 SEM and PSD for Batch 2 (dispersed through Cowles Mill)

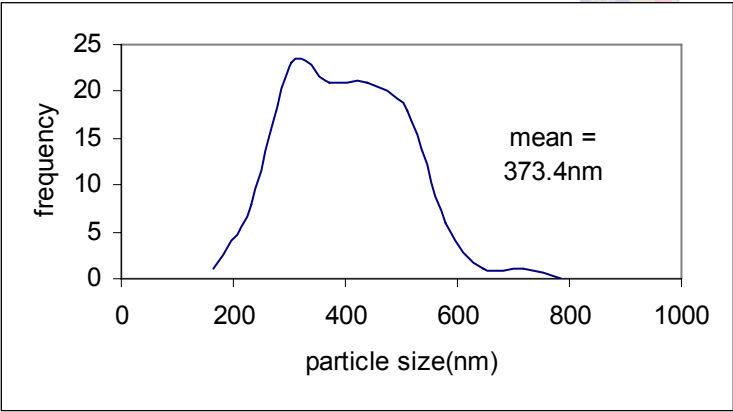
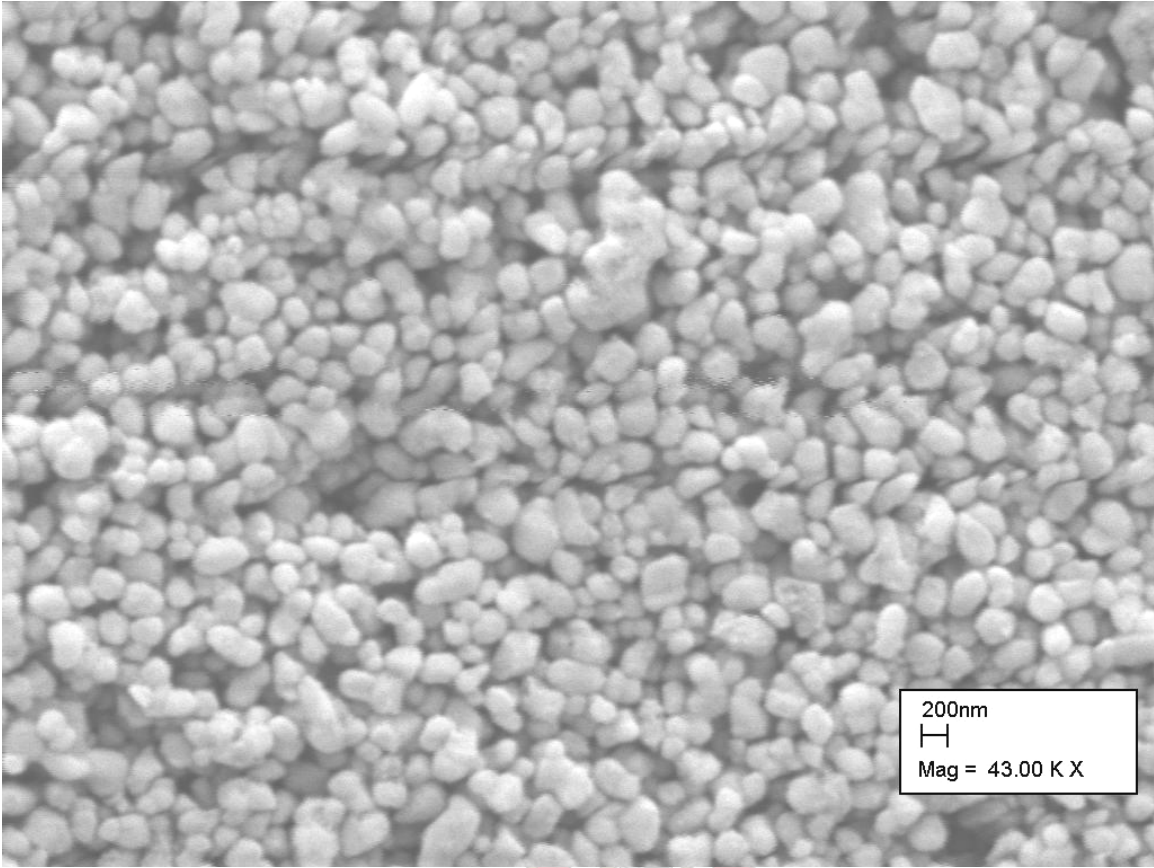
Batch 2 - 10min

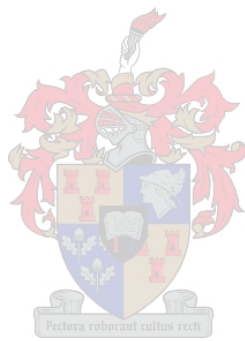


Batch 2 - 15min



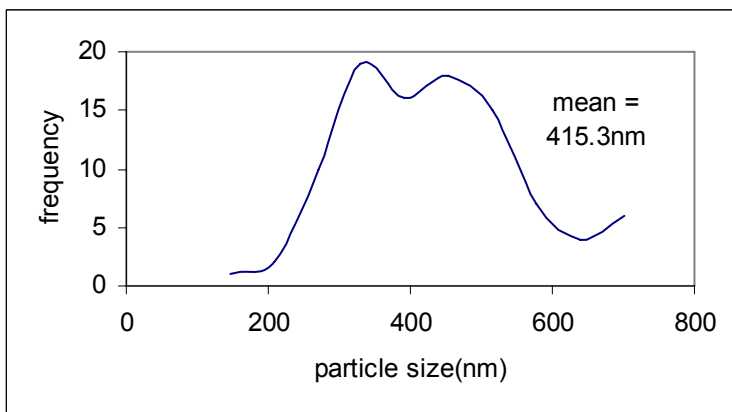
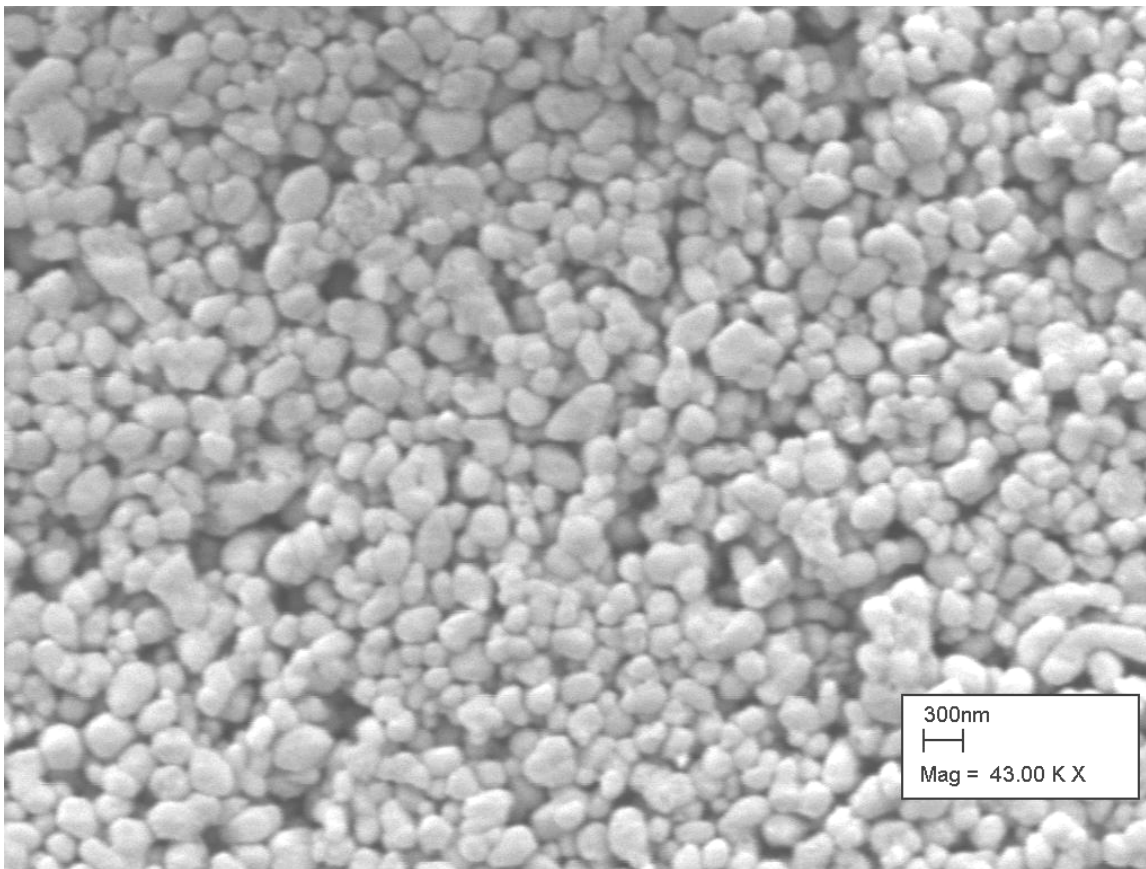
Batch 2 - 20min



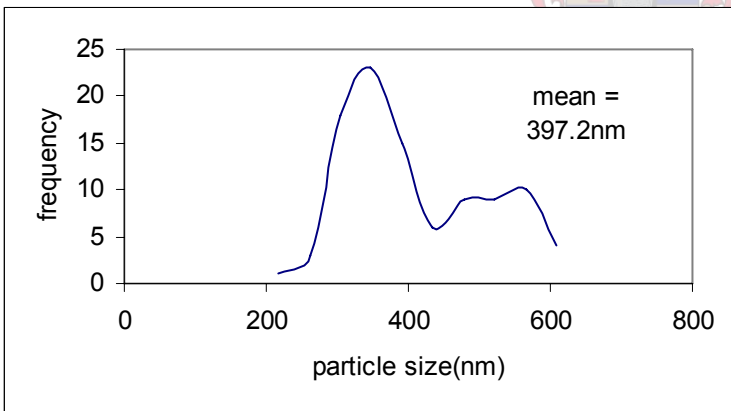
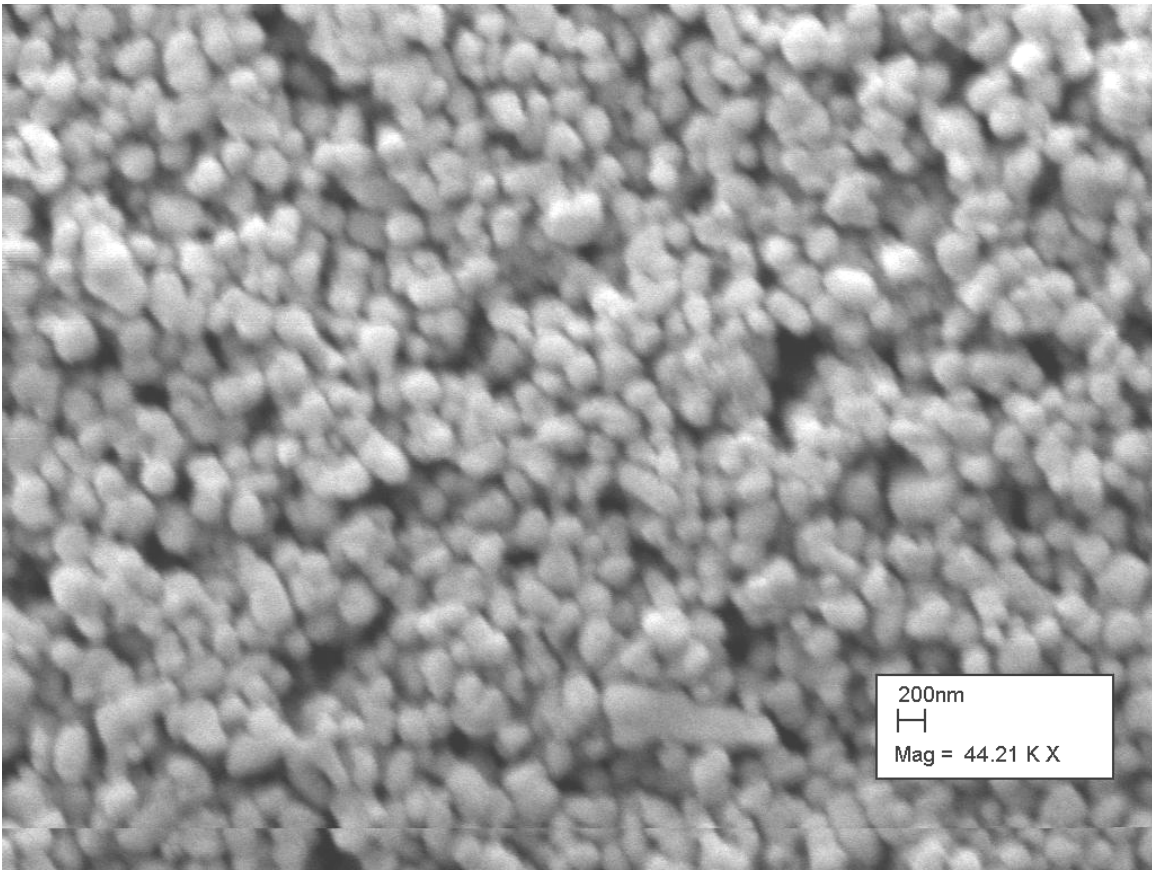


C.1.3 SEM and PSD for Batch 3 (dispersed through Cowles Mill)

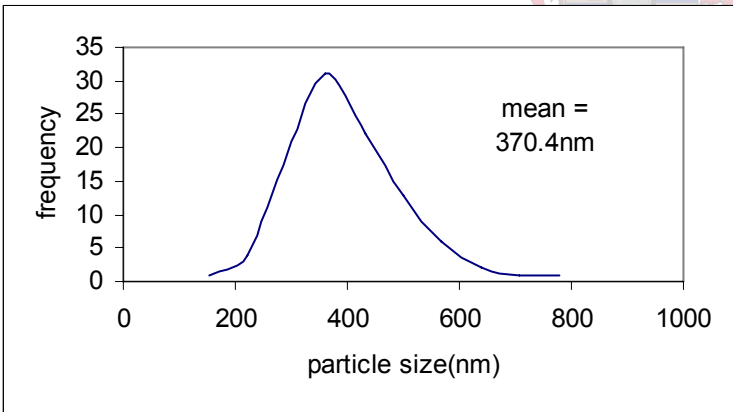
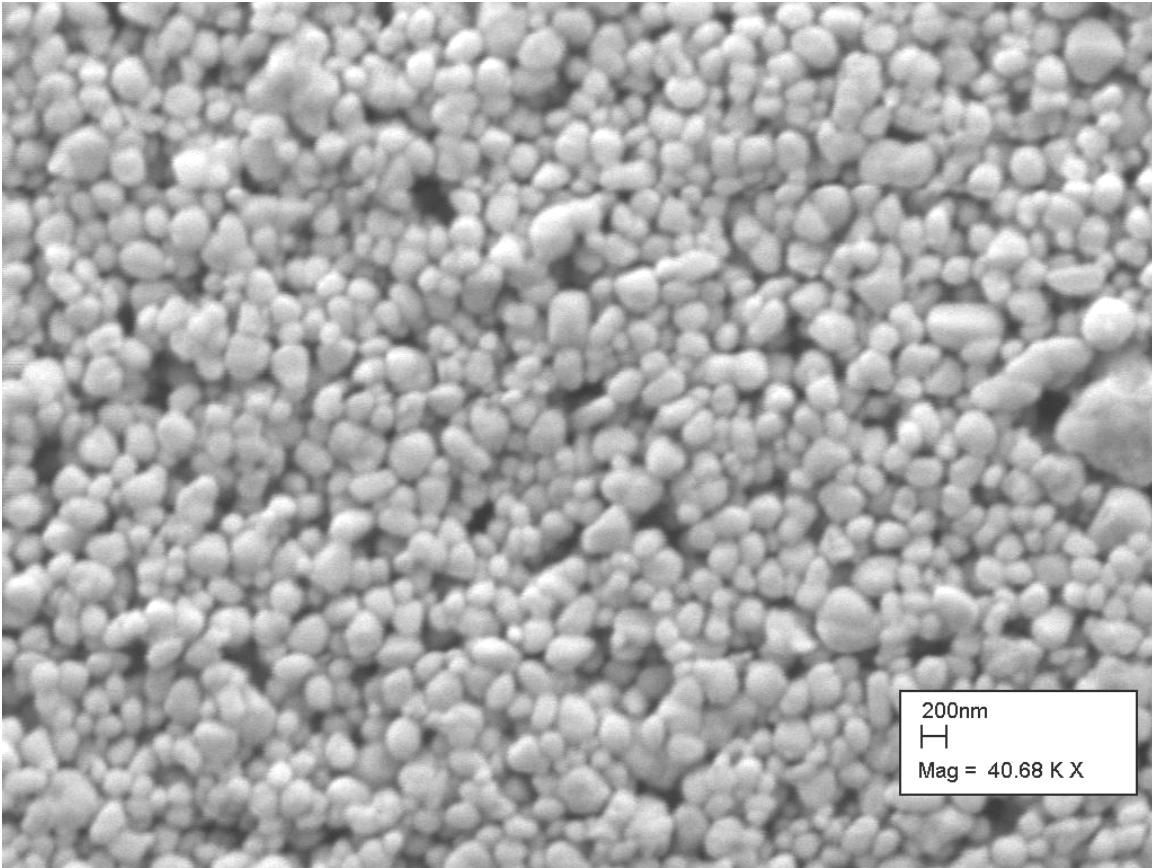
Batch 3 - 10min



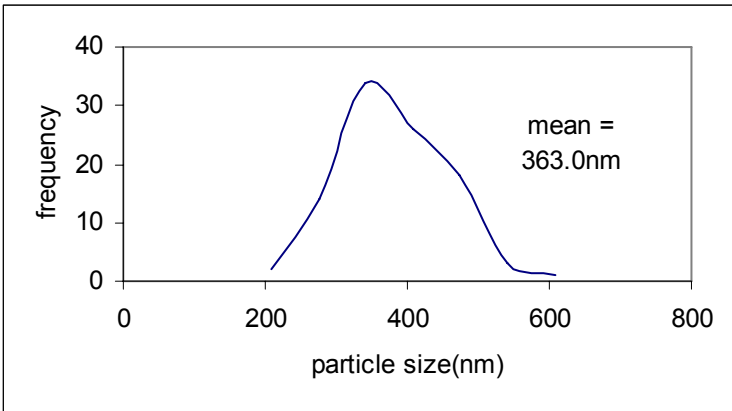
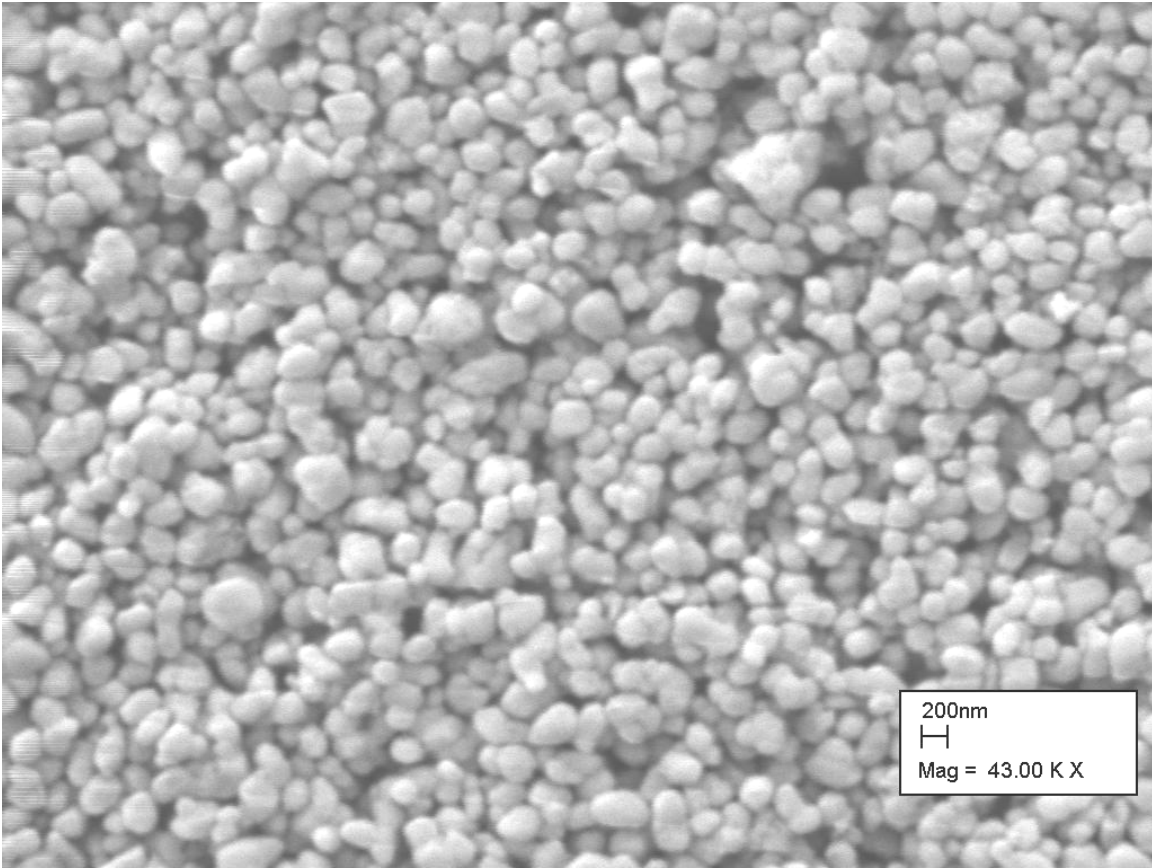
Batch 3 - 15min



Batch 3 - 20min

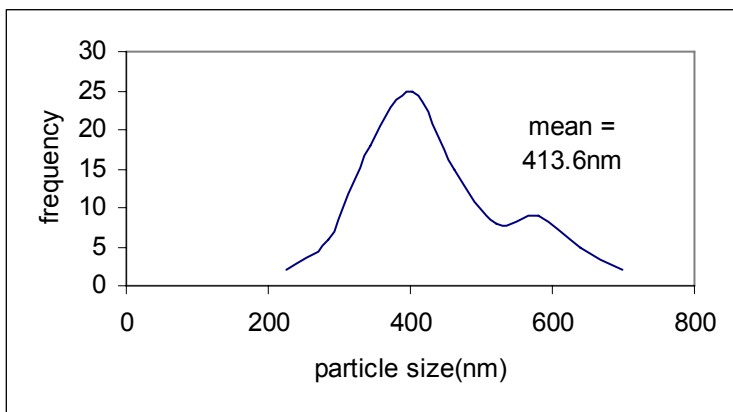
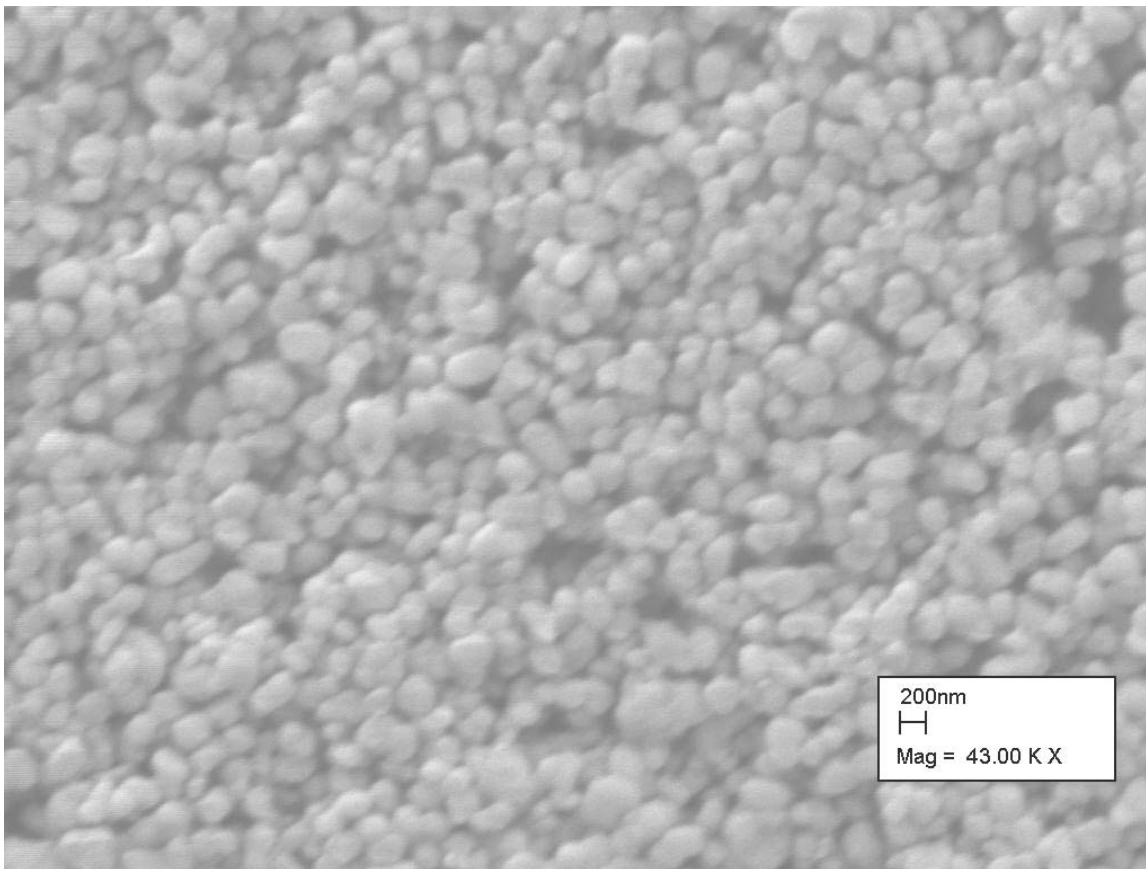


Batch 3 - 30min

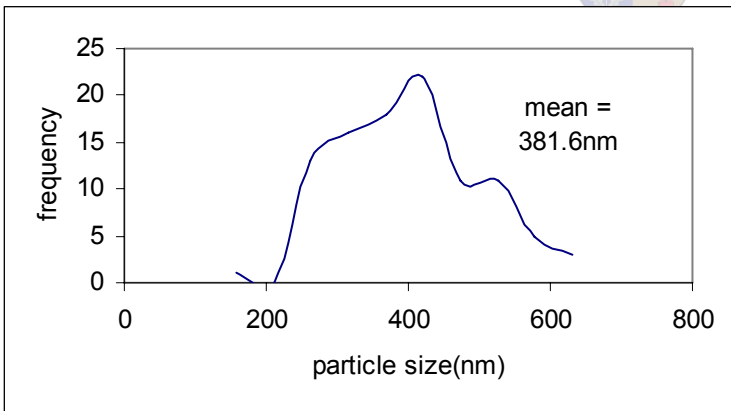
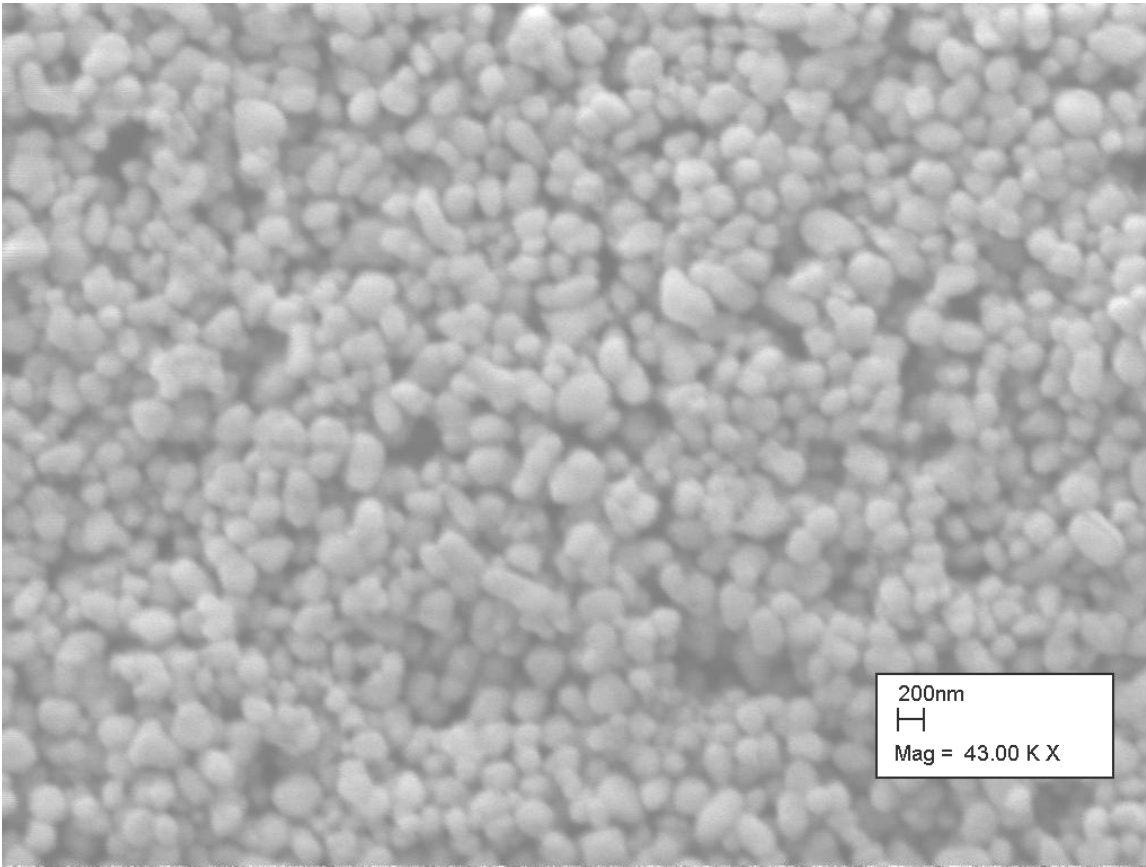


C.1.4 SEM and PSD for Batch 4 (dispersed through Cowles Mill)

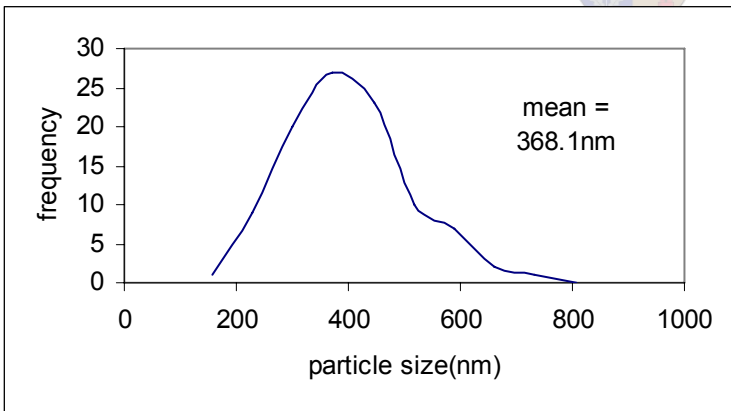
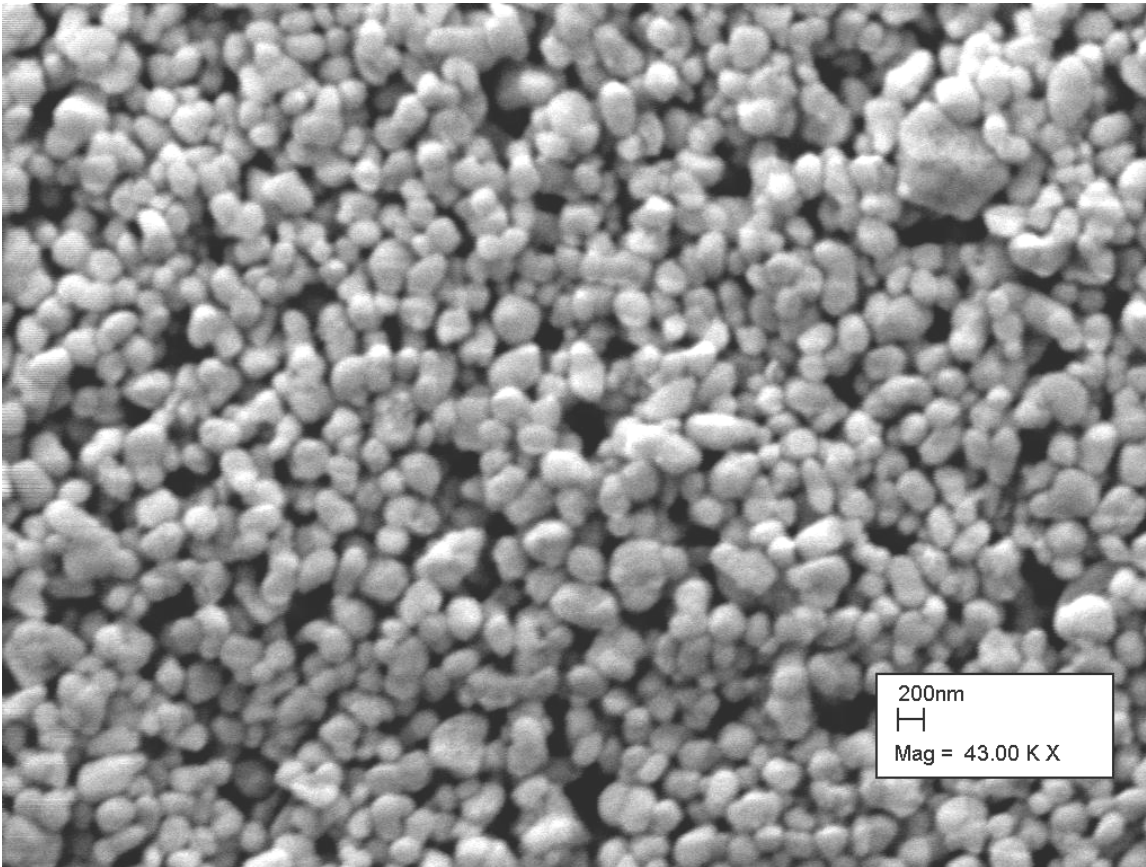
Batch 4 - 10min



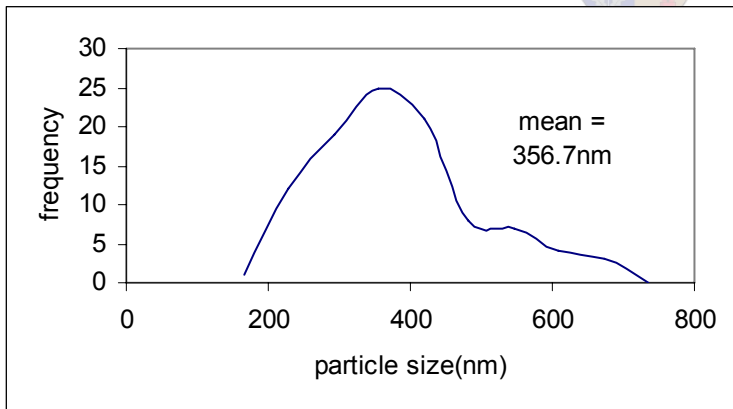
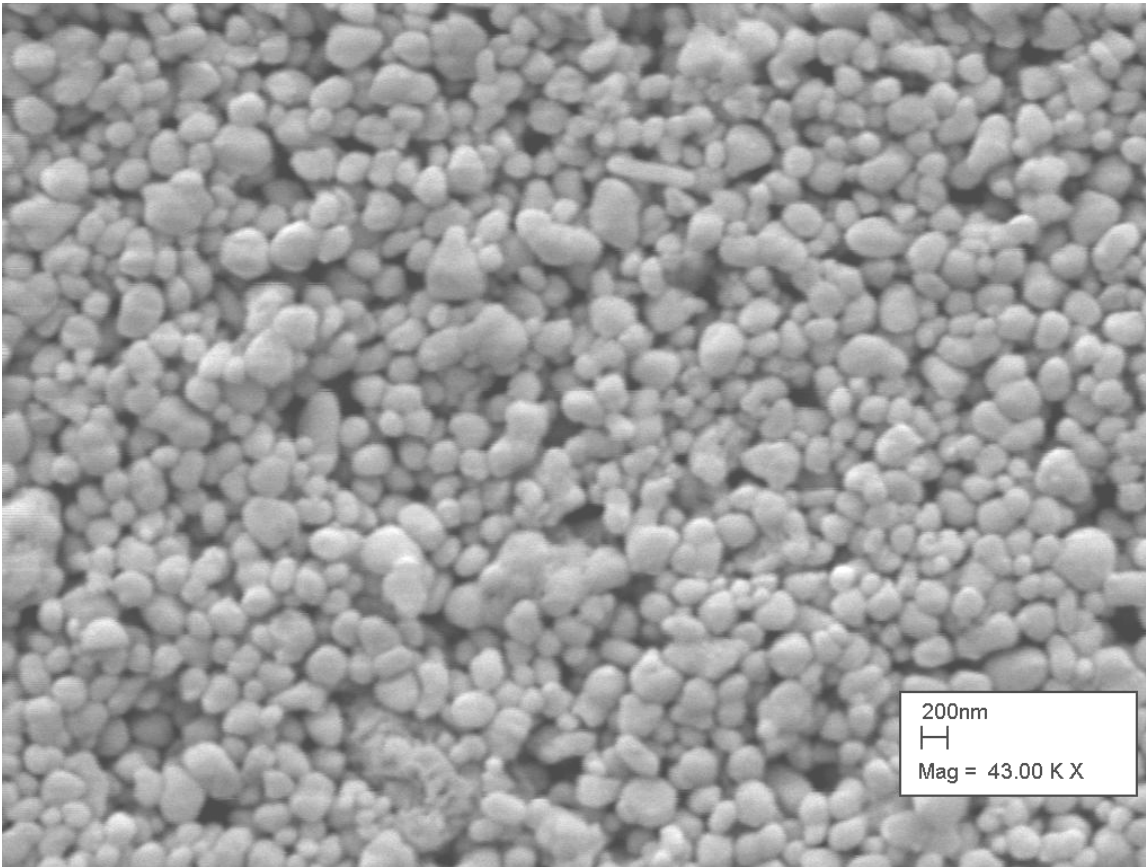
Batch 4 - 15min



Batch 4 - 20min

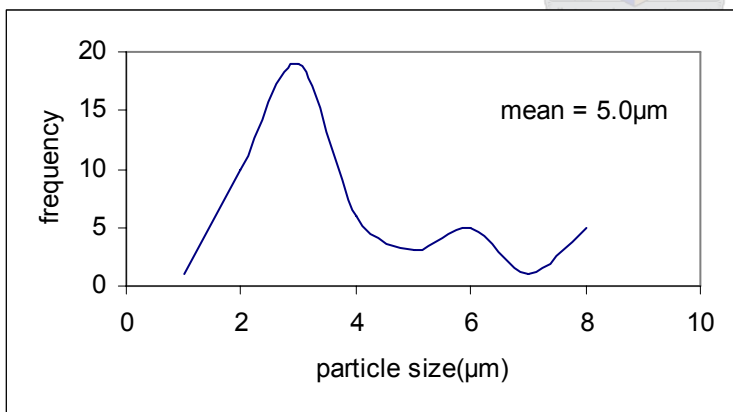
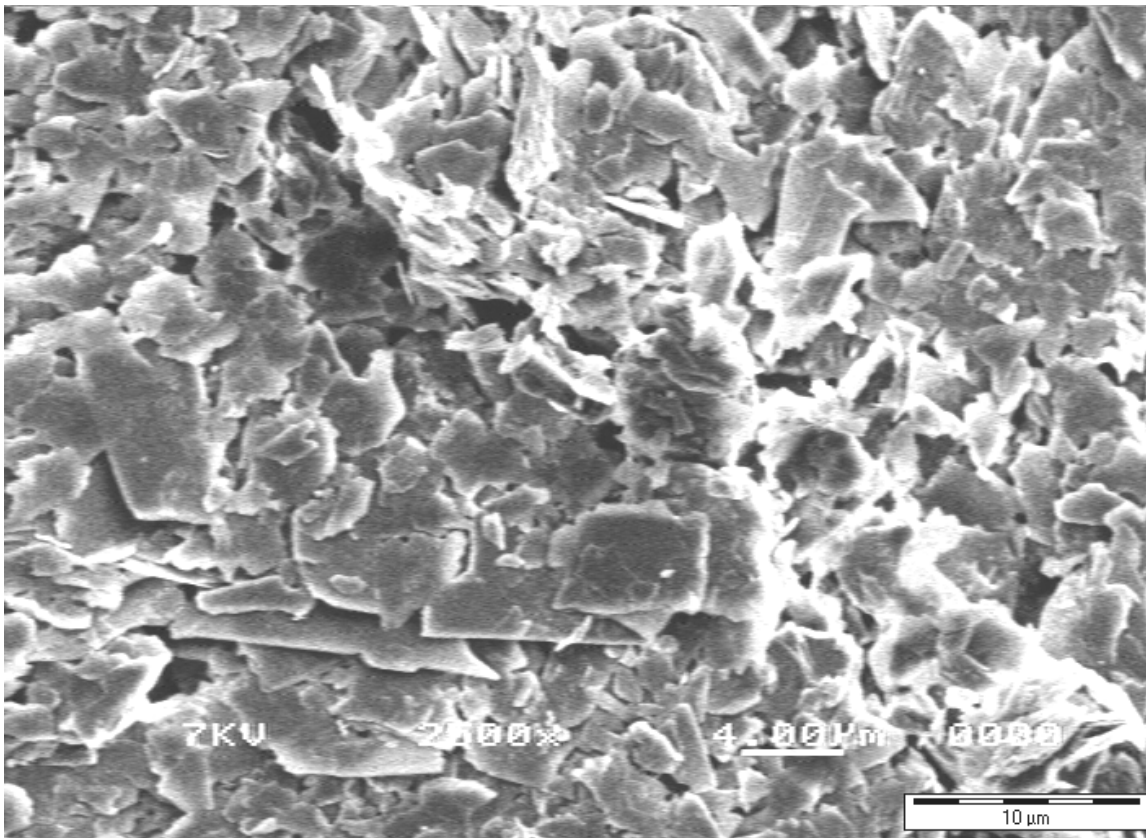


Batch 4 - 30min

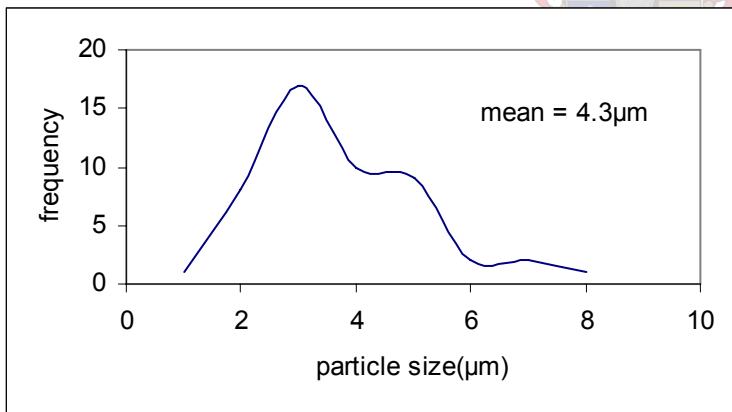
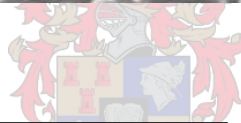
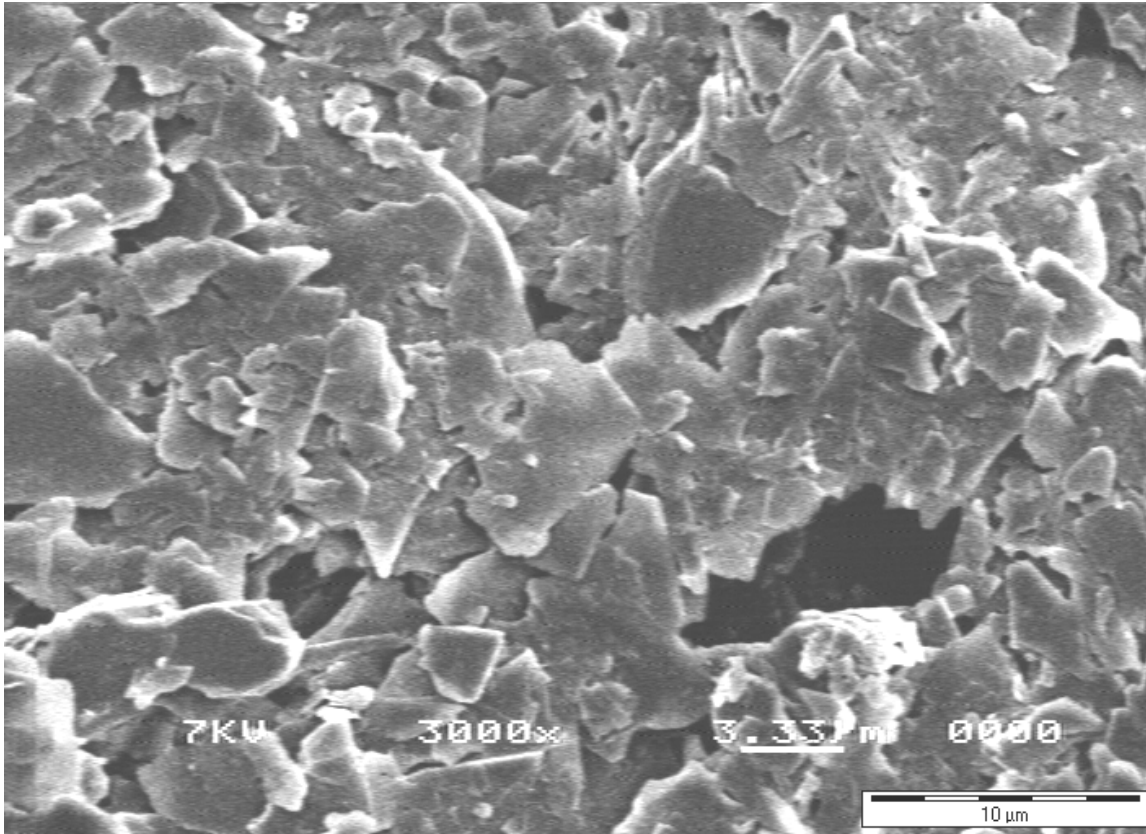


C2.1 SEM and PSD for Talc Dispersed in Cowles Mill – Batch F

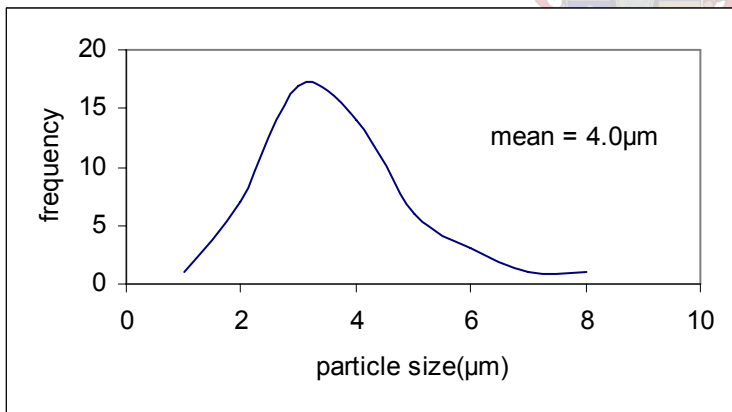
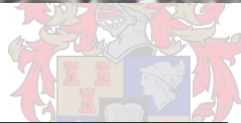
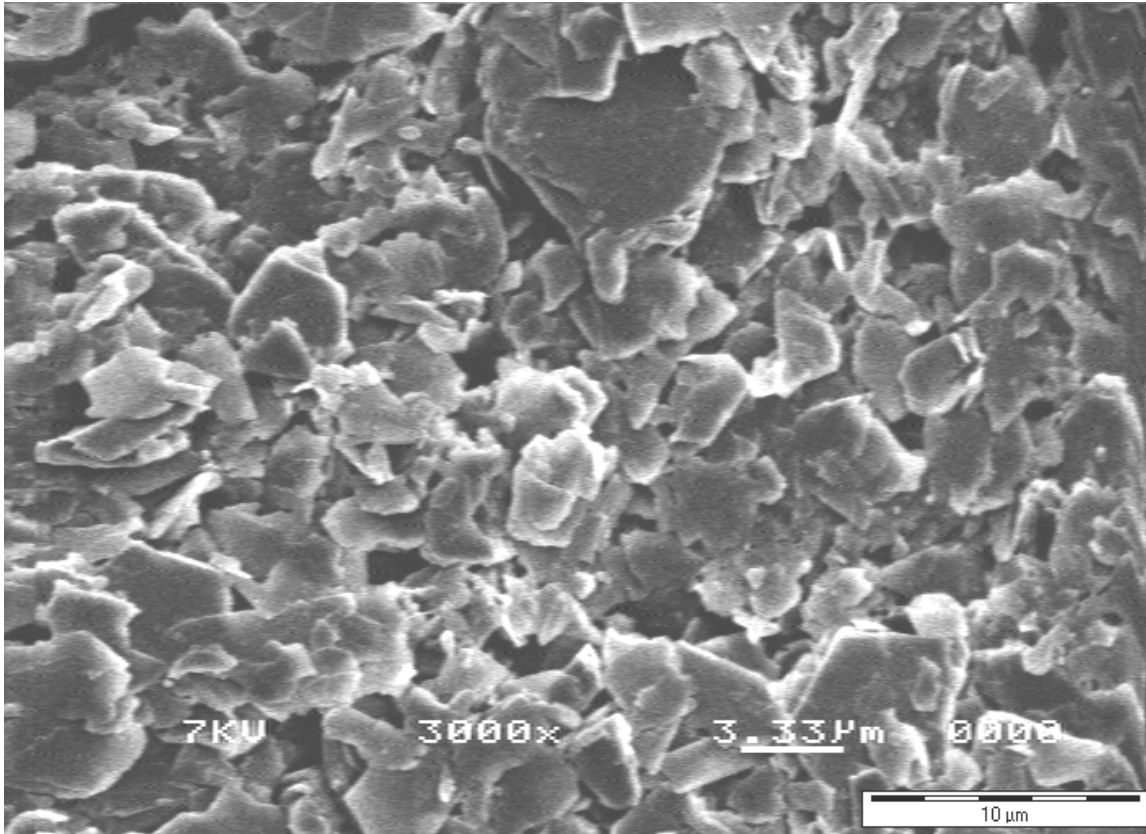
Batch F - 10min



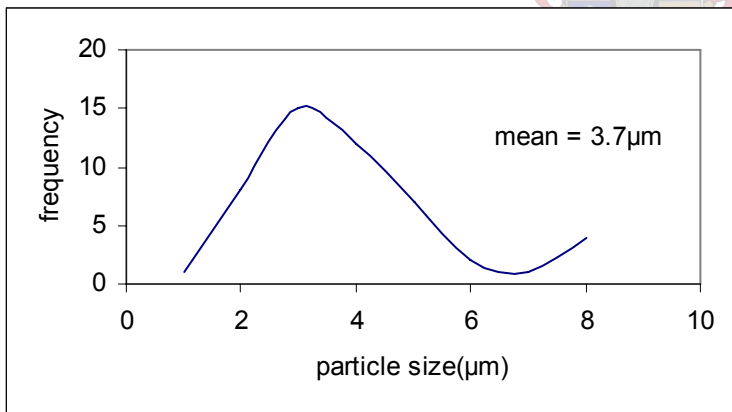
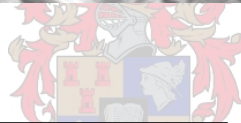
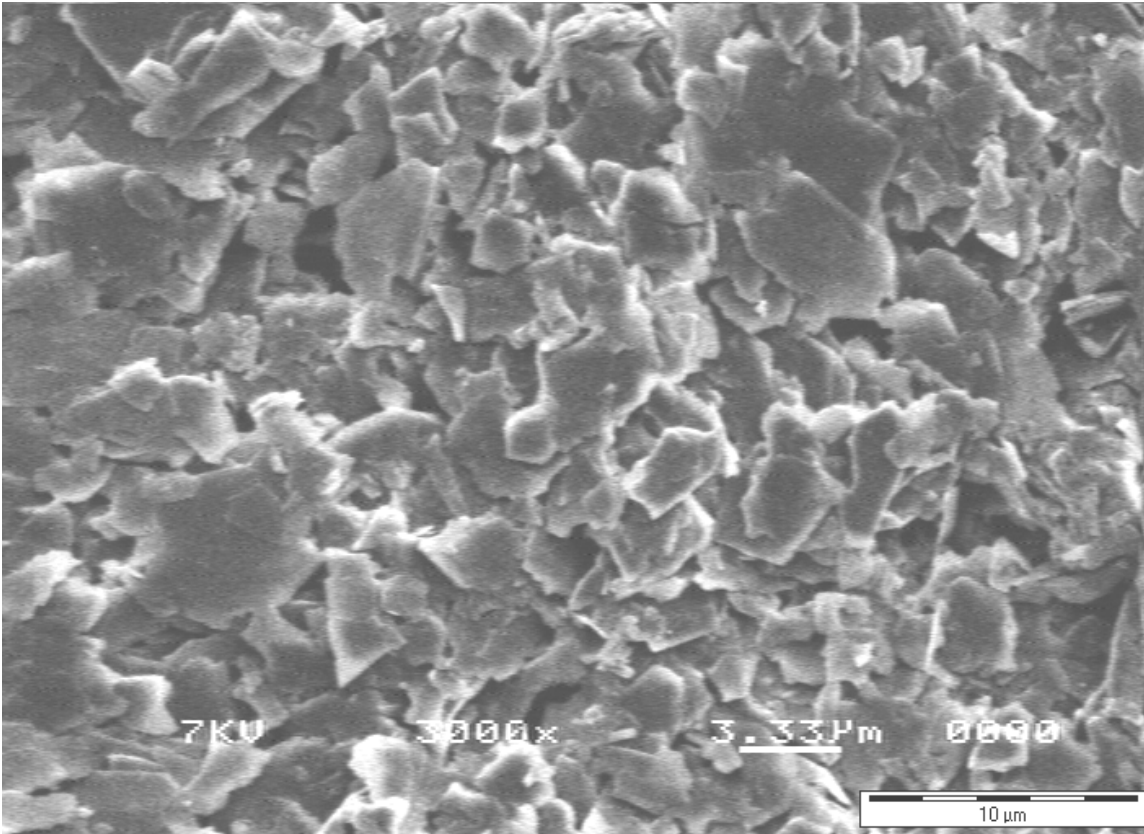
Batch F - 15min



Batch F - 20min

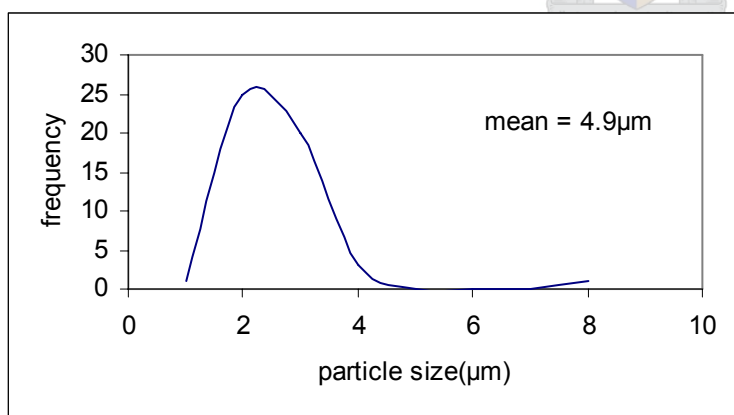
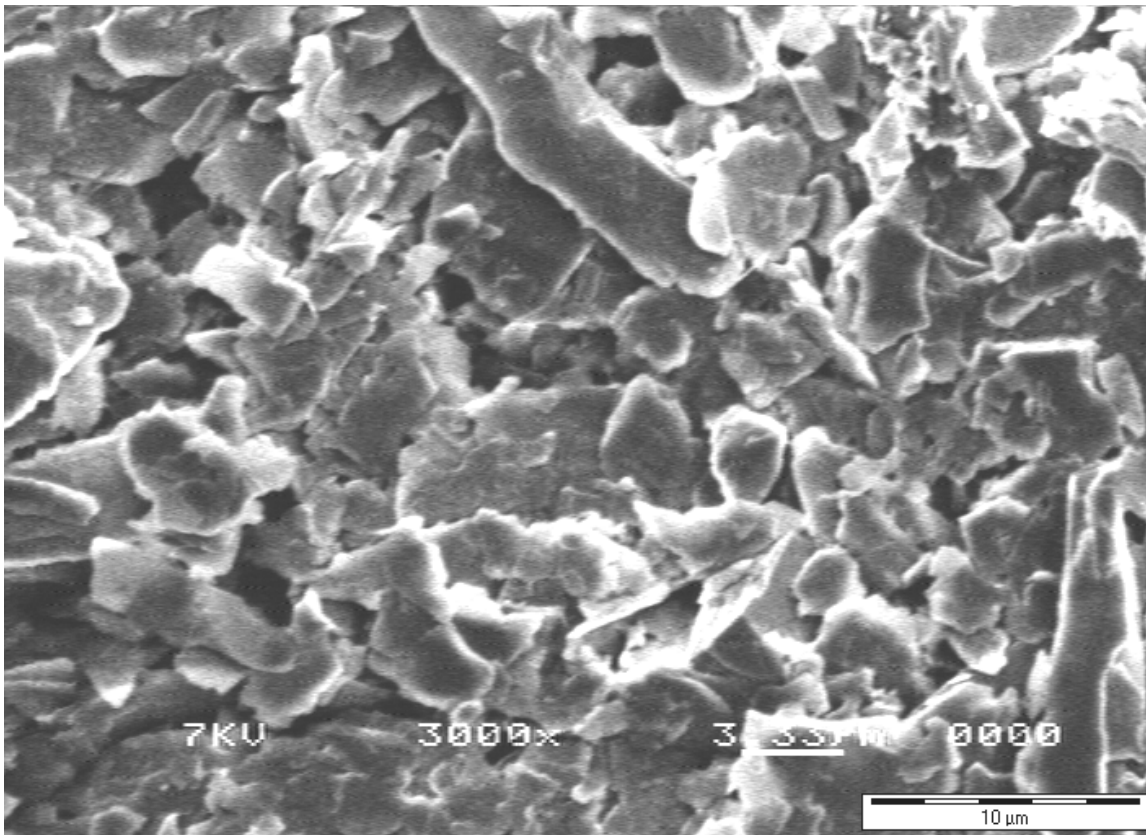


Batch F - 30min

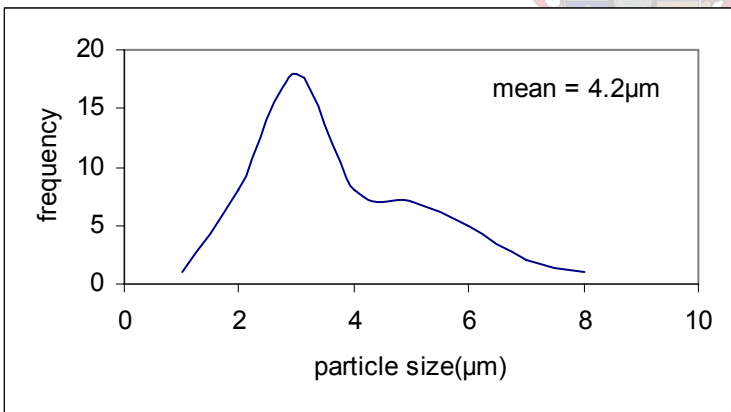
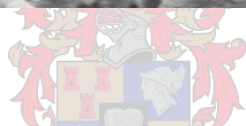
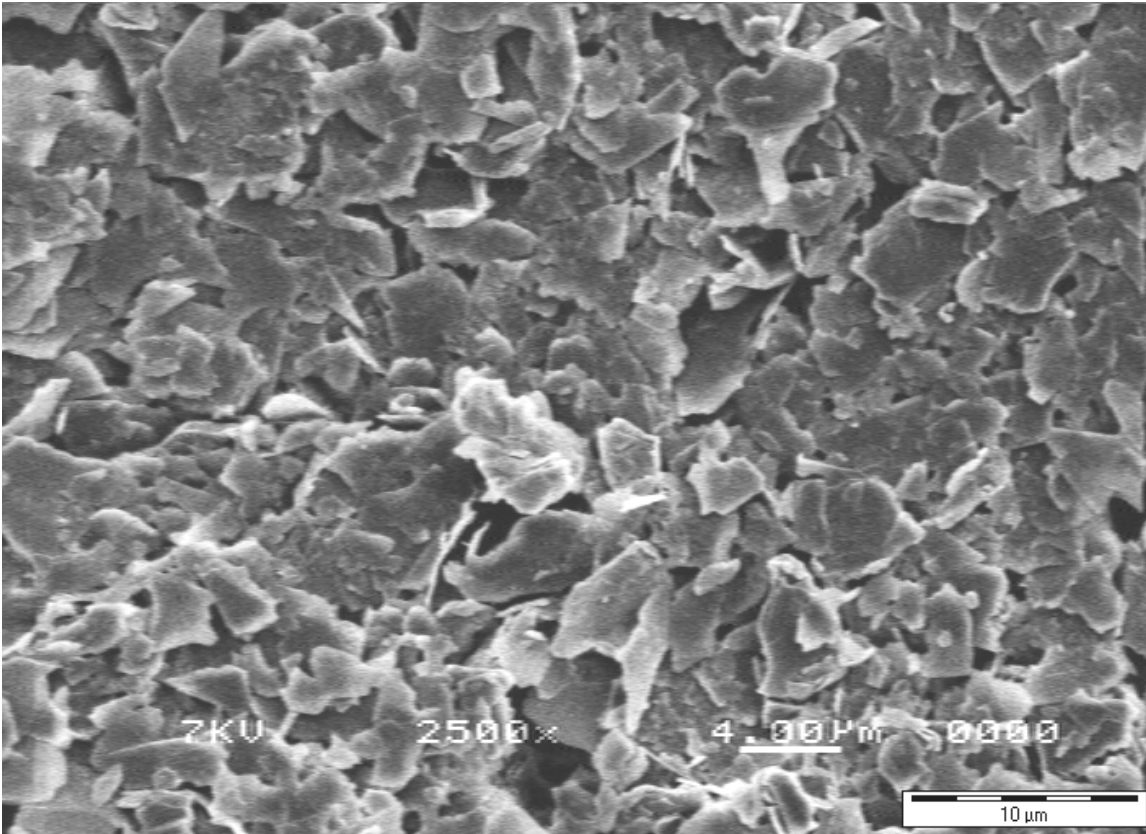


C2.2 SEM and PSD for Talc Dispersed in Cowles Mill – Batch G

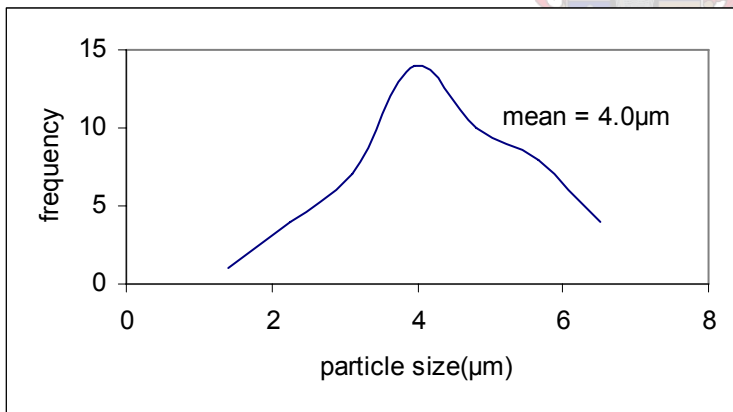
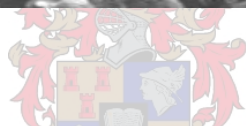
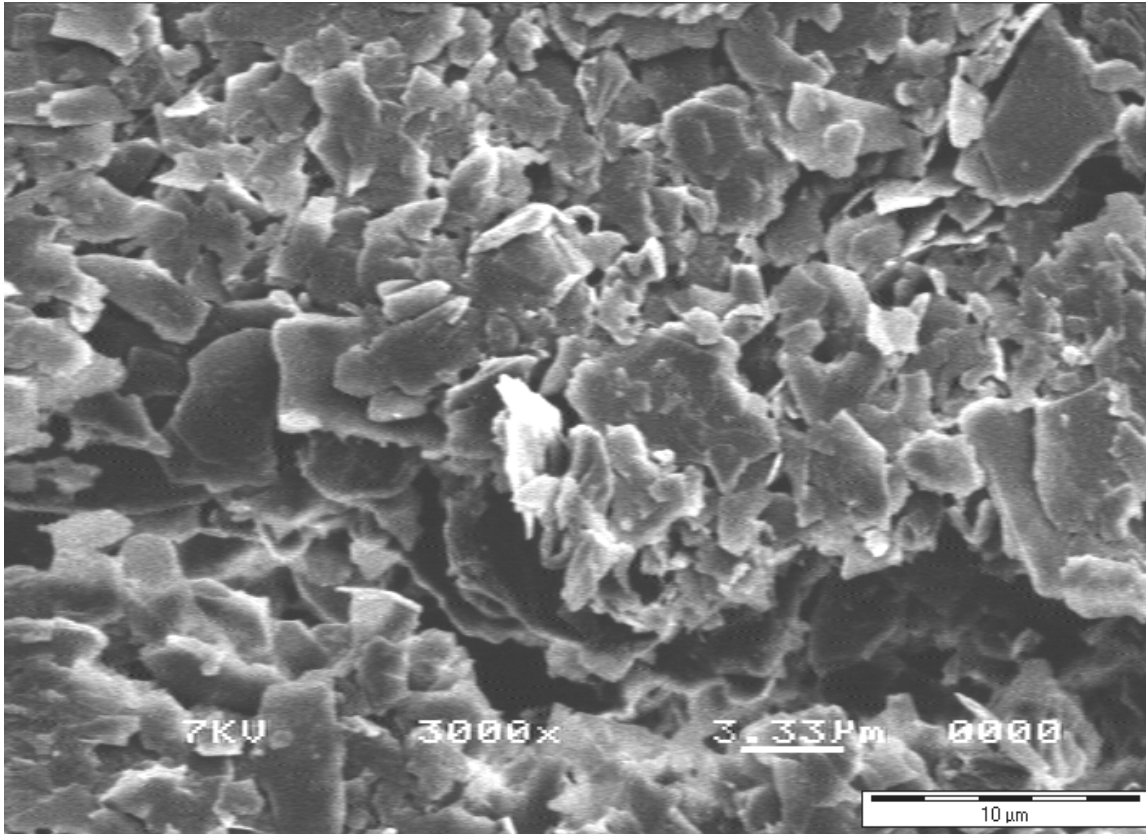
Batch G - 10min



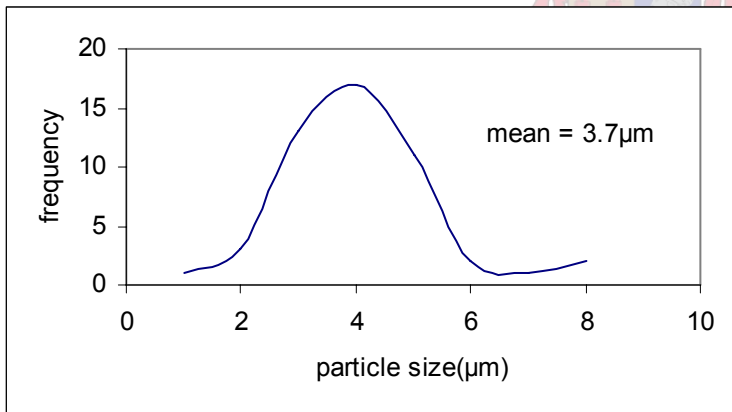
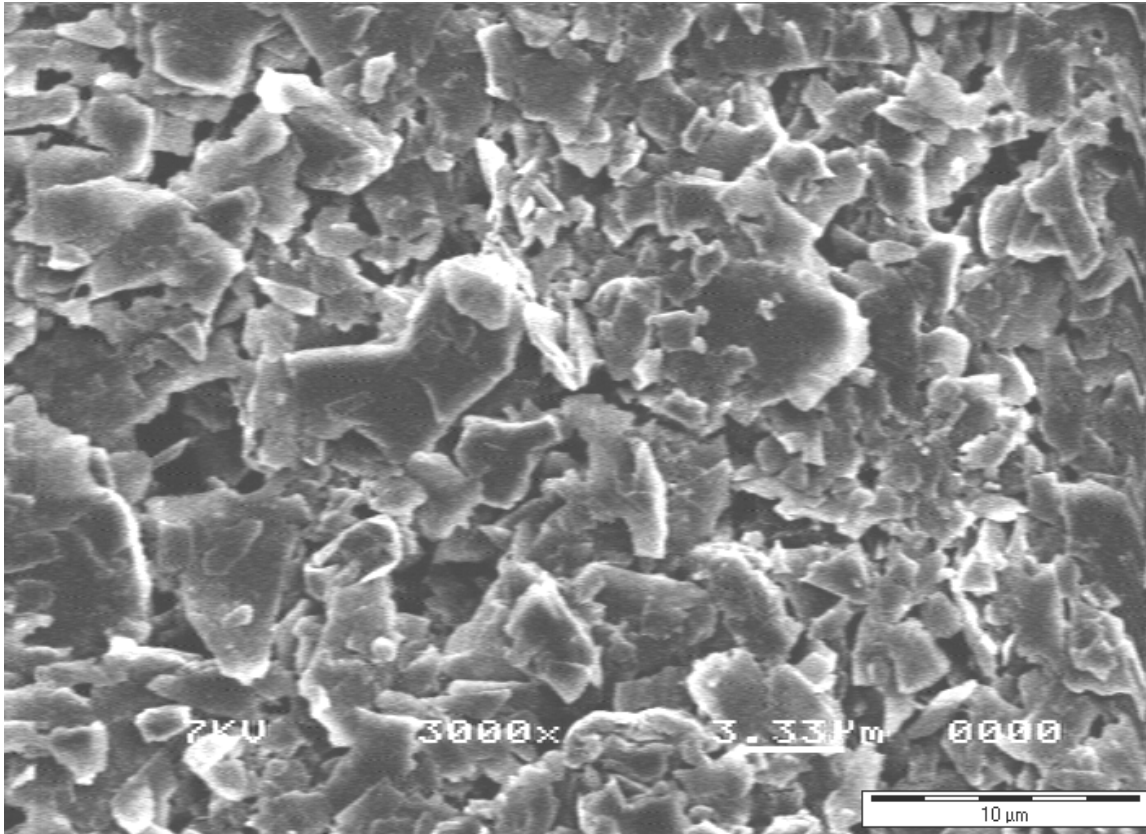
Batch G - 15min



Batch G - 20min

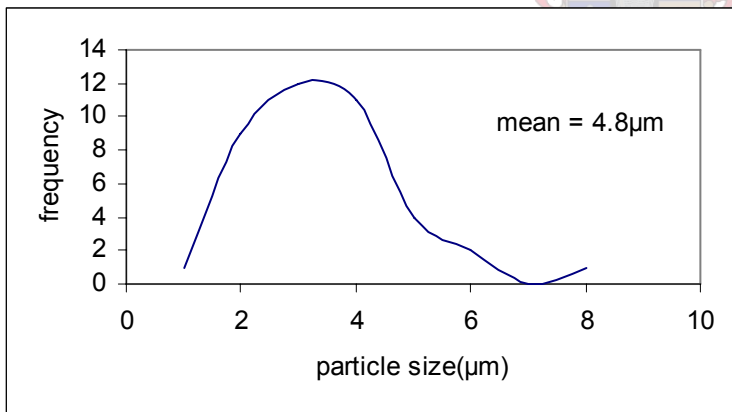
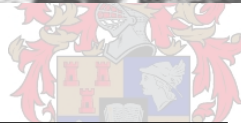
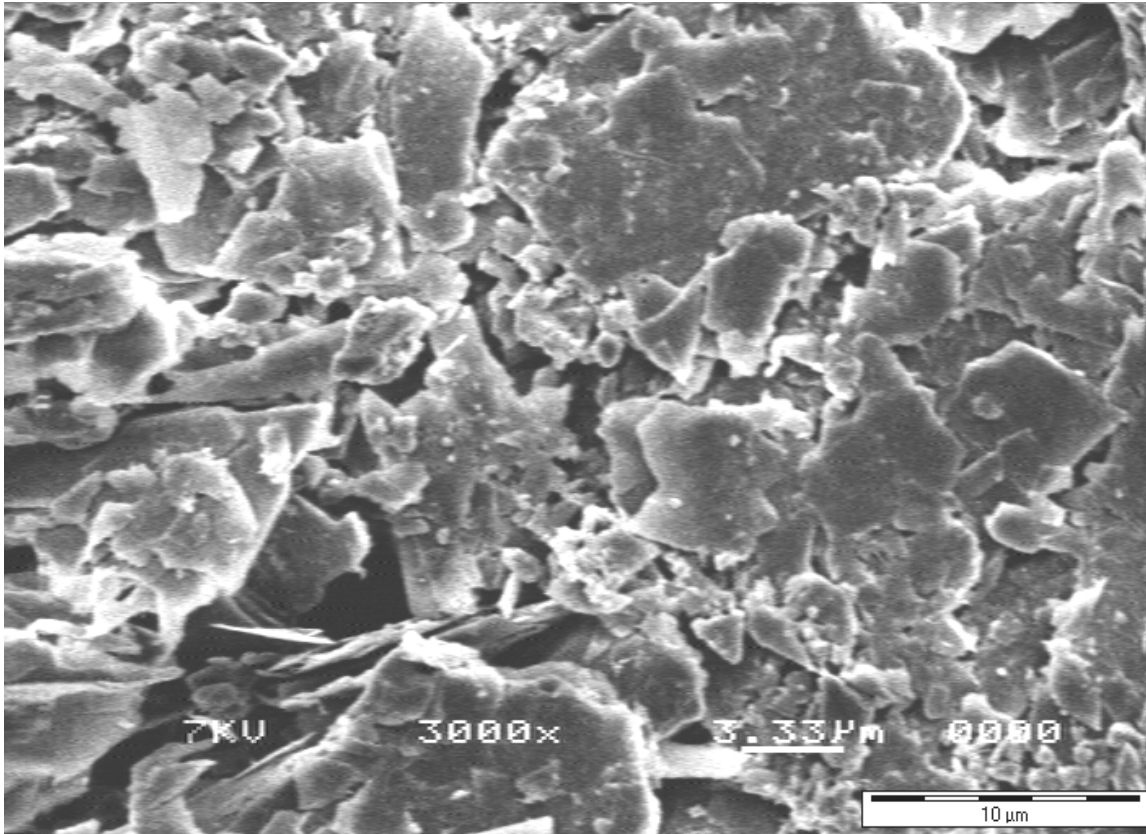


Batch G - 30min

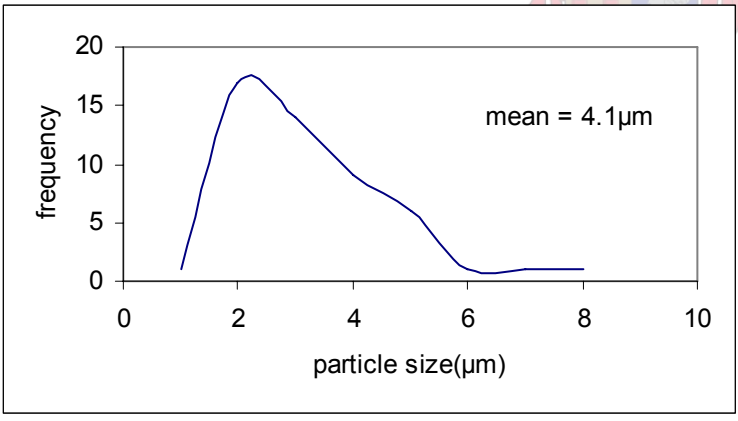
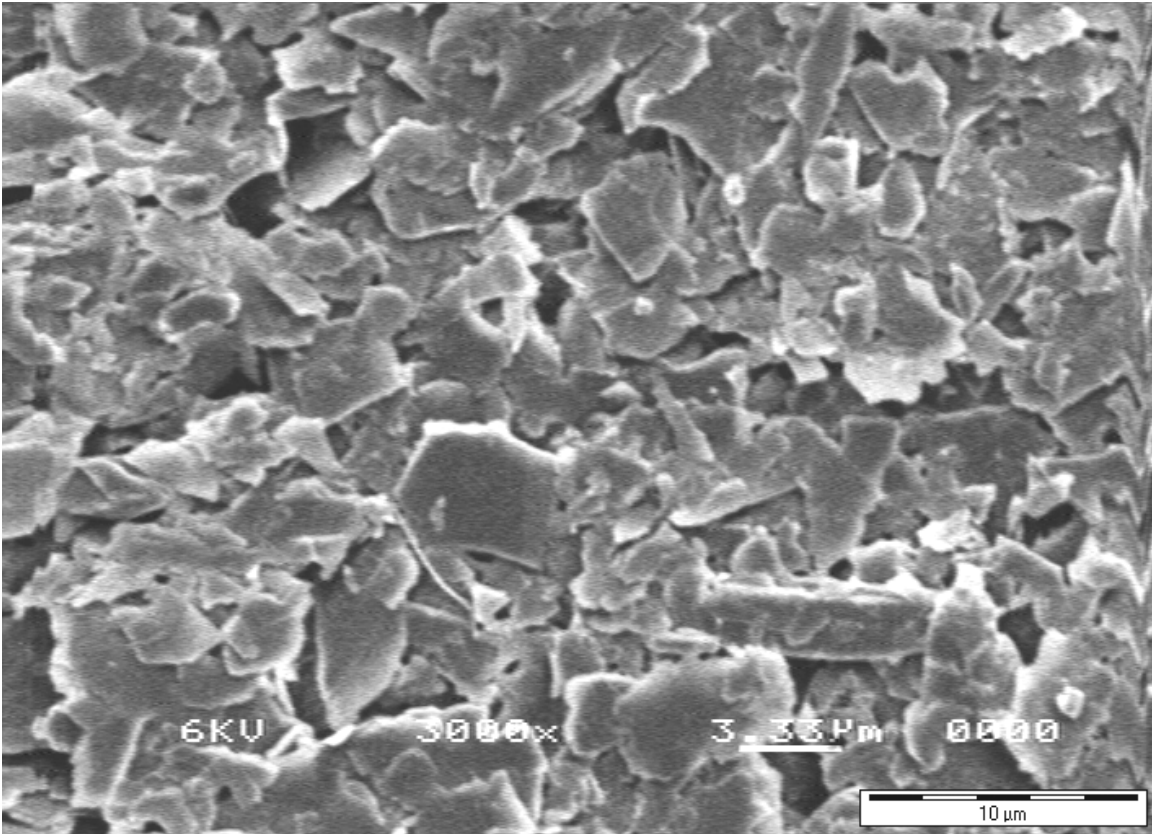


C2.3 SEM and PSD for Talc Dispersed in Cowles Mill – Batch H

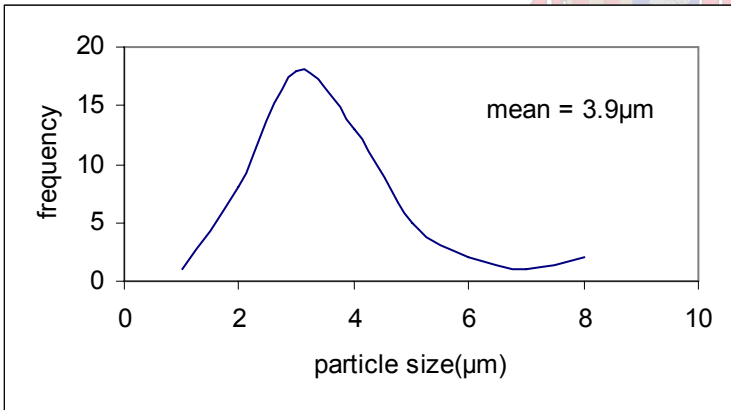
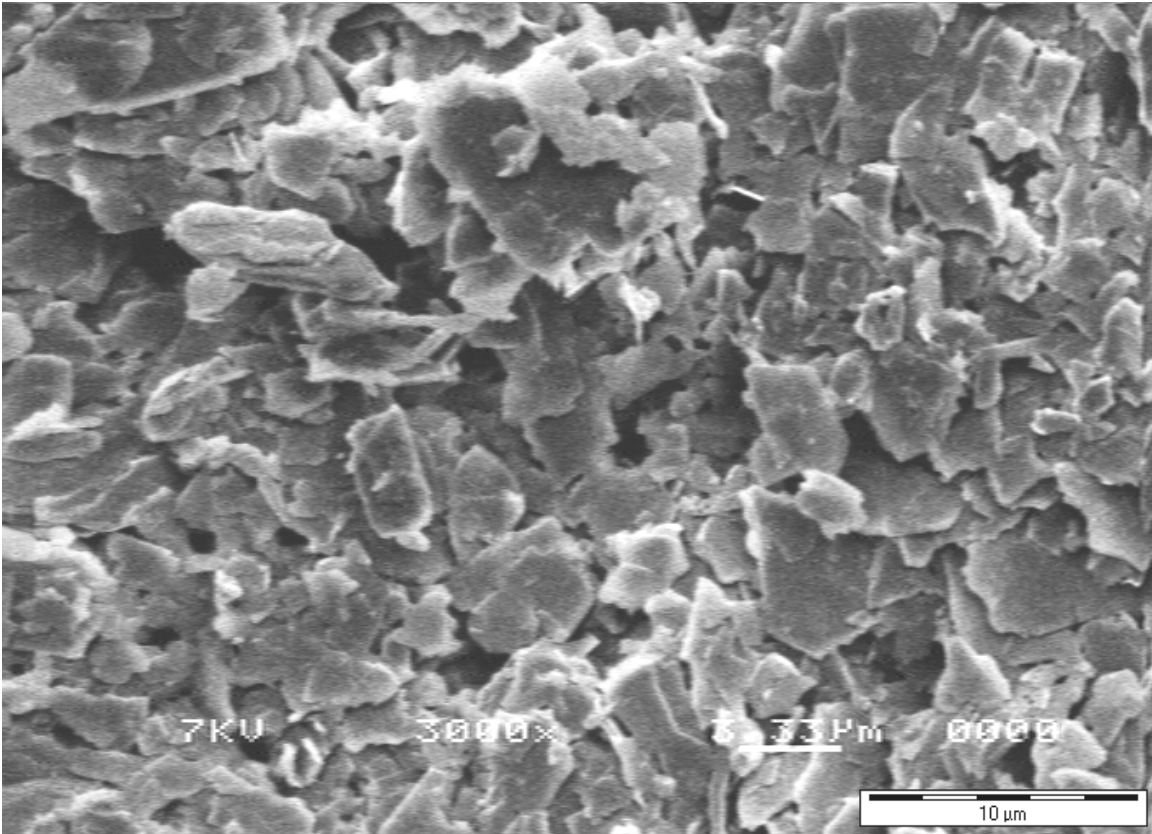
Batch H - 10min



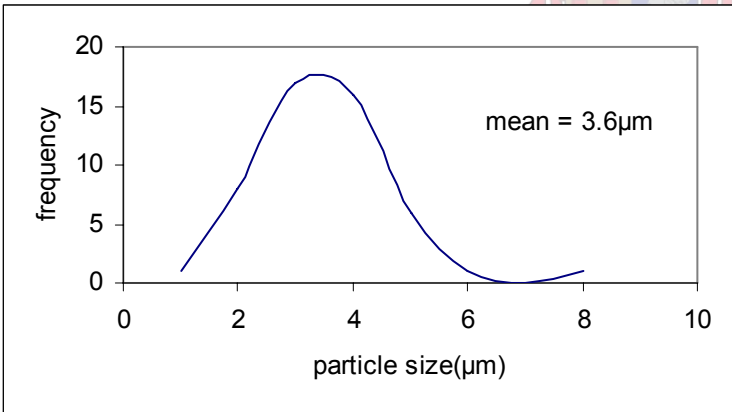
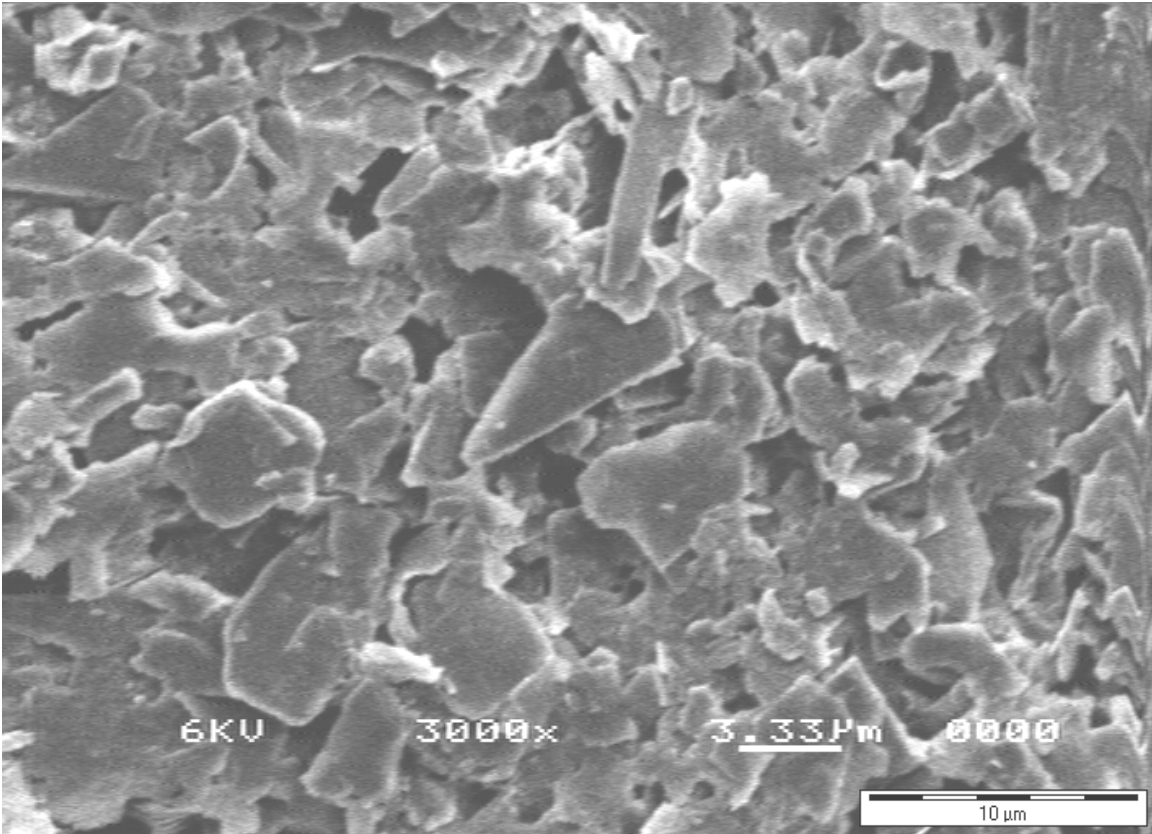
Batch H - 15min



Batch H - 20min

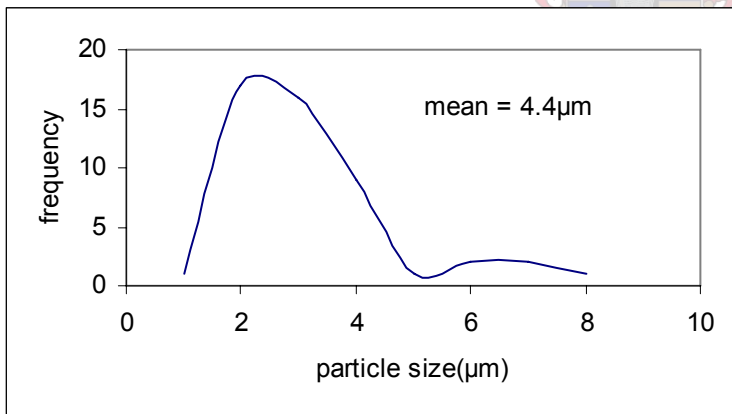
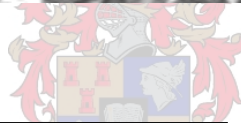
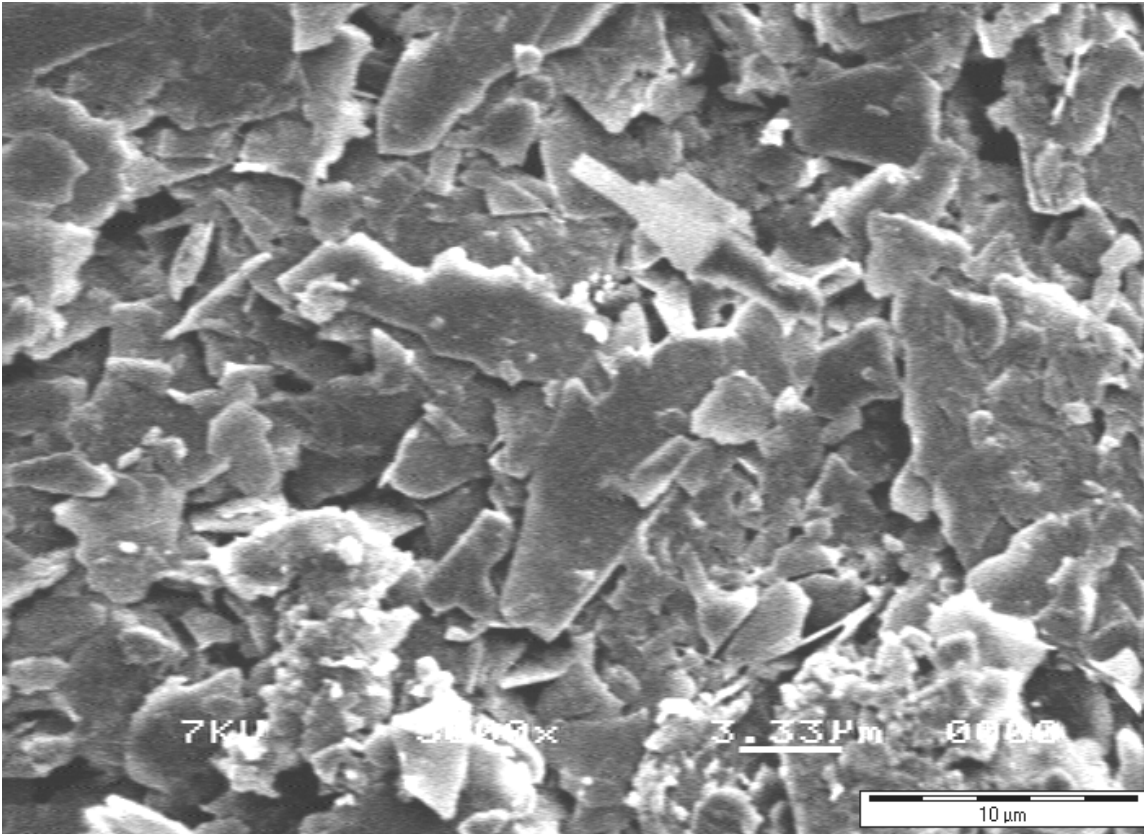


Batch H - 30min

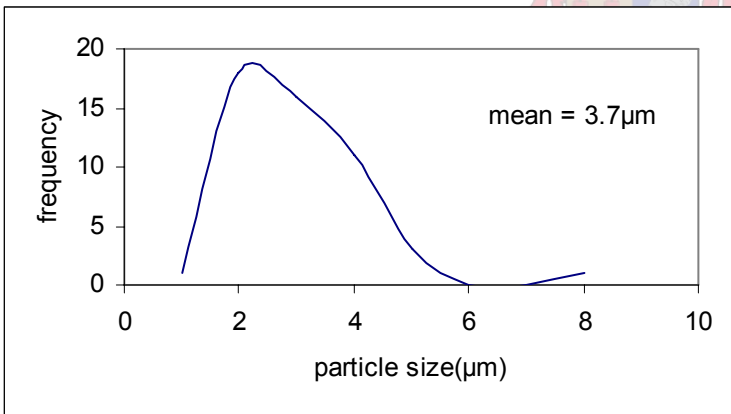
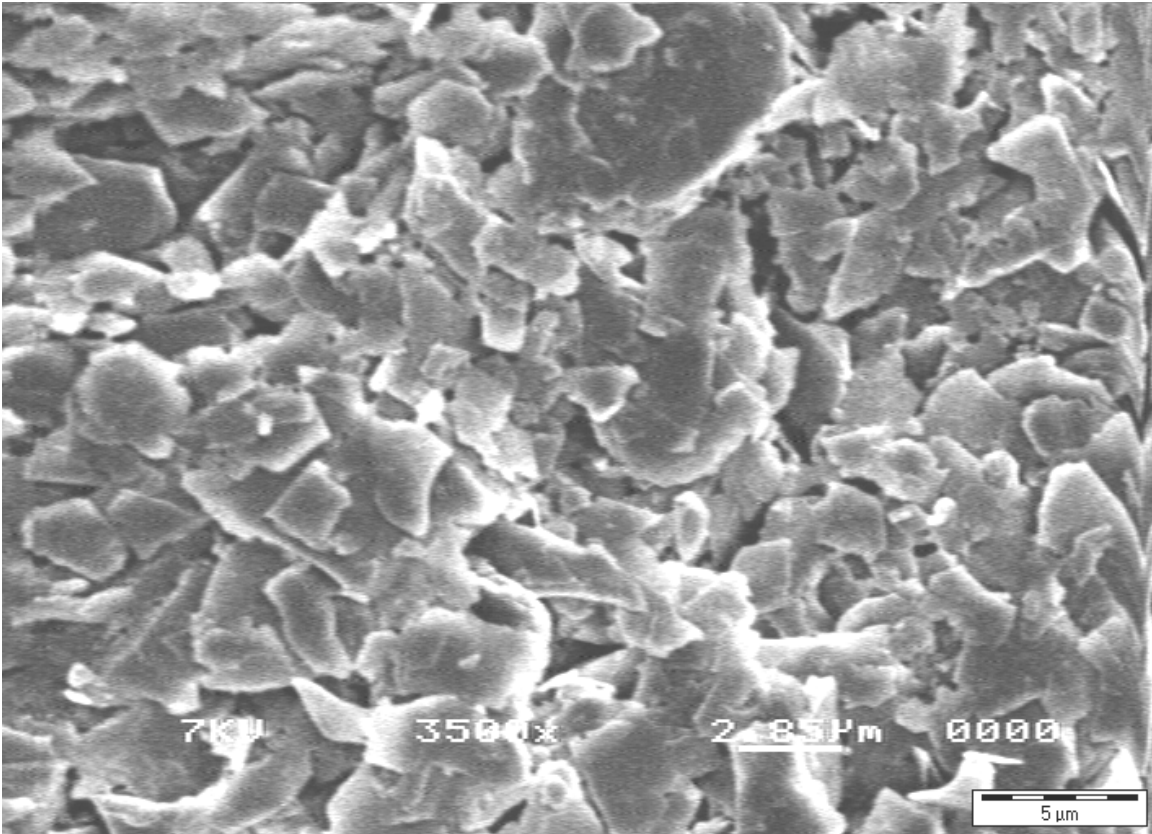


C2.4 SEM and PSD for Talc Dispersed in Cowles Mill – Batch J

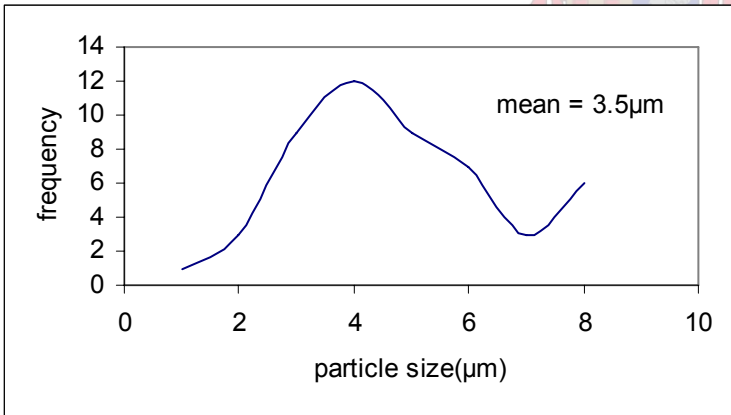
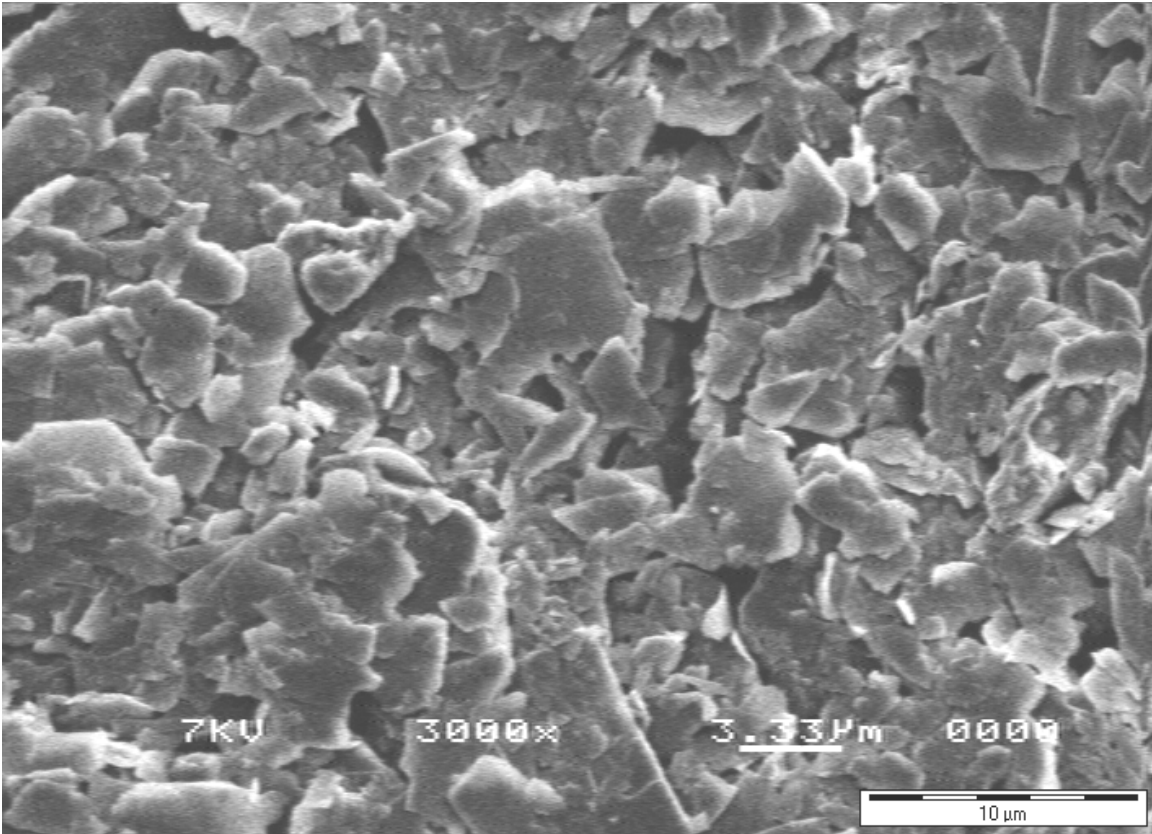
Batch J - 10min



Batch J - 20min

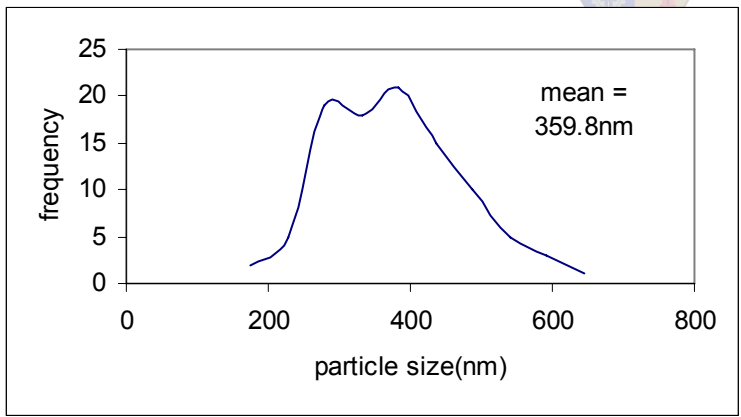
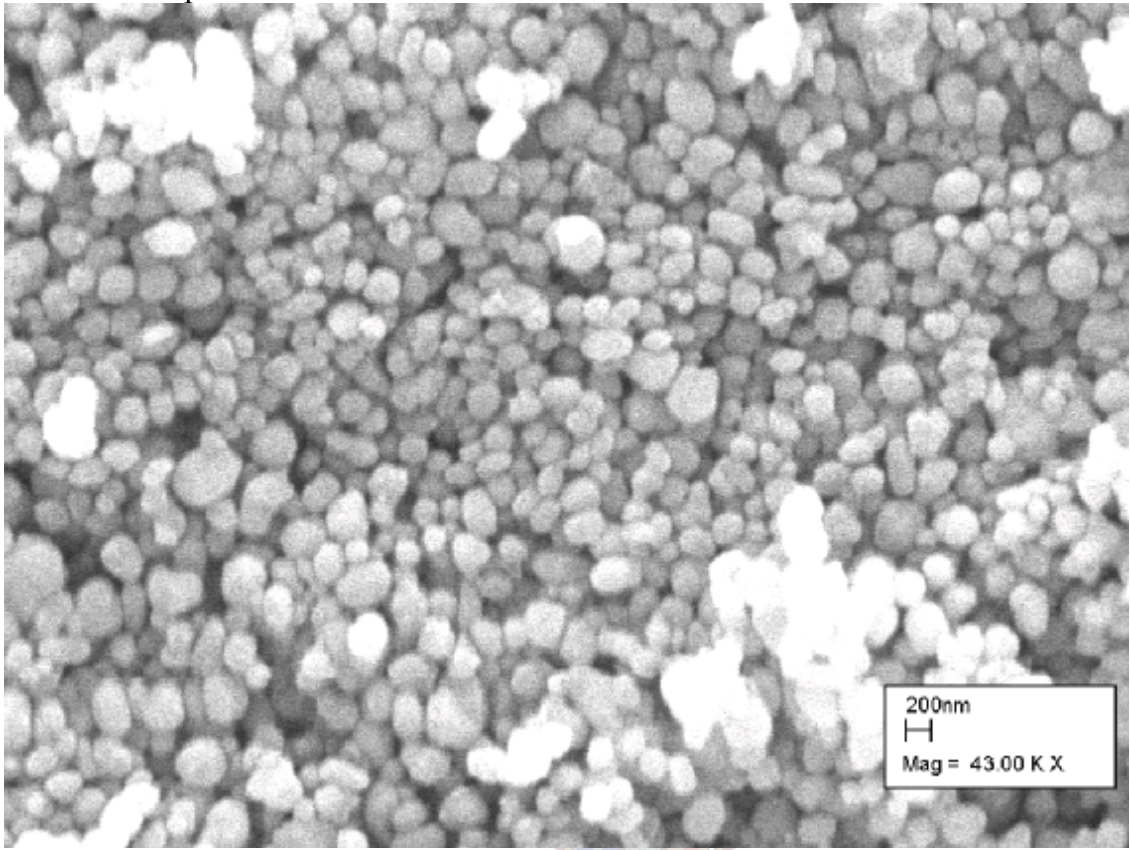


Batch J - 30min

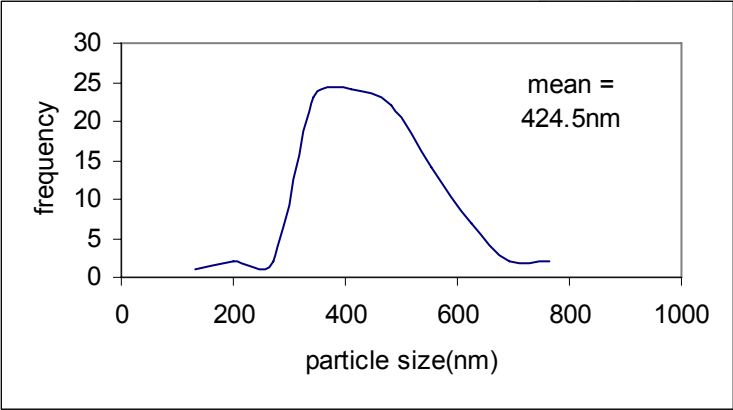
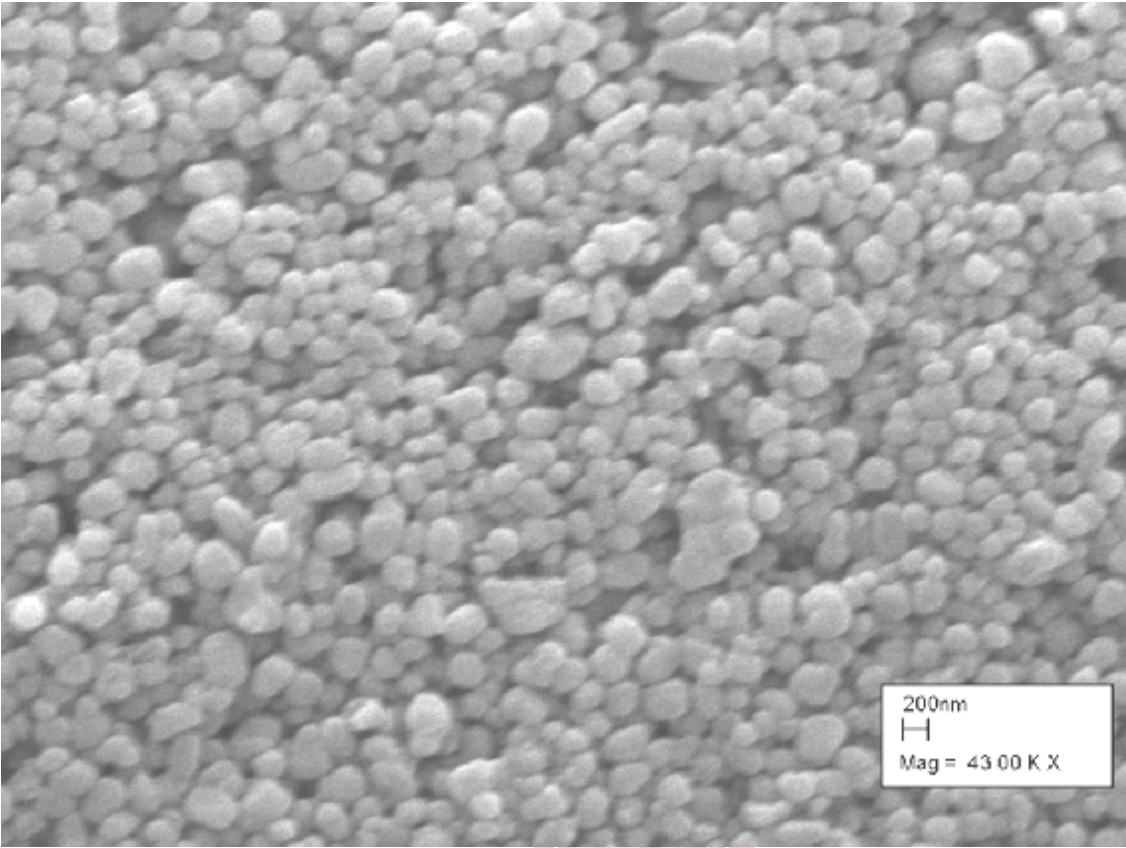


C3.1 SEM and PSD for The Homogenisation of Batch A

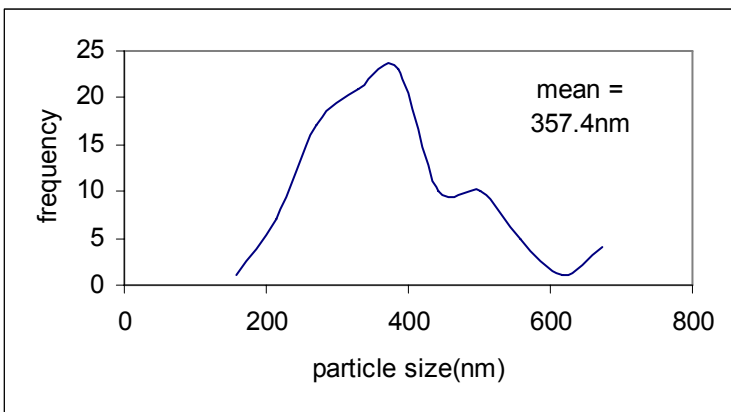
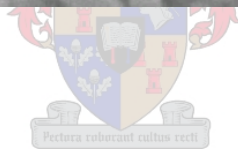
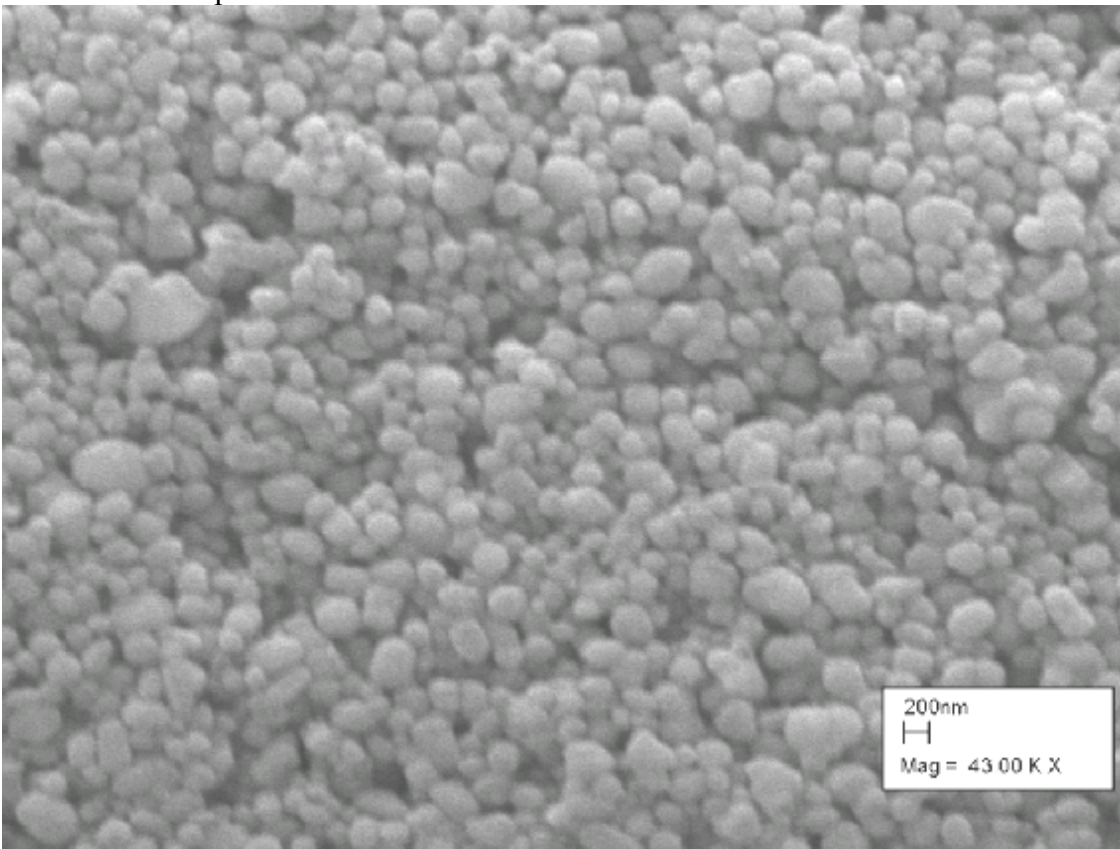
Batch A - 2passes



Batch A - 4passes

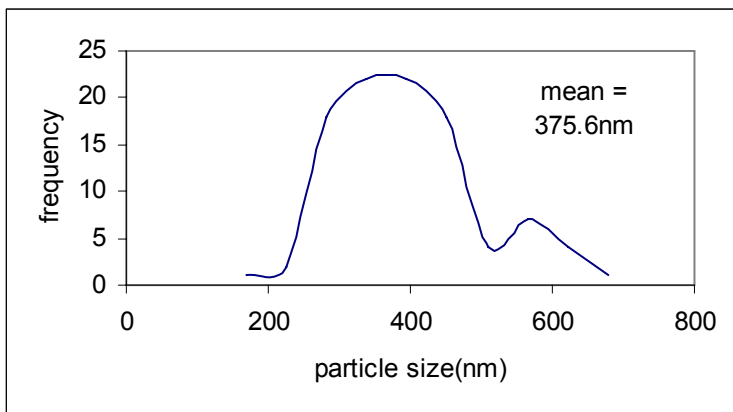
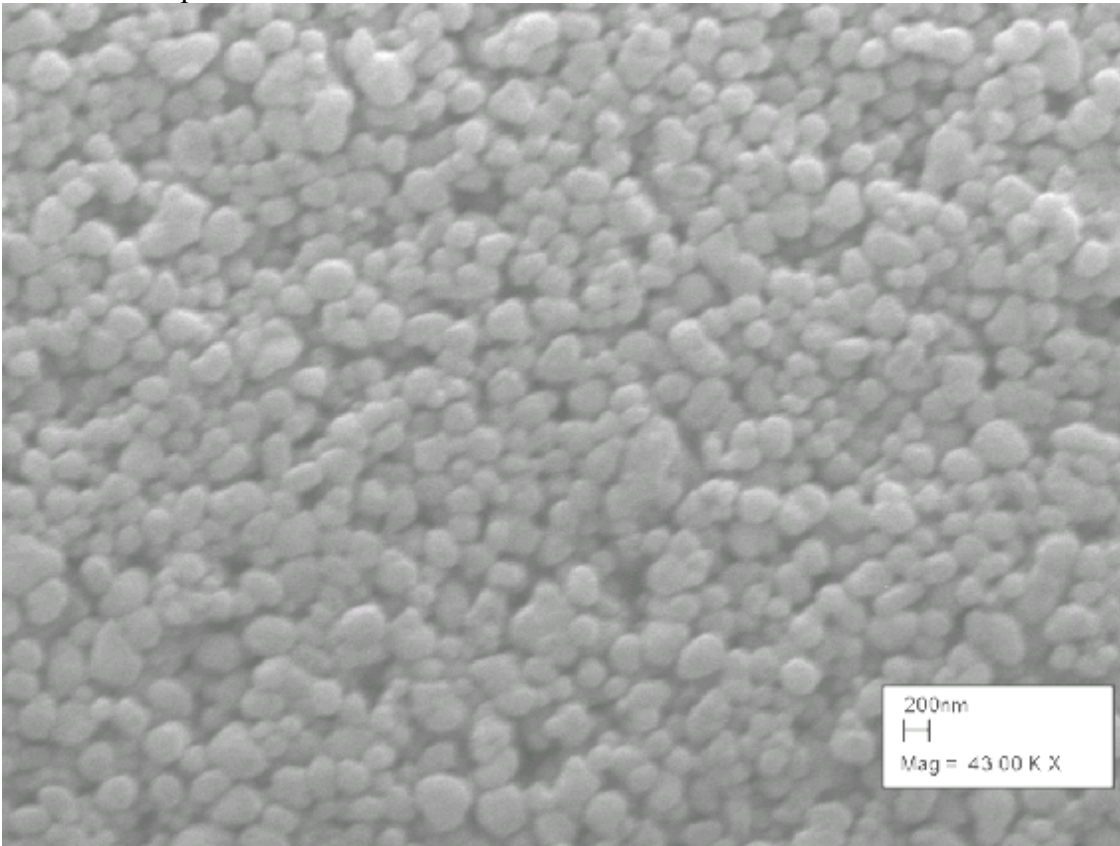


Batch A - 10passes

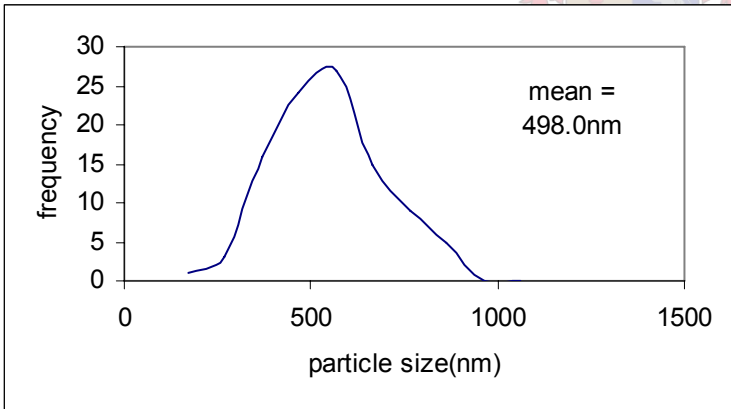
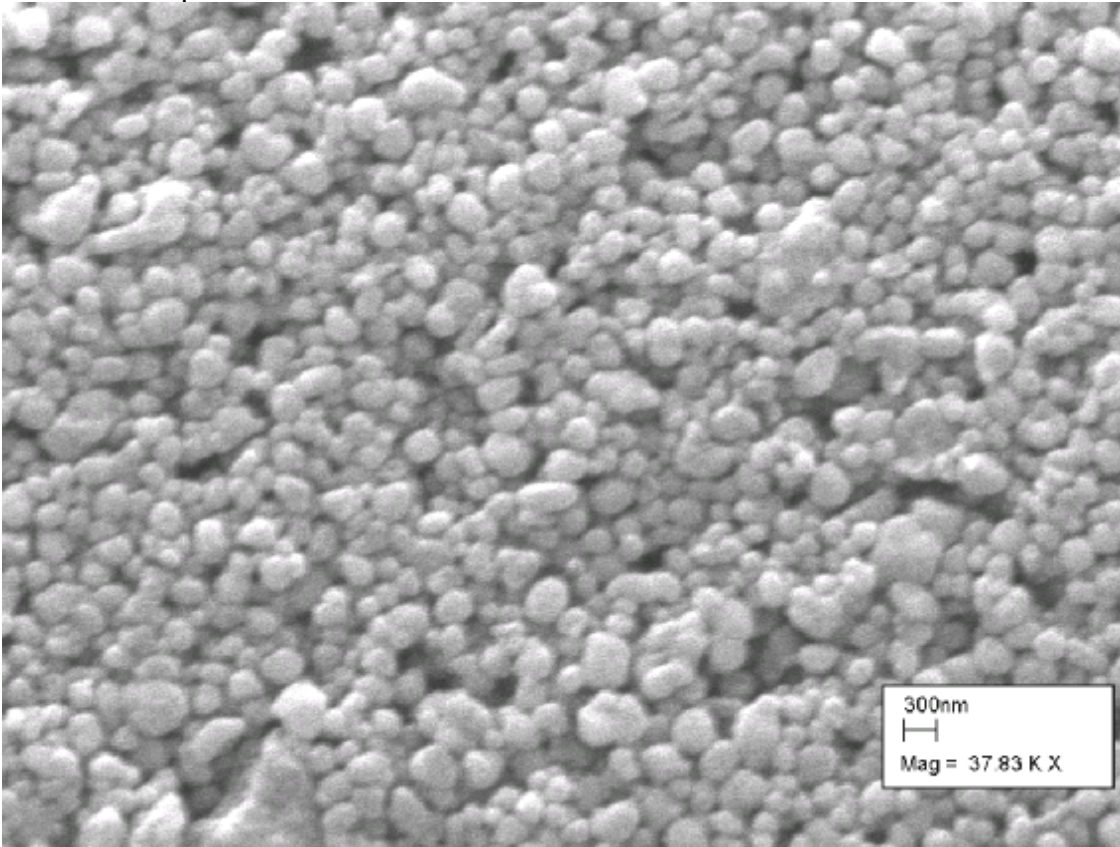


C3.2 A SEM and PSD for The Homogenisation of Batch B

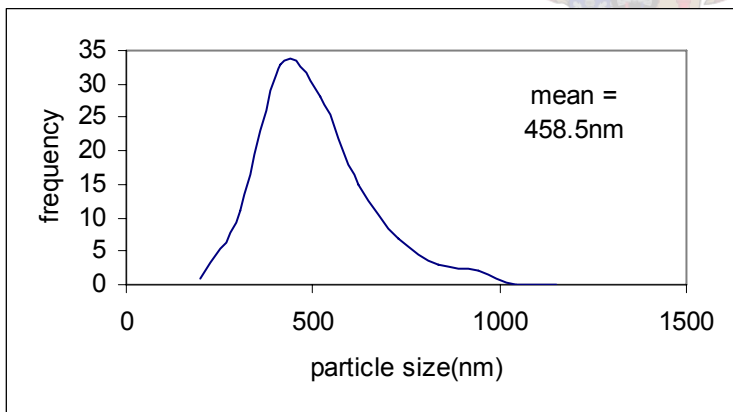
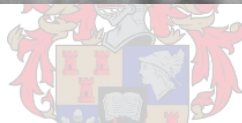
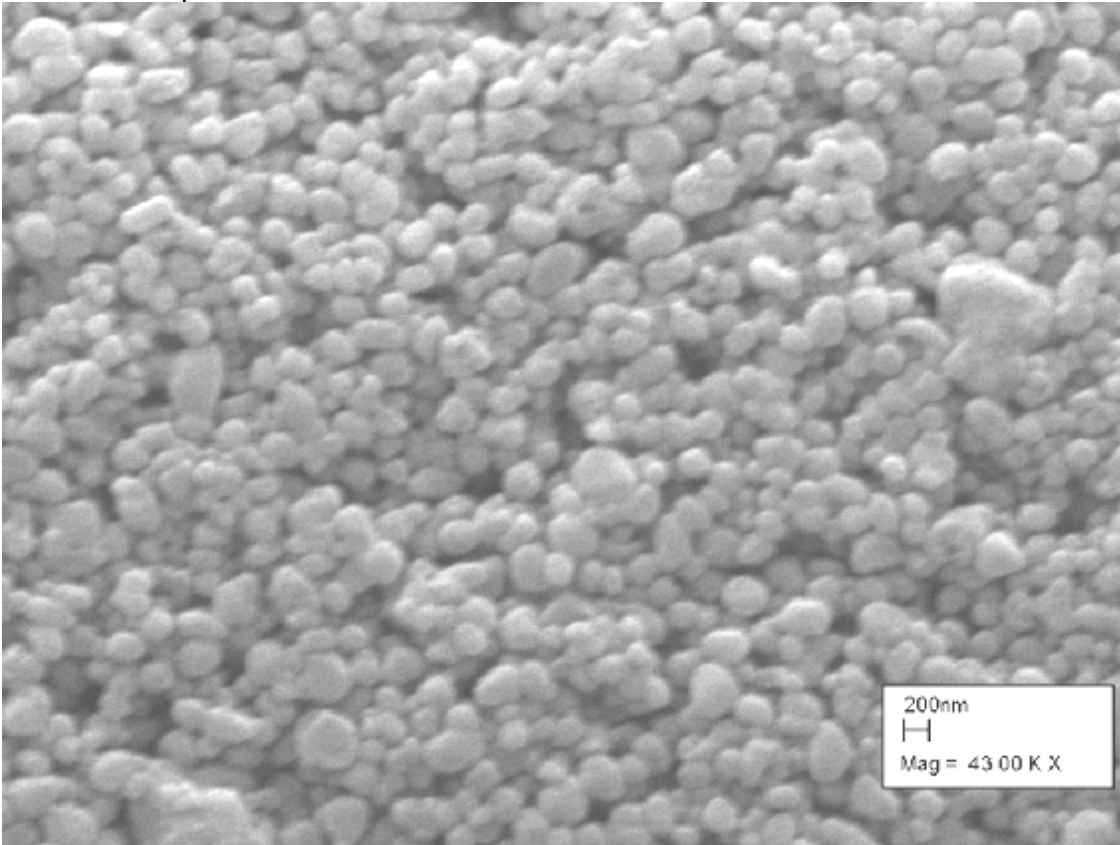
Batch B - 2passes



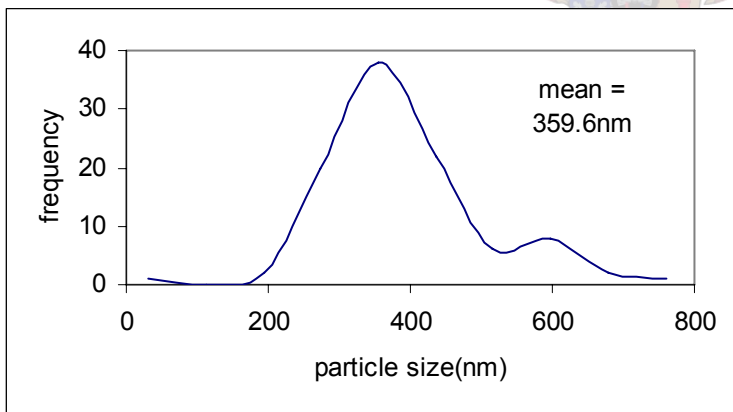
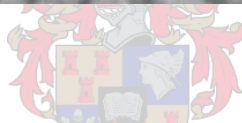
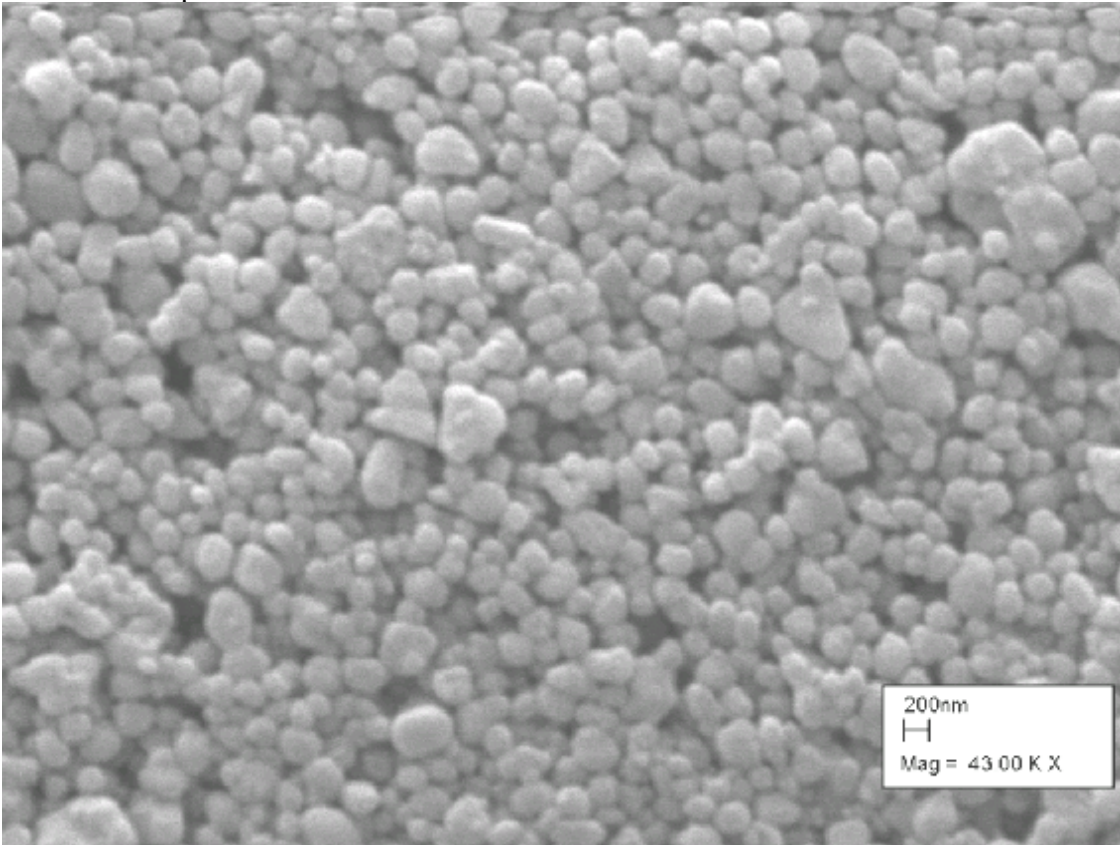
Batch B - 4passes



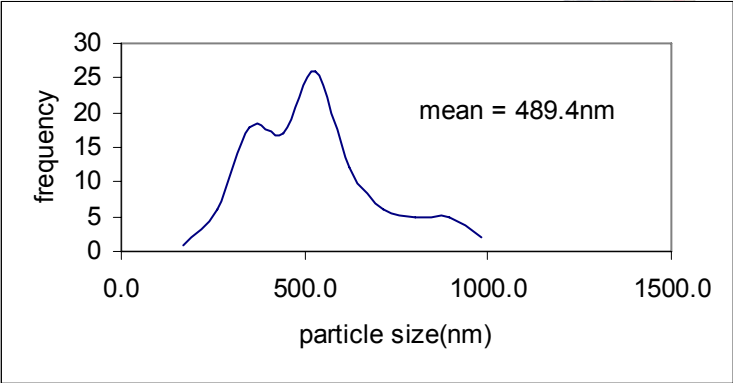
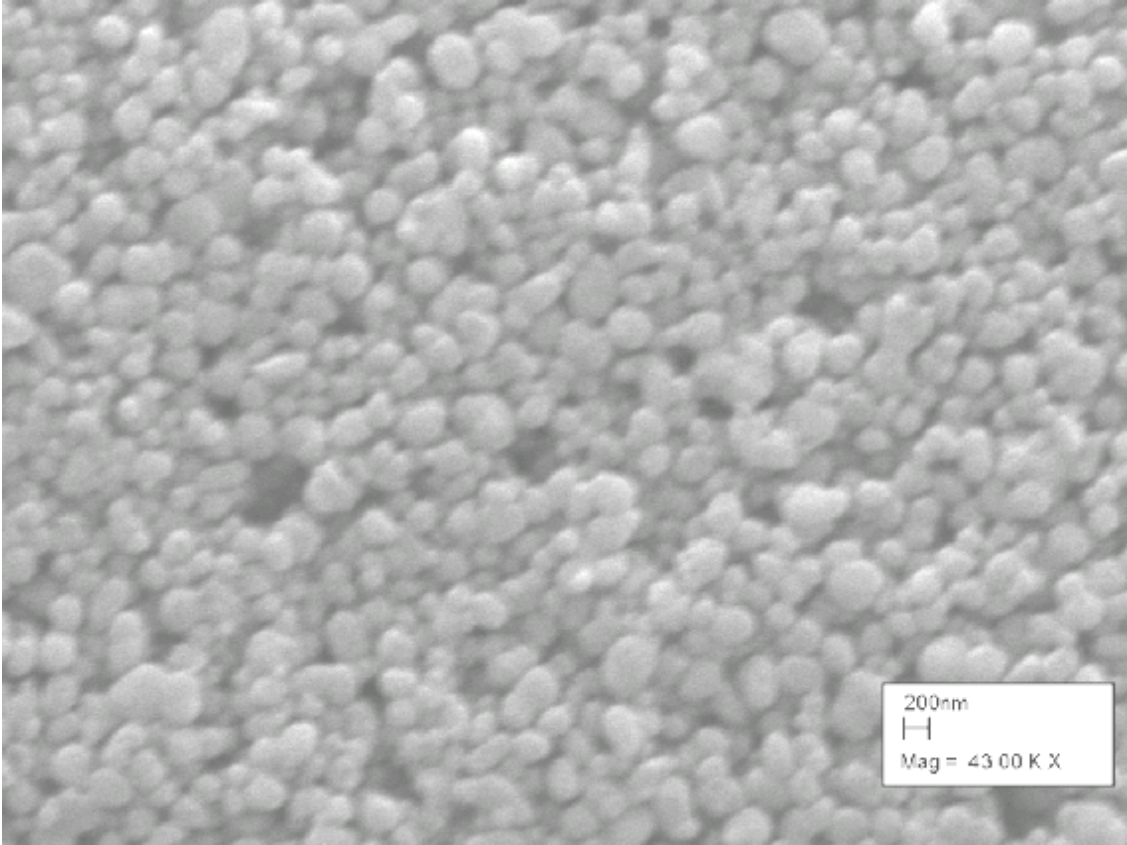
Batch B - 6passes



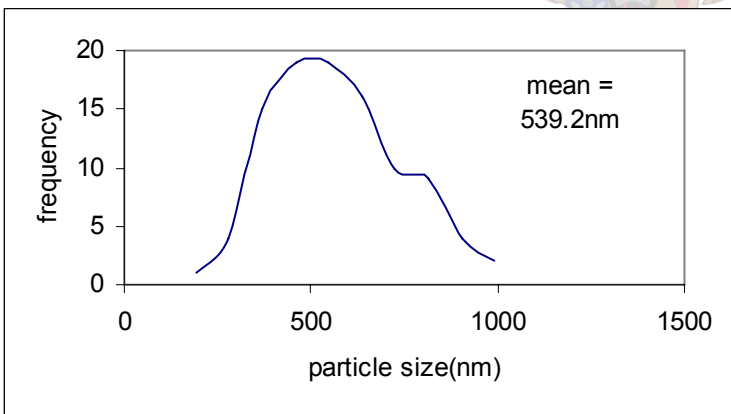
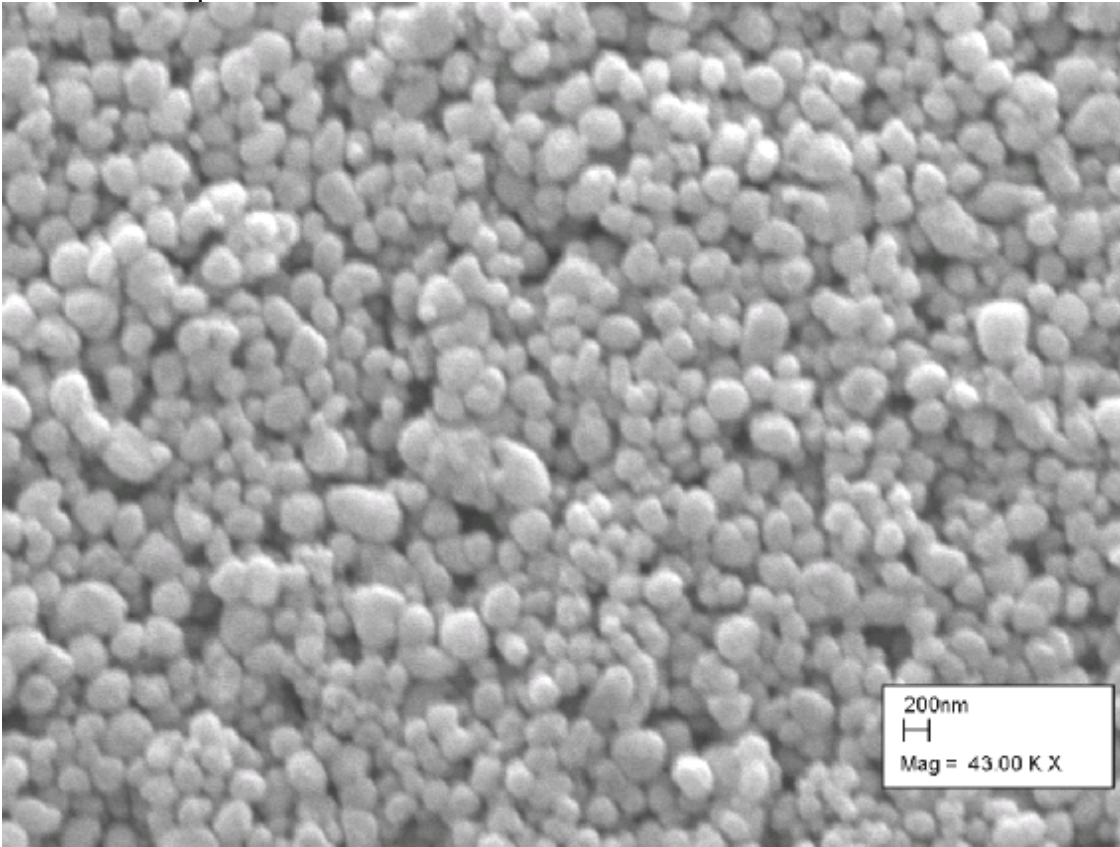
Batch B - 8passes



Batch B - 10passes

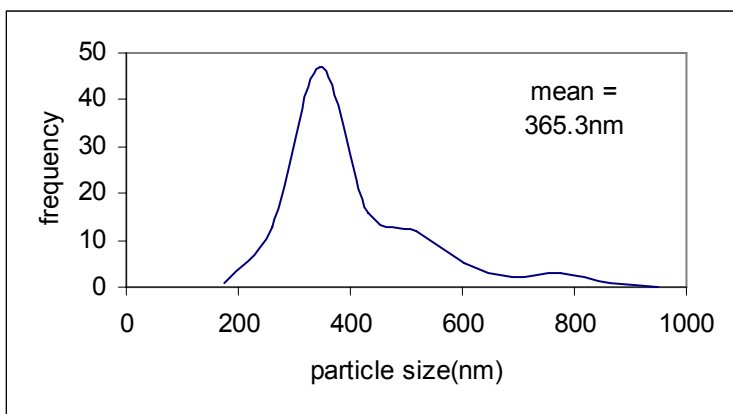
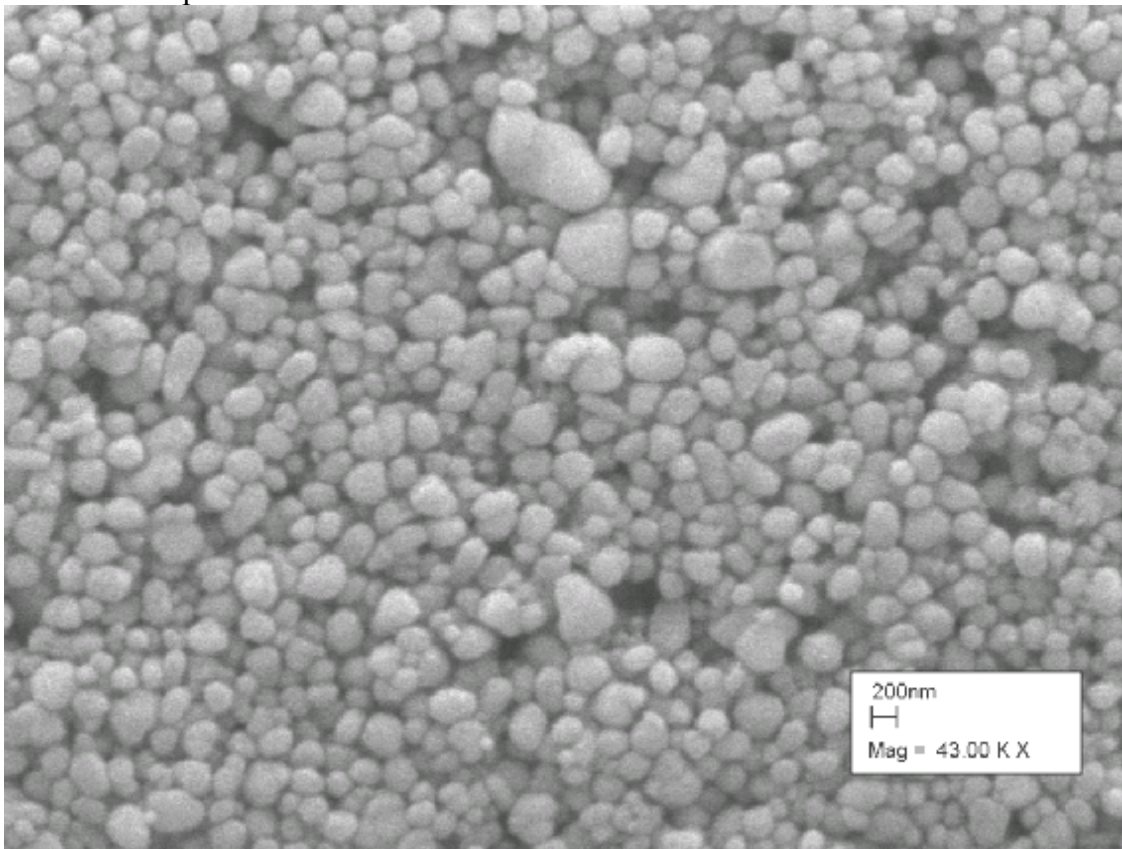


Batch B - 10passes

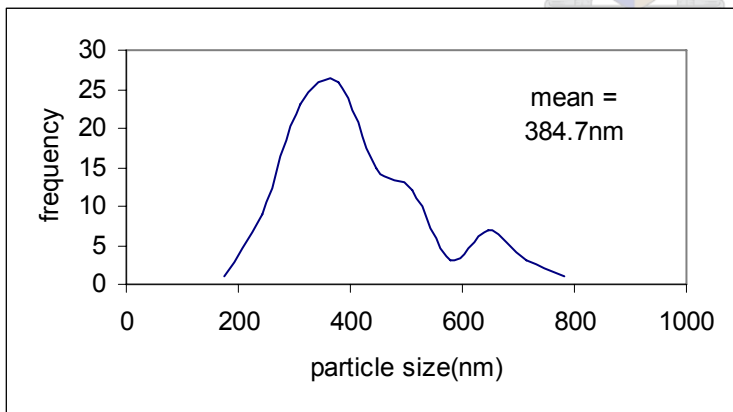
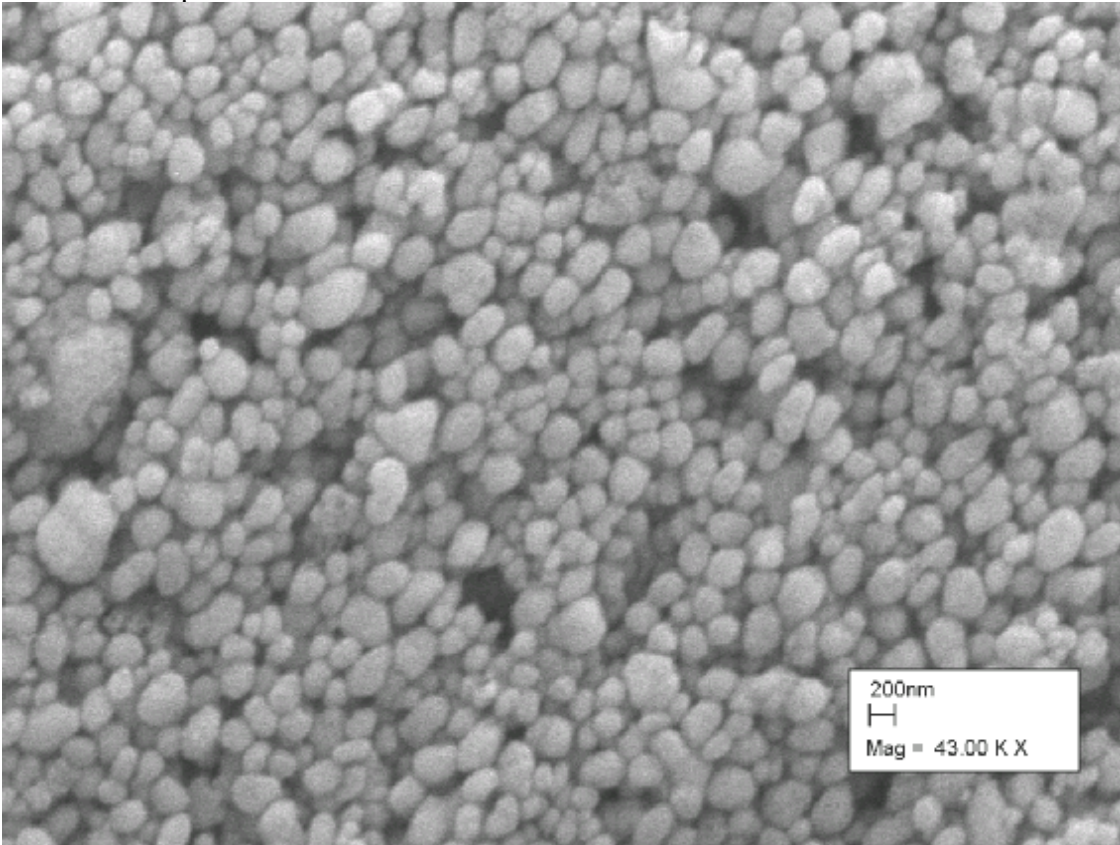


C3.3 A SEM and PSD for The Homogenisation of Batch C

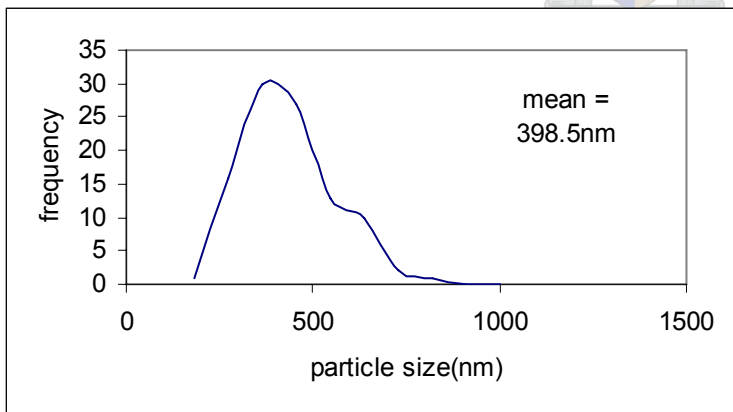
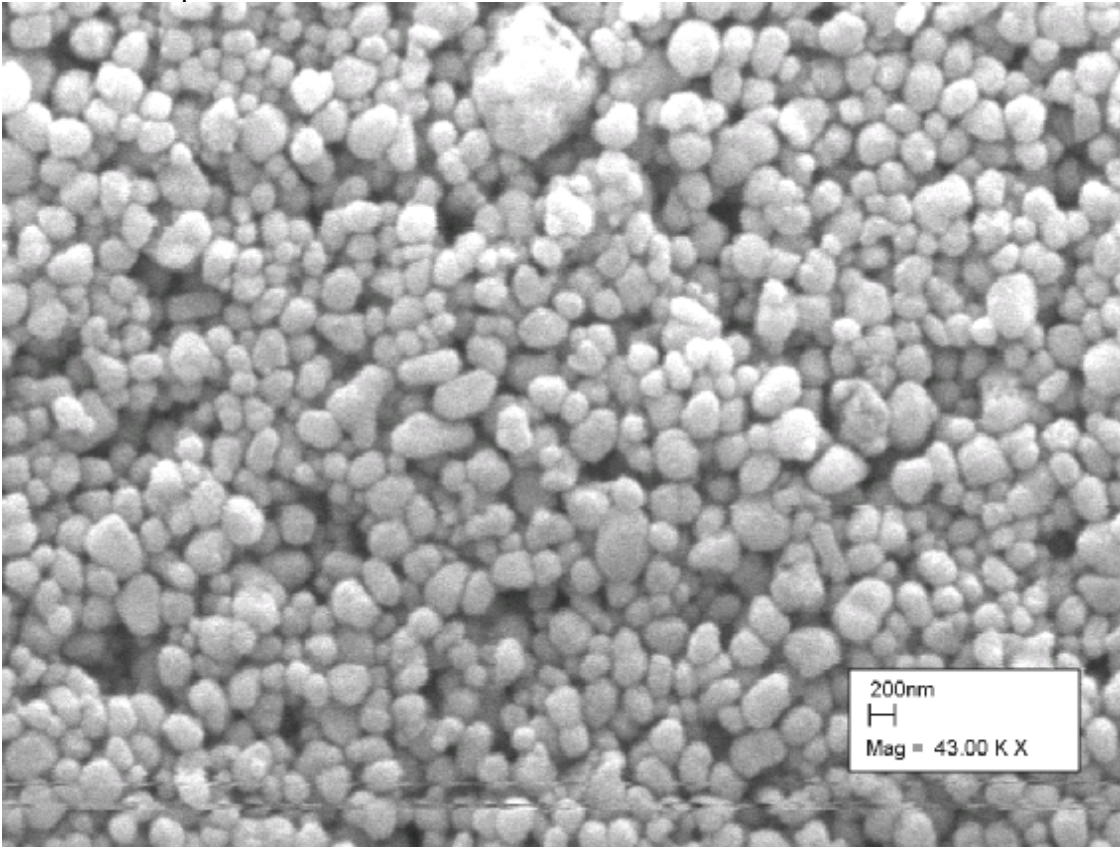
Batch C - 2passes



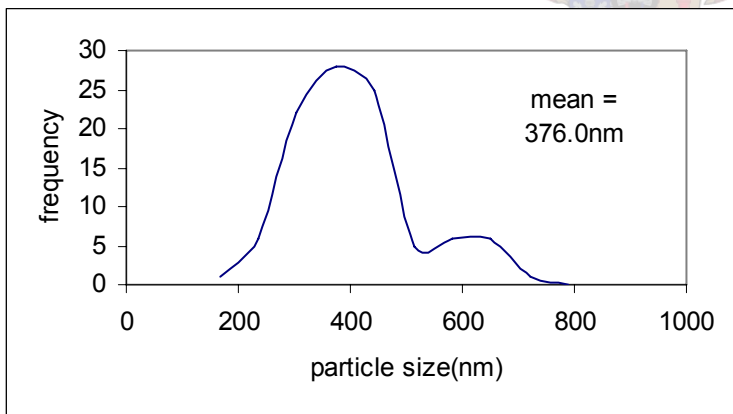
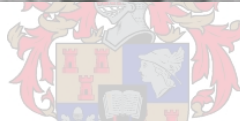
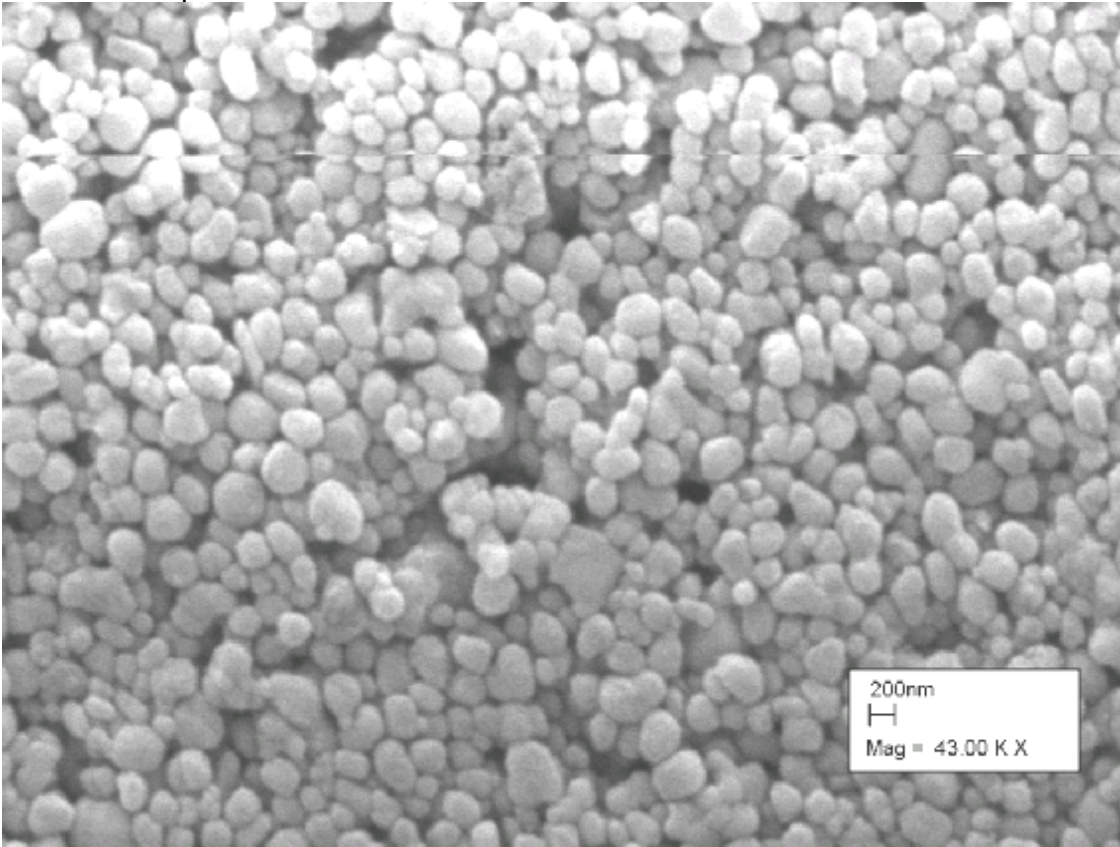
Batch C - 4passes



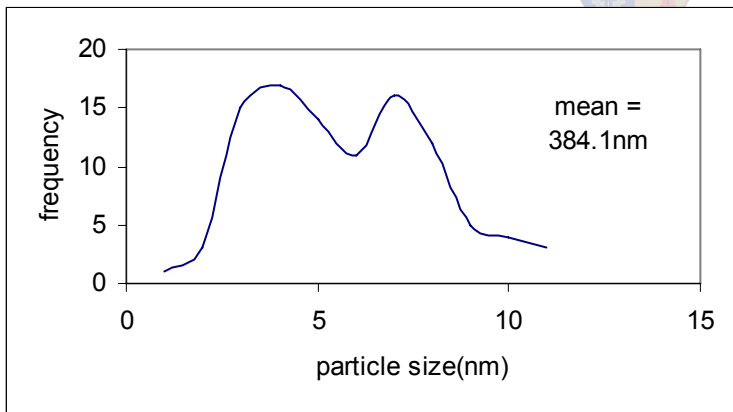
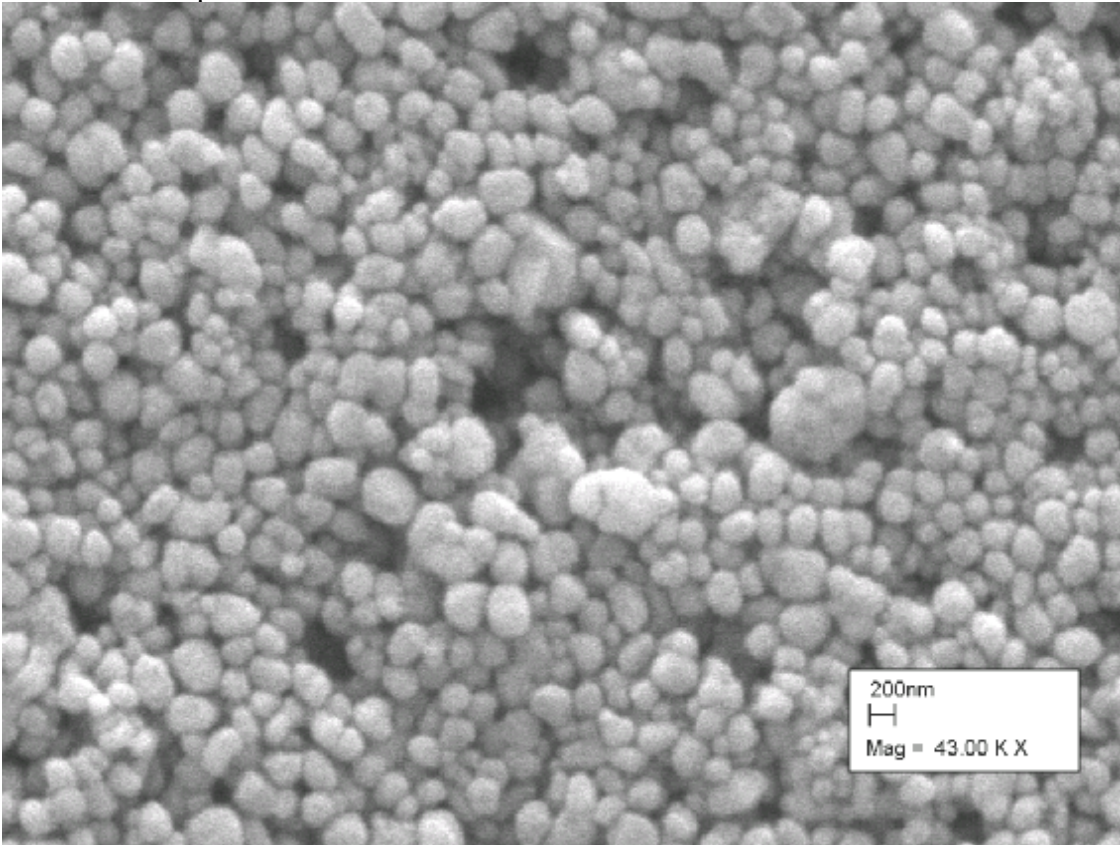
Batch C - 6passes



Batch C - 8passes

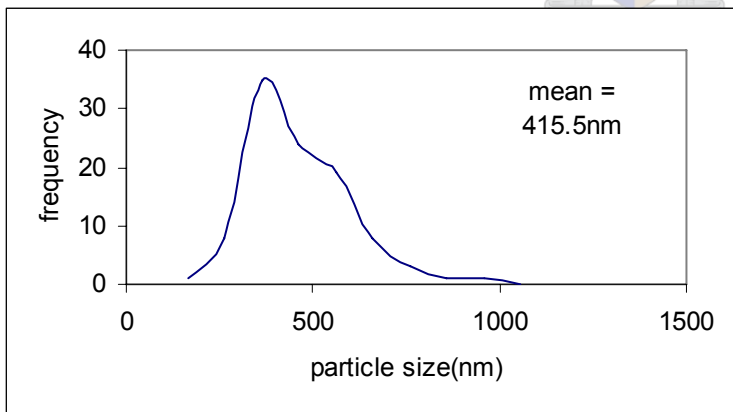
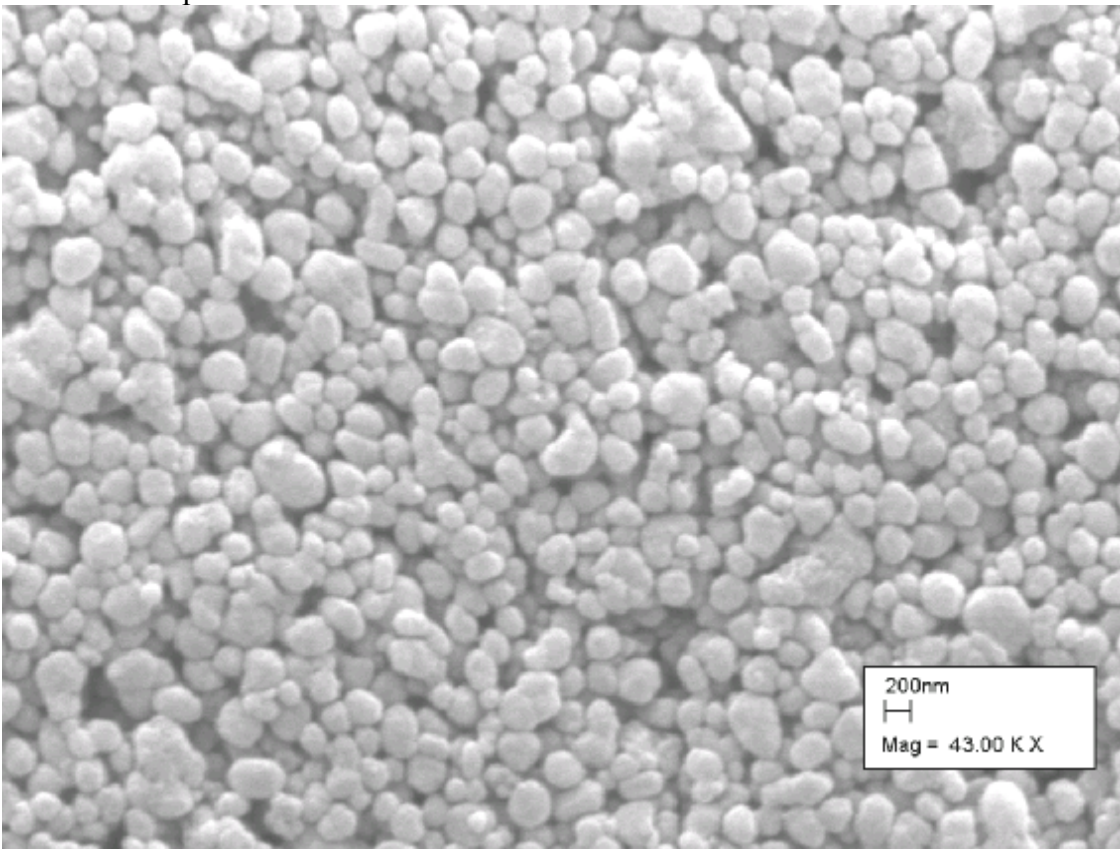


Batch C - 10passes

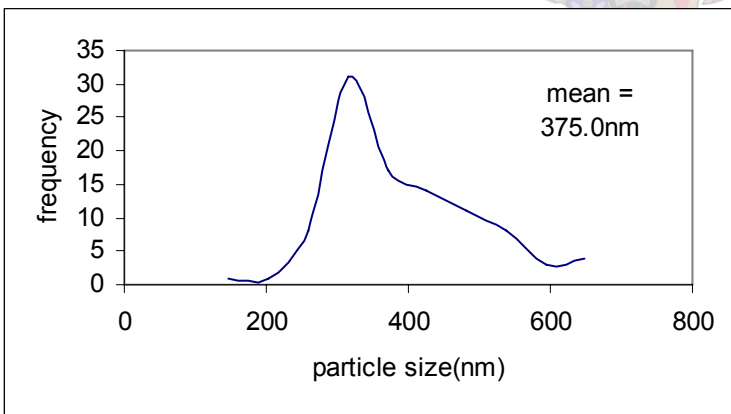
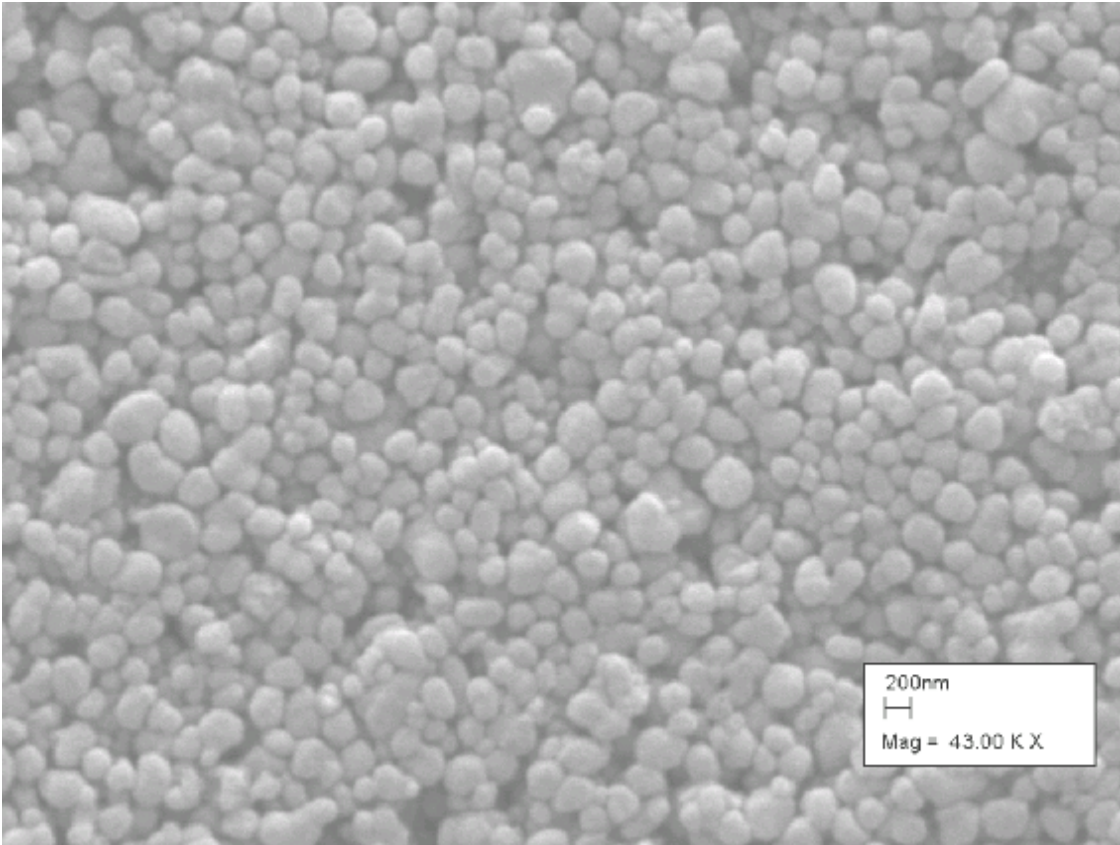


C3.4 – A SEM and PSD for The Homogenisation of Batch D

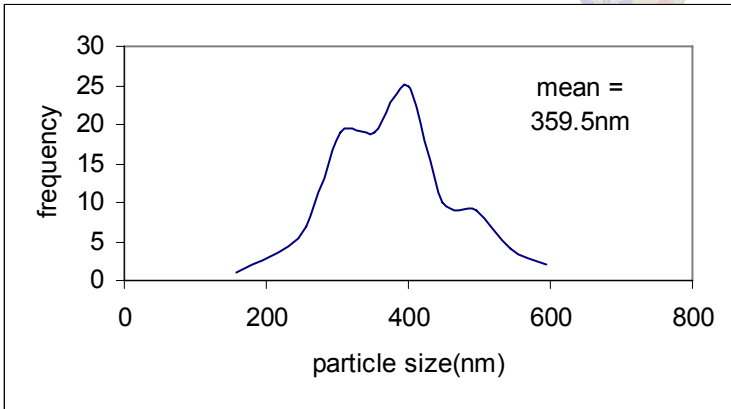
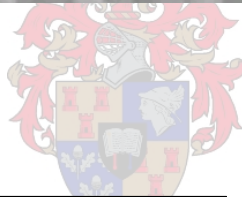
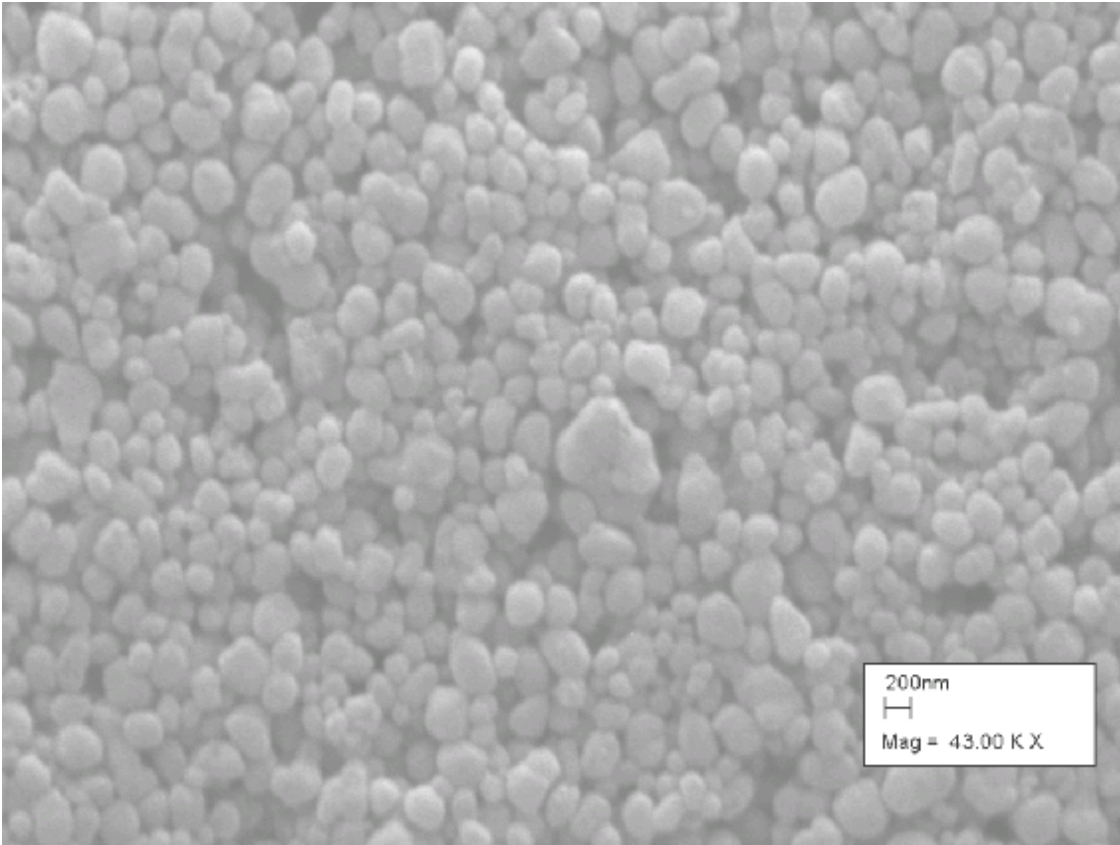
Batch D - 2passes



Batch D - 4passes

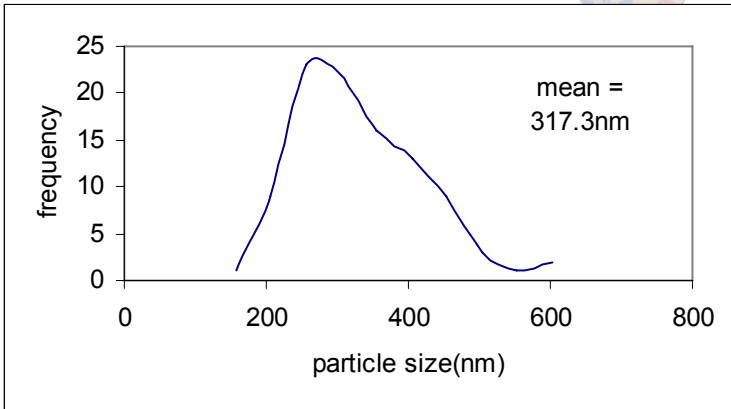
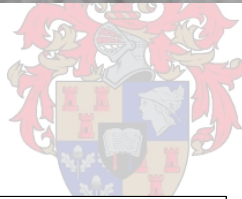
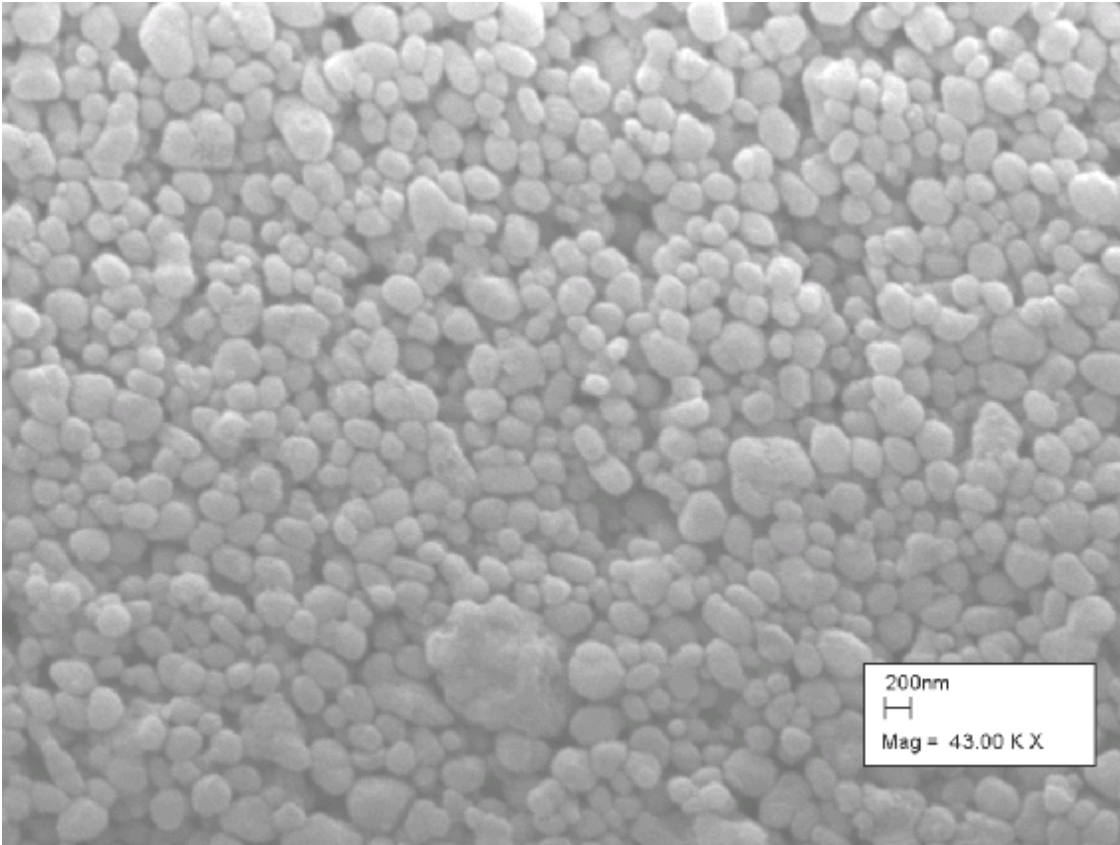


Batch D - 6passes





Batch D - 10passes





D Contrast Ratio of Pigment Dispersions

D.1 Contrast ratio of Titanium Dioxide Dispersed in Cowles Mill

| Batch 1 | | | |
|--------------------|----------------|----------------|-------|
| Sampling Time(min) | R _B | R _W | CR |
| 10 | 95.6 | 98.3 | 0.973 |
| 15 | 95.7 | 98.3 | 0.974 |
| 20 | 96.0 | 98.4 | 0.976 |
| 30 | 96.4 | 98.5 | 0.978 |

| Batch 2 | | | |
|--------------------|----------------|----------------|-------|
| Sampling Time(min) | R _B | R _W | CR |
| 10 | 95.6 | 98.2 | 0.974 |
| 15 | 96.0 | 98.4 | 0.976 |
| 20 | 96.3 | 98.5 | 0.977 |
| 30 | 96.3 | 98.5 | 0.978 |

| Batch 3 | | | |
|--------------------|----------------|----------------|-------|
| Sampling Time(min) | R _B | R _W | CR |
| 10 | 95.7 | 98.3 | 0.974 |
| 15 | 95.7 | 98.2 | 0.975 |
| 20 | 96.0 | 98.3 | 0.976 |
| 30 | 96.7 | 98.5 | 0.981 |

| Batch 4 | | | |
|--------------------|----------------|----------------|-------|
| Sampling Time(min) | R _B | R _W | CR |
| 10 | 95.8 | 98.3 | 0.974 |
| 15 | 96.2 | 98.5 | 0.977 |
| 20 | 96.7 | 98.5 | 0.982 |
| 30 | 96.8 | 98.6 | 0.983 |

D.2 Contrast Ratio of Steopac Talc Batches Dispersed in Cowles Mill

| Batch F | | | |
|--------------------|----------------|----------------|-------|
| Sampling Time(min) | R _B | R _W | CR |
| 10 | 93.4 | 98.8 | 0.946 |
| 15 | 94.7 | 99.7 | 0.950 |
| 20 | 94.6 | 99.5 | 0.951 |
| 30 | 94.7 | 99.6 | 0.951 |

| Batch G | | | |
|--------------------|----------------|----------------|-------|
| Sampling Time(min) | R _B | R _W | CR |
| 10 | 93.4 | 98.7 | 0.946 |
| 15 | 93.6 | 98.9 | 0.947 |
| 20 | 94.2 | 99.1 | 0.951 |
| 30 | 94.8 | 99.7 | 0.951 |

| Batch H | | | |
|--------------------|----------------|----------------|-------|
| Sampling Time(min) | R _B | R _W | CR |
| 10 | 93.7 | 98.9 | 0.947 |
| 15 | 93.9 | 99.0 | 0.948 |
| 20 | 94.1 | 99.0 | 0.951 |
| 30 | 94.3 | 99.1 | 0.951 |

| Batch J | | | |
|--------------------|----------------|----------------|-------|
| Sampling Time(min) | R _B | R _W | CR |
| 10 | 93.6 | 98.9 | 0.947 |
| 15 | 94.4 | 99.4 | 0.950 |
| 20 | 95.1 | 99.8 | 0.953 |
| 30 | 95.2 | 99.8 | 0.954 |

D.3 Contrast Ratio of Homogenised Titanium Dioxide Batches

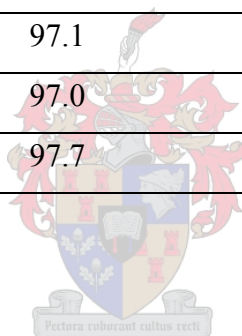
| Batch A | | | |
|------------------|----------------|----------------|-------|
| Number of Passes | R _B | R _W | CR |
| 2 | 97.2 | 99.3 | 0.978 |
| 4 | 97.3 | 99.4 | 0.979 |
| 6 | 97.3 | 99.4 | 0.979 |
| 8 | 97.1 | 99.1 | 0.980 |
| 10 | 97.1 | 99.0 | 0.981 |

| Batch B | | | |
|------------------|----------------|----------------|-------|
| Number of Passes | R _B | R _W | CR |
| 2 | 97.1 | 99.1 | 0.980 |
| 4 | 97.1 | 99.0 | 0.981 |
| 6 | 97.9 | 98.9 | 0.991 |
| 8 | 97.9 | 98.8 | 0.991 |
| 10 | 97.7 | 98.3 | 0.994 |

| Batch C | | | |
|------------------|----------------|----------------|-------|
| Number of Passes | R _B | R _W | CR |
| 2 | 97.2 | 99.3 | 0.978 |
| 4 | 97.4 | 99.5 | 0.979 |
| 6 | 97.4 | 99.4 | 0.979 |
| 8 | 96.6 | 97.6 | 0.989 |
| 10 | 97.8 | 98.5 | 0.993 |

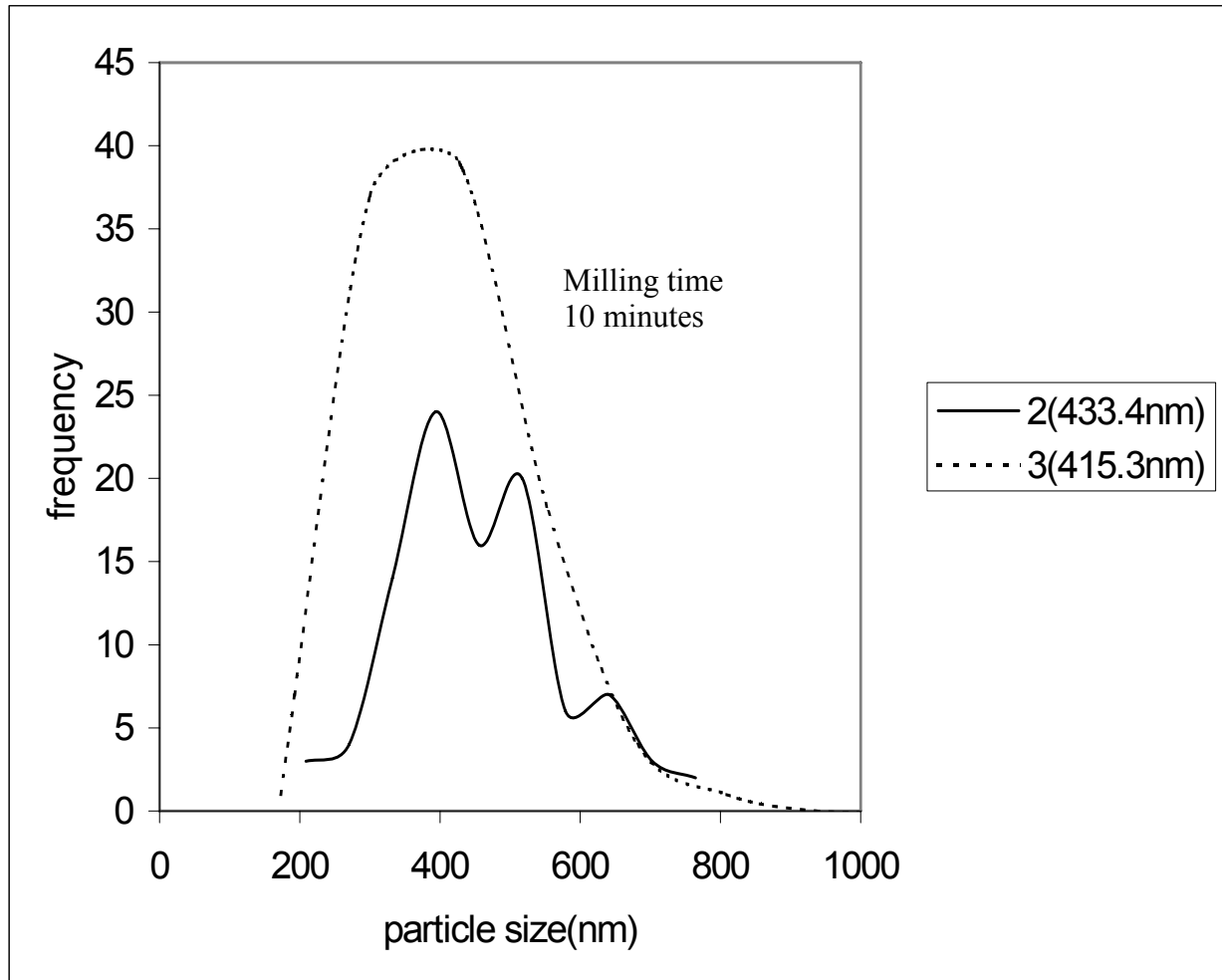
| Batch D | | | |
|------------------|----------------|----------------|-------|
| Number of Passes | R _B | R _W | CR |
| 2 | 97.5 | 99.6 | 0.979 |
| 4 | 97.5 | 99.6 | 0.979 |
| 6 | 97.3 | 99.3 | 0.980 |
| 8 | 97.0 | 98.9 | 0.980 |
| 10 | 96.6 | 97.6 | 0.989 |

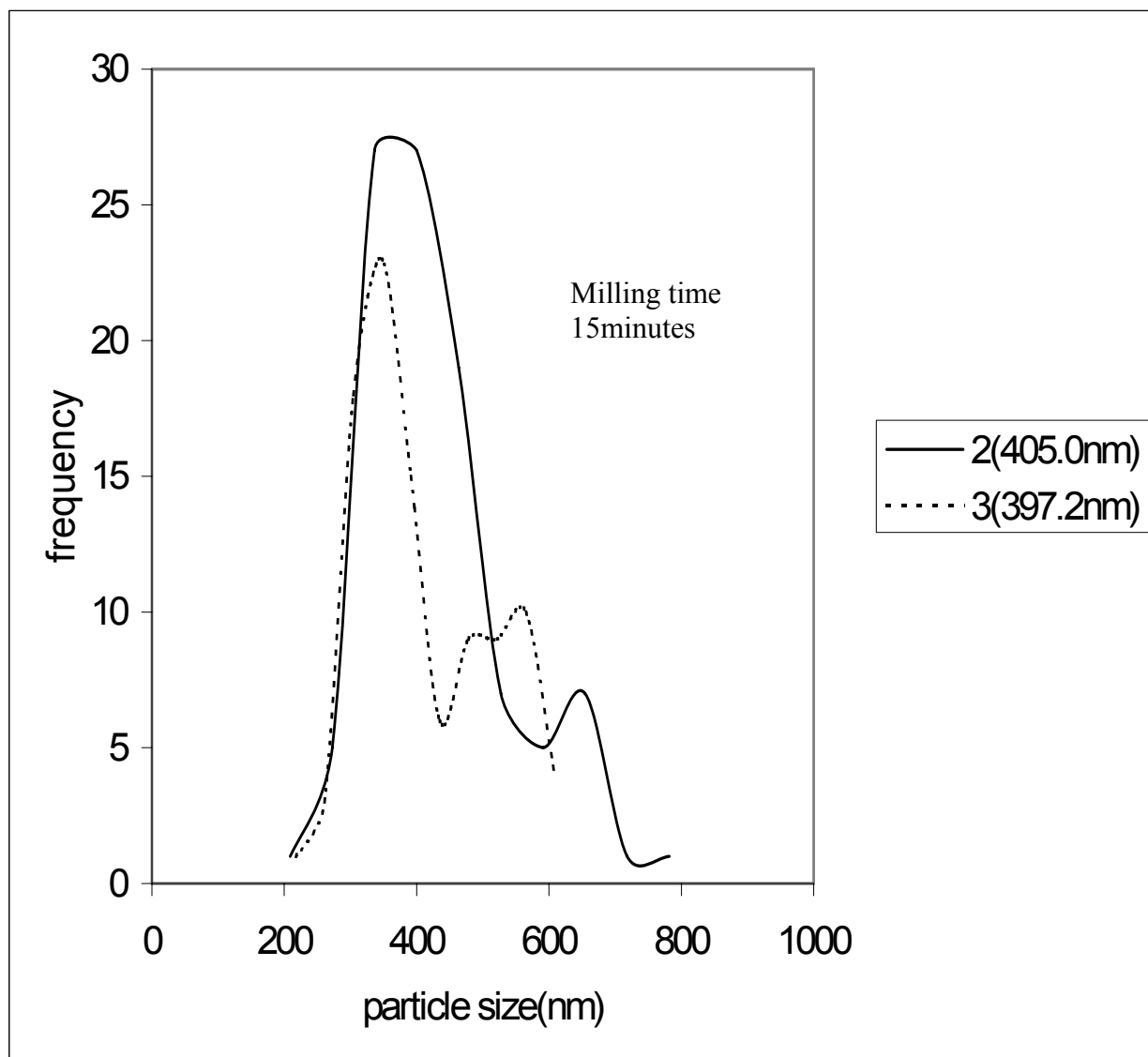
| Batch E | | | |
|------------------|----------------|----------------|-------|
| Number of Passes | R _B | R _W | CR |
| 2 | 97.4 | 99.5 | 0.979 |
| 4 | 97.3 | 99.4 | 0.979 |
| 6 | 97.1 | 99.1 | 0.980 |
| 8 | 97.0 | 98.9 | 0.980 |
| 10 | 97.7 | 98.0 | 0.997 |

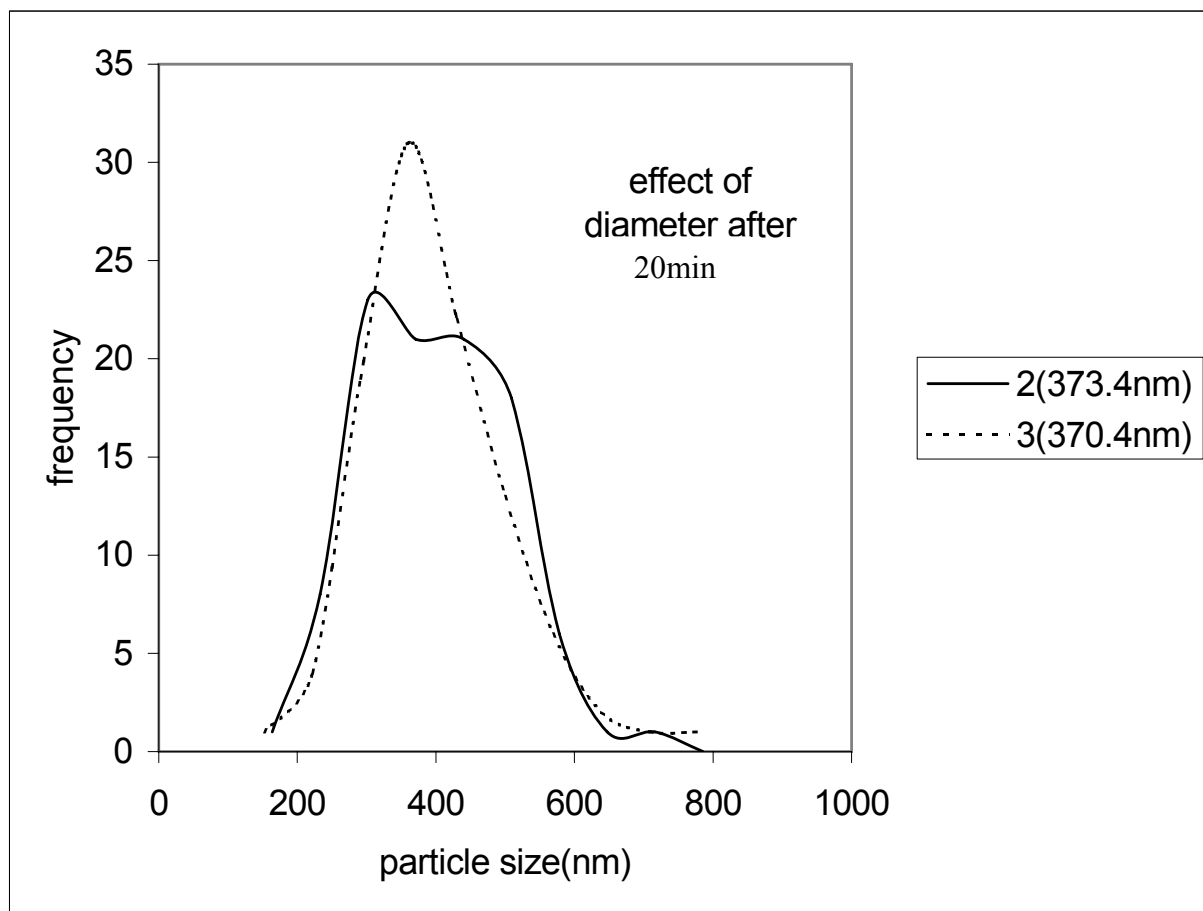


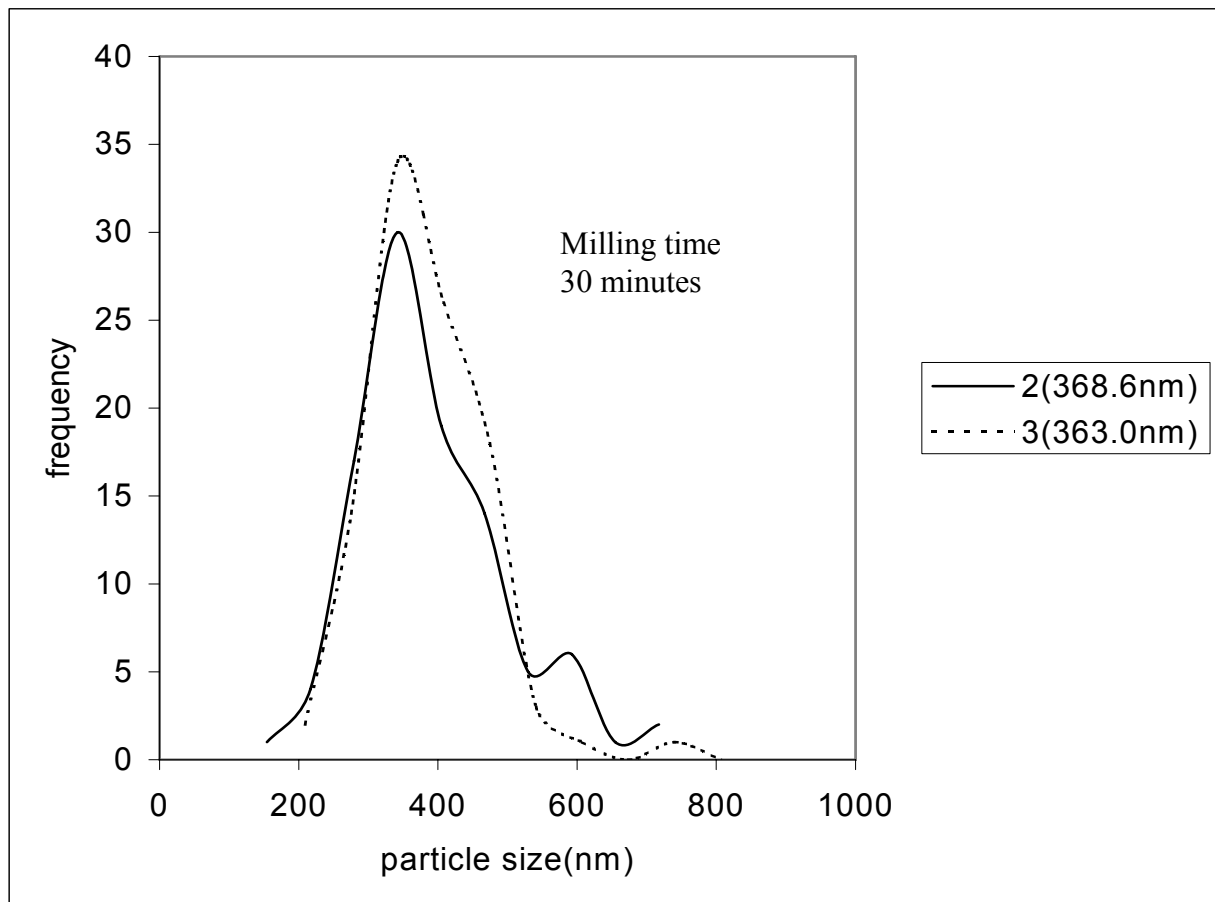
E Other variables with an effect on the dispersion process

E.1 The effect of Agitator diameter on the dispersion of Titanium Dioxide



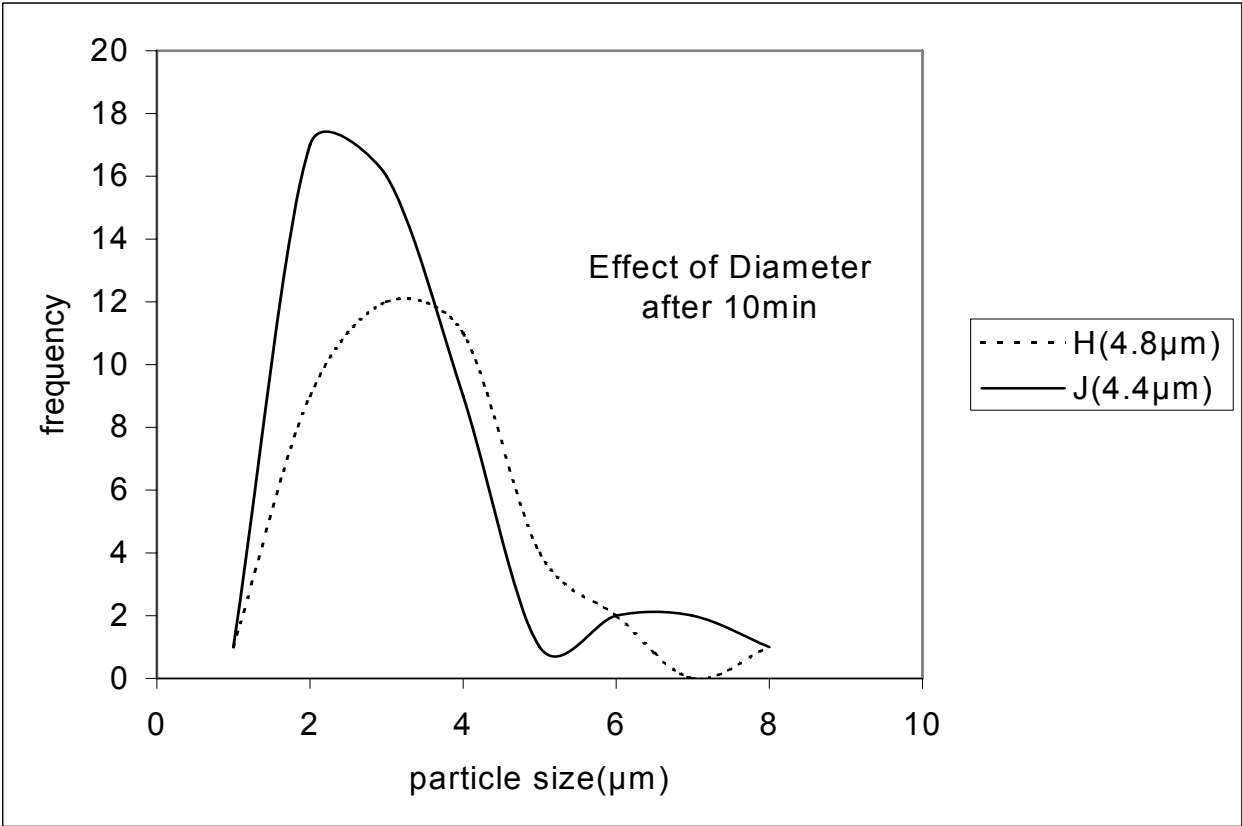


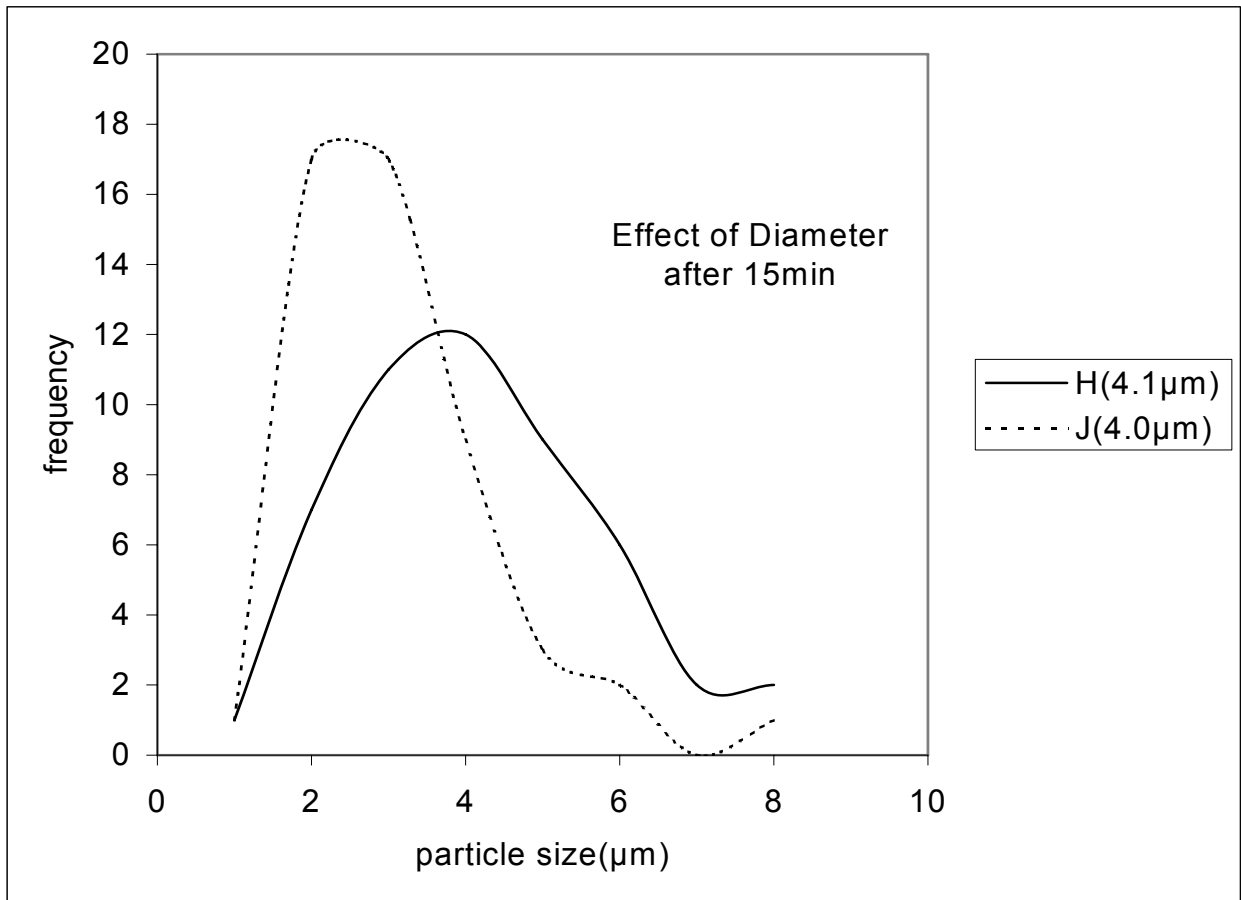


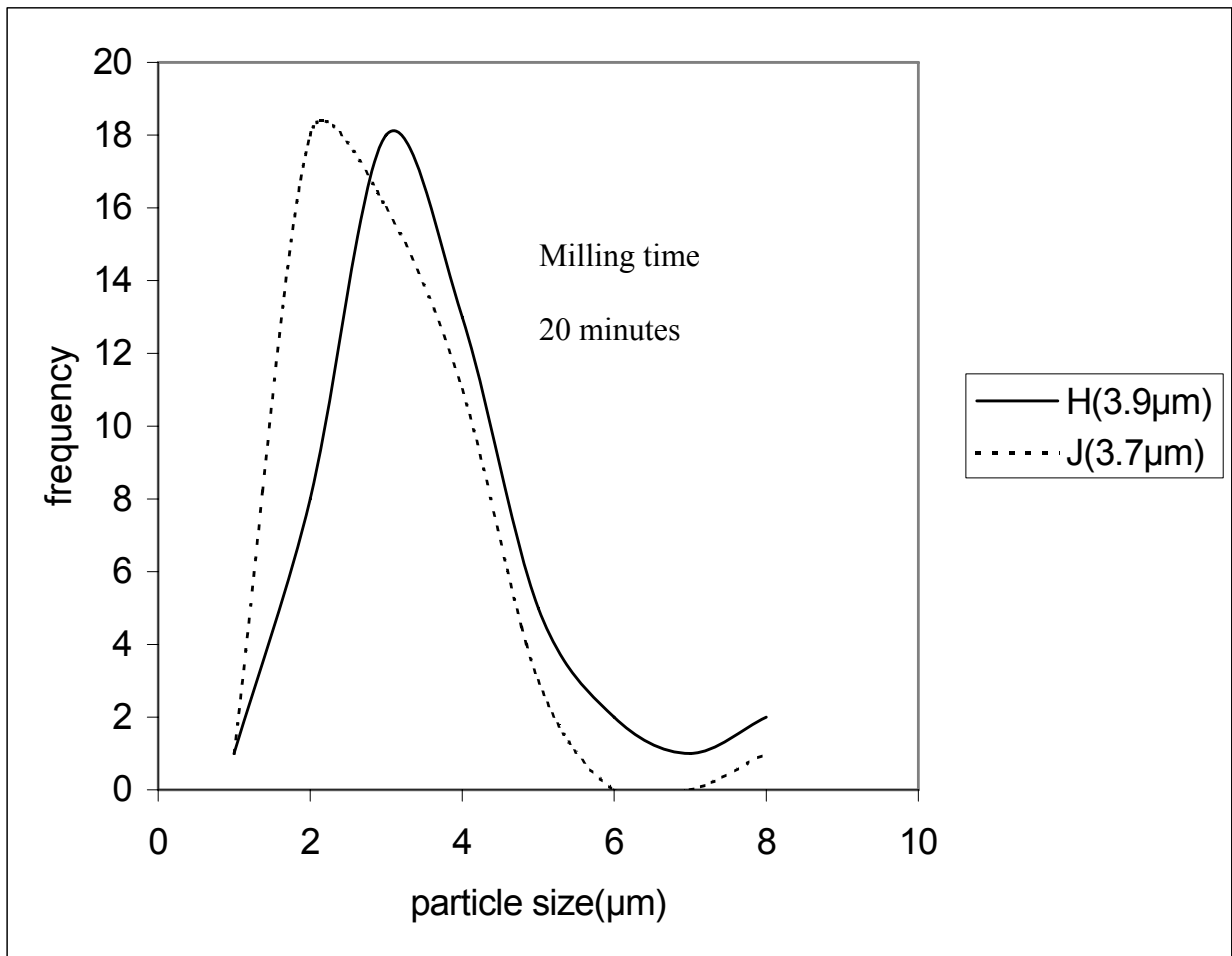


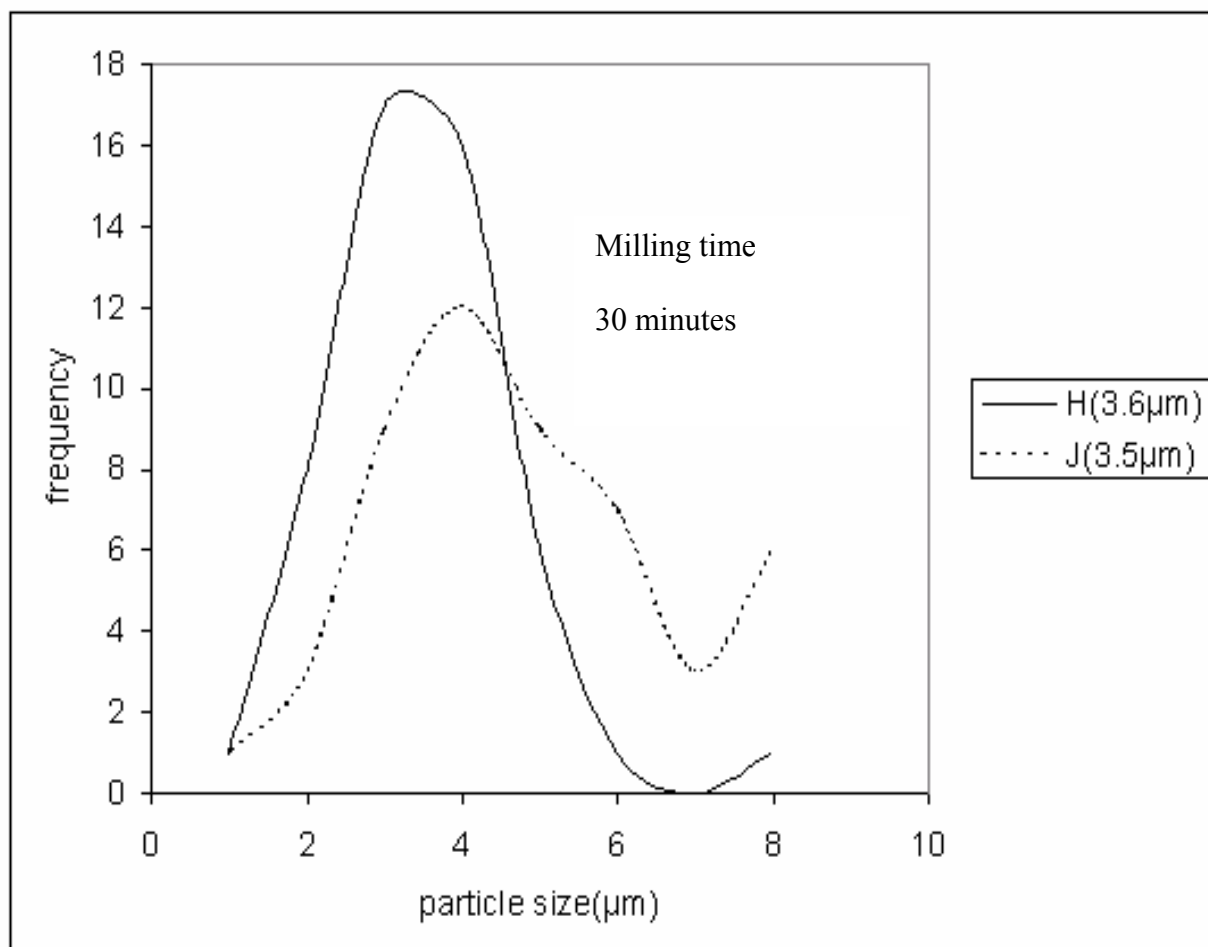
Agitator diameter exerts an effect similar to agitator speed on the dispersion process of titanium dioxide. These two variables impart similar particle sizes and distribution when they act on the process for the same time period.

E.2 The effect of agitator diameter on the dispersion of steopac talc



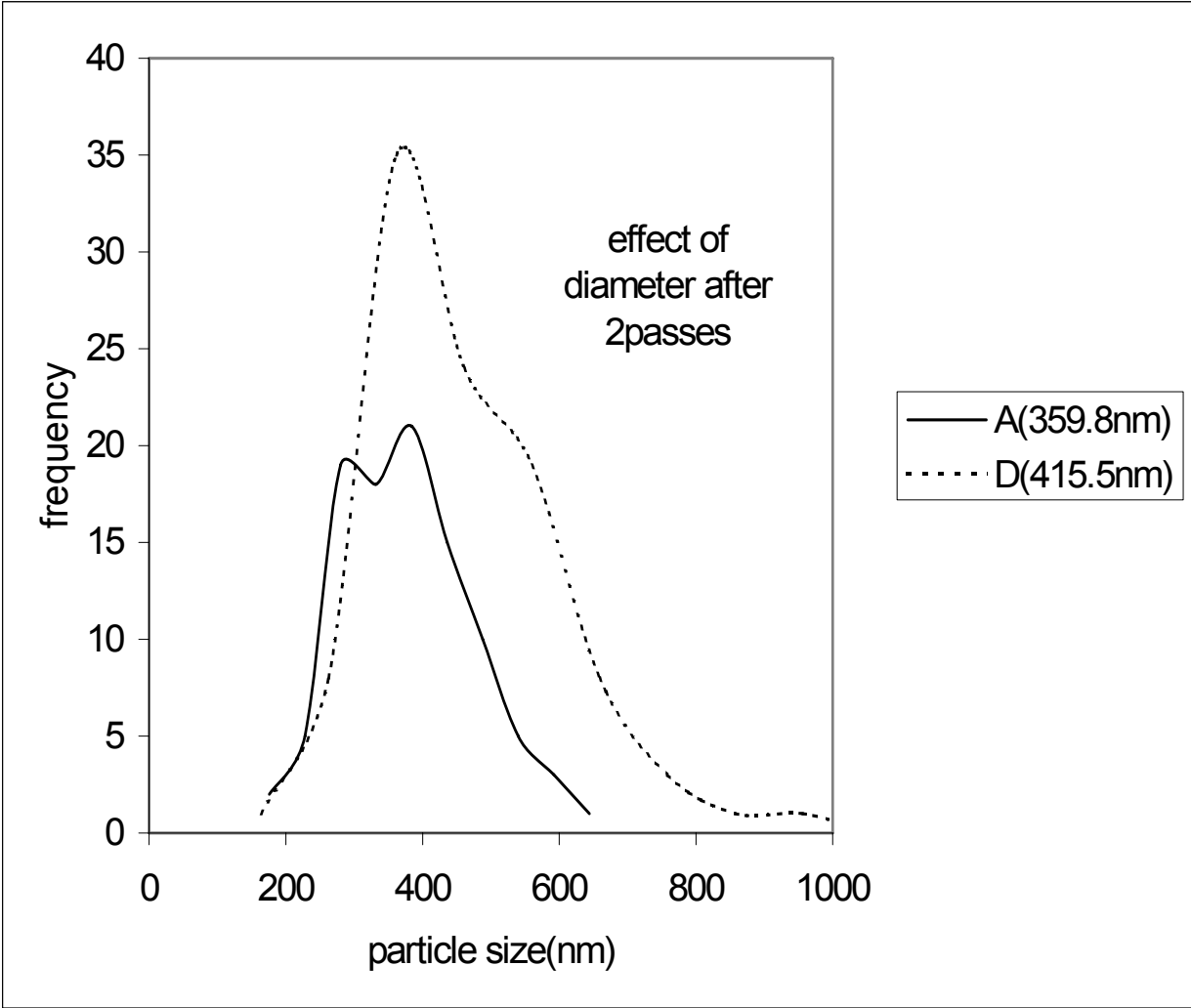


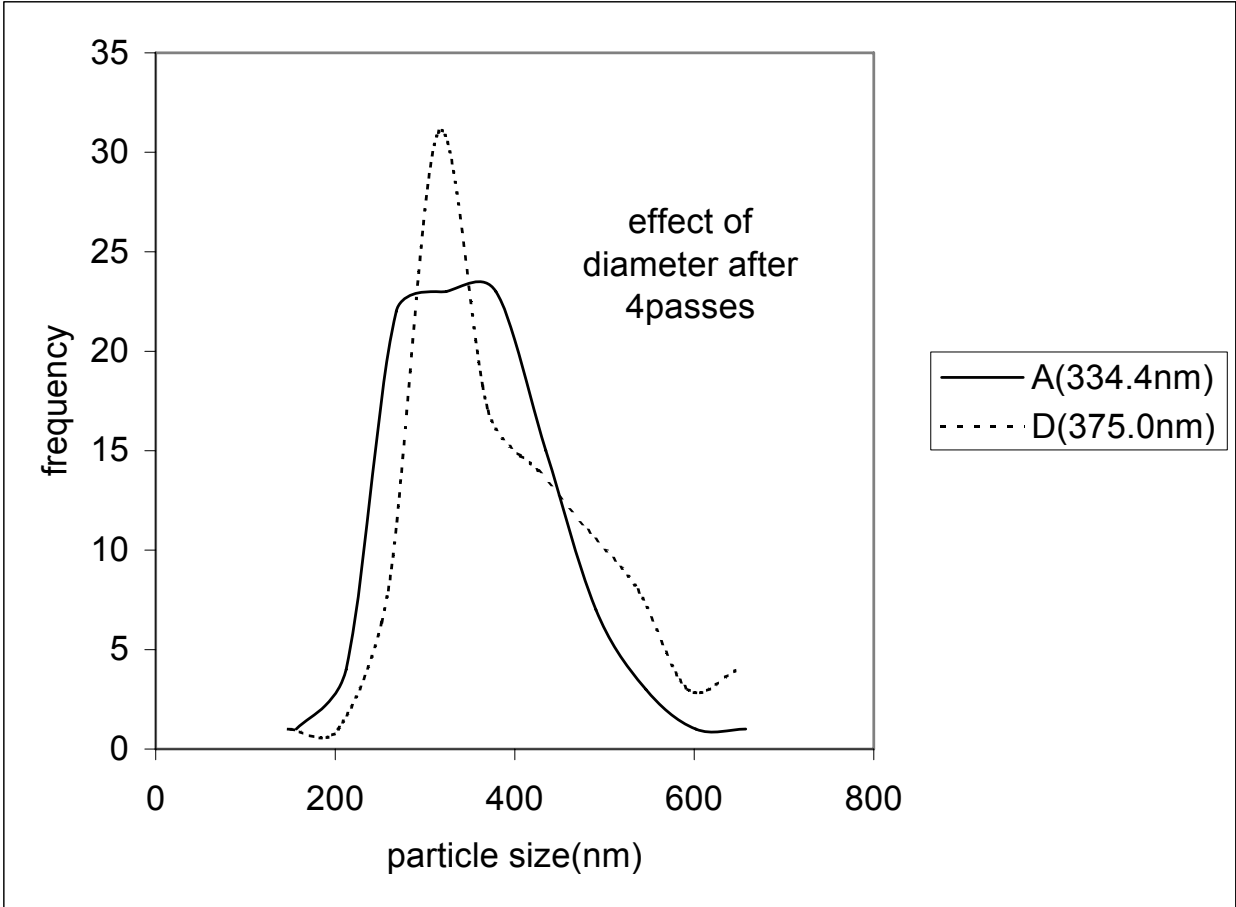


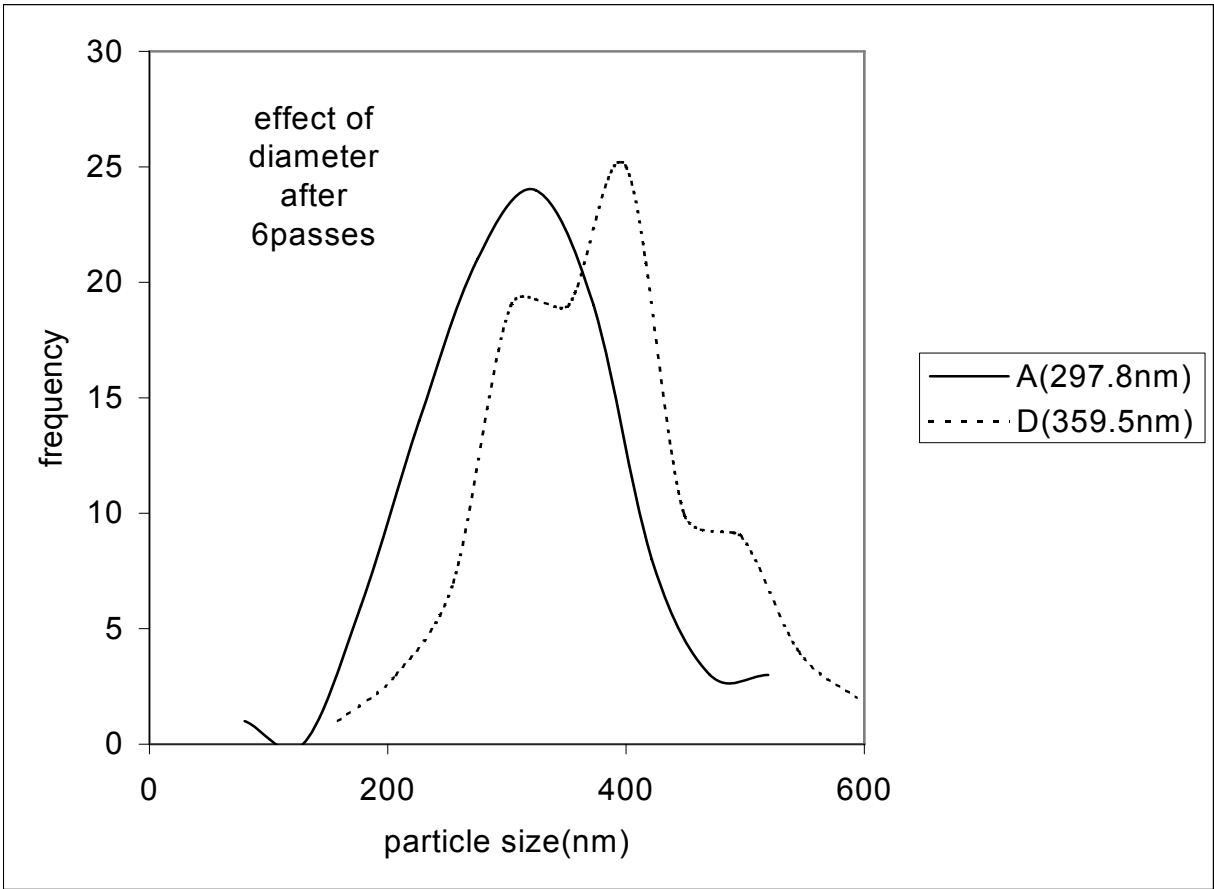


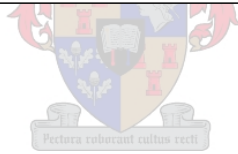
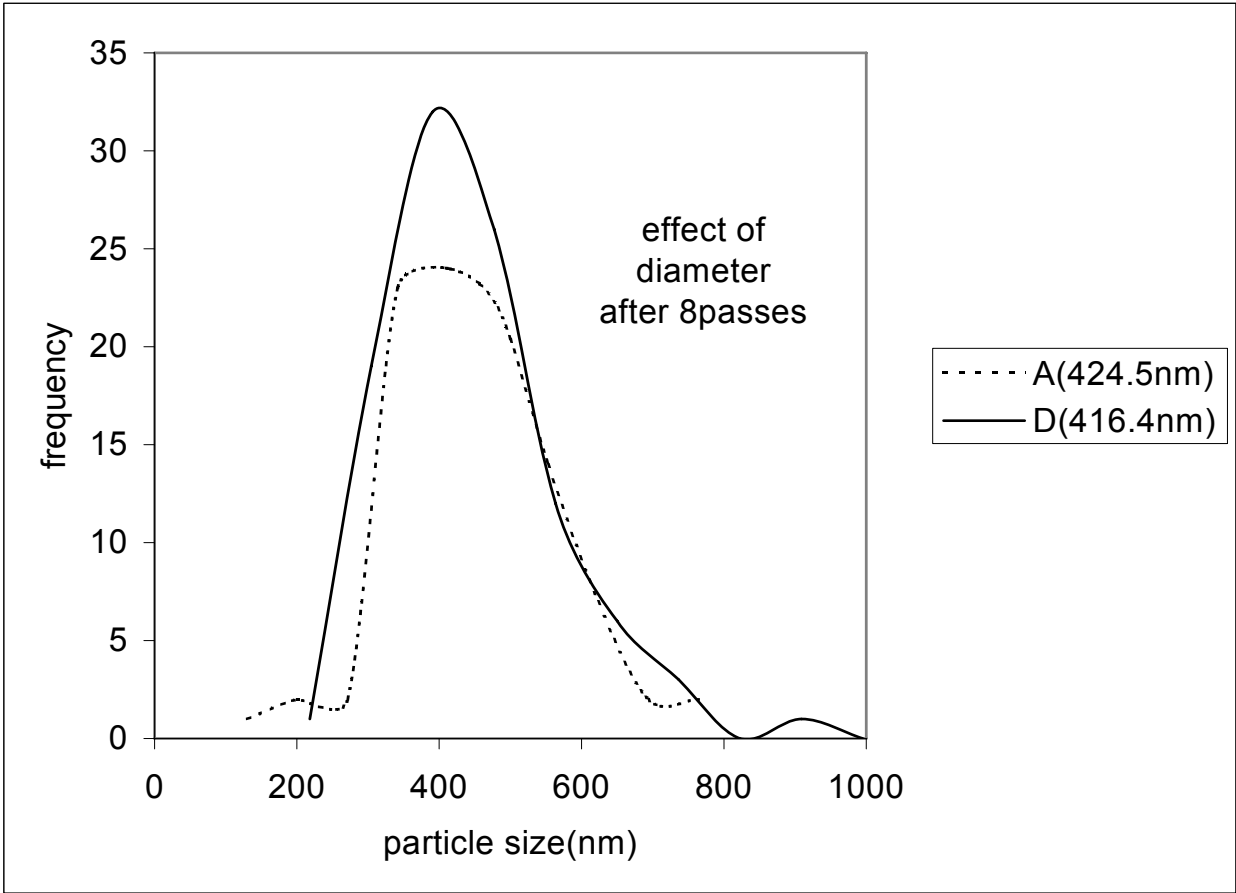
Agitator diameter exerts an effect similar to agitator speed on the dispersion process of titanium dioxide. These two variables impart similar particle sizes and distribution when they act on the process for the same time period.

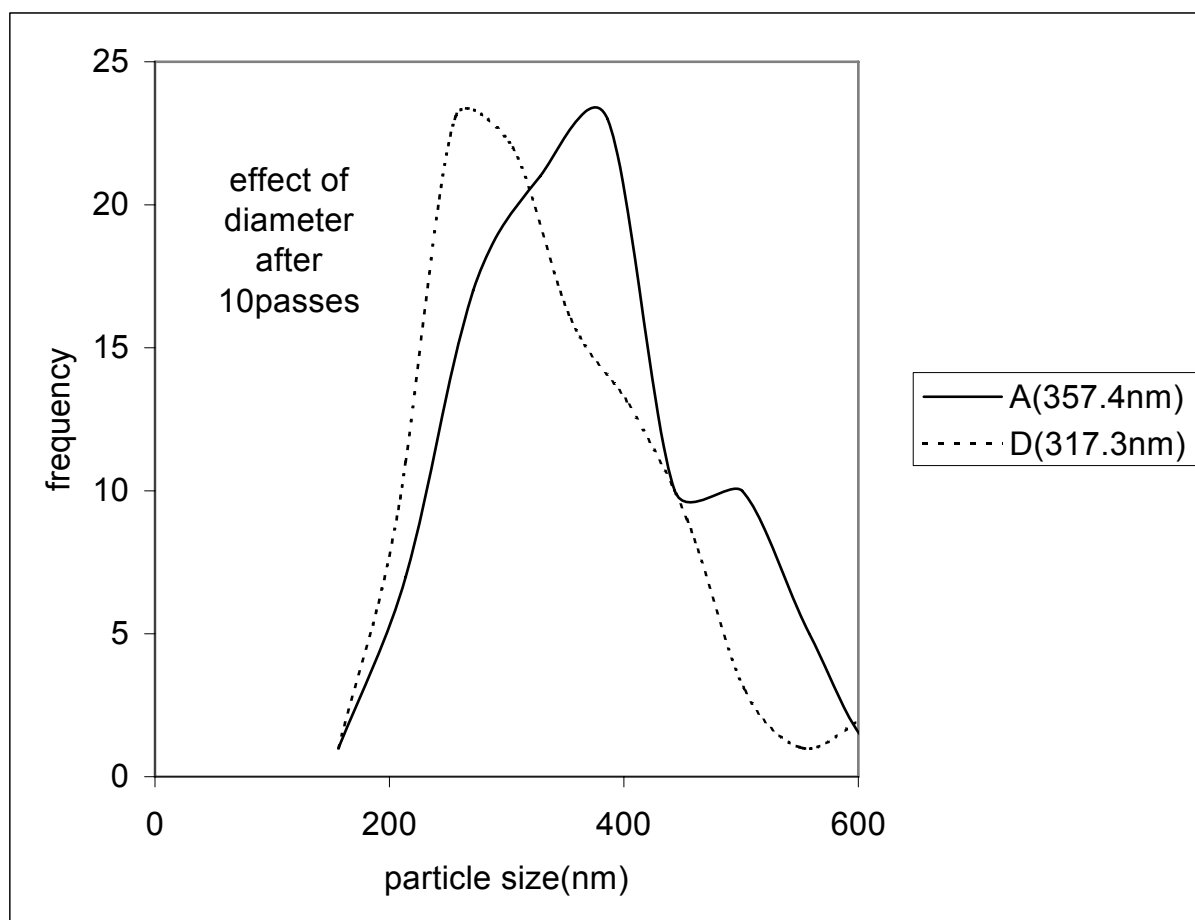
E3 the effect of plunger diameter on the homogenisation of titanium dioxide







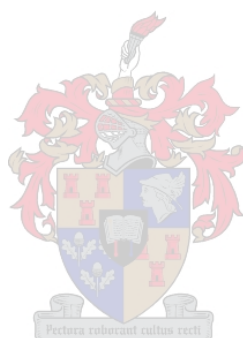




Plunger diameter exerts an effect similar to flow rate on the dispersion process of titanium dioxide.

F Temperature Changes in The Cowles Dispersion of Titanium Dioxide

| Batch \time(min) | 10 | 15 | 20 | 30 |
|------------------|----|----|----|----|
| 2 | 28 | 32 | 35 | 40 |
| 3 | 30 | 33 | 38 | 43 |
| 4 | 32 | 35 | 40 | 46 |

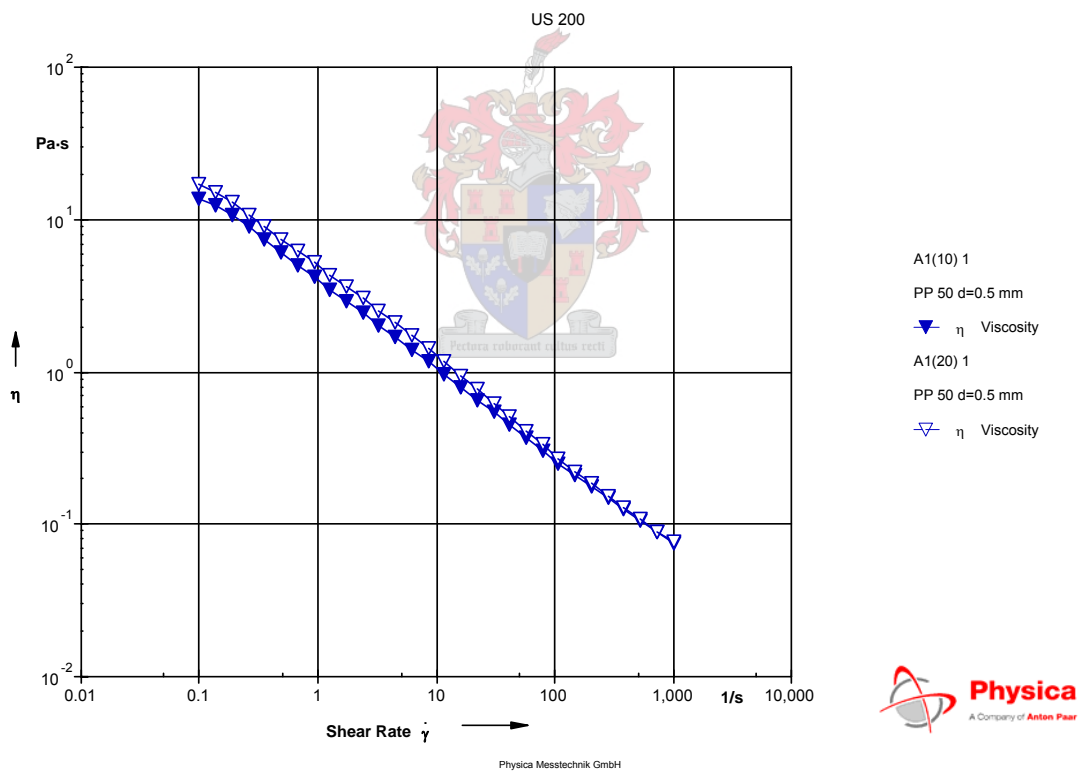


G Rheology of The Dispersion Process

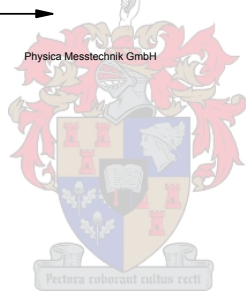
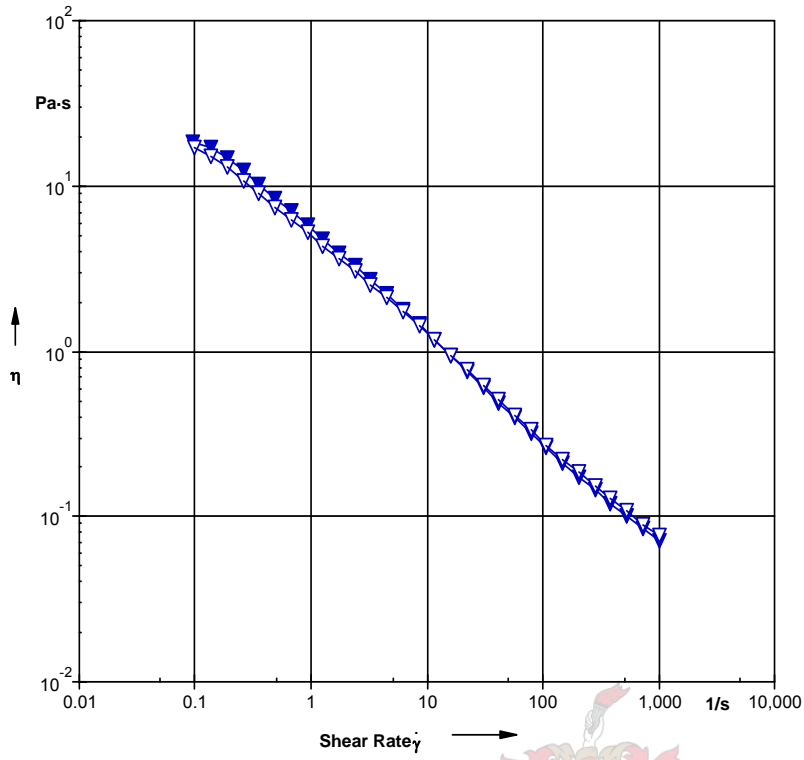
G1 Flow Curves For Batches A1, A2, and A3

The processing time is shown in brackets after the batch number

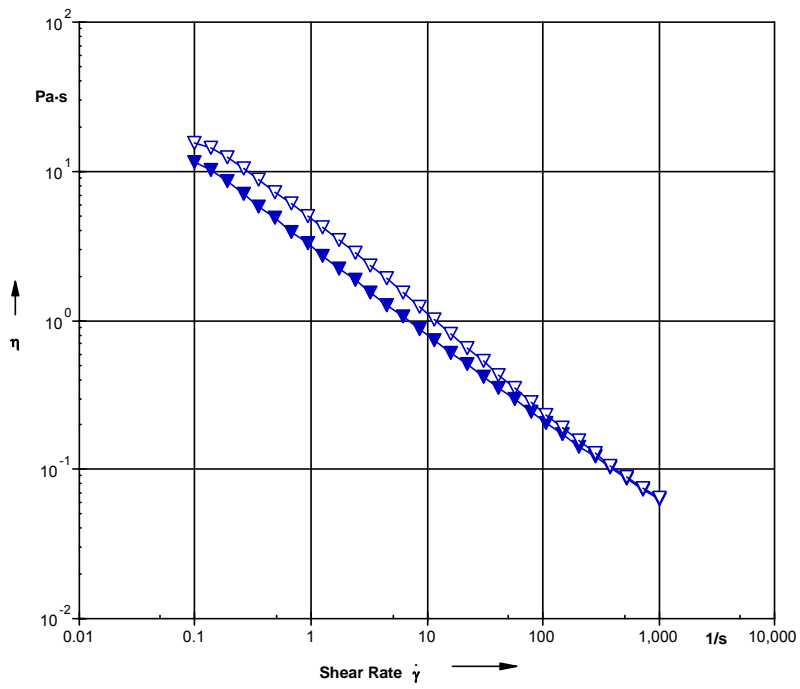
| Batch | Agitator speed(Hz) | Dispersant level |
|-------|--------------------|--|
| A1 | 30 | As given in formulation of Titanium dioxide dispersion |
| A2 | 35 | As given in formulation of Titanium dioxide dispersion |
| A3 | 30 | Fifty percent of the level given in the formulation of Titanium dioxide dispersion |



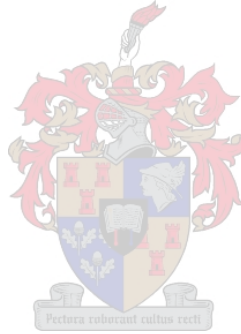
US 200



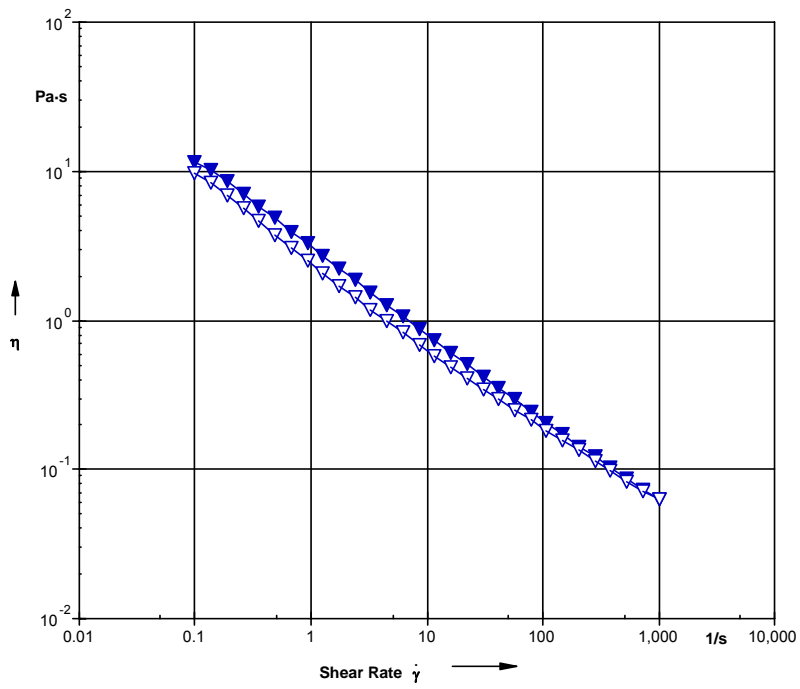
US 200



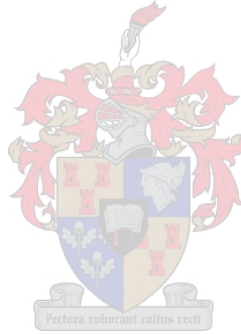
Physica Messtechnik GmbH



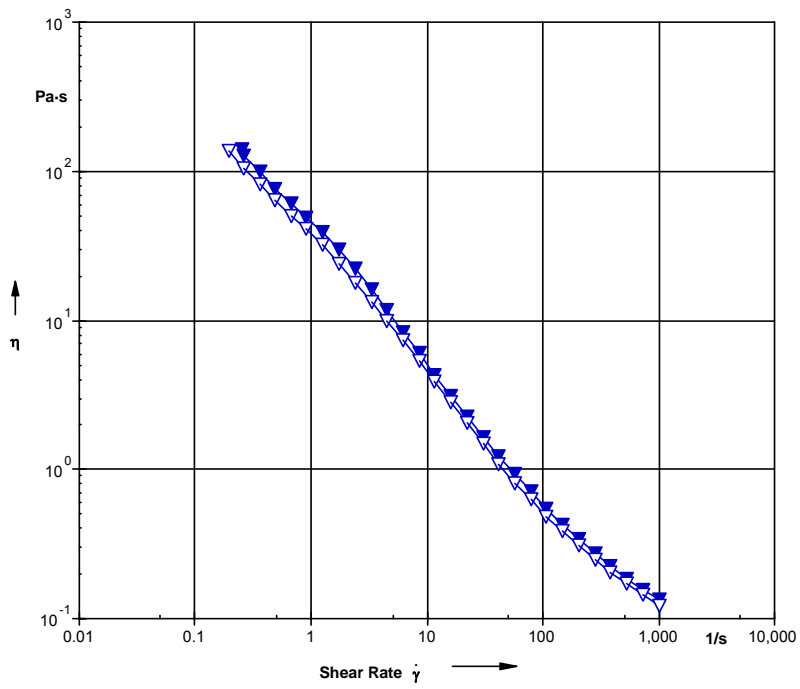
US 200



Physica Messtechnik GmbH



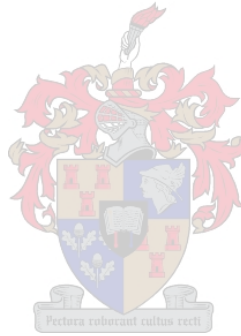
US 200



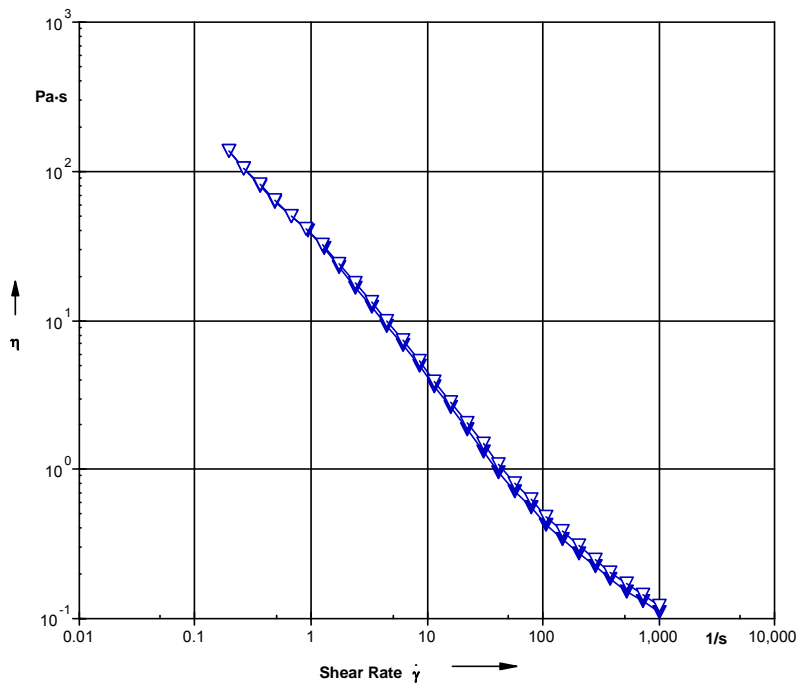
A3(10) 1
PP 50 d=0.5 mm
▼ η Viscosity
A3(20) 1
PP 50 d=0.5 mm
◻ η Viscosity



Physica Messtechnik GmbH



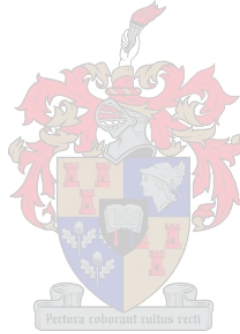
US 200



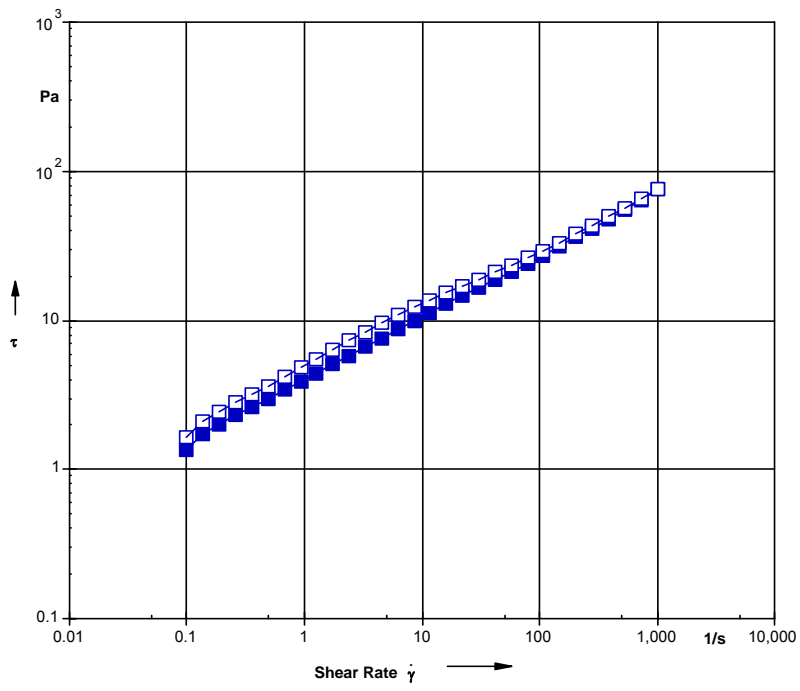
A3(30) 2
PP 50 d=0.5 mm
▼ η Viscosity
A3(20) 1
PP 50 d=0.5 mm
▲ η Viscosity



Physica Messtechnik GmbH



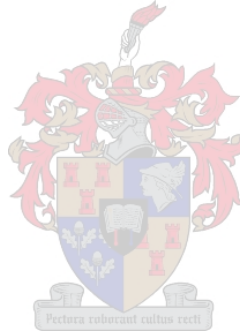
US 200



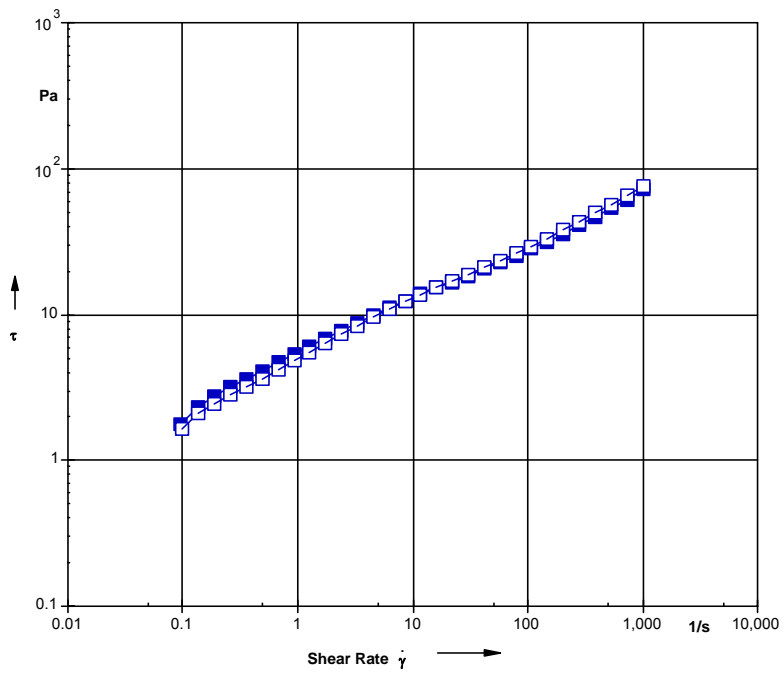
A1(10) 1
PP 50 d=0.5 mm
■ τ Shear Stress
A1(20) 1
PP 50 d=0.5 mm
□ τ Shear Stress



Physica Messtechnik GmbH



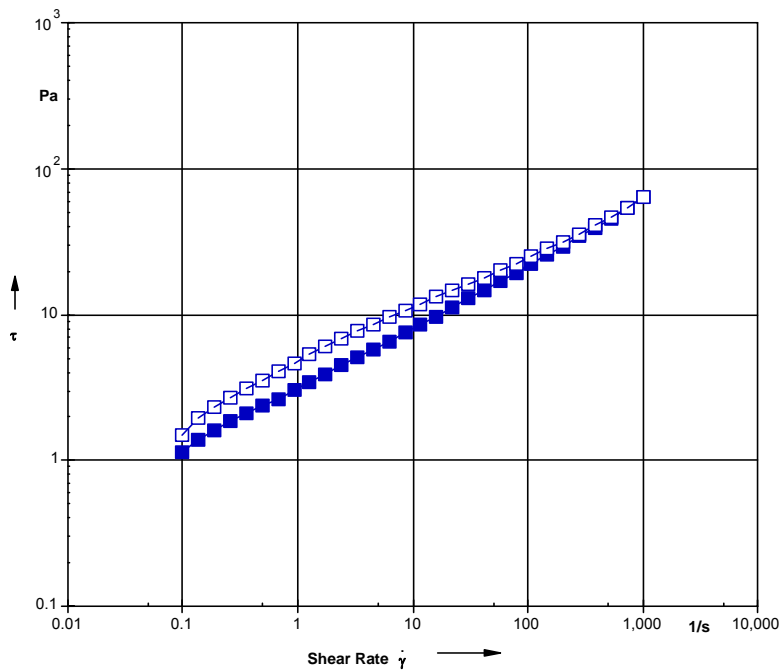
US 200



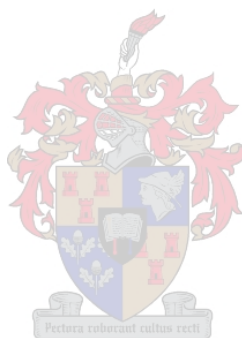
Physica Messtechnik GmbH



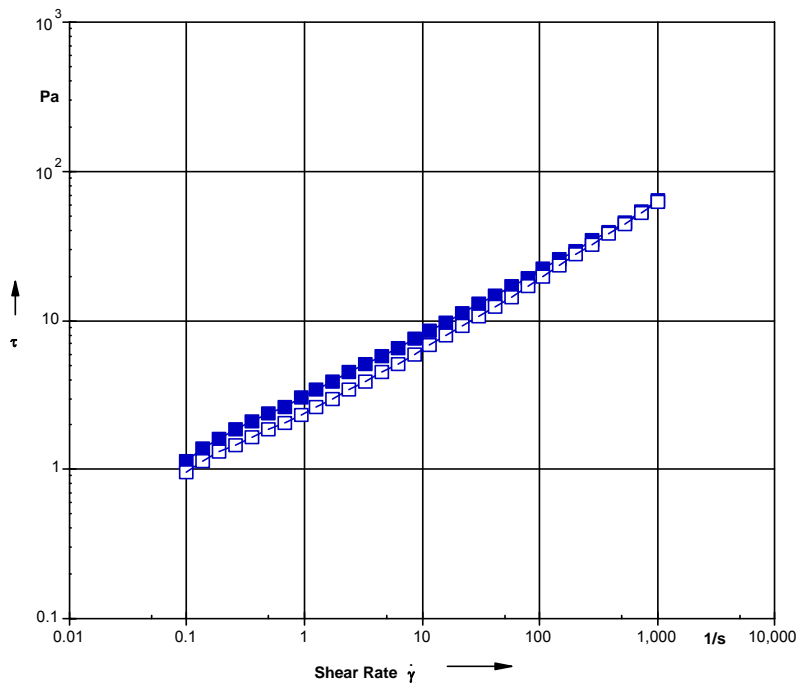
US 200



Physica Messtechnik GmbH



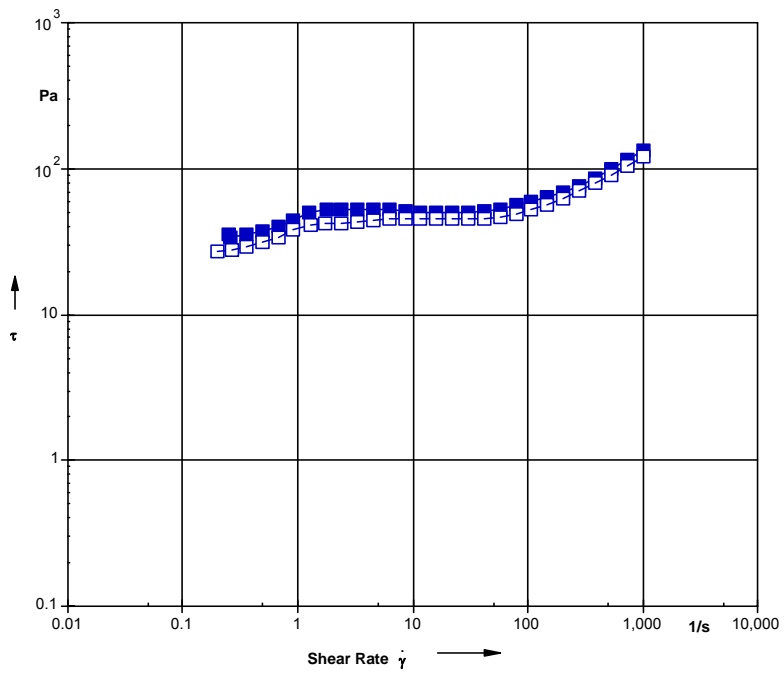
US 200



Physica Messtechnik GmbH



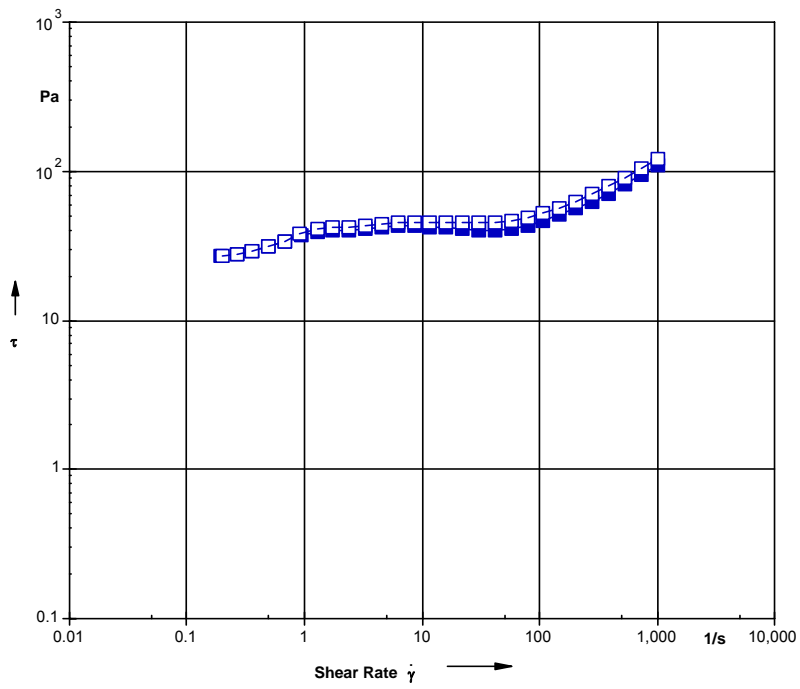
US 200



Physica Messtechnik GmbH



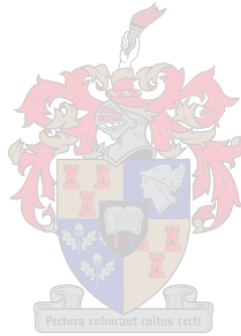
US 200



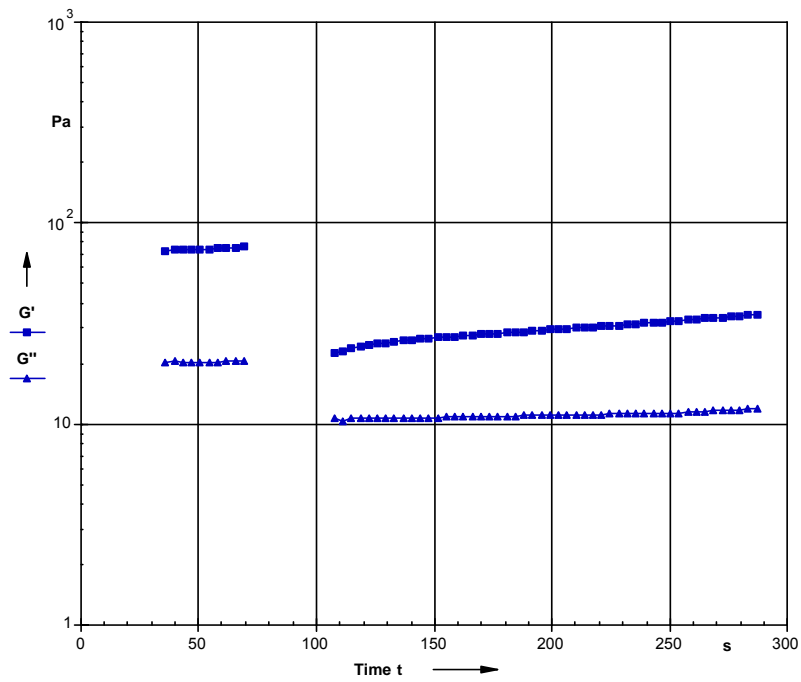
A3(30) 2
PP 50 d=0.5 mm
■ τ Shear Stress
A3(20) 1
PP 50 d=0.5 mm
□ τ Shear Stress



Physica Messtechnik GmbH



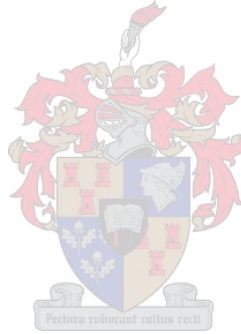
US 200



Callisto 3
PP 50 d=0.5 mm
—■— G' Storage Modulus
—▲— G'' Loss Modulus



Physica Messtechnik GmbH



G.1 Viscosity of Titanium Dioxide Batches Dispersed in Cowles Mill

Dimensions of the Krebbs-Stormer viscometer

| | | |
|-----------------------------------|----------|--------------------|
| Breadth of Spindle | 0.5 | Cm |
| Diameter of Spindle | 6 | Cm |
| Area of Spindle | 3.00E-04 | M ² |
| Speed of Spindle | 200 | Rpm |
| Shear rate(s ⁻¹) | 43.33 | |
| Density of Titanium dioxide paste | 2000 | Kg.m ⁻² |

| | | | | |
|----------------------------------|----------|----------|---------|---------|
| Batch 1 | | | | |
| Time(min) | 10 | 15 | 20 | 30 |
| Mass(g) | 340 | 320 | 305 | 290 |
| F(N) | 3.34 | 3.14 | 3.00 | 2.85 |
| Shear stress(N.m ⁻²) | 11129.33 | 10474.67 | 9983.67 | 9492.67 |
| Viscosity(Pa.s) | 256.83 | 241.72 | 230.39 | 219.06 |
| Re | 0.09 | 0.10 | 0.10 | 0.11 |
| Viscosity(KU) | 99 | 97 | 95 | 94 |

| | | | | |
|----------------------------------|----------|----------|---------|---------|
| Batch 2 | | | | |
| Time(min) | 10 | 15 | 20 | 30 |
| Mass(g) | 330 | 310 | 290 | 265 |
| F(N) | 3.24 | 3.04 | 2.85 | 2.60 |
| Shear stress(N.m ⁻²) | 10802.00 | 10147.33 | 9492.67 | 8674.33 |
| Viscosity(Pa.s) | 249.28 | 234.17 | 219.06 | 200.18 |
| Re | 0.10 | 0.10 | 0.11 | 0.12 |
| Viscosity(KU) | 98 | 96 | 94 | 91 |

| | | | | |
|----------------------------------|----------|---------|---------|---------|
| Batch 3 | | | | |
| Time(min) | 10 | 15 | 20 | 30 |
| Mass(g) | 330 | 305 | 280 | 250 |
| F(N) | 3.24 | 3.00 | 2.75 | 2.46 |
| Shear stress(N.m ⁻²) | 10802.00 | 9983.67 | 9165.33 | 8183.33 |
| Viscosity(Pa.s) | 249.28 | 230.39 | 211.51 | 188.85 |
| Re | 0.10 | 0.10 | 0.11 | 0.13 |
| Viscosity(KU) | 98 | 95 | 93 | 89 |

| | | | | |
|----------------------------------|----------|---------|---------|---------|
| Batch 4 | | | | |
| Time(min) | 10 | 15 | 20 | 30 |
| Mass(g) | 325 | 300 | 265 | 230 |
| F(N) | 3.19 | 2.95 | 2.60 | 2.26 |
| Shear stress(N.m ⁻²) | 10638.33 | 9820.00 | 8674.33 | 7528.67 |
| Viscosity(Pa.s) | 245.50 | 226.62 | 200.18 | 173.74 |
| Re | 0.10 | 0.11 | 0.12 | 0.14 |
| Viscosity(KU) | 96 | 95 | 91 | 87 |

G3 Viscosity of Titanium Dioxide Dispersed through Homogeniser

Dimensions of the Krebbs-Stormer viscometer

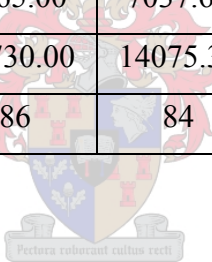
| | | |
|-----------------------------------|----------|--------------------|
| Breadth of Spindle | 0.5 | Cm |
| Diameter of Spindle | 6 | Cm |
| Area of Spindle | 3.00E-04 | M ² |
| Speed of Spindle | 200 | Rpm |
| Shear rate(s ⁻¹) | 43.33 | |
| Density of Titanium dioxide paste | 2000 | Kg.m ⁻² |

| | | | | | |
|----------------------------------|----------|----------|----------|----------|----------|
| Batch A | | | | | |
| Passes | 2 | 4 | 6 | 8 | 10 |
| Mass(g) | 230 | 215 | 200 | 195 | 180 |
| F(N) | 2.26 | 2.11 | 1.96 | 1.91 | 1.77 |
| Shear stress(N.m ⁻²) | 7528.67 | 7037.67 | 6546.67 | 6383.00 | 5892.00 |
| Viscosity(Pa.s) | 15057.33 | 14075.33 | 13093.33 | 12766.00 | 11784.00 |
| Viscosity(KU) | 87 | 84 | 82 | 81 | 78 |

| | | | | | |
|----------------------------------|----------|----------|----------|----------|----------|
| Batch B | | | | | |
| Passes | 2 | 4 | 6 | 8 | 10 |
| Mass(g) | 230 | 235 | 230 | 225 | 220 |
| F(N) | 2.26 | 2.31 | 2.26 | 2.21 | 2.16 |
| Shear stress(N.m ⁻²) | 7528.67 | 7692.33 | 7528.67 | 7365.00 | 7201.33 |
| Viscosity(Pa.s) | 15057.33 | 15384.67 | 15057.33 | 14730.00 | 14402.67 |
| Viscosity(KU) | 87 | 88 | 87 | 86 | 85 |

| | | | | | |
|----------------------------------|----------|----------|----------|----------|----------|
| Batch C | | | | | |
| Passes | 2 | 4 | 6 | 8 | 10 |
| Mass(g) | 220 | 215 | 200 | 190 | 175 |
| F(N) | 2.16 | 2.11 | 1.96 | 1.87 | 1.72 |
| Shear stress(N.m ⁻²) | 7201.33 | 7037.67 | 6546.67 | 6219.33 | 5728.33 |
| Viscosity(Pa.s) | 14402.67 | 14075.33 | 13093.33 | 12438.67 | 11456.67 |
| Viscosity(KU) | 0.021215 | 84 | 82 | 80 | 77 |

| | | | | | |
|----------------------------------|----------|----------|----------|----------|----------|
| Batch D | | | | | |
| Passes | 2 | 4 | 6 | 8 | 10 |
| Mass(g) | 230 | 225 | 215 | 210 | 200 |
| F(N) | 2.26 | 2.21 | 2.11 | 2.06 | 1.96 |
| Shear stress(N.m ⁻²) | 7528.67 | 7365.00 | 7037.67 | 6874.00 | 6546.67 |
| Viscosity(Pa.s) | 15057.33 | 14730.00 | 14075.33 | 13748.00 | 13093.33 |
| Viscosity(KU) | 78 | 86 | 84 | 83 | 82 |



| | | | | | |
|----------------------------------|----------|----------|----------|----------|----------|
| Batch E | | | | | |
| Passes | 2 | 4 | 6 | 8 | 10 |
| Mass(g) | 230 | 230 | 220 | 215 | 210 |
| F(N) | 2.26 | 2.26 | 2.16 | 2.11 | 2.06 |
| Shear stress(N.m ⁻²) | 7528.67 | 7528.67 | 7201.33 | 7037.67 | 6874.00 |
| Viscosity(Pa.s) | 15057.33 | 15057.33 | 14402.67 | 14075.33 | 13748.00 |
| Viscosity(KU) | 87 | 887 | 85 | 84 | 83 |

G4 Viscosity Data for the Rheology of Titanium Dioxide Dispersed through The Cowles Mill

G.4.1 The effect of speed on rheology of titanium dioxide dispersions

G.4.1.1 Low Shear Conditions(Read off from the relevant flow curve)

| Low shear conditions \ Batch | | |
|--------------------------------|--------|--------|
| Effect of speed (10min) | A1 | A2 |
| Shear rate(s^{-1}) | 0.3558 | 0.3559 |
| Shear stress(Pa) | 2.627 | 3.097 |
| Viscosity(Pa.s) | 7.385 | 8.701 |
| Mill speed(Hz) | 3.33 | 3.33 |
| Re | 90.2 | 76.5 |
| T($^{\circ}$ C) | | |
| Mean particle size(nm) | 416.2 | 403.9 |
| Particle size distribution(nm) | 663.6 | 457.1 |

| Effect of speed (20min) \ Batch | A1 | A2 |
|---------------------------------|--------|--------|
| Shear rate(s^{-1}) | 0.3557 | 0.3561 |
| Shear stress(Pa) | 3.196 | 2.086 |
| Viscosity(Pa.s) | 8.985 | 5.858 |
| Mill speed(Hz) | 3.33 | 3.33 |
| Re | 74.1 | 113.7 |
| T($^{\circ}$ C) | | |
| Mean particle size(nm) | 393.1 | 382.4 |
| Particle size distribution(nm) | 672.7 | 636.4 |

| Effect of speed (30min) \ Batch | A1 | A2 |
|---------------------------------|--------|--------|
| Shear rate(s^{-1}) | 0.3557 | 0.3562 |
| Shear stress(Pa) | 3.619 | 1.643 |
| Viscosity(Pa.s) | 10.17 | 4.614 |
| Mill speed(Hz) | 3.33 | 3.33 |
| Re | 65.5 | 144.3 |
| T($^{\circ}$ C) | | |
| Mean particle size(nm) | | 369.8 |
| Particle size distribution(nm) | | 518.2 |

G.4.1.1 High Shear Conditions(Read off from the relevant flow curve)

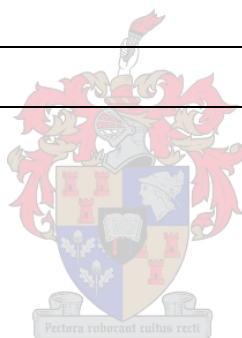
| Effect of speed (10min) \ Batch | A1 | A2 |
|---------------------------------|---------|---------|
| Shear rate(s^{-1}) | 385.7 | 529.8 |
| Shear stress(Pa) | 47.96 | 46.81 |
| Viscosity(Pa.s) | 0.1243 | 0.08834 |
| Mill speed(Hz) | 30 | 30 |
| Re | 48270.3 | 67919.4 |
| T($^{\circ}$ C) | 30 | 33 |
| Mean particle size(nm) | 416.2 | 403.9 |
| Particle size distribution(nm) | 663.6 | 457.1 |

| Effect of speed (20min) \ Batch | A1 | A2 |
|---------------------------------|---------|---------|
| Shear rate(s^{-1}) | 385.7 | 529.8 |
| Shear stress(Pa) | 49.61 | 45.62 |
| Viscosity(Pa.s) | 0.1286 | 0.08609 |
| Mill speed(Hz) | 30 | 30 |
| Re | 46656.3 | 69694.5 |
| T($^{\circ}$ C) | 39 | 42 |
| Mean particle size(nm) | 393.1 | 382.4 |
| Particle size distribution(nm) | 672.7 | 636.4 |

| Effect of speed (30min) \ Batch | A1 | A2 |
|---------------------------------|---------|---------|
| Shear rate(s^{-1}) | 385.7 | 529.8 |
| Shear stress(Pa) | 46.35 | 44.25 |
| Viscosity(Pa.s) | 0.1202 | 0.08352 |
| Mill speed(Hz) | 30 | 30 |
| Re | 49916.8 | 71839.1 |
| Mill Temperature($^{\circ}C$) | 43 | 45 |
| Mean particle size(nm) | | 369.8 |
| Particle size distribution(nm) | | 518.2 |

Mill and Dispersion information for low and high shear behaviour

| | |
|-------------------------------------|------|
| Density of mill base($Kg.m^{-3}$) | 2000 |
| Diameter of agitator(m) | 0.1 |



G.4.2 The effect of Dispersant on rheology of titanium dioxide dispersions

G.4.1.2 Low Shear Conditions (Read off from the relevant flow curves)

| Effect of dispersant (10min) \ Batch | A1 | A3 |
|--------------------------------------|--------|--------|
| Shear rate(s^{-1}) | 0.3558 | 0.3588 |
| Shear stress(Pa) | 2.627 | 35.3 |
| Viscosity(Pa.s) | 7.385 | 98.37 |
| Mill speed(Hz) | 3.33 | 3.33 |
| Re | 90.2 | 6.8 |
| T($^{\circ}$ C) | | |
| Mean particle size(nm) | 416.2 | 458.5 |
| Particle size distribution(nm) | 663.6 | 681.8 |

| Effect of dispersant (20min) \ Batch | A1 | A3 |
|--------------------------------------|--------|--------|
| Shear rate(s^{-1}) | 0.3557 | 0.3603 |
| Shear stress(Pa) | 3.196 | 29.29 |
| Viscosity(Pa.s) | 8.985 | 81.19 |
| Mill speed(Hz) | 3.33 | 3.33 |
| Re | 74.1 | 8.2 |
| T($^{\circ}$ C) | | |
| Mean particle size(nm) | 393.1 | 427.8 |
| Particle size distribution(nm) | 672.7 | 754.5 |

| Effect of dispersant (30min) \ Batch | A1 | A3 |
|--------------------------------------|--------|--------|
| Shear rate(s^{-1}) | 0.3557 | 0.3615 |
| Shear stress(Pa) | 3.619 | 28.95 |
| Viscosity(Pa.s) | 10.17 | 80.07 |
| Mill speed(Hz) | 3.33 | 3.33 |
| Re | 65.5 | 8.3 |
| T($^{\circ}$ C) | | |
| Mean particle size(nm) | 393.1 | 411 |
| Particle size distribution(nm) | 672.7 | 736.4 |

G.4.1.2 High Shear Conditions (Read off from the relevant flow curves)

| Effect of dispersant (10min) \ Batch | A1 | A3 |
|--------------------------------------|---------|---------|
| Shear rate(s^{-1}) | 385.7 | 385.7 |
| Shear stress(Pa) | 47.96 | 86.48 |
| Viscosity(Pa.s) | 0.1243 | 0.2242 |
| Mill speed(Hz) | 30 | 30 |
| Re | 48270.3 | 26761.8 |
| T($^{\circ}$ C) | 30 | 34 |
| Mean particle size(nm) | 416.2 | 458.5 |
| Particle size distribution(nm) | 663.6 | 681.8 |

| Effect of dispersant (20min) \ Batch | A1 | A3 |
|--------------------------------------|---------|---------|
| Shear rate(s^{-1}) | 385.7 | 385.7 |
| Shear stress(Pa) | 46.61 | 78.83 |
| Viscosity(Pa.s) | 0.1286 | 0.2044 |
| Mill speed(Hz) | 30 | 30 |
| Re | 46656.3 | 29354.2 |
| T($^{\circ}$ C) | 39 | 45 |
| Mean particle size(nm) | 393.1 | 427.8 |
| Particle size distribution(nm) | 672.7 | 754.5 |

| Effect of dispersant (30min) \ Batch | A1 | A3 |
|--------------------------------------|---------|---------|
| Shear rate(s^{-1}) | 385.7 | 385.7 |
| Shear stress(Pa) | 46.35 | 70.71 |
| Viscosity(Pa.s) | 0.1202 | 0.1833 |
| Mill speed(Hz) | 30 | 30 |
| Re | 49916.8 | 32733.2 |
| T($^{\circ}$ C) | 43 | 50 |
| Mean particle size(nm) | | 411 |
| Particle size distribution(nm) | | 736.4 |

Mill and Dispersion information for low and high shear behaviour

| | |
|---|------|
| Density of mill base(Kg.m ⁻³) | 2000 |
| Diameter of agitator(m) | 0.1 |

